Institute of Agronomy and Plant Breeding I

Department of Plant Breeding

Justus Liebig University Giessen

Professor Dr. Dr. h.c. Wolfgang Friedt

The pathosystem wheat (*Triticum aestivum*) root-*Fusarium graminearum*: complex plant responses and fungal strategies

A thesis submitted for the requirement of the doctoral degree in

Agricultural Sciences from the Faculty of Agricultural and

Nutritional Sciences and Environmental Management

Justus Liebig University Giessen, Germany

Submitted by

Qing Wang

Giessen 2015

Institute of Agronomy and Plant Breeding I

Department of Plant Breeding

Justus Liebig University Giessen

The pathosystem wheat (*Triticum aestivum*) root-*Fusarium graminearum*: complex plant responses and fungal strategies

A thesis submitted for the requirement of the doctoral degree in

Agricultural Sciences from the Faculty of Agricultural and

Nutritional Sciences and Environmental Management

Justus Liebig University Giessen, Germany

Submitted by

Qing Wang

Examiners

Supervisor: Prof. Dr. Dr. h.c. Wolfgang Friedt

Co-supervisor: Prof. Dr. Karl-Heinz Kogel

Giessen 2015

Table of contents

List of figures

List of tables

List of abbreviation and symbols

CMC	Carboxymethyl cellulose sodium salt
D3G	DON-3-glucoside
DON	Deoxynivalenol
dai	days after inoculation
ELISA	enzyme-linked immunosorbent assay
FAR	FRR adult stage resistance
FCR	Fusarium crown rot
FDI	FRR disease index
FHB	Fusarium head blight
FRR	Fusarium root rot
FSB	Fusarium seedling blight
FSS	FRR symptom severity
FSR	FRR seedling stage resistance
JA	Jasmonic acid
LOX	Lipoxygenase
LC-MS	Liquid chromatography mass spectrometry
PCD	Programme cell death
PCR	Ploymerase chain reaction
qRT-PCR	quantitative Real-Time-Polymerase chain reaction
QTL	Quantitative Trait Loci
RBR	Root biomass reduction
RFB	Relative fungal biomass
RI	Reduction index
RLR	Root length reduction
SI	Severity index
SLR	Shoot length reduction
WGA	Wheat Germ Agglutinin

1 Introduction

Bread wheat (*Triticum aestivum* L.ssp. *aestivum*) is one of the most important cultivated crops of the world. Together with maize and rice, wheat can be grown over a wide range of climatic and soil condition. In 2013, 708.5 million tons of bread wheat and durum wheat (*T. durum*) were produced in the world, of which 144.3 million tons were produced in the EU followed by China, India and USA (FAO 2013). However recent agricultural practices like the reduction of soil tillage and pesticides use raise the risk of re-emerging or new wheat diseases.

One of the most important fungal pathogens which frequently cause serious damages in small grain cereals and maize belong to the genus *Fusarium*, assigned to the phylum ascomycota (Van Eeuwijk et al., 1995; Ma LL et al., 2010). *Fusarium* diseases have a broad host spectrum and can cause significant loss of grain yield and quality in crops such as wheat, maize, oat (*Avena sativa L.*), barley (*Hordeum vulgare L.*) and rice (*Oryza sativa L.*) (Parry et al., 1995; Trail et al., 2003; Pereyra & Dill-Macky, 2008). *Fusarium graminearum* Schwabe (teleomorph *Gibberella zeae* [Schwein] Petch) is one of the main pathogens of wheat, causal agent of Fusarium head blight (FHB), root and stem (also named culm or stalk in cereals) rot, especially under warm and humid conditions. Moreover, *F. graminearum* produces mycotoxins which are harmful to human and animal health. Recently, although there are possible tools to be adapted to control *Fusarium* disease epidemic, to cultivate wheat varieties with significant *Fusarium* disease resistance is still considered as the most economical and effective strategy. Therefore, *Fusarium* (FHB) resistance is one of the main goals of wheat breeding as a basis for disease control.

Roots represent the hidden half of plants and thus, were not sufficiently explored for quite a long time (Raaijmakers et al., 2009). Nowadays, much more attention is given to the roots, their architecture, functioning and interactions which have promising features to enable a new green revolution via increased and more stable yields without causing unacceptable environmental damage (Den Herder et al., 2010). In fact, also root diseases are typically overlooked or underestimated and basically a challenge for research, but nevertheless account for a large part of the current yield reductions (Raaijmakers et al., 2009). Other than FHB, the knowledge on Fusarium root rot (FRR) is still very limited. There are several reports on *Fusarium* soil-borne infestations typically addressing the crown or stem rot disease caused by *F. culmorum* and *F. pseudograminearum*, associated with relatively early visible symptoms at aboveground lower stem internodes. However, possible soil-borne infestations by *F. graminearum* and the emergence of *Fusarium* root diseases are usually underestimated. Therefore, it is urgently necessary to investigate the agronomical important root-microbe interaction of *F. graminearum* and wheat.

2 Background

2.1 The evolution of wheat: Challenges and current opportunities for wheat breeding

The origin of wheat breeding reaches far back into mankind's history. Approximately 7,000 to 8,000 years ago people have started to select wheat plants for their own need. Therefore, wheat became one of the first domesticated crops. Since wheat is essential for human nutrition, there has always been a co-evolution of wheat together with man (Charmet, 2011).

Modern wheat cultivars usually belong to the hexaploid bread wheat (*Triticum aestivum*, 2n = 6x = 42, AuAuBBDD) and the tetraploid durum wheat (*T. durum*, 2n = 4x = 28, AuAuBB) (Peng et al., 2011). Bread wheat and durum wheat nowadays account for about 95% and 5% of world wheat production, respectively. About 6.5 million years ago (mya), a common ancestor start to evolve into the A and B genome lineages (*Triticum* and *Aegilops*). The evolutionary history of modern wheat is summarized in Figure 1.

About 5,500,000 years ago the diploid ancestor of modern wheat, *T. urartu* (2n = 2x = 14, genome AuAu) hybridized with the B genome ancestor *Aegilops speltoides* (2n = 2x = 14, genome SS) to generate the D genome *Ae. tauschii* (2n = 2x = 14, genome DD). Around 800,000 years ago, hybridization happened between a close relative (BB) of *Ae. speltoides* and *T. urartu* (AA), produce the allotetraploid emmer wheat (*T. turgidum*; AABB) by polyploidization. Then around 400,000 years ago, the emmer wheat (T. dicoccum, 2n = 4x = 28, genome AuAuBB) hybridized with *Ae. tauschii* (2n = 2x = 14, genome DD) to generate the early hexaploid spelt wheat (T. spelta, 2n = 6x = 42, genome AuAuBBDD) (Marcussen T et al,. 2014). About 8,500 years ago free threshing ear types were selected in emmer and spelt wheat, finally leading to the modern types of durum wheat (*T. durum*) and bread wheat (*T. aestivum*) (Peng et al., 2011).

The genome of bread wheat (*T. aestivum*) is hexaploid and consists of 42 chromosomes with an estimated genome size of 17 Gbp which is 40 times larger than, for instance, the rice genome (Paux et al., 2006). Approximately 80% of the genome consists of extensive repetitive elements (Berkman et al., 2012). In fact, the high level of repetitive DNA together with the hexaploidy basically challenges the development of genomic resources that can facilitate the necessary improvements in wheat breeding (Belova et al. 2013). However, to address this issue, the International Wheat Genome Sequencing Consortium (IWGSC) was founded to generate a reference genome sequence of the cv. Chinese Spring 42 (Feuillet & Eversole, 2007). In 2012, a first survey sequence was generated from Illumina high throughput paired end sequence data, representing a ≥30-fold depth of wheat chromosome arms. 10.2 Gigabytes (Gb) of sequence was assembled in contigs of more than 200 bp and assigned to individual chromosomes. A total of 133,090 high confidence gene models were defined using a combination of wheat RNASeq and

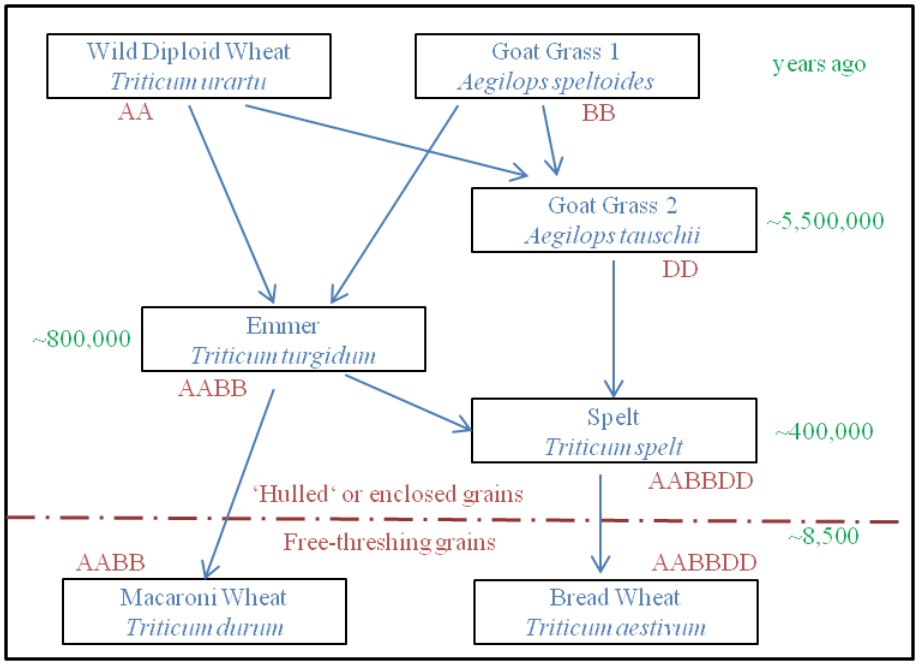

Figure 1: The evolution of bread wheat. (The figure was modified from Peng et al., 2011 and Marcussen T et al., 2014).

full-length cDNA datasets, as well as reference gene sets from sequenced grass genomes. Recent analyses at chromosomal and sub genome levels have revealed new insights on the intra-chromosomal duplications, the genome evolution following polyploidisation and the transcriptional activity of the genome. Finally, all publicly available sequence-based markers, for instance SSR (simple sequence repeat) and SNP (Single Nucleotide Polymorphism) markers, have been assigned to the sequence assemblies to provide integrated marker platform to breeders and scientists for mapping in wheat (Brenchley et al., 2012; Raats et al. 2013; Spannagl et al., 2013; The International Wheat Genome Sequencing Consortium. [http://www.wheatgenome.org/]).

Such anchored genetic-physical maps represent a powerful tool for understanding the molecular basis of complex traits such as *Fusarium* resistance as well as for accelerating gene cloning. In fact, the localization of target genomic regions and candidate genes which influence the phenotypic expression of a certain resistance is the basis for understanding the molecular cross-talk between pathogen and host which, on the other hand, is the prerequisite for discovering selective markers such as SNPs for high throughput marker-assisted selection in wheat (resistance) breeding (Philippe et al., 2013). However, the increasing availability of tools such as high density SNP genotyping platforms, integrated physical/genetic genome maps and bioinformatics approaches including genomic selection and systems biology, turns phenotyping to the most critical point for the research on complex traits.

Hitherto, limitations in genome-wide approaches and high-throughput phenotyping have prevented a substantial progress in research and breeding of wheat towards improved resistance against the floral FHB disease. In fact, FHB phenotyping is a demanding task, and the ability to improve FHB resistance has long been complicated by difficulties in phenotyping (Van Sanford et al. 2001). However, in case of resistance research advanced phenotyping refers not only to innovations in the accuracy and rate of data generation, but also to improved knowledge on relevant and critical events during host-pathogen interactions for a pinpoint application of advanced genomic tools.

2.2 *F. graminearum*: Taxonomy, life cycle and virulence

Besides abiotic stress factors such as drought, heat and nutrient deficiency, biotic stressors including pathogens like viruses, bacteria and fungi threaten wheat performance. Amongst the most important fungi causing serious damage in small grain cereals and maize are *Fusarium* species, belonging to the phylum of *Ascomycot*a. Major diseases such as Fusarium head blight (FHB), root and crown rot (FRR and FCR) are caused by fungal pathogens such as *F. graminearum, F. culmorum, F. pseudograminearum* and *F. sporotrichoides*.

F. graminearum Schwabe [teleomorph *Gibberella zeae* (Schw.) Petch] is a haploid homothallic fungus that has both a sexual and an asexual life cycle. In the asexual cycle, *F. graminearum* produces spores known as macroconidia. Those conidia are slender, thick-walled, curved to straight, tapered at both ends, with five to seven septa or partitions. They are produced in globose chlamydospores which are thick-walled resting spores, but are also formed in mycelia. Chlamydospores allow *F. graminearum* to survive unfavourable conditions and thus, allow the fungus to over-winter in soil or on crop residues until suitable temperature and humidity facilitate a new cycle of infections. In addition, chlamydospores are assumed to cause the primary infections on common bean roots (Nash et al., 1961). Generally, while macroconidia play an important role in the pathogen dissemination by wind, microconidia and chlamydospores are essential for the infection of host tissues (Katan et al., 1997). Macroconidia can be transported from soil or infected leaves to flowering spikes by rain-splash or wind dispersal, thus causing FHB. In fact, this way *F. graminearum* can infect spike tissues from flowering to late stages of kernel development (Del Ponte *et al.*, 2007). A flower infection manifests initially watersoaked lesions which later turn to a yellowish-red colour. Orange spots formed on the surface of infected spikelet are called sporodochium and contain many macroconidia. Besides the internal growth of mycelium in host tissues, dispersal of macroconidia can also be initiated from other infections on the same plant or from neighbouring plants. Whether, macroconidia can

also infect wheat roots and hypocotyls which cause FRR was not known at the start of this study. The sexual stage of *F. graminearum* starts from overwintered small bluish-black round bodies on the crop debris called perithecia. Perithecia are reported to retain viability for up to 16 months, and abundant in spring and warm moist weather conditions which are favourable for their maturation (Markell & Francl, 2003) leading to the release of ascospores (Trail et al., 2002). Ascospores are sexual spores dispersed by wind, rain or insects (Sutton, 1982; Parry et al., 1995) and cause initial disease of aerial plant parts (Agrios, 2004).

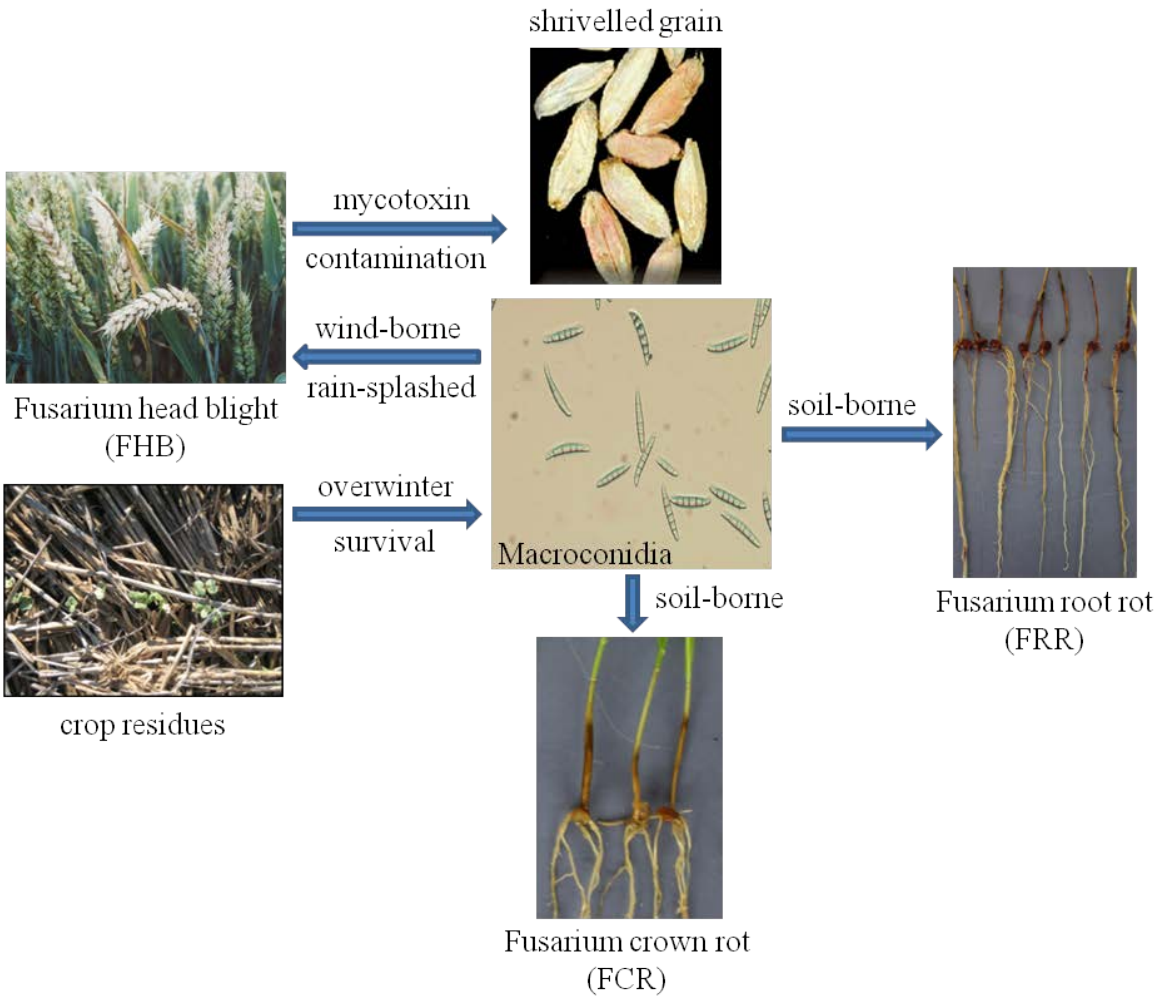

Figure 2: The life cycle of *Fusarium graminearum* Schwabe (teleomorph Gibberella zeae (Schwein) Petch) in wheat.

It is still under discussion whether *F. graminearum* exhibits a biotrophic lifestyle during the initial stages of infection of floral tissues (Trail, 2009; Brown et al., 2010). In fact, a recent microscopic study of the *F. graminearu*m infection process in wheat spikes did not find an indication for necrotrophy at the initial stages of infection which was therefore, symptomless (Brown et al., 2010). Generally, intercellular hyphae were found to grow through living host cells in flower and rachis tissues. However, this colonization mode throughout the spike was

observed only for a short period and was exceptionalness followed by the onset of host cell alterations. During biotrophic colonization no specialised feeding structures were observed and no intracellular hyphae were found within living host cells. Therefore, it was assumed that the *F. graminearum* hyphae were initially feeding from extracellular exudates in the apoplast (Brown et al., 2010). However, once host cell death is initiated, this was found to be accompanied by intracellular colonisation and necrotrophic feeding off dead host cells. The necrotrophic stage is generally associated with an increased fungal colonization, subsequent cell death and necrosis.

Over the course of spike colonization and after successful invasion of the main spike parts, the proportion of the fungal infection in association with living host cells gradually decreases, but remains present. For instance, advancing *F. graminearum* hyphae were found to remain in the intercellular spaces of wheat rachis and thus, during all phases of the spike infection process, *F. graminearum* maintains a zone where the most advancing hyphae are surrounded by living host cells (Brown et al., 2010). Moreover, one strategy of the *Fusarium* fungi to successfully establish and spread within host tissues is to live epiphytically, non-parasitic, without causing symptoms (Clement et al. 1998). Such asymptomatic colonisations of plant tissues by *F. graminearum* have been observed for stalks of corn (Bushnell et al., 2003), or grass hosts (Farr et al., 1989; Inch & Gilbert, 2003). Finally, *F. graminearum* could be classified as a hemibiotrophic pathogen, but with the restriction or distinctiveness that *F. graminearum* probably displays a unique lifestyle which is different from other described hemibiotrophic lifestyles (Kazan et al., 2012). In another words, Brown et al. (2010) concluded that the uncovered mode of nutrition during FHB disease does not resemble any of the three classical definitions, namely, biotroph, hemibiotroph or necrotroph (Agrios, 2004).

F. graminearum has also the ability for a saprotrophic growth. Generally, the chemical composition of crop biomass differs within a species and from other species as well as between different plant parts. This influences the decomposition of the crop residues by microbial colonisers and thereby, the saprotrophic survival of pathogens such as *F. graminearum* (Khonga & Sutton, 1988; Nicolardot et al., 2007). In a study on the *F. graminearum* exoproteome has been demonstrated that 30 xylanase-related genes were transcribed with different expression patterns according to the respective plant material tested (Phalip et al., 2005). Therefore, it was suggested that *F. graminearum* can firstly, adapt to a range of variations in its environment (Hatsch et al., 2006) and secondly, can survive overwinter on crop residues due to its enzymatic ability to degrade and use different residues as nutrients (Leplat et al., 2012).

F. graminearum has been well investigated for many years to understand the genetic basis of the life cycle, pathogenicity, evolution, and population biology. Availability of the full genome sequence (Cuomo et al., 2007; Ma et al., 2010) and efficient genetic transformation system of *F. graminearum* has facilitated analyses of gene functions. Meanwhile, transcriptome (Stephens et al., 2008; Hallen-Adams et al., 2011; Lysøe et al., 2011), metabolome (Chen et al., 2011) and proteome (Paper et al., 2007; Taylor et al., 2008) analyses have been conducted by using *F. graminearum* or mutants of it to study infection processes in barley and wheat, the fungal sexual development and conidial germination, the evolution of virulence and toxin biosynthesis as well as the fungal defences against fungicides (Kazan et al., 2012).

The *F. graminearum* proteome during host colonization was found to be composed of several extracellular proteins which probably are either involved in compromising the host to facilitate disease establishment and spread, or in establishing nutrient acquisition (Divon & Fluhr, 2007). Those proteins include degradative enzymes (hydrolases, oxidoreductases, esterases, and proteases), small non-enzymatic and housekeeping proteins, as well as proteins of unknown or predicted function. More than 50% of proteins secreted during pathogenesis contained putative secretion signals and therefore, might function as effectors to promote virulence, commonly by interacting with plant host proteins (Paper et al., 2007). In addition, numerous proteins involved in iron uptake, sterol trafficking, nitrate transport, and reactive oxygen species (ROS) production have been linked to pathogenesis (Walter et al., 2010). 42 protein kinase genes and 62 transcription factor genes were found to be required for wheat head infection (Son et al., 2011; Wang C et al., 2011).

Particularly, *F. graminearum* is characterized by a large arsenal of virulence factors which are secreted in all phases of diseases caused by this species and which aim at the manipulation of plants´ physiology for its own benefit (Walter et al., 2010). Among these virulence-factors plant cell wall–degrading enzymes (cellulases, hemicellulases, and pectinases) represent an essential and large group since they facilitate early flower infection as well as the rapid colonization of wheat spikes (Wanjiru et al., 2002; Martinez et al., 2008; Kikot et al. 2009; King et al. 2011). Moreover, cell-wall degrading enzymes might not only be relevant during the pathogenic part of the *F. graminearum* life cycle, but also during its saprotrophic part of life cycle (Belien et al. 2006; Van den Brink & de Vries, 2011).

Another important group of virulence factors are hydrolytic enzymes (subtilisin-like and trypsin-like proteases) which were found during almost the entire course of FHB disease. Such proteases are supposed to be involved in the suppression of plant defence by degrading pathogenesis-related (PR) proteins or defence-signalling compounds according to their property to cause

proteolytic protein digestion (Jackowiak et al., 2002; Olivieri et al., 2002; Pekkarinen et al., 2007). For instance, in the spikes of the resistant wheat cv. Wangshuibai the down-regulation of different housekeeping proteins was reported already 6 to 24 h after *F. graminearum* inoculation as a consequence of fungal proteases and mycotoxins (Wang Y et al., 2005). In the transcriptome of resistant wheat cv. Dream several serine proteases as well as serine protease inhibitors were found to be exclusively enriched upon *F. graminearum* infection, indicating a complex crosstalk between *F. graminearum* and wheat proteases and their inhibitors (Gottwald et al., 2012). Such defence counter-defence mechanisms in which both, host and pathogen release specific sets of proteases and protease inhibitors which mutually impair each other, have been reported for other diseases (Xia, 2004; Tian et al., 2008).

Since 2003 the complete *F. graminearum* genome sequence is available and more than 11,600 genes were detected, indicating *F. graminearum* as one of the most gene-rich fungi (Goswami & Kistler, 2004). Particular genes for the biosynthesis of secondary metabolites, including toxic compounds were found to typically cluster in the *F. graminearum* genome at a single locus and to be co-expressed. Estimations suggest that more than 190 gene clusters are present with a gene density greater than 10 ORFs per 25 kb (Hammond-Kosack et al., 2004), indicating a common mechanism of transcriptional co-regulation for associated genes (Postnikova et al., 2011). These clusters include the mycotoxin producing TRI5-cluster on chromosome 2, together with several clusters suggested to be responsible for the production of other secondary metabolites than mycotoxins (Hammond-Kosack et al., 2004). It is still unknown whether or at which timepoint during the general disease progression the pathogen produces toxic secondary metabolites, other than the *F. graminearum* characteristic toxin deoxynivalenol (DON).

Trichothecene mycotoxins produced by *F. graminearum* are essentially responsible for the severe economic damages caused by FHB and other *Fusarium* diseases since they significantly reduce grain yield and quality (Maier et al., 2006; Walter et al. 2010). Those toxins are grouped into four types: A, B, C, and D. *F. graminearum* isolates mainly produce the toxins deoxynivalenol (DON), nivalenol (NIV) and zearalenone (ZEA) of which DON and NIV belong to the type B trichothecenes (Bennett & Klich, 2003). The potential toxicity of NIV versus DON toxin-producing *F. gram*inearum isolates is still controversial (Puri & Zhong, 2010; Gale et al., 2011). Mycotoxins are not only phytotoxic, but also cause serious toxic effects on farm animals and humans even at very low concentrations (Pestka & Smolinski, 2005; Rocha et al., 2005). *Fusarium* disease essential affects the aspect of food security and consequently, in the European Union regulations exist which state the levels of maximum tolerable DON contents in nutritional products: 1.25 mg/kg in unprocessed cereals except durum wheat; 1.75 mg/kg (ppm) in durum

wheat; and 0.75 mg/kg (ppm); in cereals' flour and pasta and bread, 0.50 mg/kg (Anonymous 2007).

The DON toxin is commonly known as a potent inhibitor of eukaryotic protein biosynthesis and considered as an essential virulence factor which determines the aggressiveness of the pathogens in host tissues. A positive, significant correlation ($r = 0.69$, $P < 0.01$) between aggressiveness and DON content was found in a field experiment with as many as 50 *F. graminearum* isolates (Cumagun & Miedaner, 2004). DON was reported to be produced in the fungal infection structures already during the initial penetration of floret tissues. The reason for this early secretion is unknown, because the initial infection is symptomless and indistinguishable between susceptible and resistant wheat cultivars. In addition, even trichothecene-deficient *F. graminearum* mutants did not lose their ability to infect flower tissues (Bai et al., 2002; Maier et al., 2006; Boenisch & Schäfer, 2011). However, the DON secretion gains importance during later disease stages in which the pathogen systemically colonizes infected tissues and/or spreads into non-infected plant parts (Jansen et al., 2005). At these disease stages the role of DON secretion can be explained by its assumed capability to suppress plant defence by inhibiting the biosynthesis of defence proteins (Rocha et al., 2005; Boenisch & Schäfer, 2011).

Recently it has been reported that DON released by *F. graminearum* at low concentrations can already inhibit the apoptosis-like programmed cell death (PCD) in *Arabidopsis*; PCD is a common plant response to arrest pathogen growth. Therefore, it was assumed that the inhibition of apoptosis-like PCD may be another important role of DON during the plant colonisation process (Diamond et al., 2013). Finally, at high concentrations DON, together with proteases, induces cell death probably to initiate and facilitate necrotrophic intracellular nutrition (Pekkarinen & Jones, 2002; Boddu et al., 2006; Brown et al., 2010, 2011).

Recent studies indicate that farming practises, such as the use of resistant cereal cultivars and fungicides, and environmental shifts, such as climate change, may affect the evolution of virulence and toxin biosynthesis in *F. graminearum*. For example, a larger number of *F. graminearum* isolates with higher aggressiveness and greater levels of grain DON content were found among current isolates compared to those isolates collected between 1980 and 2000 in North Dakota (Puri & Zhong, 2010). Another study examining *F. graminearum* isolates throughout the USA has found that NIV-producing isolates have already established in small-grain-growing regions of southern Louisiana (Gale et al., 2011), despite earlier reports showing that such chemotypes were rare (e.g. Desjardins et al., 2008).

2.3 Recent status of Fusarium head blight (FHB) research

Major FHB epidemics have occurred in the last two decades, resulting in billions of dollars of wheat yield and quality loss in the USA during the 1990s and early 2000s (McMullen, 1997, 2003). For instance, from 1993 to 2001 the cumulative direct economic loss attributable to FHB in wheat and barley for the entire period was US $2.491 billion, with $1.074 billion (43.1%) of the total being lost between 1998 and 2001 (Nganje et al., 2004). In 2003, a regional epidemic occurred that involved much of the soft red winter wheat grown in the United States, with a total dollar loss estimated at $13.6 million (McMullen et al., 2012). In the period of 2007 to 2008 FHB damage occurred in several states causing US $13.3 and 57 million losses respectively. FHB was at low level in 2010, but the impact in Kansas was still estimated at US $13 million.

Currently, several FHB-management approaches are applied for reducing the economic damage and potential health hazards associated with this disease. Strategies have been developed to target each of the three major components which are necessary for an outbreak: i) inoculum source, ii) susceptible hosts, and iii) favourable environmental conditions. The inoculum source of FHB is usually present in the form of soil-borne ascospores. Here, crop-rotation, tillage, chemical or biological control, and the use of FHB resistant cultivars can contribute to reduce the amount of inoculum from contaminated crops and/or crop debris (He *et al*., 2009; Petti *et al*., 2010; Henkes *et al*., 2011). However, FHB outbreaks in the past decade demonstrate that the currently available FHB-management approaches are still insufficient to avoid *Fusarium* epidemics. Moreover, current agronomical farming practices are rather inclined to facilitate further outbreaks in the future. In fact, reduced, non-plough or minimal tillage and cereal-based crop rotations in regions of intensive agriculture constantly enrich the fungal inoculum in soils of agricultural areas (Chakraborty et al., 2008; Luck et al., 2011). In addition, the climate change which is accompanied by higher average temperatures and infection propagating environmental conditions during sensitive wheat growth stages such as flowering (more rainfall during this season), seedling and juvenile stages (milder temperatures during one or both seasons) propagate rather a rise of infestation by allowing the pathogen to exploit their broad spectrum of infection routes (Chakraborty & Newton, 2011).

Worldwide a significant increase in the risk of FHB epidemics is expected which may lead to grain yields with mycotoxin levels above the permitted limit (*cf.* Chakraborty & Newton, 2011), for instance in the United Kingdom around 2050 (Madgwick et al., 2010). Generally, the use of cultivars with stable resistance is considered to be the most efficient strategy to avoid FHB epidemics in wheat (Buerstmayr et al., 2008; Kazan et al., 2012; Yang F et al., 2013). However, this strategy is still hampered by insufficient knowledge on the molecular basis of FHB

resistance and hence, functional resistance genes were not cloned yet (Liu S et al., 2008). Wheat resistance to *Fusarium* is a complex trait since it is controlled by many small effect genetic loci (Massman et al., 2011) with a low heritability that changes depending on environment, location and year (Buerstmayr et al., 2009; Miedaner et al., 2012; Massman et al., 2011). Such circumstances, indeed, turn resistance research into a time consuming and moderately efficient task (Balmer et al., 2013). In addition, besides a limited selection of registered cultivars with decent FHB resistance, farmers preferentially select cultivars with good agronomics, which often have insufficient resistance (Foroud & Eudes, 2009). A prominent example for this negative correlation is the currently released high yielding German cv. Tobak (Table 1).

The known FHB resistances include active, passive and/or tolerance mechanisms. In wheat, five resistance components or types are described, which rely on active resistance mechanisms: Type 1 - resistance against initial infection (Schroeder & Christensen, 1963); Type 2 - resistance to pathogen spreading within infected tissue (Schroeder & Christensen, 1963); Type 3 - resistance to kernel infection (Mesterhazy, 1996); Type 4 - tolerance against FHB (Mesterhazy, 1996); and Type 5 - resistance to toxins (Miller et al., 1985).

Major reactions against FHB combine the Type 2 and Type 5 resistances. Quantitative trait loci (QTL) for Type 2 resistance originate mainly from Chinese sources such as Sumai 3 and have been located primarily on chromosomes 3B and 5A (Waldronet et al., 1999; Anderson et al., 2001). Until today the most important QTL identified in the cultivars Sumai 3 and Ning 7840 is *Qfhs.ndsu-3BS* (Waldron et al., 1999; McCartney et al., 2004), currently re-designated as *Fhb1* (Liu et al., 2006). A second significant QTL was found on chromosome 6BS of cv. Sumai 3 and was designated as *Fhb2* (Waldron et al., 1999; Shen et al., 2003; Lin et al., 2004; Yang et al., 2005b; Cuthbert et al., 2007; Häberle et al., 2007). Investigations on a Chinese Spring-Sumai 3 chromosome 7A disomic substitution line (CS-Sumai 3-7ADSL) have identified *Fhb7AC* as a novel QTL near the centromere of chromosome 7A (Jayatilake et al., 2011).

The Chinese cv. Wangshuibai was used for QTL mapping and stable QTL were found on the chromosomes 3B, 4B and 5A. Those were the resistance QTL *Fhb4* (on chromosome 4B), the QTL detected on chromosomes 3B which is assumed to be identical or allelic to *Fhb1*, and the chromosome 5A QTL *Qfhs.ifa-5A* (McCartney et al., 2004; Lin et al., 2004; Zhang et al., 2004; Zhou et al., 2004; Ma et al., 2006; Yu et al., 2008; Xue et al., 2011). Recently two further QTL were identified on the chromosome arms 5AS (*Qfhb.rwg-5A.1*) and 5AL (*Qfhb.rwg-5A.2*) of the FHB resistant Spanish wheat accession PI277012. This line has a pedigree of ‘Extremo Sur’/‘Argelino’//T. timopheevii. Both QTL explain up to 20 and 32% of the variation in FHB

severity, respectively and showed major effects on reducing the disease spread and DON accumulation in seeds (Chu et al., 2011). In a 'CM-82036' (resistant)/Remus (susceptible, Table 1) DH population two significant QTL were mapped to chromosomes 3BS (*Fhb1*) and 5A (*Qfhs.ifa-5A*). Using spray inoculations, the effects of both QTL were indistinguishable, but after single floret inoculation *Fhb1* showed a much stronger effect than *Qfhs.ifa-5A* leading to the assumption that *Qfhs.ifa-5A* might contribute more towards type 1 resistance (Buerstmayr et al., 2002, 2003). Recently, in a study on transcriptional differences in near-isogenic lines (NILs) segregating either for *Fhb1* or *Qfhs.ifa-5A* or both QTL, a lipid transfer protein (LTP) was identified as constitutively more abundant in relation to the resistant *Qfhs.ifa-5A* allele (Schweiger et al., 2013).

Generally, the Type 1 resistance against initial infection (Schroeder & Christensen, 1963) has only rarely been observed. The Brazilian cv. Frontana is one of the few genetic sources of a moderate Type 1 resistance to initial fungal infection (Schroeder & Christensen, 1963; Buerstmayr et al., 2009). In cv. Frontana the major QTL for type 1 resistance has been mapped on chromosome 3AL and was found to mediate low FHB incidence and severity (Steiner et al., 2004). Another, but minor effect QTL has been located on chromosome 7AS (Mardi et al., 2006). Berzonsky et al. (2007) found that loci on the cv. Frontana chromosomes 3A, 6A and 4D were responsible for significantly reducing symptoms of FHB. In a recent study it was found that chromosome 3A likely carries a major gene responsible for expressing type 1 resistance. In addition, also Frontana chromosome 4D was found to carry one gene or few genes involved in type 1 resistance, although the effect was less than observed for chromosome 3A (Yabwalo et al., 2011).

Since 1999 more than 200 QTL were identified in different wheat genotypes and were located on all chromosomes, except chromosome 7D. However, only the QTL *Fhb1*, *Qfhs.ifa-5A* and *Fhb2* which all originated from Chinese wheat were found to be stable by explaining 25-60% of the variation in FHB resistance and by providing reliable resistances under different environmental conditions (Buerstmayr et al., 2009). However, poor agronomic performance and the frequent occurrence of genetic linkage drag make them less suitable donors of resistant genes (Lulin et al., 2010).

To overcome knowledge gaps in *Fusarium* resistance research, several transcriptome studies have been conducted to understand the molecular mechanisms behind FHB resistance and to identify resistance related genes. Several genes were shown to be differentially expressed between resistant and susceptible genotypes and therefore, might be involved in the *F.*

graminearum- wheat interactions (Li & Yin, 2008; Jia et al., 2009; Ding et al., 2011; Gottwald et al., 2012; Schweiger et al., 2013; Xiao et al., 2013).

Particularly the signalling pathways mediated by jasmonate (JA) and ethylene (ET) were assumed to play essential roles for the control of FHB resistance in different wheat genotypes with different levels of resistance and geographical origins (cv. Sumai 3: Li & Yin, 2008; cv. Wangshuibai: Ding et al., 2011; cv. Dream: Gottwald et al., 2012). For instance, in the cv. Wangshuibai both JA and ET defence-signalling pathways were supposed to mediate the early basal defences at 12 to 24 h after *F. graminear*um infection. Generally, JA-mediated defense seems to act especially against necrotrophic pathogens (Laluk et al., 2010). In a more recent study of cv. Wangshuibai pathogenesis-related proteins such as PR-5, PR-14 (Table 2), ABC transporter and the JA signaling pathway were found to be crucial for FHB resistance mediated by *Fhb1*. The ET and ROS pathways, however, were not activated and thus, were considered as less relevant (Xiao et al., 2013). An induction of the JA-responsive genes *PR-2, PR-4* and *PR-5* in cv. Sumai 3 after *F. graminearum* inoculation has also been observed in a comparison with two FHB susceptible near-isogenic lines (Golkari et al., 2009).

Comparative analyses of *F. graminearum* interactions in wheat and barley revealed a large set of conserved transcript accumulation patterns which besides ET- and JA-related proteins also include genes that are likely associated with the DON detoxification (Walter et al., 2008; Jia et al., 2009; Karlovsky et al., 2011; Gottwald et al., 2012). Previous studies indicated that the highly DON-inducible barley gene *HvUGT13248*, encoding a glycosyltransferase (Table 2), has the ability to convert DON into the less toxic compound DON-3-glucoside (Schweiger et al., 2010). Also other UDP-glucosyltransferases such as *TaUGT3* (Ma L et al., 2010) (Table 2), and ABC transporter genes such as *TaPDR1* (pleiotropic drug resistance 1) and *TaMDR1* (MDR-like ABC transporter gene Table 2) were reported to act as detoxification genes during wheat spike infections by *F. graminearum* (Sasaki et al., 2002; Shang Y et al., 2009). In addition, different cytochrome P450 genes were found to be involved in defences against fungal pathogens (Kong et al., 2005; Walter et al., 2008). For example, the wheat P450 gene *CYP709C1* (Table 2), which was found to be induced by the stress hormone methyl jasmonate (MeJ), was in response to *Fusarium* pathogens or trichothecene mycotoxins during FHB as well as during Fusarium seedling blight (Li X et al., 2010).

The resistance to kernel infection (Type 2) expressed by Chinese QTL is assumed to be associated with resistance against the accumulation of DON mycotoxin (Type 5), because a suppression of this essential virulence factor would impair the spike colonization by the pathogens (Parry et al., 1995; Bai et al., 2001; Nasri et al., 2006). In case of the gene behind the

QTL *Fhb1*, different concepts have been discussed with regard to its functional role in FHB resistance. First concept stated that *Fhb1* represents either a detoxification gene, for instance the gene *TaUGT3* (Ma L et al., 2010), or a major regulator of DON detoxification (Lemmens et al., 2005). A different concept was suggested that the Fhb1 resistance derived from the wheat genotype Nyubai is mainly associated with cell wall thickening due to deposition of hydroxycinnamic acid amides, phenolic glucosides and flavonoids, but not with the DON detoxification (Gunnaiah et al., 2012). Finally, expression QTL mapping in a Sumai 3/Y1194-06 (susceptible) RIL population by using candidate resistance genes obtained from Sumai 3 transcriptomics (Li & Yen, 2008) has identified *WFhb1_c1* (wheat Fhb1 candidate gene 1, Table 2). This gene was both functionally and physically associated with *Fhb1* and its sequence was found to be weakly similar to an encoding pectin methyl esterase inhibitor gene from *Arabidopsis* (Zhuang et al., 2013). The expression pattern has been described as a relatively slight increase associated with resistance, while susceptibility was associated with a sharp drop of about 20-fold between 8 to 21 hours after flower inoculation (hai). Based on this expression pattern it was stated that Fhb1 could contribute to a delay of FHB spreading by reducing susceptibility rather than increasing FHB resistance. However, studies in our lab on FHB resistance have recently demonstrated that *WFhb1_c1* is in fact strongly up-regulated in cv. Sumai 3, but not in the FHB susceptible cv. Florence-Aurore (Fig. A5). This induction was present specifically at the timepoint 6 hai, a timepoint that has not been investigated by Zhuang et al. (2013).

Finally, to understand the molecular pathogen-host interactions during the FHB pathogenesis is still an indispensable task. Important support for the development of novel FHB management strategies come also from histopathological examinations on the mode of spike infection and colonization processes. These studies have uncovered important yielded relevant timepoints associated with relevant changes in pathogen-host interactions as well as relevant tissues such as rachis nodes which were found to be a critical obstacle in the disease spread towards the infection of hitherto uninfected flowers (Jansen et al., 2005; Brown et al., 2010, 2011). Moreover, the observation that during all phases of *F. graminearum* spike colonization the most advancing hyphae are surrounded by living host cells (Brown et al., 2010) allows to consider approaches in which these cells are enabled to continuously supply antifungal onto the intercellular advancing hyphal tips.

Knowledge on the mode of disease progression allows to precisely direct investigations for combining this knowledge with recent developed technologies such as systems biology combining genomics with ‘omics’ platforms. For instance, studies have demonstrated that non-

target metabolomics is a highly valuable tool to search for resistance- or pathogenesis-related metabolites (Hamzehzarghania *et al.*, 2005; Bollina *et al.*, 2010; Gunnaiah *et al.*, 2012) or biomarkers (Hamzehzarghania *et al.*, 2008).

2.4 Current research status of soil-borne *Fusarium* diseases

In contrast to the floral disease FHB which has been in the focus of *Fusarium* resistance research in the past 40 years, soil-borne *Fusarium* diseases were much less explored. However, the diseases root and crown rot (FRR and FCR) recently became more prevalent and are nowadays considered to account for a substantial part of *Fusarium* infections in wheat (Backhouse et al., 2004; Burgess et al., 2005; Smiley et al., 2005). For two main reasons soil-borne *Fusarium* infections are of increasing importance nowadays also in the temperate agricultural regions of Europe: First, maize growing has constantly increased, particularly within bioenergy crop rotations. Infected stubble of maize, however, is a major source of FRR infestations on wheat (Khonga & Sutton, 1988; Beccari et al., 2011). Second, *Fusarium* diseases in general and their soil-borne diseases in particular can be seen as winners of global warming due to climate change (Chakraborty & Newton, 2011). Particularly, *F. culmorum* and *F. pseudograminearum* were referred to as the major agents for FCR and FRR in cereal crops, while *F. graminearum* was, so far, only sporadically related to these diseases (Sutton, 1982; Paulitz et al., 2002, 2006). Moreover, for a long time root rot has been seen as a dryland disease which mainly occurs in areas with arid and/or mediterranean climate or with sub-optimal growing conditions (Chongo et al., 2000; Backhouse et al., 2002). For example, in Australia yield losses due to FCR can be 25% (Daniel & Simpfendorfer, 2008) and annual losses in wheat can reach $79 millionthis. In Pacific Northwestern of the United States, yield losses of 35% have been documented (Smiley et al., 2005), and global yield losses over 30% have been reported (Poole et al., 2012). In fact, soil-borne fusariosis are meanwhile increasing in all regions of intensive agriculture in Europe, America and in particular the more marginal cereal production areas of Western Asia, Northern Africa, Australia and Canada.

Soil-borne *Fusarium* diseases have specific characteristics which convert common plant protection into an ineffective instrument, and the cultivation of resistant varieties becomes the most promising strategy. In case of root rot *Fusarium* attacks host plants via the infection and colonization of seedling roots. Since roots are the ‘hidden half of plant’ at early disease stages FRR severity remains typically invisible (Li X et al., 2010). Successful root infections lead to rotten roots, diminished nutrient and water uptake, and finally reduced seedling vigour. Consequently, root rot symptoms typically mimics symptoms of nutrient and/or deficiencies. A

successive colonization of distal plant tissues is potentially associated with plant lodging, damage to leaves, interference of water/nutrient translocation and reductions of grain yield and quality, accompanied by the "whitehead" symptom (Strausbaugh et al., 2005; Mitter et al., 2006). FRR is difficult to distinguish from FCR which attacks host plants via the hypocotyl. However, for both diseases successful root colonization is a necessary stage prior to further plant colonization, because roots provide an excellent nutrient supply (Beccari et al., 2011). Thus, in the case of soil-borne *Fusarium* diseases, the roots have to be seen as the critical defense line to prevent further plant colonization and toxin accumulation.

Similar to observations on FHB that DON production enables the fungus to spread from infected florets into the wheat rachis in FHB (Bai GH et al., 2002; Jansen et al., 2005; Maier et al., 2006), the DON toxin seems to be not essential for *F. graminearum* or *F. pseudograminearum* at early infection stages during FCR, but gains in importance during later systemic stem colonization (Mudge et al., 2006). Studies on FCR revealed that trichothecenes can be translocated in the plant tissues in advance of fungal growth following *F. culmorum* infection (Covarelli et al., 2012). In addition, in wheat spikes DON was detected in uninfected cells which are in advance of the *F. culmorum* hyphae (Kang & Buchenauer, 2002). Although there is first evidence that mycotoxins are translocated into wheat spikes, the magnitude and destruction potential of these contaminations is still a matter of discussion (Mudge et al., 2006; Wang et al., 2006). In addition, the translocation of fungal biomass in aerial plant parts is a matter of debates, too. In fact, FCR was characterized by a relatively long symptomless period, followed by massive tissue necrosis and a rapid increase of fungal biomass (Stephens et al., 2008). In a comprehensive study *F. culmorum* and *F. graminearum* was isolated from flag leaf nodes and spike tissue after stem base inoculations. Limited colonization of the vascular tissues occurred at the infection site as well as in the vascular bundles of non-inoculated upper internodes (Mudge et al., 2006). Another study reported that after stem base inoculation *F. culmorum* can extensively colonize stem tissues, but not reach the spikes until plant maturity (Covarelli et al., 2012). Other studies, however, concluded that none of the *Fusarium* species can colonize spikes by this route (Purss, 1971; Burgess et al., 1975; Snijders, 1990; Clement & Parry, 1998; Gèlisse et al., 2006). Differences in environmental factors and the relative aggressiveness of the different *Fusarium* species and strains are probably important reasons for the contrasting results (Diaz & Mercedes, 2012). FCR disease development caused by *F. graminearum* involves three distinct phases of colonization associated with well defined fungal gene expressions (Stephens et al., 2008). The initial infection process showed sequentially penetration of stem base leaf sheaths, and then the fungal systemic colonization by *F. culmorum* and/or *F. graminearum* occurred in distal parts of stem (Beccari et

al., 2011). In comparison with FHB and FCR, only few researches refer to FRR which reveal that *F. culmorum* invaded the rhizodermal layer and cortex but was not seen to colonize the stele (Beccari et al., 2011). In a recent review it was stated that to the author's knowledge no microscopic investigation of root infection by *F. graminearum* has been reported (Kazan et al., 2012).

Until today breeding for FRR/FCR resistance is restricted by limited insights into the *Fusarium*-wheat root pathosystem (Mudge et al., 2006; Wang et al., 2006, Kazan et al., 2012). Particularly, the *F. graminearum*-wheat root pathosystem represented a white spot in the research fields of *Fusarium* diseases and wheat resistances. In addition, roots are the hidden half of a plant and their diseases not only remain typically undetected, but also challenge their assessment and research. Accordingly, only a limited number of wheat cultivars have been screened for their responses to FCR and even fewer for responses to FRR. To date, only few QTL studies have reported QTL conferring FCR resistance. A locus was identified on chromosome 4B near the semi-dwarfing gene Rht1 (Wallwork et al., 2004). Two QTL, which located on chromosome 1DL and 1AL, were detected in breeding line '2-49' (Collard et al., 2005). The study on genotype 'W21MMT20' showed several putative QTLs, but none of them reached to significant levels. The most tow significant QTLs were located on 5D and 2D (Bovill et al., 2006). Two QTLs, designated as Qcrs.cpi-3B on the long arm of chromosome 3B and Qcsr.cpi-4B on chromosome 4B were identified from genotype 'CSCR6' (Ma J et al., 2010). Significant QTL on chromosome 3BL respectively in W21MMT70 and Ernie inherited from CSCR6 was reported (Bovill et al., 2010; Li HB et al., 2010). A single significant QTL inherited from Sunco on chromosome 2B (QCr.usq-2B.2) was identified (Bovill et al., 2010). All of these QTLs studies conducted for FCR adopted either seedling assay (Collard et al., 2005, 2006; Bovill et al., 2006, 2010; Ma J et al., 2009; Li HB et al., 2010) or adult assay (Wallwork et al., 2004). Recent study showed that QTLs for FCR at seedling stage and adult stage were different (Poole et al., 2012). Moreover, quantitative trait loci (QTL) which attributed to FCR and FHB resistances were also different (Wu AB et al., 2005; Tamburic-Ilincic et al., 2009; Li HB et al., 2010). So far, no published researches focus on FRR resistance QTLs identification at seedling and adult stages or comparative study between QTLs of FRR, FCR and FHB.

3 Objectives

Until the presented study, to my knowledge no systematic examination of *F. graminearum* growth patterns in wheat roots and the host-pathogen interaction had been reported. Therefore, information on the Fusarium root rot (FRR) disease was sparse in comparison to the related soil-borne disease crown rot (FCR) and especially head blight (FHB). Hence, the *F. graminearum*-wheat root pathosystem represented a blank area in the field of *Fusarium* diseases of wheat. In general, roots are the hidden half of a plant. Root diseases often remain undetected, and their assessment and research is a challenge. Nowadays, *F. graminearum* has become subject of intensive molecular research. Although molecular tools have been developed to enhance research into virulence determinants of the pathogen, knowledge on mechanisms and strategies of the infection and colonization is still rather limited (e.g. Rittenour & Harris, 2010). Such knowledge is required to effectively apply the molecular tools that are currently available and help to advance our knowledge on *F. graminearum* infection.

The main objective of the present study was a systematic examination on the *F. graminearum*-wheat root interactions. The following tasks were addressed: (1) Establishment of a FRR bioassay considering the specific requirements of a root disease. (2) Characterizing the pathogen action and wheat reaction at seedling and post-seedling plant developmental stages. This task comprised screenings and classification the response of a diverse set of wheat genotypes to FRR, as well as investigations on the ability of *F. graminearum* to infect and colonize wheat roots. (3) Histopathological studies on the mode of *F. graminearum* root infection and colonization. This task also included examinations on fungal strategies in different aerial plant parts. (4) Studies on the potential of *F. graminearum* to spread from the roots to the aerial plant tissues. (5) Analysis of the molecular *F. graminearum*-wheat root interactions based on gene expression using known FHB/DON resistance candidate genes.

Finally, an important task was to identify timepoints and tissues which are critical during the FRR disease as targets for future applications of ‘omics’ technologies to uncover the molecular and metabolic basis of FRR as well as targets for reliable phenotyping for genetics approaches such as QTL mapping and genome wide association studies.

4 Material and methods

4.1 Plant material

The analysed genotype set comprised a diversity set of 12 hexaploid spring and winter wheat cultivars and pre-breeding lines (Table 1). The pedigree of the assembled wheat genotypes was either obtained from the Wheat Pedigree database (http://genbank.vurv.cz/wheat/pedigree/), the International Crop Information System (ICIS version 5.4) (http://www.icis.cgiar.org:8080/index.htm) or provided by the breeding company W. von Borries Eckendorf GmbH & Co. KG, Leopoldshöhe, Germany (WvB). The genotype set represents different geographical origins and the whole spectrum of wheat responses to the floral FHB disease ranging from high resistance to high susceptibility. Information on the respective responses to FHB was obtained from the literature (Badea et al., 2008; Buerstmayer et al., 2009) and from the breeding company WvB. All seed material was kindly provided by WvB.

4.2 Fungal material

Macroconidia of *F. graminearum* isolate 'IFA 65' (IFA, Department for Agrobiotechnology, Tulln, Austria) was grown on synthetic nutrient agar medium 'Spezieller Nährstoffarmer Agar (SNA)' (Leslie et al., 2006) at 20 °C under cool-white and near-UV light illumination. After nine days, macroconidia were collected by washing into 0.02% (v/v) Tween-20 solution. After a filtration of the spore suspension through four layers of cheesecloth, the concentration of macroconidia suspension was determined using a haemocytometer and was adjusted to $5*10^4$ macroconidia ml^{-1}.

4.3 Inoculation, plant cultivation and sampling

Inoculation: For root infections in the seedling stage (FRR seedling testing), wheat seeds were sterilized in 6% sodium hypochlorite for 40 min on a magnetic stirrer and then washed 10 times with distilled water. Subsequently, seeds were sown in autoclaved sand in the climate chamber with a 16 h photoperiod of 22℃/18℃ day/night and 60% humidity until the seedling growth stage, i.e. 1^{st} leaf unfolded, Zadoks scale (Z) 11 according to Zadoks et al. (1974). The seedling roots were inoculated with *F. graminearum* spore suspension as described below. For studies on the *F. graminearum* colonization of aerial plant parts (FRR spread testing) the same procedure has been applied.

Table 1: Origin, pedigree, FHB reactions of spring and winter wheat accessions

Accession	Origin	Pedigree	FHB reaction	Type
Sumai 3	China	Funo/Taiwan-Xiaomai; Jingzhou/Sumai2;	highly resistant	Spring
Ning 7840	China	Avrora/Anhui11(F2)//Sumai3	highly resistant	Spring
Wangshuibai	China	LV-CHN; LV-Suyang; LV-Jiangsu	highly resistant	Spring
Line 1105.16	Germany	Hana/Estica	highly resistant	Winter
Frontana	Brazil	Fronteira/Mentana	resistant	Spring
Tabasco	Germany	ZE 90-2666/LW 86Z099-09//CPB 93-27	intermediate	Winter
Line 1105.13	Germany	unknown, from Romania	intermediate	Winter
Line 172.11*	Germany	Qualibo/ Tommi// Tulsa	intermediate	Winter
Tobak	Germany	Ellvis/ Drifter// Koch	susceptible	Winter
Remus	Germany	Famos/Mexican //Sappo	susceptible	Spring
Florence-Aurore	France	Florence/Aurore	highly susceptible	Spring
Line 162.11	Germany	Tyberius/Opus	highly susceptible	Winter

* since 2014 called Siegfried, under variety registration

For post-seedling root infections (FRR adult plant testing), wheat seeds were sterilized in 6% sodium hypochlorite for 40 min on a magnetic stirrer and then washed 10 times with distilled water. Seeds were sown in a mixture (1:2, v/v) of autoclaved sand and soil (Fruhstorfer Erde, Hawita Gruppe GmbH, Germany) in a climate chamber with a 16h photoperiod of 22℃/18℃ day/night and 60% humidity until early stem elongation stage (2^{nd} detectable node, Z32). The plant roots were inoculated with *F. graminearum* as described below.

Prior to inoculation, plants were carefully removed from the sand or sand/soil mixture to avoid root injury. To guarantee root inoculation, stem parts above the seminal root system were covered by a protective coating made of alufoil. For inoculation, plants were either placed into a small flat tray for seedling roots or in a 250 ml plastic rectangular cup for adult roots (Wächter & Co. Germany), each with 5 ml or 15 ml (5×10^4 macroconidia mL^{-1}) inoculum and were gently shaken for 2 h on a rotary shaker. For control plants mock inoculations were performed with

0.02% (v/v) Tween-20 instead of fungal suspension. Plants were arranged in such a way that only roots came into contact with the respective suspension.

Plant cultivation and sampling: (A) For FRR seedling testing, after root inoculation each five seedlings were planted in a pot (7.5x7.5x8.0 cm) with autoclaved sand and grown in a cultivation room at a 16/8 h day/night rhythm. For successful infection *F. graminearum* requires a temperature in the range of 15-32°C (Sutton, 1982). Hence, the temperature in the culture room was set to constant 20°C. All plants were watered once a week with 250 ml of water and thus, drought stress was avoided. Control plants were grown in autoclaved sand at the same time.

The examined cultivation period comprised eight timepoints evenly distributed throughout the seedling development between the stages first leaf unfolded (Z11) and early tillering (Z21). At the timepoints 0.5, 1, 3, 5, 7, 10, 14 and 21 days after inoculation (dai), 15 plants each were collected per treatment and genotype. The roots of each plant were washed in distilled water, examined for visible symptoms, measured, frozen in liquid nitrogen and finally, stored in -80°C until further use. Three pools of each five plants were sampled: (i) two samples were subjected to DNA extractions and qPCR quantifications of fungal and root biomasses; and (ii) one sample was used for RNA extraction and qPCR gene expression analysis.

(B) For FRR spread testing, after root inoculation each five seedlings were cultivated per pot (11.5x11.5x12 cm) in a 1:2 (v/v) mixture of sterilized silica sand and soil (Fruhstorfer Erde). The examined cultivation period comprised the plant development between seedling (Z13) and flowering stage (Z60-64). Tissue sampling was done at four plant developmental stages: seedling stage (Z13), tillering (Z21-22), stem elongation (Z32) and flowering (Z60-64). The respective sampling strategy is shown in Figure 3. At each developmental stage 10 plants each were collected per treatment and genotype. The respective wheat tissue samples were frozen in liquid nitrogen and finally, stored in -80°C until further use. Roots were washed in distilled water, examined for visible symptoms and prior to sampling. Two pools of each five plants were sampled: (i) one sample was subjected to DNA extraction and qPCR quantification of fungal and root biomass; and (i) one sample was used for quantifications of the mycotoxin deoxynivalenol (DON).

(C) For FRR adult plant testing, after root inoculation a single plant was cultivated per pot (11.5x11.5x12 cm) in a 1:2 (v/v) mixture of sterilized silica sand and soil (Fruhstorfer Erde). The examined cultivation period comprised seven timepoints evenly distributed throughout the plant development between early stem elongation (two nodes, Z32) and flowering (Z60-64). At the timepoints 1, 3, 5, 7, 10, 14 and 21 dai, 15 plants each were collected per treatment and genotype. Sampling at each timepoint was performed as described for FRR seedling testing (A).

For studies which included adult plant developmental stages (B and C), care was taken to grow wheat plants in the greenhouse under optimal conditions to avoid additional environment stress and/or other plant diseases. In case of powdery mildew infestation fungicide applications (0.1-0.2% vol.) with Corbel® (BASF, Limburgerhof, Germany) were done during adult plant stages. The fungicide is not effective against *Fusarium* pathogens and care has been taken that application was two weeks the latest in advance of tissue sampling. Fertilizer applications (1.0% vol.) with Wuxal Super® (NPK 8-8-6; Wilhelm Haug GmbH & Co. KG, Düsseldorf, Germany) were done regularly together with watering (each 250 ml) during the particularly sensitive growth period between stem elongation and flowering.

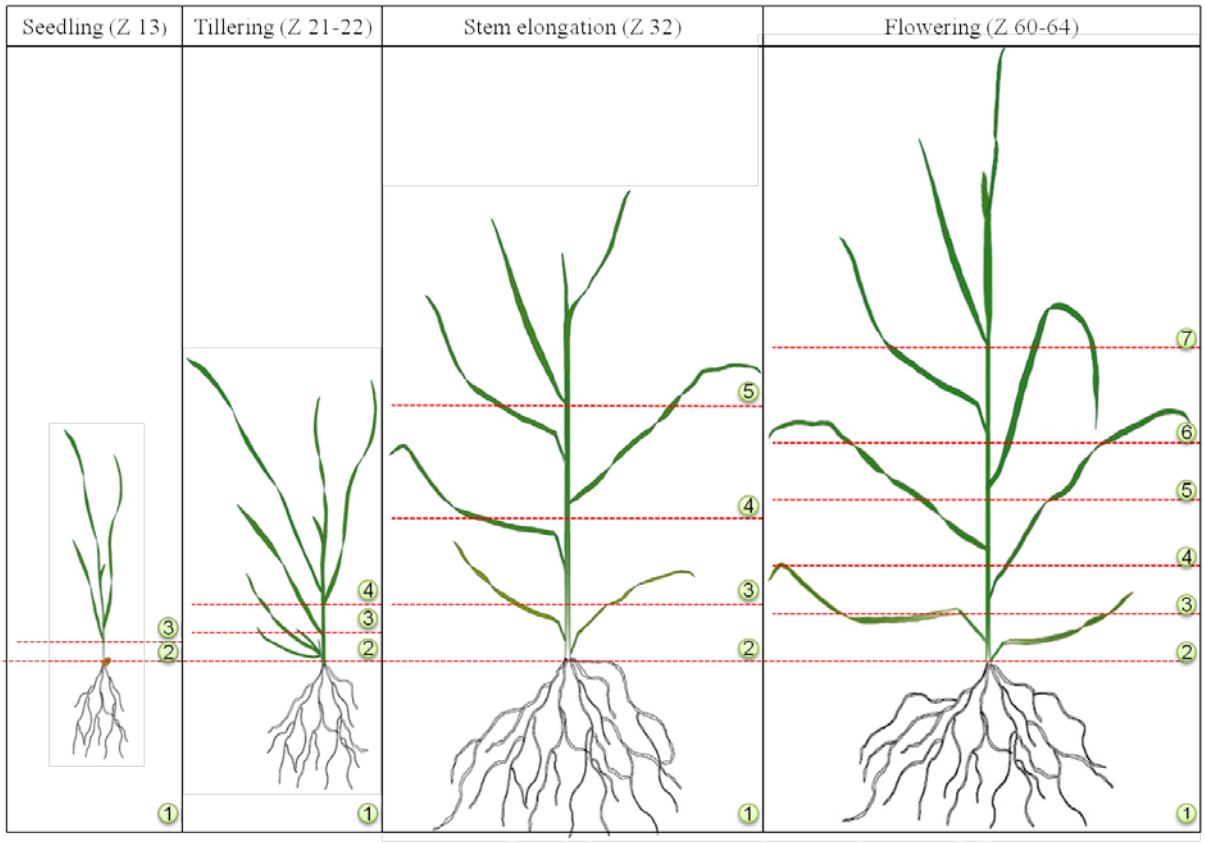

Figure 3: Diagram of wheat tissue selection in four growth stages after seedling root inoculation with *F. graminearum* IFA65. The tissue sampling was done at four plant developmental stages: seedling (Z13), tillering (Z21-22), stem elongation (Z32) and flowering stage (Z60-64). Numbers represent different target zones. 1) entire root; 2) stem base; 3) first to second node & leaflet at first node; 4) second to third node & leaflet at second node; 5) third to fourth node & leaflet at third node; 6) fourth to fifth node & leaflet at fourth node; 7) flag leaf & spike.

4.4 Plant and fungal gDNA extraction

For qPCR quantification of wheat DNA from inoculated and non-inoculated samples of root, leaf, stem and spike tissues gDNA extraction was carried out according to the protocol described by Doyle & Doyle (1990). The total DNA concentration was determined using the NanoDrop ND 1000 (Thermo Fisher Scientific Inc., Waltham, USA). The gDNA of all samples was diluted to a 50 ng/µl work solution. Leaves from young, mock-inoculated control plants were used to produce gDNA as standards for wheat. For the Ubiquitin assay (wheat root DNA), the gDNA of standard curve was diluted into 100, 50, 25, 6.25, 1.5625, 0.39 ng wheat gDNA/µl.

As DNA standard for absolute qPCR-based quantifications of fungal biomass, gDNA was extracted from *F. graminearum* mycelium. Plates with 100 ml potato dextrose broth (PDB) agar were inoculated with $2*10^5$ macroconidia suspension of *F. graminearum* and incubated on a rotary shaker at 28°C for 3 to 5 days. The harvested mycelium was used for fungal gDNA isolation as described by Doyle & Doyle (1990). For establishing the standard curve the gDNA of for the Fg16N assay (*F. graminearum* DNA) was diluted into 50, 10, 5, 1, 0.5, 0.1 ng *F. graminearum* gDNA/µl.

4.5 Plant RNA extraction and cDNA synthesis

RNA extraction: Prior to RNA extractions root material was crushed under liquid nitrogen. The RNA extraction from root material was conducted by using the guanidinium thiocyanate-phenol-method (Chomczynski et al., 1987). RNA samples were purified according to Sambrook et al., (1989). Finally each RNA pellet was resuspended in 50 µl Milli-Q water and RNA concentration was measured on NanoDrop ND 1000 (Thermo Fisher Scientific Inc.), and the RNA quality was checked by using 1% agarose gel electrophoresis.

In order to remove DNA from the samples `DNase I RNase free´ from Fermentas (Fermentas Life Sciences, Germany) was used. The samples were filled to a final volume of 60 µl with Milli-Q water and 1µl DNase I and 6 µl 10 x buffers were added. Samples were incubated at 37°C for 30 minutes. Afterwards an aliquote was used for cDNA synthesis.

cDNA synthesis: The cDNA synthesis was done by using RevertAidTM H Minus First Strand cDNA Synthesis Kit (Fermentas Life Sciences, Darmstadt Germany). Finally the prepared cDNA was kept at -20°C until use.

4.6 Fusarium root rot bioassay

4.6.1 Quantitative real time PCR (qPCR) for wheat root and *F. graminearum* biomass quantifications

Primer selection and testing: The qPCR analyses were performed by using a 7500 Fast Real-Time PCR System (Applied Biosystems, Darmstadt, USA). In this study the plant and fungal external standard dilution series (chapter 4.3) were tested for the amplification efficiency of primer Ubiquit and Fg16N (Table 2) as well as the correlation between Ct value and DNA concentration. Each reaction mix contained 1 µl template gDNA, 5 µl Roche FastStart Universal SYBR Green Master (Roche Diagnostics GmbH, Mannheim, Germany), 2 µl sterile water, and 1 µl forward and inverse primer (10 pmol/µl) each; reactions were run in triplicate. Melting curves were analyzed using Dissociation Curves Software (Applied Biosystems) to ensure that only a single product was amplified; 90%-110% amplification efficiency can be accepted by adjusting the reaction system (Bustin & Nolan, 2009).

The PCR was performed according to the following cycling protocol. Initial denaturation was done for 1.5 min at 95°C, followed by 35 cycles with 30 s at 94°C, 45 s at 64°C, and 45 s at 72°C. The final elongation was performed for 5 min at 72°C. Fluorescence was determined during the annealing step of each cycle. After amplifications, the melting curves were acquired by heating the samples to 95°C for 1 min, cooling to 55°C for 1 min and then slowly increasing the temperature from 65°C to 95°C at the rate of 0.5°C 10 s^{-1}, with continuous measurement of the fluorescence.

Relative fungal biomass (RFB) assessment: The relative fungal biomass (RFB) in roots was measured at each timepoint by qPCR analysis as the ratio between fungal DNA quantity and wheat DNA quantity. To quantify the fungal DNA, the *F. graminearum* specific 280bp gDNA fragment Fg16NF was used (Nicholson et al., 1998). An external standard calibration was generated by analyzing dilution series (50, 10, 5, 1, 0.5, 0.1 ng *F. graminearum* DNA/µL) of DNA from pure fungal cultures (chapter 4.3). The wheat ubiquitin gene was used for quantification of wheat root DNA. An external standard calibration was generated by analyzing dilution series (100, 50, 25, 6.25, 1.5625, 0.39 ng wheat DNA/µL) of DNA from wheat leaves. qPCR was conducted according to the same cycling protocol as described above.

Based on the obtained C_T values the average amount of *Fusarium* and wheat root DNA was calculated for each technical repetition. According to Brunner et al. (2006), the C_T values of the standard dilution series were plotted against the natural logarithm of the DNA concentration. With the gradient equation ($f(x) = ax + b$) of the standard curve the total amount of wheat DNA and fungal DNA was calculated according to the following formula, in which C_T is the

crossing threshold: $DNA\,(ng) = 10\text{^}\frac{(C_T - b)}{a}$. The RFB was calculated according to the following formula 1 (Brunner et al., 2009):

$$Relative\ fungal\ biomass\ (RFB) = \frac{Fusarium\ DNA(ng)}{Total\ DNA(ng)} * 100$$

where total DNA = *Fusarium* DNA+ wheat DNA. Finally, the infection percentage of the cultivars for each timepoint was calculated as the average of the four values (two pools, each repeated twice).

4.6.2 Root and shoot length assessments

At each measurement timepoint wheat plant responses to FRR were measured as relative reductions in root length (RLR) and shoot length (SLR). Root and shoot length measurements were performed for each 15 *F. graminearum* or mock inoculated plants per genotype and timepoint. In order to remove the effect of genetic variation in seedling and root growth which has to be expected in a diverse set of wheat genotypes, relative reductions were calculated as the ratio between trait expression under FRR and trait expression in healthy plants. The same approach was applied to the studies on FRR after seedling and adult root inoculations.

4.6.3 Visible symptom assessments

Visible symptom development was rated as root symptom index (RSI) and stem base symptom index (SbSI), respectively. The RSI was used to rate symptom appearance on seminal roots and the SbSI was used to rate symptom appearance on the seedling stem part between the root-stem-junction and the first leaf node. Visible symptoms on roots and stem bases of 15 plants per genotype were assessed at each timepoint using two parameters: browning and symptom extension based on a five point scale.

The browning scale ranged from 0 to 4 (0, symptomless; 1, slightly necrotic; 2, moderately necrotic; 3, severely necrotic; 4, completely necrotic). The extension (length of necrotic discoloration) scale ranged from: 0, no lesions; 1, 1-24%; 2, 24-49%; 3, 50-75%; 4, >75% of roots/stem bases. Finally, a genotype-timepoint-specific root and stem base symptom index (RSI and SbSI) was calculated using the equation: RSI/SbSI = $\sum$B1$\cdots$BN/N + $\sum$E1$\cdots$EN/N; where B and E each represent the parameter browning and extension index, and N the number of assessed individuals (according to Piccinni et al., 2000). In this study, the stem base was referred to sub-crown and first stem internode.

4.7 Microscopic examinations

4.7.1 Sampling and tissue section preparation

To investigate the systematic colonization development of *F. graminearum* in wheat, primary root, stem and leaf blades from infected and water control wheat plants were taken 0.5,1, 3, 5, 7, 10, 14, 21 and 28 dai for histopathological analysis.

Wheat seedling roots were incubated in a mixed chloroform, 96% ethanol and trichloroacetic acid solution (1:4:0.15%) for fixation. If not used immediately, tissues were kept in the fixation solution at 4°C until analysis. Root cross sections were prepared by hand-sectioning from root tissues fixed in a polystyrene block. Subsequently, root sections were placed on glass slides (VWR International, Darmstadt, Germany) with water and covered by a cover slide.

Fresh stem and leaf tissues were frozen in a metal mold with 4% (w/v) CMC (Carboxymethyl cellulose sodium salt , Sigma Life Science, location, USA) solution by immerging the mold into a coolant mixer (hexane and dry ice). The obtained CMC block was used to obtain cross sections of 20 µm thickness by using a cryrostat (HM 525 cryostat, Thermo Scientific, Dreieich, Germany). The embedding material was carefully removed with a painting brush preventing the distortion of tissue. Then the section was thaw mounted on a microscope glass slide. After adding one-two drop/s of water the sample was covered with a cover slide. All glass slides were stored in a plastic box at 4℃ to keep humidity until analysis.

4.7.2 WGA Alexa Fluor 488® and Typan blue staining

To visualize internal hyphae, root and plant tissues were stained by using a WGA (Wheat Germ Agglutinin) Alexa Fluor 488® conjugate (Invitrogen, Life technologies, Darmstadt, Germany) solution in 1*PBS (pH 7.4) for 20 min at room temperature. Finally, tissues were washed twice by using double distilled water.

To investigate external fungal structures on root surfaces, root tissues were stained with a 0.1% (w/v) typan blue solution (Fluka analytical) in 10% (v/v) acetic acid for 20 min at room temperature. Finally, tissues were washed twice by using double distilled water.

4.7.3 Bright-field and fluorescence microscopy

Bright-field and fluorescence microscope studies in inoculated vs. non-inoculated roots were conducted in three biological replications, each with five different plants per treatment and timepoint. Non-infected roots were used to test for the absence/presence of *F. graminearum* and other possible fungal hyphae. Bright-field microscopy was done with transmitted light using a ‘Zeiss Axioplan 2 imaging and Axiophot 2’ microscope equipped with a Zeiss Apotome to

observe typan blue stained *F. graminearum* hyphae and infection structures. Fluorescence microscopy was done by using the above mentioned microscope with the same equipment to observe WGA Alexa Fluor® stained fungal hyphae and infection structures. A UV lamp HAL 100 served as UV light source. GFP was excited with 480 to 500 nm and detected at 510 to 530 nm wavelength. Images were taken with Zeiss Axio Cam MRm CCD camera. Images were processed with Zeiss Axio Vision software (version 4.8.1).

4.7.4 Confocal laser scanning microscopy

Inoculated and non-inoculated plant tissues (roots, stem base, stem, leaf blades) were analyzed under a Leica TCS SP2 microscope (Leica Microsystems, Heidelberg, Germany) after WGA Alexa Fluor® 488 staining. WGA was excited by the 488-nm line of the argon/krypton laser (Omnichrome, Chino, CA). For observation at the 510 nm wavelength and the autofluorescence detection wavelength of 550–650 nm, a long pass filter was used. Digital images were processed with Adobe Photoshop to optimize brightness, contrast, and colour and to enable an overlay of the photomicrographs. The same procedure was also used for non-inoculated (control) roots. [Spectral data were collected by excitation with 488 nm Argon Ion Laser and by using a GFP specific detection window (500–530 nm) and an autofluorescence detection wavelength of 550–650 nm. Confocal image overlays of the two channels were obtained by using IMAGEJ version 1.410 (Collins, 2007).]

4.8 Deoxynivalenol (DON) quantifications in wheat tissues

Tissue was sampled at four plant developmental stages: seedling stage (Z13), tillering (Z21-22), stem elongation (Z32) and flowering (Z60-64). The respective sampling strategy is shown in Figure 3. Plant generation, sampling and tissue handling were as described in chapter 4.3.

No previous knowledge on possible DON accumulations in root tissues was available at the beginning of this case study, Ridascreen Fast DON kit (R-Biopharm AG, Darmstadt, Germany) was chosen with a relatively low limit of DON detection at < 0.2 mg/kg (ppm) and a maximum limit at 6.0 mg/kg (ppm), defined by DON standard solutions. Only small quantities of seedling root tissue samples were available, particularly from FRR infected seedling roots (< 5g), the minimum sample amount recommended by the manufacturer. Therefore, the manufacturer's protocol was modified and the following procedure was used. All samples were weighed, ground in liquid nitrogen and then a solution of acetonitrile and water (86/14, v/v, and 15-fold sample volume) was added. The mixtures were shaken for 1.5 h and then the extract was filtered. Afterwards, samples were subjected to a vacuum centrifuge drying in a freeze dryer system

(Thermo scientific, Darmstadt, Germany), and dissolved in distilled water (20-fold sample weight). Each sample was present in three repeats per ELISA plate. The mycotoxin DON was detected and quantified in the plant tissues samples on a Tecon Sunrize 96 well microplate reader (Tecan GmbH, Crailsheim, Germany). Finally, the DON concentration (ppm) was calculated by Rida Soft Win (R-Biopharm AG, Darmstadt, Germany).

4.9 Gene expression analyses

Primer selection and testing: qPCR was performed by using an ABI Step One Plus real-time PCR system (Applied Biosystems). In this study FHB resistance related primers were used which have been described earlier. The individual primers for the target and reference genes are show in Table 2. The amplification efficiency of primer and the correlation between Ct value and cDNA concentration were tested to quantify the of gene expression. From each genotype 7 dai and 21 dai infected samples were diluted to 1:8, 1:80, 1:800 and 1:8000. For each primer pair q-PCR was performed in an ABI Step One Plus real-time PCR system (Applied Biosystems). For each reaction 1µL template cDNA was mixed with 5µL Roche FastStart Universal SYBR Green Master (Roche Diagnostics GmbH, Mannheim, Germany), 3µl sterile water, forward and inverse primer 1µl (each 10pmol/µl). Each reaction was run in triplicate. Melting curves were analyzed using Dissociation Curves Software (Applied Biosystems) to ensure that only a single product was amplified. Ubiquitin was used as an endogenous reference; 90%-110% amplification efficiency can be accepted by adjusting the reaction system (Bustin & Nolan, 2009).

PCR was performed according to the following cycling protocol. Initial denaturation for 10 min at 94°C was followed by 44 cycles with 45 s at 94°C, 45 s at 60°C, and 45 s at 72°C. The final elongation was executed for 5 min at 72°C. Fluorescence was determined during the annealing step of each cycle. Following amplification, the melting curves were acquired by heating the samples to 95°C for 15 sec, cooling to 60°C for 1 min and then slowly increasing the temperature from 60°C to 95°C at a rate of 0.5°C 10 s^{-1}, with continuous measurement of the fluorescence, cooling to 60°C for 15 sec.

Gene expression analysis: Gene expression was measured by qPCR under the same conditions described above. The cDNA working solutions consist of a 1:10 diluted stock solution. All cDNA of infected and control plants for all investigated timpoints of each genotype were present in triplicate on one qPCR plate. Moreover, data of the target and reference gene were collected from the same qPCR run to avoid distortions. To compare the relative change in gene expression between infected and control samples the $2^{-\Delta\Delta C}{}_{T}$ method was used (Livak & Schmittgen, 2001).

4.10 Data analyses

The FRR disease index: As a benchmarking of wheat seedling and adult plant responses to *F. graminearum* root infections a FRR disease index (FDI) has been developed that combines information from different FRR severity traits. For the study on FRR after seedling root inoculation FDI incorporated besides the relative fungal biomass (RFB), the relevant severity traits root biomass (RBR), root length (RLR) and shoot length (SLR) reductions as well as root symptom (RSI) severity.

All values were beforehand transferred into dimensionless susceptibility index (SI) values to allow a direct comparison between different types of values (ratio and score values). Moreover, SI values also allow removing environment effects on variations in the scored traits coming from different test environments during seedling/plant evaluations. SI values were calculated using the equation: SI = (XTx) / (Y); where X represents the parameters RFB, RBR, RLR, SLR, RSI, CSI for each genotype and sampling timepoint (Tx) and Y the corresponding mean calculated over all wheat germplasms and timepoints.

For the calculation of FDI only RBR, RLR and SLR data with statistically significant treatment effects were considered and generally, all traits were handled with equal valence: $FDI = \sum RFB^{SI}$, RBR^{SI}, RLR^{SI}, SLR^{SI}, RSI^{SI}. In these terms lower FDI is considered synonymous with higher resistance or tolerance against FRR. For the study on FRR after adult root inoculation, the FDI was calculated in the same way, but with the difference that the trait RSI could not be incorporated.

Statistical analyses: All statistical analyses were performed by using the software SPSS 20 for Windows (IBM SPSS Statistics 20; IBM Corp., USA). All statistical tests mentioned in the following were applied to FRR studies performed for seedling and adult plant developmental stages.

Treatment effects were statistically tested by one-way ANOVA. As the homogeneity of variance was not given for all data (Levene's test), the one-way ANOVA was complemented by the Welch's t-test and the Kruskal-Wallis one-way ANOVA. A significant difference was assumed if confirmed by all three tests. Treatment effects were tested for each timepoint and genotype. ANOVA statistics has been performed for the traits: wheat root biomass (quantified by qPCR and by dry and fresh weight), root length and shoot length.

Genotypic mean values for relative fungal biomass and FDI were tested for significant differences by using the nonparametric Mann-Whitney U-test, which does not require the assumption of normally distributed values. Genotype-specific RFB and FDI values measured at

each of the eight timepoints were handled as independent samples and were each subjected to pairwise comparisons to test for significant differences between the respective medians.

Since FRR examinations were performed as time-course studies and even an ANOVA analysis of treatment effects at each time point does not make statistical comparisons among times, all available FRR severity data were also subjected to repeated measures ANOVA (rANOVA). In all used rANOVA models the following aspects were considered likewise. Since the Mauchly's test for sphericity violated the equality assumption for most data, a Greenhouse-Geisser correction was applied to adjust the degrees of freedom appropriately. For multiple comparisons the Bonferroni adjustment (correction for Type I error) was applied for p-values and confidence intervals. Where the rANOVA revealed significant ʻTimeʼ effects or ʻTime × Genotypeʼ interactions, the respective pairwise comparisons tables of treatment group means were considered for interpretation. The mean profile plots (estimated marginal means) were applied to interpret significant time × treatment interactions for the developmental traits root biomass, root length, and shoot length measured (inoculated vs. non-inoculated wheat seedlings). In case of significant effects or interactions, the trend analysis table was considered to determine the degree of change across examined timepoints, respectively whether the relationship between time and measurement data (fungal biomass, reductions in root biomass, root and shoot length, visible symptom developments) fits linear or non-linear trend. The rANOVA was performed by using three different models:

(I) Two-way rANOVA has been performed to test for significant ʻTreatmentʼ and ʻTimeʼ effects as well as for significant ʻTreatment × Timeʼ interactions in the measurment means of the developmental traits root biomass, root length and shoot length. This design included all 12 wheat genotypes in case of seedling and the four genotypes in case of adult plants; the within-subjects factors ‘Time’ [independent factor with eight (FRR seedling testing) and seven (FRR adult plant testing) levels, respectively sampling timepoints], and ‘Treatment’ [independent factor with two levels, FRR inoculated vs. non-inoculated]. For the traits root length and shoot length each ‘Treatment’ level comprised measurements of 14 individual plants, and for the trait root biomass each level comprises four repeated qPCR measurements, each sampling included five individual plants. Thus, the assumption of equal sample level sizes was given for each trait.

(II) Mixed rANOVA was performed to test for significant ʻTimeʼ effects and ʻTime × Genotypeʼ interactions in the FRR disease progression in terms of fungal growth, reduction in seedling root and shoot biomass, and visible symptom development. This design considered all 12 wheat genotypes in case of seedling and the four genotypes in case of adult plants; the within-subjects factor ‘Time’ (as described for model I) and the between-subjects factor ‘Genotype’ (with 12

(FRR seedling testings) and four (FRR adult plant testing) wheat genotypes). This design allowed testing significant effects and interactions for the dependent variables RFB, RBR, RLR, SLR, RSI and CSI. For the traits RBR, RLR, SLR, RSI and SbSI each 'Treatment' level comprised measurements of 14 individual plants, and for the traits RFB and RBR each level comprises four repeated qPCR measurements, each sampling included five individual plants. Thus, the assumption of equal sample level sizes was given for each trait.

(III) One-way rANOVA was performed to test for significant 'Time' effects and 'trends (linear or non-linear)' in the FRR disease progression by taking into consideration three categories of FRR severity (different responses to FRR): partial resistance (cv. Florence-Aurore; Line 162.11); susceptibility (cv. Tabasco; cv. Wangshuibai; cv. Remus; Line 1105.13; Line 172.11), and high susceptibility (cv. Frontana; cv. Tobak; cv. Ning 7840; Line 1105.11). The 'category rANOVA' was applied on mean disease ratings for wheat genotypes assembled to the three three categories of FRR severity, and included the within-subjects factor 'Time' (as described for model I), because genotype effects were anticipated by testing each category separately. In this design was applied to the dependent variables RFB, RBR, RLR, SLR, RSI and SbSI.

Table 2: Nucleotide sequences of the primers used for qRT-PCR.

Annotated functions	GenBank ID	Primers	Reference
Ubiquitin	Ta28553.1	F: CCCTGGAGGTGGAGTCATCTGA R: GCGGCCATCCTCAAGCTGCTTA	(Gottwald et al., 2012)
Fg16N		F: ACAGATGACAAGATTCAGGCACA R: TTCTTTGACATCTGTTCAACCCA	(Nicholson et Al., 2008)
Fusarium-induced detoxification			
Cytochrome P450 (CYP709C1)	AY641449	F:TGGCATCAAAGTGACCGAAGG R:GGCCCACTGGAGAAAGACAAT	(Li et al., 2010a)
UDP-glucosyltransferase protein (TaUGT3)	FJ236328	F: GTTCGAGGAGCGTGTCAAAG R: ACCTGCACAAGATGCCCTCTA	(Gottwald et al., 2012)
UDP-glucosyltransferase (HvUGT13248)	BQ281752	F: TCTTGTGGGTATTCCGCATT R: CCTTTTGCATCCACTTCACA	(Gottwald et al., 2012)
MDR-like ABCtransporter (TaMDR1)	AB055077	F: CTTTCGCTACCCTGCAAGAC R: GCCGATCTTCCCTCTTATCC	(Gottwald et al., 2012)
JA-mediated defence			
Lipoxygenase (Lox-2)	CK152466	F: CCAGAGTGCCATAGTCCTTG R: TCTCCCTTGTCCTCTCCTTG	(Zhuang et al., 2013)
Coronatine Insensitive1 (COI1)	Unigene 29682	F: CCTTTGGCAAGAACCGTATC R: ATCAAAGCACGGAGCAACTT	(Xiao J et al., 2013)
MYC2	TaAffx.65732.1.A1_at[1)]	F:TAACCTTTGGACGGCTATATGACC R:TGCAGGAAGAGGAAGGATATATGTG	(Gottwald et al., 2012)
Jasmonate ZIM domain (JAZ)	Unigene 51573	F:CCGTAGCACGGTCTTACCAT R:ATATGAGGCGAGCAACTTGG	(Xiao J et al., 2013)
Vacuolar defense Proteins (PR-4)	CA692789	F: AAGATCAACTGGGACCTCAAC R: GCCAGGCGTACGACATG	(Zhuang et al., 2013)
non-specific lipid transfer proteins (PR-14)	Unigene 17832	F: AGCGGCGTTAGGAGTCTAGC R: TGCTCGATCAGCGAATCTTA	(Xiao J et al., 2013)
Miscellaneous			
C2H2 zinc finger protein (WZF-1)	D16416	F: ACCCAAGCAACCACACTC R: CATGGCAGTCACAAACGAAG	(Zhuang et al., 2013)
WFhb1-C1	CA640991	F: AGGAGGCGCTGTCTGAATCTAT R: GCCCCAGCATACAGTTGAAAC	(Zhuang et al., 2013)

[1)] Affymetrix ID

5 Results

5.1 Examinations of root rot severity and *F. graminearum*-wheat seedling root interactions

5.1.1 Assessment of relative fungal biomass accumulations in wheat seedling roots

The progression of *F. graminearum* biomass accumulation in the roots of wheat seedlings is a critical aspect since it allows fundamental insides into the hidden pathogen-plant interactions by uncovering (i) the general capability of the pathogen to infect seedling roots and its aggressiveness during root invasion, as well as (ii) the spectrum and degree of wheat responses to pathogen infection and accumulation. RFB was referred to as the quantity of a seedling root that is affected by the disease and has been assessed in a time-course study comprising eight timepoints evenly distributed throughout the seedling stage.

For all 12 wheat genotypes the established qPCR assay revealed a successful *F. graminearum* root infection and invasion already at the early evaluation between 0.5 to 1 dai (Fig. 4a-c, 5a-c). The exceptionalness presence of the pathogen in the root tissues confirms both, the general capacity of *F. graminearum* to penetrate seedling roots and the absence of wheat resistance to initial root infection. The further progression of fungal hyphae accumulation, however, uncovered differences between the wheat genotypes which indicates differential *F. graminearum*-wheat interactions in response to successful root infection (Fig. 4a-c, 5a-c).

The repeated measures ANOVA (rANOVA) was applied in a mixed design on the *F. graminearum* development which included the within-subjects factor ‘Time’ (mean RFB levels of 12 wheat genotypes for each of the eight timpoints) and the between-subjects factor ‘Genotype’. A strong, significant effect of ‘Time’ ($p < 0.001$) has been observed for the fungal growth in seedling roots (Table 3) which confirms the observed developmental changes over time (Fig. 4a-c, 5a-c). However, the pathogen did not develop with the same level and time pattern in all tested genotypes which is demonstrated by the significant ‘Time × Genotype’ interaction (Table 3). Since the significance of this interaction ($p < 0.001$) shows that the factor genotype had an influence on the fungal development during the examined time-course, it was reasonable to assume the presence of a genotypic variation in the *F. gramiearum*-wheat root interactions within the tested wheat set. The post-hoc pairwise comparisons provided by rANOVA indicated a genotype variation that was characterized by three groups defined by Florence-Aurore and Line 162.11 with minim, and Tobak, Ning 7840 and Line 1105.16 with maximum mean accumulations in roots.

To further dissect this variation and to allow a direct comparison of fungal biomass accumulations between the 12 wheat genotypes, the respective mean RFB values across all

Figure 4: Time-course assessment of *F. graminearum*-wheat root interaction

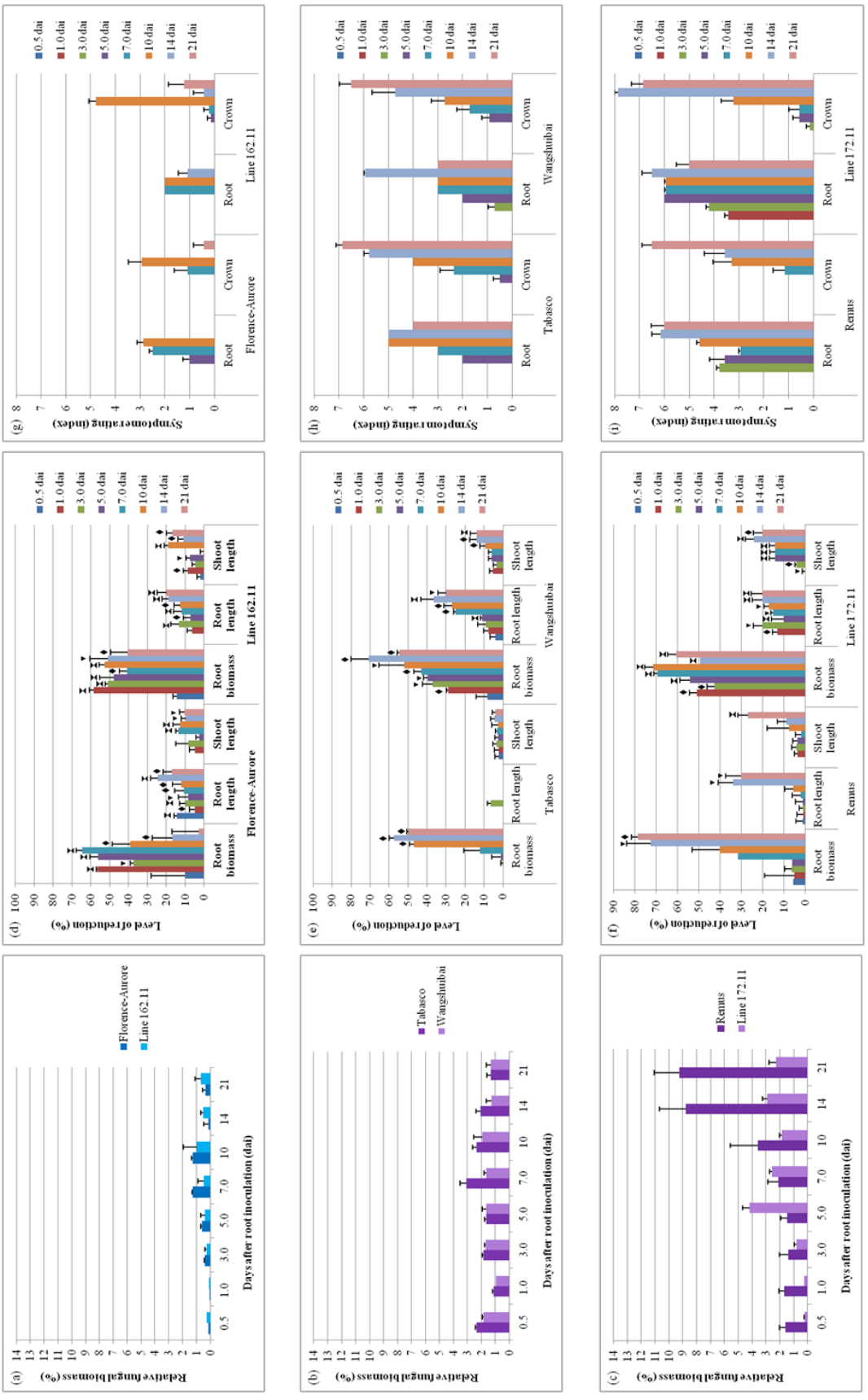

Figure 4: Time-course assessment of *F. graminearum*-wheat root interaction in seedlings of cv. Florence-Aurore, pre-breeding line 162.11, cv. Tabasco, cv. Wangshuibai, cv. Remus and pre-breeding line 172.11. (a-c) Relative fungal biomass (RFB) measured by quantitative qPCR. The RFB was estimated as ratio between fungal and wheat root DNA. (d-f) FRR impact on root and plant biomass. Relative reduction of root biomass (RBR), root length (RLR) and shoot length (SLR) was estimated as respective ratio between trait expression under FRR and under healthy conditions. Treatment differences were tested for significance per genotype and timepoint using one-way ANOVA complemented by a Welch's t-test and the Kruskal-Wallis one-way ANOVA. In the case of significant differences the levels are given as symbols above the bar graphs: inverted triangle, $p \leq 0.05$; rhombus, $p \leq 0.01$; hourglass, $p \leq 0.001$). (g-i) Visible symptom developments on roots (RS) and crowns (CS). Symptoms were rated using a four point scale each for a browning and the symptom extension index, finally allowing a disease rating between 0 (no symptom) and 8 (severe necrosis on >75% of root/crown). In each diagram the error indicator represents the average standard error of the mean (SEM).

timepoints were ranked in an ascending order (Fig. 6). This benchmarking revealed a spectrum of mean RFB values ranching from 17.3% to 0.45% fungal biomass accumulation in wheat seedling roots. The genotypes Florence-Aurore and Line 162.11 showed the lowest RFB values, while cv. Ning 7840 and pre-breeding Line 1105. 16 had the highest ranks.

To test whether the obtained RFB ranking yield differential groups of wheat responses which could serve as first characterization of pathogen-host interactions, the nonparametric Mann-Whitney U-test has been applied. Based on these statistics, the wheat genotypes were assigned into three groups (a, b, c) which are illustrated by the different coloured bars in Figure 6.

No significant differences in the fungal accumulation were found between the cv. Florence-Aurore and Line 162.11, both characterized by minimum RFB values with an average of 0.5% (group a). In this group the amplitude of RFB values remained nearly constant over time with a maximum at 1.27% fungal biomass observed for cv. Florence-Aurore at 10 dai (Fig. 4a), indicating a significantly impaired fungal accumulation in the roots of these genotypes. The genotypes Tobak, Ning 7840 and Line 1105.16 (group c) were representing the opposite end of the ranking with the average of 10.2% fungal accumulation in roots (Fig. 6). With 36.7% the highest inoculum load was obtained in this group, measured in the roots of pre-breeding Line 1105.16 at the timepoint 21 dai (Fig. 5c). The seven remaining genotypes (group b) had intermediate RFB values with an average of 2.2% (Fig. 6). Typical representatives of group b are cv. Sumai 3 (mean RFB 1.4%) and cv. Remus (mean RFB 3.7%).

Considering that partial resistance is mainly characterized by a quantitative limitation of pathogen growth, the terms relative partial resistance (group a) and relative high susceptibility (group c) were used to denote the opposite ends of the RFB ranking scale. Different levels of

Figure 5: Time-course assessment of *F. graminearum*-wheat root interaction

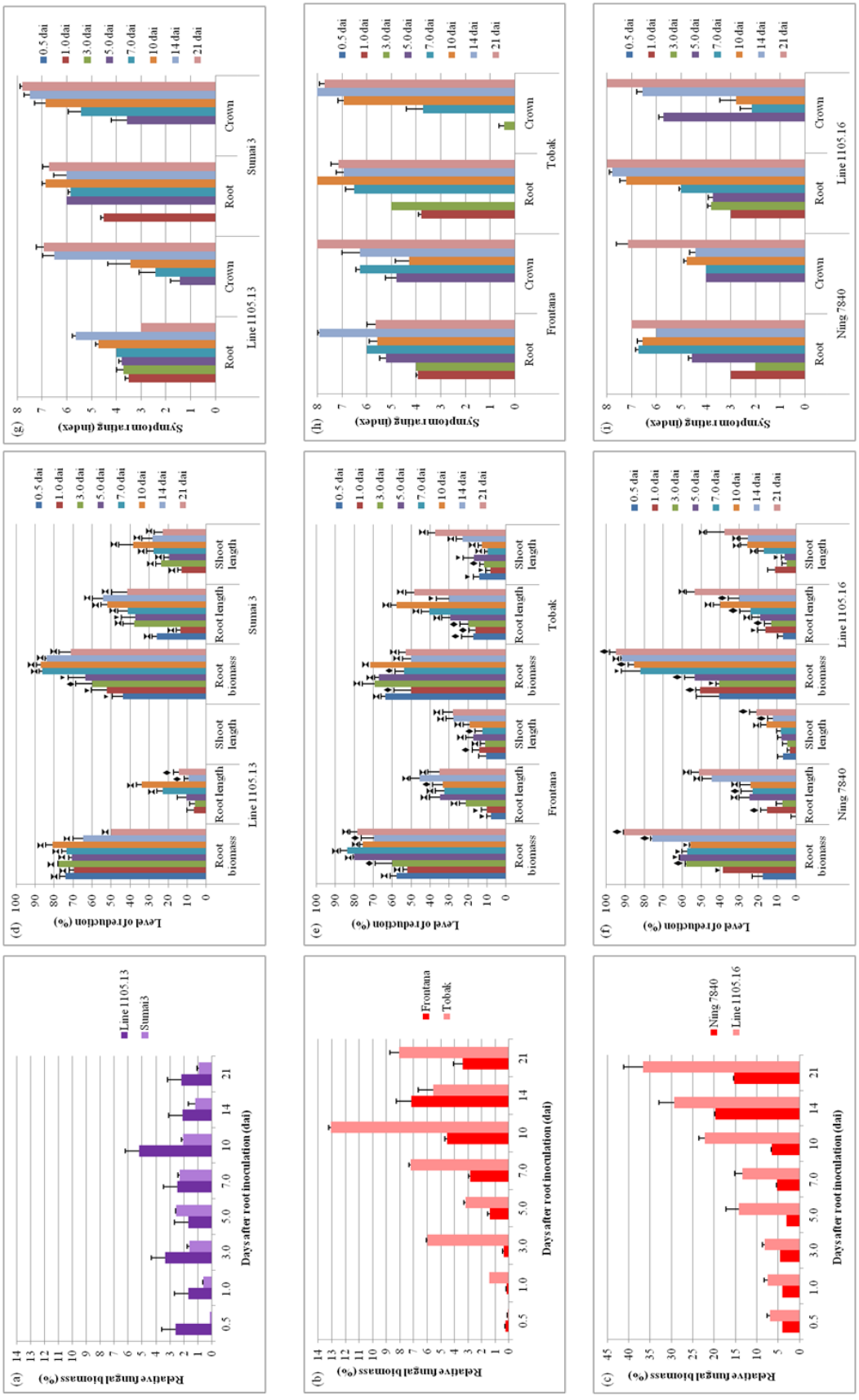

Figure 5: Time-course assessment of *F. graminearum*-wheat root interaction in seedlings of pre-breeding line 1105.13, cv. Sumai 3, cv. Frontana, cv. Tobak, cv. Ning 7840 and pre-breeding line 1105.16. (a-c) Relative fungal biomass (RFB) estimated by quantitative qPCR. RFB was estimated as ratio between fungal and wheat root DNA. (d-f) FRR impact on root and plant biomass. Relative reduction of root biomass (RBR), root length (RLR) and shoot length (SLR) was estimated as respective ratio between trait expression under FRR and under healthy conditions, respectively. Treatment differences were tested for significance per genotype and timepoint using one-way ANOVA complemented by a Welch's t-test and the Kruskal-Wallis one-way ANOVA. In the case of significant differences the levels are given as symbols above the bar graphs: inverted triangle, $p \leq 0.05$; rhombus, $p \leq 0.01$; hourglass, $p \leq 0.001$). (g-i) Visible symptom developments on roots (RS) and crowns (CS). Symptoms were rated using a four point scale each for a browning and the symptom extension index, finally allowing a disease rating between 0 (no symptom) and 8 (severe necrosis on >75% of root/crown). In each diagram the error indicator represents the average standard error of the mean (SEM).

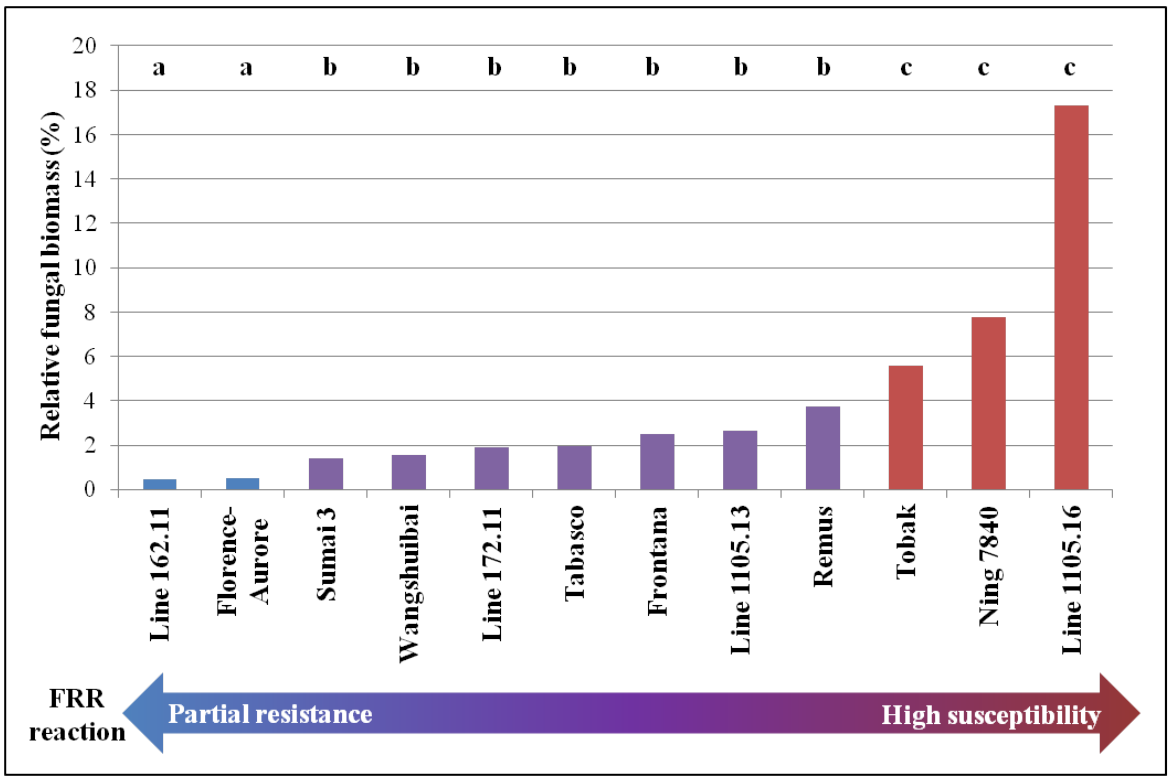

Figure 6: Fusarium root rot severity ranking based on increasing relative fungal biomass (RFB) values per genotype. Wheat genotypes are ranked according to mean values of RFB (ratio between fungal DNA and wheat root DNA) over a time period between 0.5 to 21 days after root inoculation. The observed FRR measures show a range of severity from partial resistance to high susceptibility. The significant grouping of wheat genotypes into the severity categories I-III is displayed by different bar colours. Grouping is based on pairwise comparisons of mean RFB values by using the Mann-Whitney-U-Test. Details on the RFB progressions over the time-course are given in the Figures 4 and 5.

susceptibility were assembled in the intermediate group b. Although, genotype classifications were at this point relative in terms of RFB ranking, for reasons of brevity the terms “partially resistant”, “susceptible” and “highly susceptible” will be used hereafter to denote the three groups. That this three groups, in fact, not only represent different pattern of *F. graminearum* development, but also different pattern in the severity and progression of FRR disease will be demonstrated subsequently in the chapter 5.1.4. In summary, the achieved sensitivity of the established qPCR assay enabled to demonstrate the capability of *F. graminearum* to infect wheat seedling roots and to uncover variation among the wheat responses over time. Therefore, the qPCR diagnosis proved to be a sensitive, non-subjective quantitative method for measuring disease severity in terms of pathogen growth in addition to more subjective methods that are based on disease symptoms as indirect measurements of fungal growth.

5.1.2 Phenotypic evaluation of wheat seedling responses to root rot

Since the RFB quantifications displayed the pathogen develop progression in the roots of different wheat genotypes, phenotypic evaluations were conducted to assess the wheat seedling reaction after successful root invasions by *F. graminearum*. FRR severity respectively was evaluated by monitoring developmental traits such as root biomass (RBR), root (RLR) and shoot length (SLR) reduction as well as visible symptom development on roots (RSI) and stem bases (CSI). In this study the reduction of plant biomass was considered a quantitative measure of FRR impact on the seedling performance. Symptom development, however, was considered as indicator of disease stages associated with corresponding root cell damage visible as necrotic lesions and, in the case of stem bases, also as indication for a disease spread into distal plant parts.

5.1.2.1 Evaluation of reductions in root biomass, root and shoot length

The evaluation of developmental traits demonstrated that a successful root invasion by *F. graminearum* was always accompanied by a quantifiable adverse impact on the root and seedling growth (Fig. 4g-i; Fig. 5g-i). For all three developmental traits (RFB, RLR and SLR) genotype and treatment effects on the qPCR quantifications and length measurements were tested for each of the eight sampling timepoints and 12 wheat genotypes by using the ANOVA. As the homogeneity of variance was not given for all data (Levene's test), the one-way ANOVA was complemented by the Welch’s t-test and the Kruskal-Wallis one-way ANOVA. A significant difference was assumed if confirmed by all three tests. For reasons of brevity this package of statistical tests will be hereinafter named ‘one-way ANOVA’. The results of the statistical tests are displayed in the Figures 4 (g-i) and 5 (g-i).

Table 3: Repeated measures ANOVA results

	Relative fungal biomass				Root biomass				Root length			
	F-value	p-value		Effect	F-value	p-value		Effect	F-value	p-value		Effect
Treatment [1)]	-	-		-	120.24	.000	***	0.84	297.28	.000	***	0.64
Time [1)]	-	-		-	32.96	.000	***	0.60	532.33	.000	***	0.76
Treat. × Time [1)]	-	-		-	21.31	.000	***	0.50	50.94	.000	***	0.24
Time [2)]	110.15	.000	***	0.75	33.47	.000	***	0.74	10.00	.000	***	0.60
Time × Genotype [2)]	24.14	.000	***	0.88	4.26	.000	***	0.80	2.15	.000	***	0.13
Cat. I (partial resistance) [3)]												
Time	12.88	.211	n.s.	-	19.59	.005	**	0.87	3.59	.004	**	0.12
Cat. II (susceptibility) [3)]												
Time	9.79	.000	***	0.30	8.46	.001	**	0.44	14.91	.000	***	0.15
Cat. III (high susceptibility) [3)]												
Time	7.83	.007	**	0.34	5.82	.013	*	0.45	24.00	.000	***	0.30

* Significant at level $p \leq 0.05$; ** significant at level $p \leq 0.01$; *** significant at level $p \leq 0.001$; n.s. non-significant. In all rANOVA analyses no sphericity could be assumed ($P < 0.05$, Mauchly's test), results were therefore corrected based on the Greenhouse-Geisser F-test. The F-value indicates that differences between timepoints are greater than would be expected by chance or by error. The effect size gives the strength of associations between effect (main effect or interaction) and dependent variable (measurement).

[1)] Two-way rANOVA on root and shoot development in infected and uninfected seedlings. [2)] Mixed rANOVA on disease progression in terms of fungal growth, reduction in seedling root and shoot biomass, and visible symptom development, including data of all 12 wheat genotypes. [3)] One-way rANOVA on disease progression, each preformed for three different responses to FRR: partial resistance (cv. Florence-Aurore; Line 162.11); susceptibility (cv. Tabasco; cv. Wangshuibai; cv. Remus; Line 1105.13; Line 172.11); and high susceptibility (cv. Frontana; cv. Tobak; cv. Ning 7840; Line 1105.11).

Table 4: Repeated measures ANOVA results

	Shoot length				Root symptoms				Crown symptoms			
	F-value	p-value		Effect	F-value	p-value		Effect	F-value	p-value		Effect
Treatment [1)]	240.72	.000	***	0.60	-	-		-	-	-		-
Time [1)]	989.40	.000	***	0.86	-	-		-	-	-		-
Treat. × Time [1)]	42.41	.000	***	0.20	-	-		-	-	-		-
Time [2)]	20.73	.000	***	0.12	611.99	.000	***	0.80	348.41	.000	***	0.69
Time × Genotype [2)]	2.81	.000	***	0.17	44.01	.000	***	0.76	14.25	.000	***	0.50
Cat. I (partial resistance) [3)]												
Time	4.77	.001	***	0.15	53.85	.000	***	0.67	27.04	.000	***	0.50
Cat. II (susceptibility) [3)]												
Time	7.26	.000	***	0.08	100.07	.000	***	0.55	192.98	.000	***	0.70
Cat. III (high susceptibility) [3)]												
Time	14.85	.000	***	0.21	105.63	.000	***	0.66	104.50	.000	***	0.66

* Significant at level $p \leq 0.05$; ** significant at level $p \leq 0.01$; *** significant at level $p \leq 0.001$; n.s. non-significant. In all rANOVA analyses no sphericity could be assumed ($P < 0.05$, Mauchly's test), results were therefore corrected based on the Greenhouse-Geisser F-test. The F-value indicates that differences between timepoints are greater than would be expected by chance or by error. The effect size gives the strength of associations between effect (main effect or interaction) and dependent variable (measurement).

[1)] Two-way rANOVA on root and shoot development in infected and uninfected seedlings. [2)] Mixed rANOVA on disease progression in terms of fungal growth, reduction in seedling root and shoot biomass, and visible symptom development, including data of all 12 wheat genotypes. [3)] One-way rANOVA on disease progression, each preformed for three different responses to FRR: partial resistance (cv. Florence-Aurore; Line 162.11); susceptibility (cv. Tabasco; cv. Wangshuibai; cv. Remus; Line 1105.13; Line 172.11); and high susceptibility (cv. Frontana; cv. Tobak; cv. Ning 7840; Line 1105.11).

The differences in root and shoot biomass between inoculated and non-inoculated seedlings-varied with time. Non-significance was typically observed for low values of biomass reduction (smaller than 10%) at early timepoints which might result from only low impact of FRR infection on seedlings. As a result, differences in the root biomass between inoculated and control plants were typically significant from 1 dai on, $p \leq 0.05$ (Fig. 4g-i, 5g-i). In fact, at this timepoint a successful root invasion by *F. graminearum* was also determined by qPCR (Fig. 4 and 5) and microscopy (Fig. 12d). In contrast, significant differences in root and shoot length became generally apparent at later timepoints, finally impacting the shoots (Fig. 4g-i, Fig. 5g-i). Exceptions from general trends were represented by the genotypes Tabasco (Fig. 4e), Remus (Fig. 4f) and Line 1105.13 (Fig. 5d), due to usually delayed or absent FRR effects on root and shoot length. Finally, the observed time sequences of significant treatment effects indicated biological reasons for non-significant differences rather than technical reasons, e.g. measurement errors and/or different experimental conditions. For instance, the observation that FRR finally impacts seedling shoot length was in accordance with the *a priori* expectation that FRR impact on the seedling development result from previously impaired root development and growth. However, the ʻone-way ANOVA' analysis of treatment effects at each timepoint does not allow a statistical comparison between timepoints.

The 'rANOVA' has been applied to the measurement data of root biomass, root and shoot length in a two-way design to test treatment effects in a time-course manner. The two-way design included the within-subjects factors 'Time' (with eight sampling timepoints) and 'Treatment' (inoculated vs. control). The two-way rANOVA confirmed strong, significant 'Treatment' ($p < 0.001$) and 'Time' effects ($p < 0.001$) for all three developmental traits, demonstrating root and shoot developments that changed over time, but at levels that differed between inoculated and uninoculated seedlings (Table 3 and 4). The significant treatment × time interactions ($p < 0.001$) indicate that roots and shoots not only developed at different rates, but also that these differences changed over time. Based on the mean profile plots provided by the rANOVA to display these interactions (Fig. 10) it became evident that from 3 dai and 7 dai on root and shoot growth increasingly diverged between both treatments due to increasingly lower growth rates of diseased tissues. To test for 'Time × Genotype' interactions, the rANOVA was additionally applied in a mixed model on the general FRR progression (across all 12 genotypes) in terms of reductions in root biomaas, root and shoot length. The significant interactions ($p < 0.001$) obtained for all three severity traits show that FRR does not progress equal for all genotypes with regard to the seedling development, demonstrating a genotypic variation in the *Fg*-wheat root interactions as stated above for the relative fungal biomass development.

To display this genotypic variation for all three developmental traits (RBR, RLR and SLR) the respective mean reduction values across all timepoints were ranked in an ascending order (Fig. 7a, b, c). The ranking demonstrates a large variation of developmental responses ranging from 35.0 to 75.0%, 0.0 to 38.0% and 0.0 to 27.0% for mean reduction of root biomass, primary root and shoot length, respectively. The comparison between rankings illustrated two essential aspects: (1) the mean reduction rates of root biomass were considerably greater than those of root and shoot length, in decreasing order (Fig. 7a, b, c); this order was consistent with the observed time sequence of significant treatment effects obtained by 'one-way ANOVA'. (2) For all FRR developmental traits differences between partially resistant and susceptible wheat genotypes was observed corresponding to the significant groups obtain from relative fungal biomass ranking (Fig. 6). The relative partial resistance of seedlings from cv. Florence-Aurore and Line 162.11 were reliably ranked as low disease severity phenotypes while the relatively highly susceptible genotypes Tobak, Ning 7840 and Line 1105.16 were reliably ranked as high disease severity phenotypes (Fig. 7a, b, c).

5.1.2.2 Evaluation of visible symptoms

Ratings of visible disease symptoms, i.e. necrotic lesions on the roots and on the developing stem-bases indicating FRR severity, were conducted using a symptom index (RSI and SbSI) (Fig. 4 and 5). Both ratings included (i) the browning of tissues (light to dark brown) as an indicator for the level of necrosis, and (ii) the symptom spread. For both parameters a general dependence on the disease phase and severity was expected. Hence, a high symptom index indicates both severe necrosis (dark brown) and lesion spread (covering >75% of root area) and thus, an unrestricted propagation of FRR. Examples of such heavy symptoms are the stem basis of cv. Sumai 3 (Fig. 8n and o) and stem basis as well as roots of cv. Tobak (Fig. 8s and t).

On the roots and stem bases of susceptible genotypes symptoms typically showed a transition from initially local, light (amber) brown discolorations to more distributed dark brown lesions at later timepoints (for example, Fig. 8q-t). Stem base necrosis typically covered about half of the stem base of initially few individuals and continued until nearly the entire stem base was affected for more or less all individual plants. In contrast, on the roots and stem bases of partially resistant genotypes lesions did not became dark brown in the examined period. Particularly root symptoms appeared more locally and showed a trend to a recovery (Fig. 8a-e). Disease lesions on the roots of susceptible and highly susceptible wheat seedlings were present already at 1 dai (Fig. 4h, i and Fig. 5g-i), while they did not appear on roots of partially resistant genotypes before 5 dai (Fig. 4g).

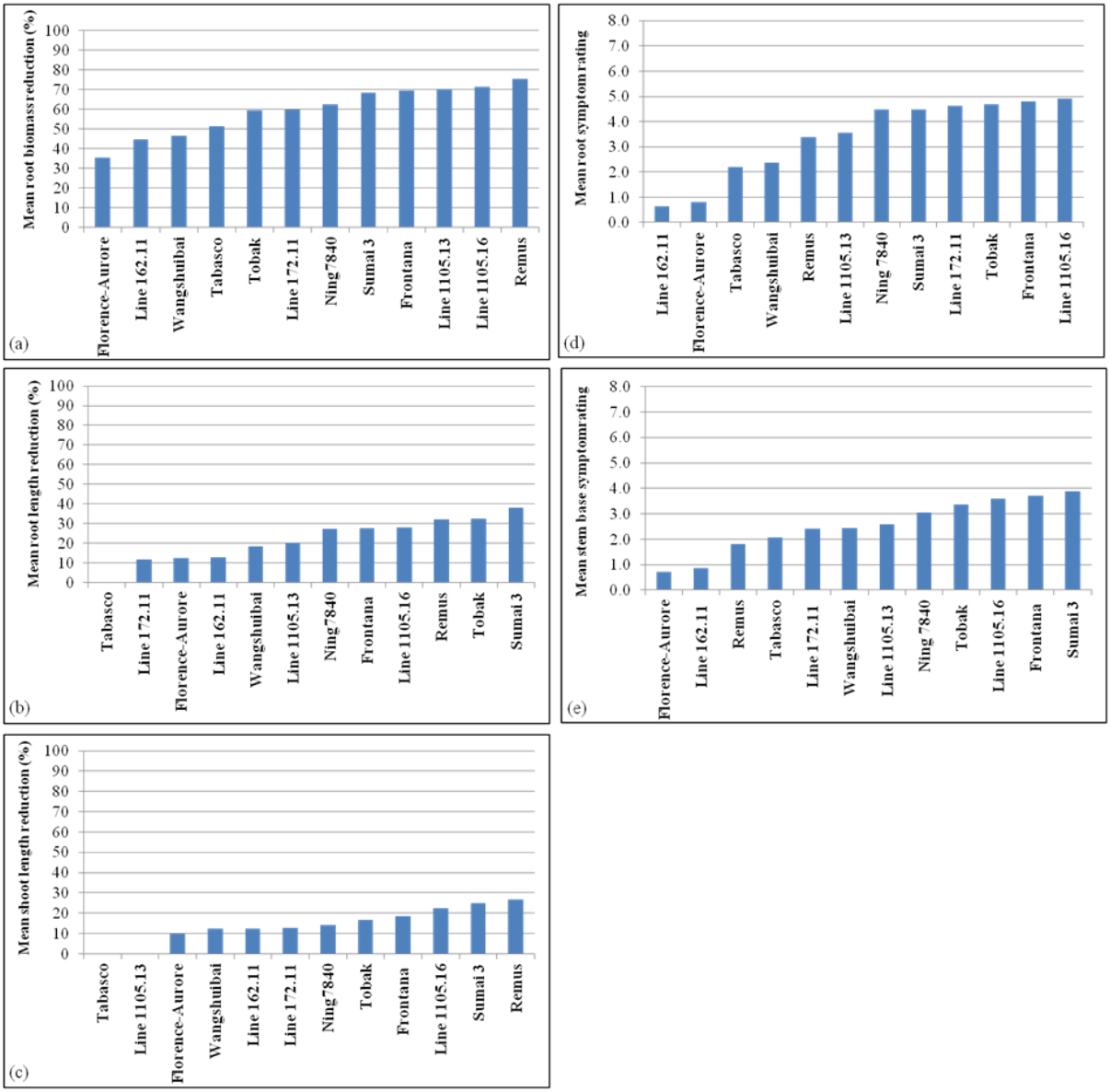

Figure 7: Wheat genotypes ranked by increasing FRR impact on seedling growth and the visible symptom development. (a) Mean root biomass reduction (%); (b) mean root length reduction (%); and (c) mean shoot length reduction (%). All reduction values were measured as biomass/length ratios between infected and uninfected plants and mean values were calculated over a time period between 0.5 to 21 dai. Detailed data from the time-course experiments are given in Fig. 4 and 5. (d) Mean root symptom rating (RSI). (e) Mean stem base symptom rating (SbSI). Root and crown symptoms were rated using a four point scale each for a browning and the symptom extension index, finally allowing a disease rating between 0 (no symptom) and 8 (severe necrosis on >75% of root/crown). All mean values were calculated over a time period between 0.5 to 21 dai. Detailed data are given in Fig. 4 and 5.

For partially resistant genotypes a strong relation between RFB progression (Fig. 4a) and symptom development (Fig. 4g) was found since cv. Florence-Aurore and Line 162.11 showed a reduced symptom appearance. Here, at maximum moderate root necroses were observed not

exceeding a scale of 3.0. Moreover, at the last two timepoints roots of both genotypes were found to recover since only low or even no disease symptoms were present then (Fig. 4g).

In contrast to root symptoms, stem base symptoms appeared always later and did not become visible before 5 dai in susceptible plants (Fig. 4h and i, Fig. 5g) and not before 7 dai in partially resistant genotypes (Fig. 4g). These observations indicate that at 5 to 7 dai the pathogen has initiated its systemic colonization of aerial plant tissue. However, for cv. Florence-Aurore and Line 162.11 the invasion of stem base tissues was found to be delayed or at least less severe since symptoms did not become marked before 10 dai and already decreased again at the following timepoint (Fig. 4g).

The mixed rANOVA applied to the time-course data of root and stem base symptoms demonstrated significant 'Time' ($p < 0.001$) as well as significant 'Time x Genotype' interactions ($p < 0.001$) for both symptom assessments (Table 4). Therefore, it was demonstrated that both symptom developments feature time pattern that differ between the wheat genotypes. To display the genotypic variation suggested by rANOVA for both symptom ratings, genotype rakings were done as previously described for the developmental traits (Fig. 7d, e). In fact, for both symptoms the lowest disease ratings were obtained for genotypes grouped as partially resistant (cv. Florence-Aurore and Line 162.11), resulting in a clear distinction between partial resistance and different levels of susceptibility (Fig. 7d, e). On the other side, the expected highly susceptible genotypes Tobak, Ning 7840 and Line 1105.16 showed accordingly high disease ratings. At the lower ranks mean RSI and SbSI ratings form a plateau since genotypic differences were not detectable (Fig. 7d, e). The cv. Tabasco showed relatively low symptoms, supporting the relatively low impact of FRR on root and shoot development observed for this cultivar. Finally, the lower mean values for stem base symptoms illustrate the generally later appearance of the disease in this tissue.

5.1.2.3 Concluding remarks on the phenotypic evaluation of wheat-Fusarium interaction

Both the rANOVA statisitcs and the genotype rankings demonstrated for the phenotypic evaluations of wheat seedling responses to FRR a genotypic variation in the observed *F. graminearum*-wheat root interactions which were in general accordance the genotypic variation that was obtained for fungal biomass accumulations (Fig. 6 and 7). Moreover, as demonstrated for the pathogen development, also the wheat responses to successful root infections were characterized by time effects, separating the respective pathogen-host interactions into periods of constant and changing disease progression (Table 3 and 4).

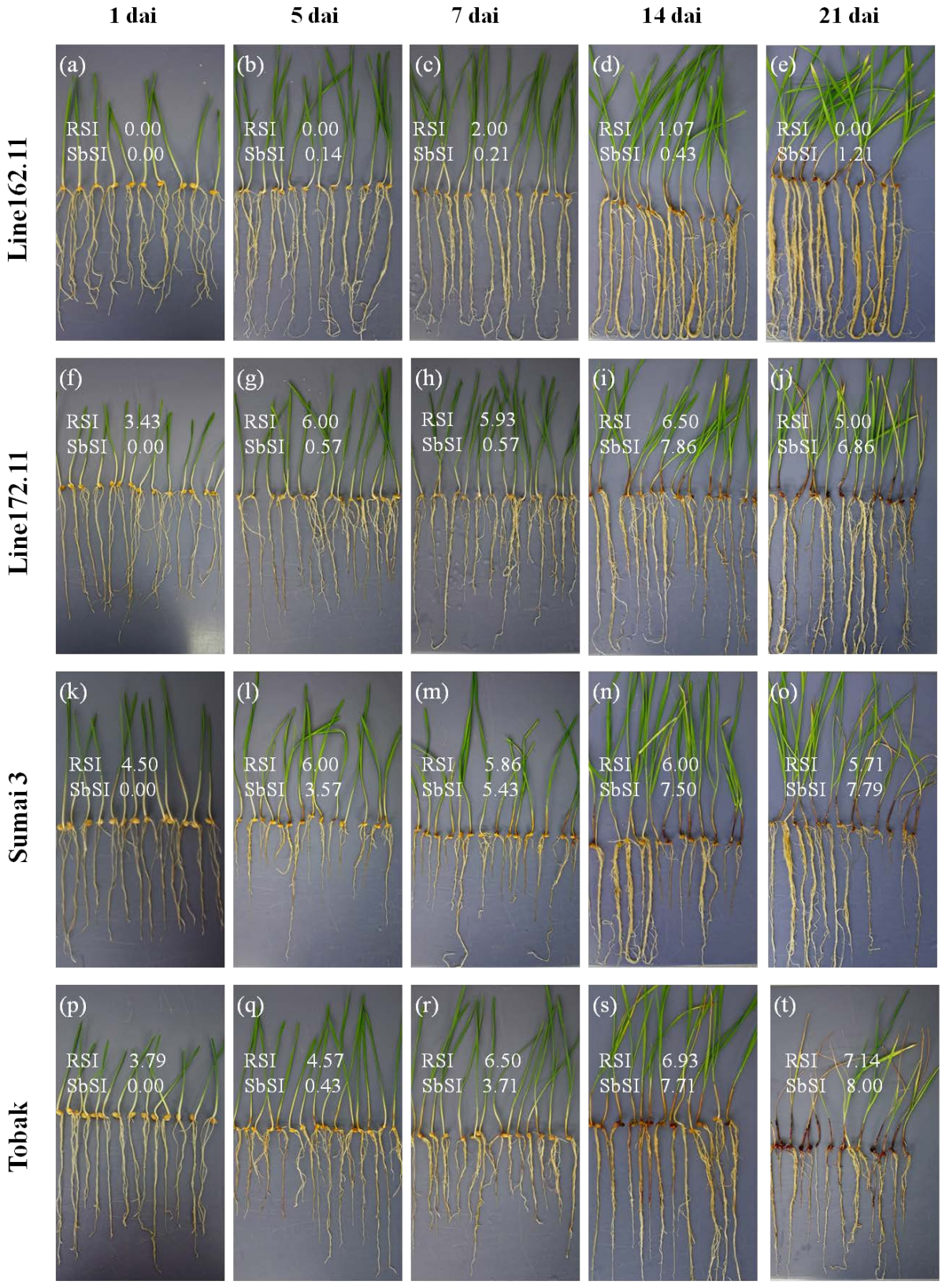

Figure 8: Time-course of visible symptom development on the roots and stem bases of the partially FRR resistant genotype Line 162.11, the susceptible genotypes Line 172.11 and Sumai 3, and the highly susceptible cultivar Tobak.

Generally, FRR impacts on the seedling development and necrotic lesions proved to be the substantially smaller threat for genotypes categorized as partially resistant. Hitherto, genotypic evaluations for soil and/or seed-borne *Fusarium* infestations were based on symptom ratings, while detailed examinations on seedling biomass reduction had not been conducted. Now, the present study demonstrates that besides root and stem base necrosis, FRR is coming along with serious threats to the generally already sensitive seedling growth and development (Fig. 7a, b, c). Especially, root biomass reductions were found to be the most immediate and severe affect of FRR on seedling development even in genotypes with relatively low fungal biomass loads in their roots. The negative association between *F. graminearum* root colonization and root/shoot development is clearly demonstrated in the susceptible cv. Remus where the fungal accumulation and seedling biomass reductions in parallel, up to highly increased values at the last timepoints (Fig. 4c, f). A similar accordance between RFB development and seedling development was also observed for the highly FRR susceptible genotypes Ning 7840 and Line 1105.11 (Fig. 5c, f).

The examinations of root and stem base symptoms revealed a time effect which confirmed the priori assumption that the successful root colonization is a necessary prerequisite for the further invasion into aerial plant parts (Fig. 4). This was clearly demonstrated by the appearance of stem base symptoms observed for partially resistant seedlings which indicated that reduced fungal root colonization not only leads to reduced necrosis, but also to a delayed and reduced fungal spread to aerial plant parts (Fig. 4a, g). Here, *F. graminearum*-wheat root interactions were indicating disease responses which are able to suppress the pathogen spread in roots and stem base accompanied by a much lower degree of cell death. In contrast, for susceptible genotypes the visible symptoms revealed developmental patterns (‘trend pattern’ and ‘curve pattern’ of change) similar to the fungal biomass developments (Fig. 4h, i and Fig. 5g, h, i). The visual diagnoses of root disease correlated with qPCR fungal biomass measurements during the entire examination period. These results also confirm that the visual assessment of disease symptoms is very well suited to estimate the extent of tissue colonization by the pathogen and thereby confirms the validity of visual assessments for disease rating and screening of breeding materials. It can be concluded that the application of different quantification and measurement procedures for the estimation of FRR disease severity and progression, essentially led to the same results. In fact, the genotype rankings of fungal accumulation (Fig. 6) were clearly related to the extent of negative effects on seedling performance (Fig. 7).

5.1.3 Genotype ranking based on FRR disease index

The FRR screenings in 12 wheat genotypes based on six different FRR severity parameters yielded genotype diversity in response to FRR. Thus, for a comprehensive benchmarking of genotype performances, FRR disease index (FDI) has been established (Fig. 9), more detail concerning the FDI of 12 genotypes was shown by Figure A1. All traits were considered with equal valence. Data on the stem base symptom development were not included since emphasis was given to the seedling root performance after *F. graminearum* infection. A lower FDI indicates a higher relative resistance against FRR, while a higher FDI is equal to a higher relative susceptibility.

It is interesting that the genotypes cv. Florence-Aurore and Line 162.11 showing partial FRR resistance in the seedling stage are highly susceptible to the head blight disease (Fig. 9). In contrast, among the highly susceptible genotypes three out of four, i.e. Ning 7840, Frontana and Line 1105.11, are described as resistant to FHB (Fig. 9). Similarly, except cv. Remus all wheat genotypes categorized as susceptible are known to react either resistant or intermediate to FHB (Fig. 8). Moreover, the cultivars Ning 7840 and Sumai 3 exhibited significantly different RFB levels, disease progression patterns and seedling performances (Fig. 4 and 5) although they both carry the stable FHB resistance QTL *Fhb1*. Consequently, the FDI ranking clearly reveals that major resistances to FHB do not necessarily protect against FRR, at least in the seedling stage of wheat.

As for the RFB ranking, the non-parametric Mann Whitney U test has been used to test the obtained ranking with regard to grouping significantly different genotypes. Figure 9 demonstrates the overall grouping of all 12 wheat genotypes into three main groups and two subgroups based on significant or non-significant differences between the respective medians The cultivars Tabasco and Wangshuibai were representing a linkage between the ʻgroup aʼ and ʻgroup bʼ which could be explained by the tolerant response to FRR associated with intermediate. RFB values in case of cv. Tabasco and by the moderate RFB values and intermediate FRR impacts on seedling in case of cv. Wangshuibai (Fig 6 and 7). Therefore, both genotypes were assigned to ʻgroup bʼ. The second subgroup was linking ʻgroup bʼ and ʻgroup cʼ, due to the high fungal biomass accumulations (Fig. 6) associated with strongly negative seedling reaction to FRR infection obsevered for cv. Frontana, Tobak and Ning 7840 (Fig. 7). Therefore these genotypes were assigned to ʻgroup cʼ. The cultivar Sumai 3, however, represented a special case by having an intermediate RFB level, but unexpected high levels of seedling biomass reductions and symptom developments. This response indicates rather sensitivity to FRR than susceptibility.

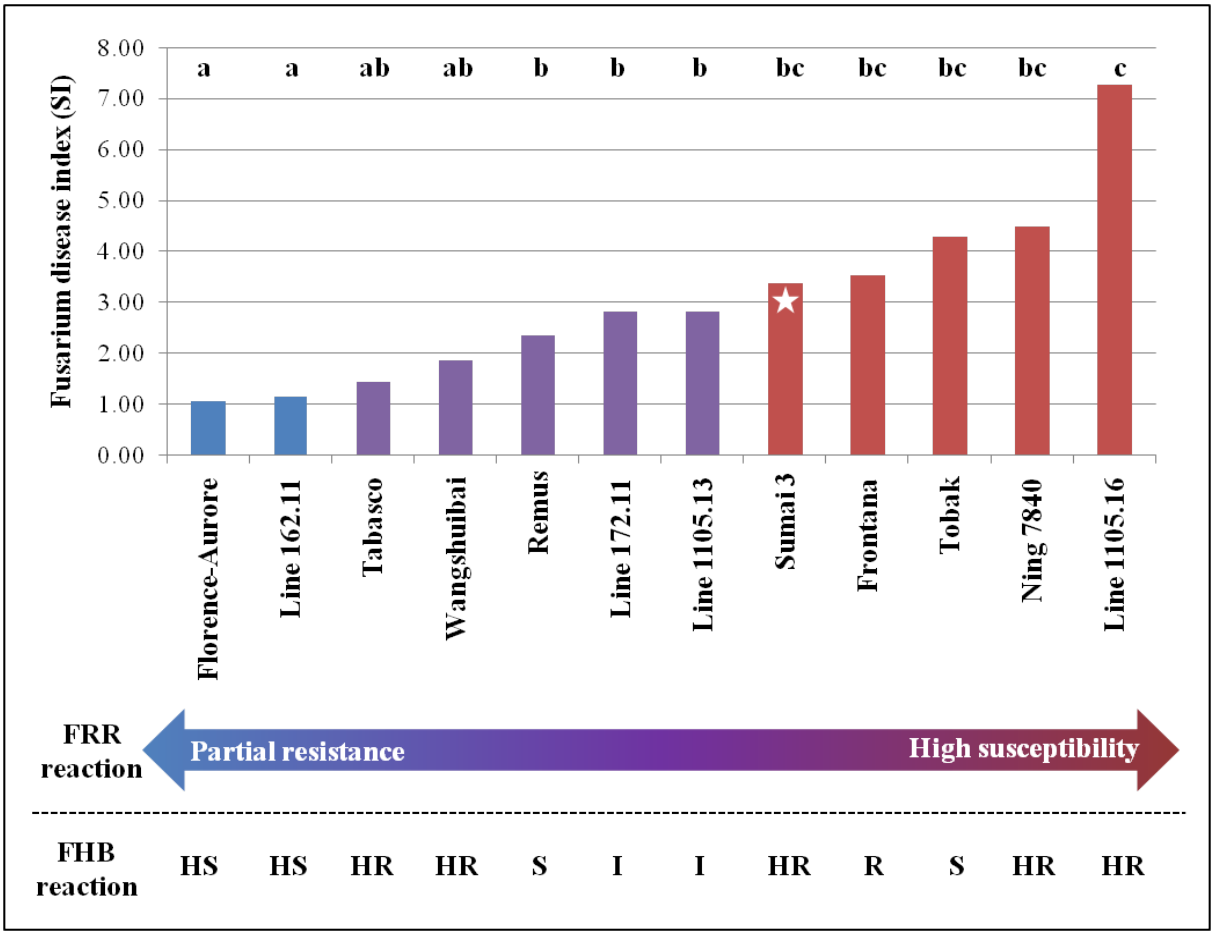

Figure 9: Wheat genotype ranking according to FRR disease index (FDI). The FDI is calculated based on susceptibility indices (SI) for (i) relative fungal biomass RFB; (ii) root biomass (RB); root length (RL) and shoot length (SL) reductions; and (iii) root symptoms (RS) [FDI= RFB^{SI} + RB^{RSI} + RL^{RSI} + SL^{RSI} + RS^{SI}]. For calculations of RB^{RSI}, RL^{RSI} and SL^{RSI} values only reductions were considered that showed significant treatment differences at $p \leq 0.05$ (one-way ANOVA complemented by a Welch's t-test and the Kruskal-Wallis one-way ANOVA). The observed FDI values show a range from partial resistance to high susceptibility. The significant assignment of wheat genotypes to three severity groups is displayed by different bar colours. Grouping is based on pairwise comparisons of mean RFB values using the Mann-Whitney-U-Test. The star in the bar of cv. Sumai 3 indicates that for this genotype rather sensitivity to FRR was observed than susceptibility. This became evident by a direct comparison with the landrace Wangshuibai which at similar moderate fungal biomass levels was accordingly FDI ranked as relative moderate susceptible genotype while Sumai 3 was ranked as a genotype with high susceptibility. For all genotypes the known reactions to FHB are listed: HR, highly resistant; R, resistant; I, intermediate; MS, moderately susceptible; S, susceptible; HS, highly susceptible.

Nevertheless, in the final ranking cv. Florence-Aurore and Line 162.11 remained to be the best performing genotypes which did not show any significance with the medians of‘group b’ genotypes (Fig. 9). Based on the FDI value, the obtained grouping allows defining three categories of FRR severity. The term category refers to a specific scenario of *Fg*-wheat root interactions with Florence-Aurore and Line 162.11 as most resistant genotypes (category I), and

two groups each representing different levels of susceptibility(category II and III). Those three categories represent a genotypic variation in FRR responses which was, indeed, found to be associated with characteristic variations in the FRR progression as will be described in the follwing chapter.

5.1.4 The dynamics of *F. graminearum*-wheat root interaction

The ranking of different wheat responses already showed many aspects of the FRR disease and indicated complex interactions between *F. graminearum* and wheat roots. However, to understand the full spectrum of this disease, the dynamics in the pathogen action and in the host reaction, i.e. the temporal changes in the progression of FRR, have to be taken into account.

For the general fungal biomass development (over all timepoints and genotypes) the mixed rANOVA demonstrated significant effects of 'Time' explaining the *F. graminearum* growth in roots measured by qPCR (Table 3). The mixed rANOVA suggested a change in the general fungal progression at one or more timepoints. Therefore the pairwise comparisons tab provided by the Bonferroni post-hoc test was applied to identify significant differences in the mean RFB values between the timepoints. The pairwise comparisons showed significant changes in the mean fungal growth between 1 to 3 dai and 7 to 10 dai, while no significant differences in the mean quantities were found in the interim periods.

Thus, the *F. graminearum* development generally proceeded in three distinct phases, typically with an initial latent period which was followed by an accelerated growth at 3 to 5 dai that proceeded during the third phase from 10 to 21 dai as shown in the mean profile plot (estimated marginal means) provided by one-way rANOVA in Figure 10d. For the disease impacts on seedling development, the congruence between the general fungal growth pattern and the general pattern of disease severity could be illustrated by the mean profile plots (estimated marginal means) provided by the two-way rANOVA (Fig. 10a-c). Those plots visualize the 'Treatment' effect and explain the significant 'Treatment × Time' interactions observed for all three traits (Table 3 and 4). For all three traits *F. graminearum* treated plants development clearly divergent from the control plants during timepoints 3 to 7 dai for root biomass and length (Fig. 10a and b), and at 7 to 10 dai for shoot length (Fig. 10c). This might be explained by the simultaneous strong increase in fungal biomass during the second period 3 to 7 dai (Fig. 10d). Finally, it became obvious that phase II (~3 to ~10 dai) is critical within the FRR disease progression.

The statistics on FDI ranking suggested a genotypic variation in the wheat responses to FRR within the tested wheat set which was assigned to three categories (Fig. 9). In fact, those three categories were found to represent characteristic variations in the FRR progression, representing

different scenarios of *F. graminearum*-wheat root interacations. For clarification, these variations were displayed as category-specific mean profile plots for each severity trait (Fig. 11a-f), and the mean values of each category were subjected to one-way rANOVA (hereafter denoted as 'category rANOVA') to examine the time effects on the category-specific disease progression (Table 3 and 4). The average disease ratings were tested for wheat genotypes assembled to the categories partial resistance (cv. Florence-Aurore; Line 162.11); susceptibility (cv. Tabasco; cv. Wangshuibai; cv. Remus; Line 1105.13; Line 172.11); and high susceptibility (cv. Frontana; cv. Tobak; cv. Ning 7840; Line 1105.11). The 'category rANOVA' included only the within-subjects factor 'Time' since genotype effects were anticipated by testing each category separately.

The 'category rANOVA' demonstrated for pathogen development that the three-phase model was only explained by the susceptible genotypes since the factor time did not reach the level of statistical significance in case of cv. Florence-Aurore and Line 162.11 (Table 3; Fig 11a). The plots in Figure 11 illustrate that relative resistance (category I) was characterized by an almost unchanged fungal growth at low levels associated with a below-average disease severity. Relative susceptibility was either associated with avearage fungal accumulations and above-average severity levels (category II); or with an accelerated fungal growth and increasing disease severity, both at above-average levels (category III). Figure 8 summarizes the phenotypic spectrum and development of root rot.

In addition, characteristic differences in the degree of change and in the trends of disesase progressions were suggested by 'category rANOVA' which are indicated in Figure 11. For resistant reactions the severity measurements over time reasonable (significant) trends were typically non-linear trends as present in the relationship between 'Time' and measured impacts caused by FRR. Quadratic trend components were suggested for root symptoms (F-value 319.46, p-value 0.000) and root biomass reduction (F-value 18.52, p-value 0.023) which display concavity with a single downward bend, demonstrating reduced disease impacts at the last timepoints (Fig. 11b and d). A cubic trend component was suggested for stem base symptoms (F-value 172.72, p-value 0.000). Thus, a curve with two reversals (second with upward bend) describes the development of necrotic lesions on stem bases of cv. Florence-Aurore; Line 162.11 (Fig. 11c). Simply SMA (simple moving average) trend components were suggested for the relationships between 'Time' and reductions in root (F-value 14.92, p-value 0.001) and shoot (F-value 16.81, p-value 0.000) length which can be described as a sequence of peaks and valleys (Fig. 11e and f). All trends were peaking at 7 to 10 dai and thereafter, root symptoms (Fig 11b) and root biomass reductions (Fig 11d) were declining (Fig 11b and d). Stem base symptoms (Fig.

11c) and shoot reductions (Fig. 11f), however, showed an increasing trend at the last timepoint, indicating an ongoing disease impact on stem bases and shoot growth.

In contrast, severity and relative fungal biomass development associated with susceptible reactions was fitting exceptionless positive linear trends which demonstrated increasing impacts on the seedling growth during the second and third disease phase (Fig 11a-c), although indications for a negative trend during the second phase were found for intermediate susceptible reactions (Fig. 11b-e). Generally, while the curves for susceptible interactions suggest a plateau in fungal biomass and root symtpom development at 21 dai (Fig. 12a, b), stem base symptoms retained an increasing trend. This indicates a proceeding disease spread into distal plant parts (Fig. 11c), wherase a quantitative limitation of pathogen growth was associated with delayed and reduced visible symptom developments (Fig. 11c). For the resistant genotypes stem bases lesions were not apparent before 10 dai and thus, about 5 days later than on susceptible stem bases. This time difference together with the considerable lower symptom rates demonstrated for the investigated time-course a delayed and reduced disease spread into above-ground plant parts.

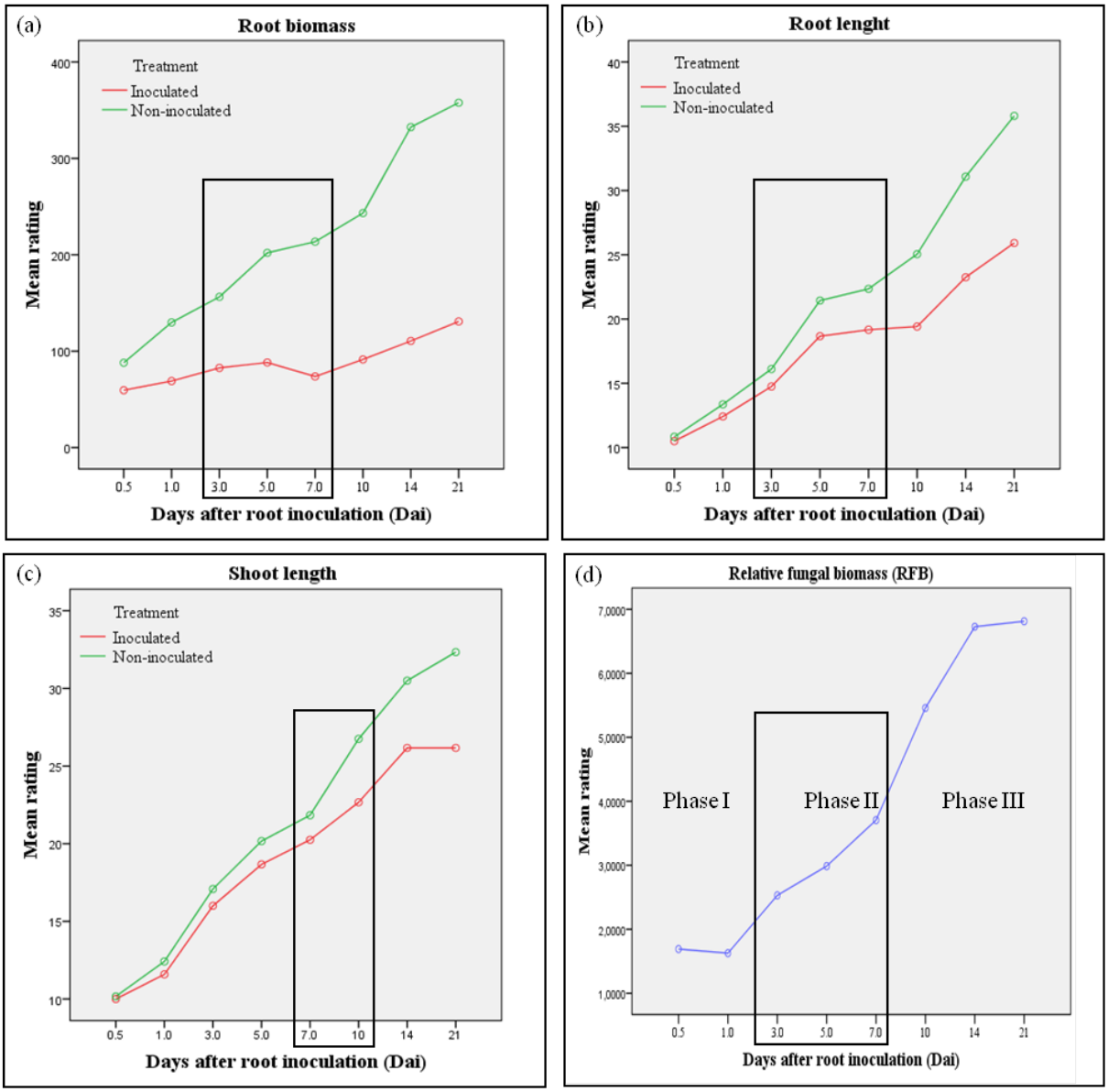

Figure 10: The mean profile plots displaying 'Treatment × Time' interactions. The mean profile plots (12 wheat genotypes) show the general trends of change present in the developments of (a) root biomass (µg); (b) root length (cm); and (c) shoot length (cm) for inoculated and non-inoculated seedlings (two-way rANOVA). (d) The graph for RFB (%) was obtained from one-way rANOVA. The black boxes in the plots of developmental traits highlight periods of non-parallel curve progressions which explain the significant 'Treatment × Time' interactions observed for these traits (Table 3 and 4) by demonstrating a marked reduction in the biomass development of infected seedlings. The black boxe in the plot of RFB demonstrates the strong increase in the fungal biomass development coincident with increasing reductions in the mean root development. Phase I to II are the three phaseses of disease progression as suggested by mixed rANOVA.

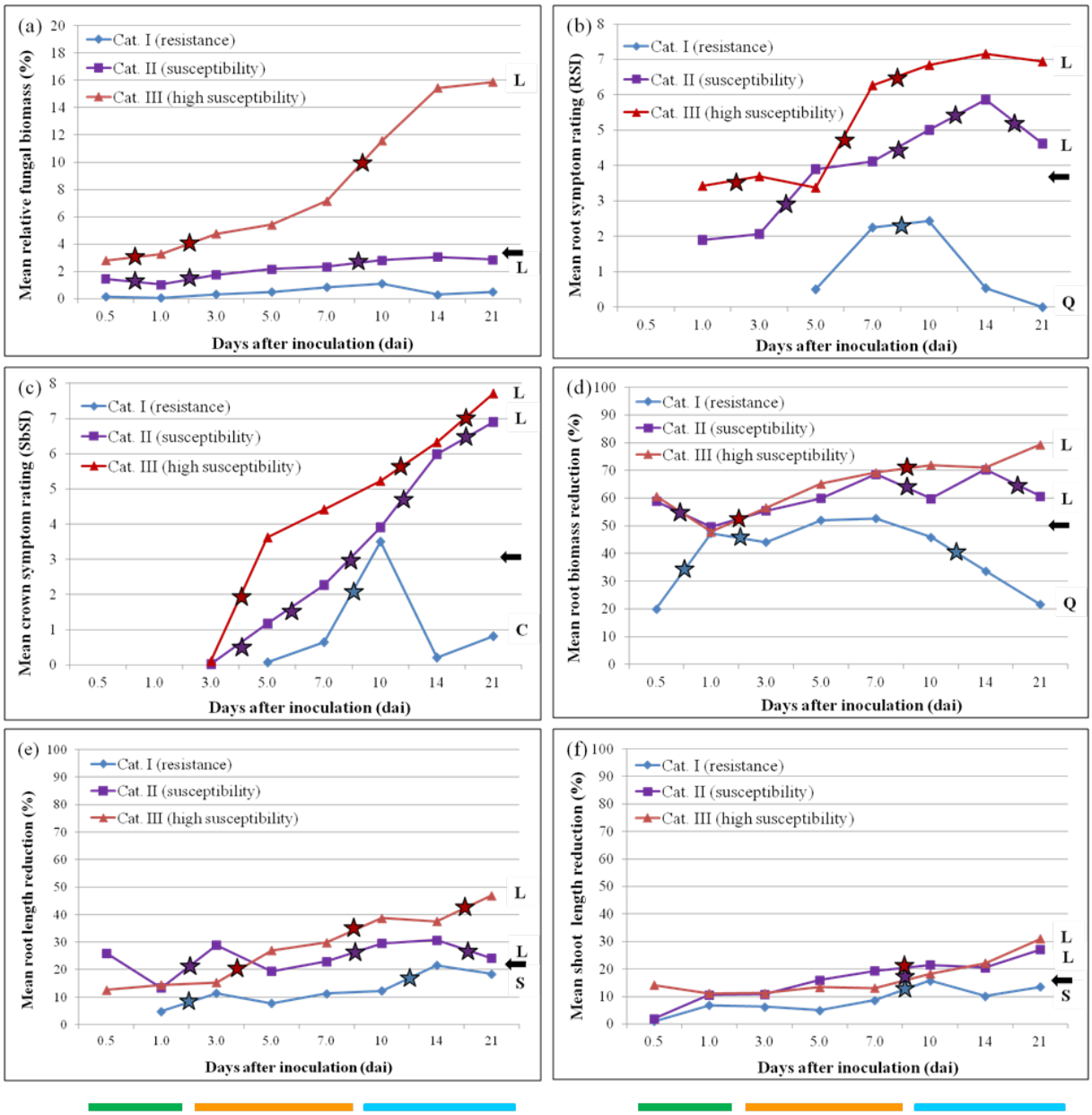

Figure 11: Fusarium root rot proceeds differentially in partially resistant, susceptible and highly susceptible wheat seedlings. Disease ratings for six severity traits (a-f) are plotted as mean curves of genotype groups (a, b, c) obtained from FDI ranking (Fig. 9). Each group represents different responses to FRR: relative partial resistance (cv. Florence-Aurore; Line 162.11); relative susceptibility (cv. Tabasco; cv. Wangshuibai; cv. Remus; Line 1105.13; Line 172.11); and relative high susceptibility (cv. Frontana; cv. Tobak; cv. Ning 7840; Line 1105.11). Black arrows on the right side represent the respective overall measurement means (over 8 timepoints and 12 genotypes) for each severity trait. Information obtained from rANOVA are given as (i) stars within graphs showing significant time effects (pairwise comparisons of measurement means), explaining the disease progression in terms of fungal growth, impacts on seedling biomass and symptom development; (ii) letters on the right side representing outcomes of the trend analysis on significant time effects, reasonable (significant) pattern in means are: L, linear trend; Q, quadratic; C, cubic; and S, simple moving average as non-linear trends; and (iii) coloured lines below the graphs showing the three phases in general F. graminearum development (pairwise comparisons of relative fungal biomass means over 8 timepoints and 12 genotypes).

5.2 Comparative histopathological examinations on the Fusarium root rot-wheat pathosystem

Hitherto, the mode of *F. graminearum*-wheat colonization upon root invasion has not been described to my knowledge. The phytopathological examinations on the *F. graminearum*-wheat root pathosystem reported above have led to a statistically significant three-category model of FRR severity in which wheat seedling responses range from relative partial resistance to relative high susceptibility including different levels of susceptibility. In addition, the conducted time-course studies have disclosed a statistically significant three-phase model of FRR disease development by subdividing the examined period into phases I (0.5 to 1 dai), II (3 to 7 dai) and III (10 to 21 dai). Generally, both models were characterized by specific events in the pathogen proliferation accompanied by respective adverse effects on the wheat seedlings. Especially, the phase II was found to be a critical period since it was associated with substantial fungal accumulations, macroscopic root symptoms, losses of seedling biomass and the beginning of the pathogenic spread into aerial plant parts.

Light and fluorescence as well as confocal microscopic observations were performed (i) to further characterize the three distinct phases of disease progression by uncovering histopathological aspects of *F. graminearum*-wheat root interactions; (ii) to investigate the supposed differences between a partial resistant and a high susceptible seedling reaction therein; and (iii) to further determine the mode and extent of *F. graminearum* colonization in different plant tissues including aerial plant parts. For all microscopic investigations the genotypes Florence-Aurore and Line 1105.16 were used as the respective representatives for a partially resistant and highly susceptible wheat seedling response to Fusarium root infection (Fig. 9).

5.2.1 The mode of *F. graminearum* development on seedling roots

To investigate the early disease phase, particularly functional hyphal structures formed on the root surface during penetration and infection processes, light and fluorescence microscope studies were conducted on the timepoints 0.5 to 7 dai by using the Zeiss Axiophot 2 microscope. Light and fluorescence microscope studies were done in three biological replications, each with five different plants per timepoint. For all examinations non-infected roots shown to be free from *F. graminearum* and other possible fungal hyphae were used. Three stages of *F. graminearum* root invasion could discriminate, covering processes such as pathogen establishment at the root surface, root infection and colonization. These phases were referred to as early infection, main infection and root colonization as described subsequently.

Early infection stage: Root tissue investigated at 0.5 dai showed characteristically germinating fungal macroconidia (Fig. 12a), while those roots investigated at 1 dai already showed an apparent hyphae spread onthe root surface. Here, hyphae growth had resulted in the formation of dense networks which entirely surrounded the seedling roots (Fig. 12b). This phenomenon was generally observed for both cv. Florence-Aurore and Line 1105.16. Otherwise, this phase was symptomless since necrosis was not visible at this stage neither micro-nor macroscopically. However, investigating root surface and root cross sections of Line 1105.16 at 1 dai already showed successful pathogen invasion into the root tissue. At this stage the simple penetration structures (hyphopodia) of root-infecting fungi formed by swellings hyphal were evident at infection sites associated with infection pegs (Fig. 12c). Moreover, both an extra- and intracellular hyphal growth was also found at this stage (Fig. 12d). This stage of FRR disease actually corresponds to phase I (0.5 to 1 dai) which was generally characterized by relatively low fungal biomass accumulation in the roots of all 12 tested wheat genotypes (Fig. 4 and 5).

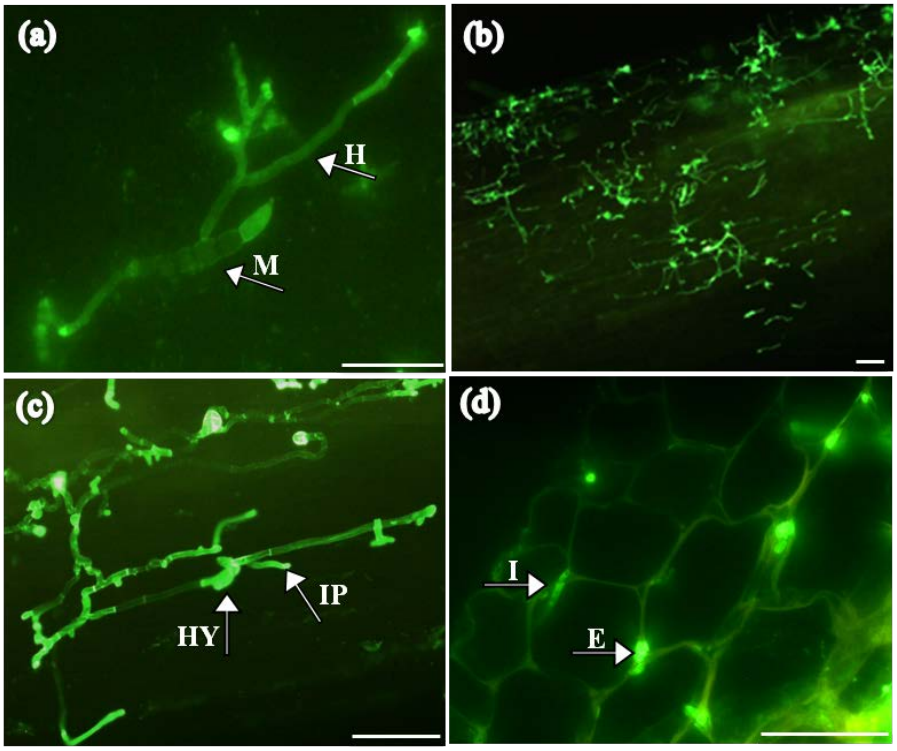

Figure 12: Infection structures of *F. graminearum* wild type isolate IFA65 on wheat roots.(a-d) Fluorescence microscopy images of infected root after WGA® Alexa Fluor 488 staining. (a) Germinating macroconidiaon the root surface at 0.5 dai. (b) Hyphae networkon the root surface at 1 dai. (C) Putative hyphopodia and infection pegsat 1 dai. (D) Extracellular and intracellular infection of root cortex at 1 dai. Abbreviations: E, extracellular hyphae; H, hyphae; HY, hyphopodia; I, intercellular hyphae; IP, infection peg; M, macroconidia. Bars: 25µm.

Main infection stage: Exclusively, the roots of Line 1105.16 at 3 dai for the first time exhibited necrotic cells on the root surface (Fig. 13a). Typically, those cells were found to be surrounded by runner hyphae and other typical fungal morphologic structures, such as foot structure (Fig. 13b) and infection cushion (Fig. 13c). In contrast, on the roots of cv. Florence-Aurore necrotic cells on the root surface were not observed.

In contrast to the previous stage, the main infection stage was characterized by remarkable symptom appearance on the roots of Line 1105.16 which, therefore, were examined micro- as well as macroscopically. However, since qPCR quantification had verified still relatively moderate fungal biomass accumulations in general, in spite of an increase in some genotypes (Fig. 5a, b), this stage was referred to as main infection stage. In term of disease progress this stage represents the transition from phase I to phase II.

Root colonization stage: For roots of Line 1105.11 investigated 5 and 7 dai the abundant presence of conidiogenous cells such as sporangium, macroconidia (Fig. 13e) and chlamydospores (Fig. 13f) at the surface was characteristic. The presence of such structures indicates both prior successful systemic root colonization and the beginning of fungal propagation into other uninfected regions of the root system. In accordance with observations made during the previous examinations, the roots of cv. Florence-Aurore appeared much healthier and necrotic cells on the surface were found only sporadically. Thus, light and fluorescence microscopic studies in the susceptible Line 1105.16 allowed to determine the period around 5 to 7 dai as colonization stage corresponding to phase II (Fig. 4 and 5). The observed differences between both wheat genotypes concerning the status of *F. graminearum* development supported the assumption of an impaired pathogenic root invasion caused by partial FRR resistance. This question is further addressed in the following chapter.

5.2.2 The mode of *F. graminearum* colonization in root, stem and leaf tissues

The confocal microscope studies were applied on cross sections of wheat seedling roots harvested7.0 to 21 dai, and on cross sections of stem bases, different stem parts and leaf blades collected 7.0 to 28 dai. Root cross sections were taken from the maturation zone (root hair zone) of seminal roots which allowed obtaining high quality sections with an average of 0.5 mm diameter. The generally high fragility of wheat roots was found to be increased after *F. graminearum* infection. Further, a diameter of <0.5 mm limited the preparation of suitable cross sections from the lower elongation zone of seminal roots or from nodal roots (adventitious or crown roots). For comparative analysis, the stem base region was separated into three zones: (i) stem base 1 (Sb1) i.e. the stem base part right above the soil surface; (ii) stem base 2 (Sb2), the

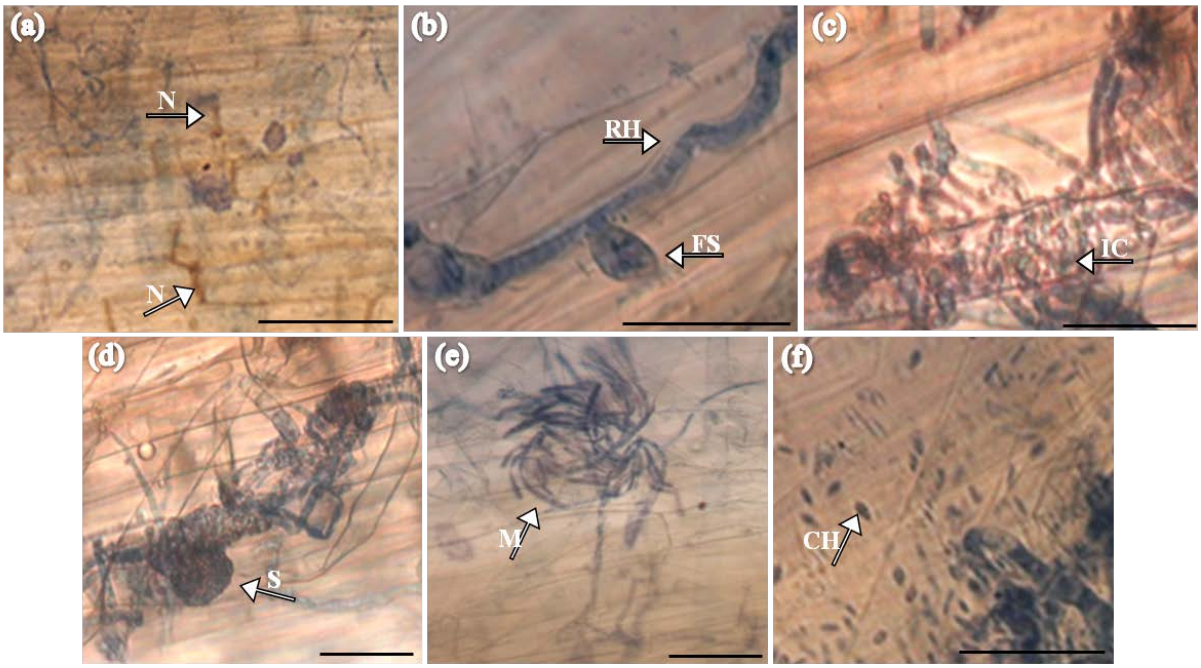

Figure 13: Infection structures of *F. graminearum* wild type isolate IFA65 on wheat roots. (a-f) Bright field microscopy images of infected root after trypan blue staining. (a) Necrotic root cell. (b) Foot structure arising from runner hyphae. (c) Magnification of trypan blue stained infection cushion. (d) Sporodochia with infection cushion. (e) Macroconidia. (f) Chlamydospores. Abbreviations: CH, chlamydospores; FS, foot structures; IC, infection cushion; M macroconidia; N, necroses; RH, runner hyphae; S sporodochia. Bars: 25µm.

area right above Sb1; and (iii)Stem base 3 (Sb3) i.e. the consecutive area below the first leaf. The anlayzed stem apex referred to a section of respective stem tip at each timepoint, containing the undeveloped stem (bud). From the first seedling leaf horizontal and cross sections of leaf blades were prepared and analyzed. Confocal microscope studies were done in three biological replications, each with five different plants, and for each tissue part 2-3 sections were analyzed. Generally, in control plants neither symptoms nor fungal hyphae were detected in the analyzed cross sections.

When studying infection processes it is important to consider the structure of the investigated tissue. The wheat seedling root (Fig. 14a) is characterized by the epidermis (rhizodermis), a single outermost cell layer which directly borders the cortex layer (parenchyma cells). The prominent cortex function is the transport and storage of nutrients/water. The central root column (stele) containing the central metaxylem and vascular bundles (xylem and phloem) is separated by the endodermis, a single cell layer. The transverse and radial endodermal cell walls include a waxy layer, the Casparian strip which regulates the water and mineral flow into the stele. The Casparian strip is visible as sharp black line inside the endodermis shown in Figure 13a. In the

maturation zone many epidermal cells have developed root hairs to absorb soil water and mineral nutrients which are transported across the cortex into the stele.

In all of the investigated root cross sections of the highly susceptible Line 1105.16 taken at 7 dai mycelium growth was detectable in the entire cortex layer (Fig. 14c). The picture detail illustrates the intercellular and intracellular fungal presence in the cortex parenchyma cells (Fig. 14d). All investigated cross sections showed an equal inter- and intracellular cortex colonization. In addition, hyphae growing from cell to cell via the symplastic pathway through the cytoplasm were clearly observable as non-stained hyphae in Figures 14c and d. These hyphae appear non-stained in the transmission images since they are located in focal planes (non confocal layer) below those in which hyphae are located that are detected by green fluorescence signals (confocal layer). Equal intense cortex invasion has been found for cross sections of Line 1105.16 roots at 10, 14 and 21 dai. In fact, concerning the magnitude of cortex invasion no differences were observed between sections obtained from necrotic and health appearing root regions.

In contrast, all investigated root cross sections from the partially resistant cv. Florence-Aurore showed a remarkably limited root invasion at 7 dai. Here, fungal hyphae were only present in or even outside the rhizodermis layer (Fig. 14e). This stage of fungal invasion was still observed for cross sections collected at the timepoint 14 dai. On the contrary, first cortex colonisations by *F. graminearum*in roots of cv. Florence-Aurore were only observed from timepoint 21 dai on. At this timepoint, inter- and intracellular cortex colonization was observed, although the hyphae presence in cortex parenchyma cells was still less pronounced than in cross sections of Line 1105.16. Of course, such microscopic analysis does not allow an exact quantification of hyphal growth. But, in both investigated genotypes fungal hyphae were not found inside the stele as shown, for instance, in Figure 13c. In addition, Figure 13e shows the general situation of the root infection process and visualizes that hyphae were found in front and within the epidermis, but were not observed in the root hairs in this work.

Confocal microscopic analyses of stem base and stem sections were conducted to investigate the magnitude and mode of *F. graminearum* migration into distal plant parts following successful root colonization. Figure 14b shows young wheat tissue enwrapped by three leaf sheaths (L1, L2 and L3). In leaf sheaths the vascular bundles are visible as dark inclusions at the epidermis. The tissue of the wheat stem is build of the outer epidermis as a single cell layer, the cortex (parenchyma cells), and the endodermis separating the vascular bundles (xylem and phloem) visible as circular arranged dark inclusions.

The stem bases of the susceptible Line 1105.16 were found to be colonized by a penetration route via the stem base leaf sheaths (Fig. 14g). At timepoint 7 dai, predominantly the outer leaf sheath (L1) was colonized, while only few hyphae were found in the second leaf sheath (L2) and in the stem (Fig. 14g). At 10 dai, the colonization of L2 and stem was found to be completed. From the beginning of stem base invasion on, all investigated cross sections uncovered the presence of hyphae inside the vascular tissues. Figure 14f shows a vascular bundle of a young stem base at 14 dai demonstrating the presence of *F. graminearum* in the sclerenchym cells as well as in the phloem and xylem cells.

Migration of fungal hyphae into the lower and upper stem parts was observed in cross sections from Line 1105.16 at timepoint 14 dai. As observed for the stem base, in all stem parts fungal invasions of leaf sheath and stem vascular bundles were predominant. The Figure 14n shows a leaf crown of Line 1105.16 which is located at the stem apex and does not contain a stem. Generally, from the timepoint 28 dai on, hyphae were observed in sections prepared from the stem apex and also here, vascular bundles were predominant targets for pathogen invasion (Fig. 14o).

In contrast, the investigated stem bases and lower stem parts of cv. Florence-Aurore were still almost pathogen-free at the timepoint 14 dai. Only a few hyphae were observed in leaf sheath tissues (Fig. 14i). Instead, particularly the stem vascular bundles were found to be heavily surrounded by green fluorescence signals (Fig. 14h, i). Moreover, identical observations were made in sections obtained from the lower and upper stem parts. Signal separation from individual channel of laser scanning microscope indicated that the signal did not radiate from the fungus and therefore, they rather originated from the plant cells surrounding the stem vascular bundles. Since such a green fluorescence was neither observed in non-stained nor in uninfected cross sections, autofluorescence as a possible reason could be excluded. On the contrary, in none of the analyzed cross sections from Line 1105.16 a comparable situation has been observed.

However, the upper stem parts of cv. Florence-Aurore were found to be colonized at timepoint 28 dai (Fig. 14p, q). This observation was made 14 days later than in upper stem sections of Line 1105.16, but at that moment fungal invasion appeared equally to the susceptible genotype (Fig. 14n, q), including predominant hyphal growth in vascular tissues. However, at that timepoint *F. graminearum* had not yet reached the stem apex of cv. Florence-Aurore.

To investigate the mode of *F. graminearum* colonization in the first leaf blades of wheat, horizontal and cross sections were prepared. The leaf blade anatomy comprises the upper and lower epidermis, the palisade layer right below the upper epidermis which is build of

parenchyma tissue with chloroplasts (Fig. 14j, l). The central body of a leaf blade consists of mesophyll cells which bear the vascular bundles, commonly known as leaf veins. Some epidermal cells produce hairs (trichome) and bear guard cells which define natural openings, the stomata, placed at the lower leaf side.

From 10 dai on and until 28 dai, the final investigation timepoint, fungal hyphae were observed in leaf blade sections from Line 1105.16 (Fig. 14j, k). From 14 dai on, hyphae were also found in the leaf blades of cv. Florence-Aurore (Fig. 14l, m). However, while leaves of Line 1105.16 always showed hyphae, half of the analysed leaves from cv. Florence-Aurore were free from hyphae. This situation remained until the timepoint 28 dai.

Concerning the mode of leaf blade colonization no considerable differences were found in the analyzed sections of both genotypes: hyphae were exclusively observed in the leaf blades either (i) in the palisade and/or epidermal cells beneath the trichome or in trichome cells themselves, or (ii) in substomatal chambers of lower epidermis. Therefore, trichome and stomata seem to be the preferential targets for *F. graminearum* leaf blade colonization, because hyphae were not observed in the vascular bundles or in the mesophyll cells in any of the investigated sections.

5.2.3 Concluding remarks on the comparative histopathological examinations

By the histopathological studies four distinct stages which constituted the course of FRR disease could be discriminated. They are characterized as (i) early and (ii) main infection stages; followed by (iii) root tissue colonization and (iv) plant tissue colonization stages (Fig. 15). Consequently, these studies support and help to further characterize the three phases of disease progression previously described on the basis of phytopathological examinations complemented by rANOVA statistics. While phase I (~0.5 to ~1 dai) is seen as early, symptomless infection stage which is identical in both analysed wheat genotypes, phase II (~3 to ~10 dai) is the main infection and root colonization stage defined on the basis of root analysis of Line 1105.16 at 5 to 7 dai. For the root colonization stage, the microscope studies demonstrated a fungal propagation on root surface and root cortex colonization (Fig. 12, 13 and 14). The consecutive phase III (~14 to ~21 dai) was then characterized as a stage in which *F. graminearum* systemically colonizes aerial plant parts. At 28 dai, seedlings of Line 1105.16 were entirely invaded by the pathogen. Based on these observations which were consistent with the previous assessments of stem base symptoms (Fig. 4 and 5), this stage was denoted as plant colonization stage. Infected roots and stem bases of Line 1105.16 displayed first necrotic lesions between 5 to 7 dai, consistent with the previous assessment of visible symptoms (Fig. 4 and 5). At 10 dai infected stem bases of Line 1105.16 showed a level of fragility which challenged the preparation of cross sections, and

at 14 and 21 dai about half of the 15 test plants were already wilting. In contrast, cv. Florence-Aurore plants appeared generally much healthier and strong necrotic lesions were not observed. However, visible symptoms such aschlorosis on leaf blades or main stem parts were not observed.

The course of FRR disease was principally similar in both investigated wheat genotypes representing two contrasting responses to FRR. However, for cv. Florence-Aurore a delayed invasion of root and aerial plant tissues was confirmed by the microscopic investigations in accordance with the phytopathological observations. In fact, characteristics of partial resistance stated for cv. Florence-Aurore could be confirmed by microscopy. These include an initially suppressed root cortex invasion and later suppressed stem colonization or invasion of stem vascular bundles, respectively. Of course, the partial resistance of cv. Florence-Aurore does not provide full protection against later systemic colonizations of root, stem and leaf tissues. Here, the timepoint 21 dai was found to be critical. This coincided with the tillering stage (Z21), typically seen as the end of seedling stage in wheat development. Finally, the histopathological study has uncovered tissue-specific modes of host colonization which give rise to tissue-specific pathogen-host interactions. Here, the finding that *F. graminearum* strictly acts as a vascular pathogen in wheat stems is considered as particularly relevant.

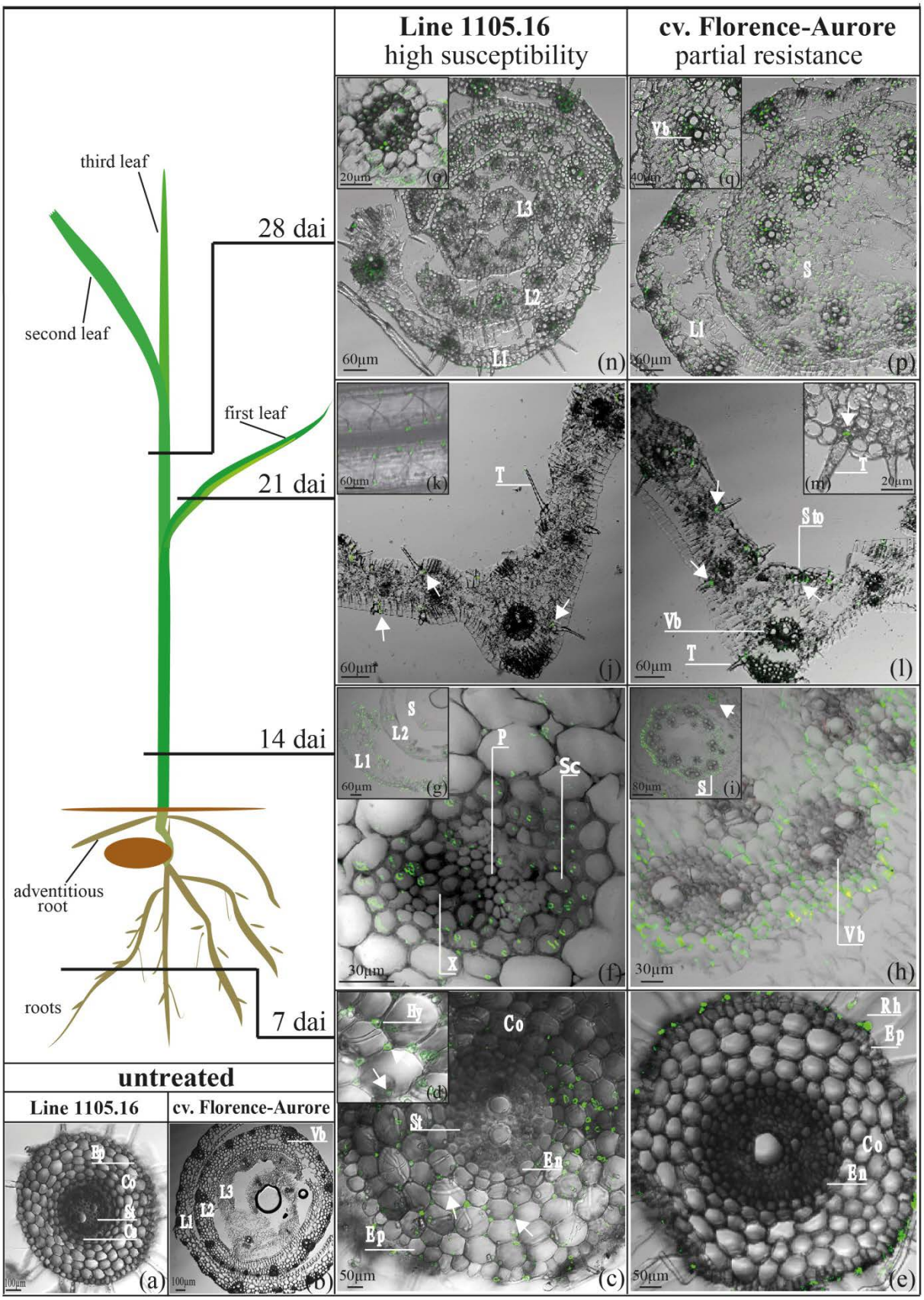
Line 1105.16
high susceptibility
cv. Florence-Aurore
partial resistance
third leaf
second leaf
first leaf
28 dai
21 dai
14 dai
7 dai
adventitious root
roots
untreated
Line 1105.16
cv. Florence-Aurore
(a)
(b)
(c)
(d)
(e)
(f)
(g)
(h)
(i)
(j)
(k)
(l)
(m)
(n)
(p)
(q)
Ep
Co
St
En
Vb
L1
L2
L3
Hy
Rh
Sc
P
X
S
T
Sto
60µm
50µm
30µm
20µm
40µm
100µm

Figure 14: Comparative analyses of *F. graminearum* infection and colonization in the roots and distal plant parts of partial resistant and highly susceptible genotypes. (a-j) Confocal laser scanning microscopy of root, stem and leaf cross-section after WGA Alexa Fluor 488® staining. (a) Untreated root of Line 1105.16. (b) Untreated stem base of cv.Florence-Aurore. (c) Root cross section of Line 1105.16 with extra- and intercellular *F. graminearum* colonization (white arrow) in the cortex at 7 dai. (d) Detailed image of extra- and intercellular *F. graminearum* colonization (white arrow) (e) Root cross sections of cv.Florence-Aurore with *F. graminearum* hyphae (green signal) at and inside epidermis. (f) Magnification image of infected vascular bundle in stem base of Line 1105.16 at 14 dai; fungal hyphae colonization (green signal) in whole vascular bundle. (g) Detailed image showing fungal colonization (green signal) in stem base leaf sheath 1 and 2. (h) Magnification image of stem base of cv.Florence-Aurore at 14 dai with strong (non-pathogen) fluorescence signals in parenchyma cells surrounding the vascular bundles. (i) Image detail low colonization by the pathogen (white arrow) in the external leaf sheath 1 and non-pathogenic signals surrounding vascular bundles. (j-m) Leaf blade cross sections with fungal signals (white arrow). (n) Stem apex showing leaf crown of Line 1105.16 with fungal colonization of vascular bundles (green signals) at 28 dai. (o) Detail image of (n) showing invaded vascular bundle. (p) Serious fungal colonization (green signals) in vascular bundles of stem apex optained from cv. Florence-Aurore at 28 dai. (q) Detailed image of (p) showing invaded vascular bundle. Abbreviations: Co, cortex; Cs, casparian stripe; Ep, epidermis; En, endodermis; Hy, hyphae; L1, leaf sheath 1; L2, leaf sheath 2; L3, leaf sheath 3; P, phloem; Rh, root hair; S stem; Sc, sclerenchyma; St, stele; Sto, stomata; T, trichomes; Vb, vascullar bundle; X, xylem.

Stage	Main characteristics
Early infection	Macroconidia germination Hyphae network Hyphopodia, infection pegs Intracellular and extracellular hyphae
Main infection	Increased fungal biomass Necrotic root cells Infection cushion Foot structures from runner hyphae DON can be detected by LC-MS
Root colonization	Macroconidia and chlamydospores Visible FRR symptoms
Distal plant colonization	Defence was overcame Colonization in aerial plant (stem, leaf)

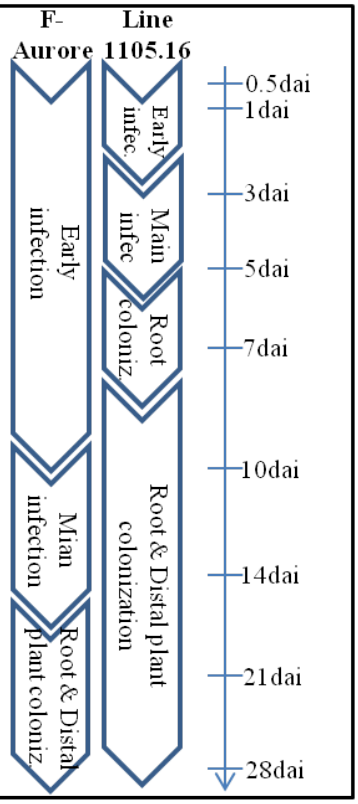

Figure 15: Summary showing the main characteristics of different FRR disease stages (right side) and timeline showing the differet disese progression in partial resistant genotype Florence-Aurore and highly susceptible genotype Line 1105.16 (left side).

5.3 *F. graminearum* colonization progress in distal plant parts of wheat

Since histopathological and comparative microscopic studies have demonstrated that *F. graminearum* begins systemic colonization of distal plant parts already 5 to 7 dai, the following experiments were designed to address agronomically relevant questions concerning the systemic plant colonization upon a successful seedling root infection. For this study the wheat genotypes Florence-Aurore, Sumai 3, Frontana and Ning 7840 were selected from the entire set of 12 genotypes since they represent the three FRR severity categories, the whole spectrum of FHB responses (Fig. 9).

To investigate the disease spread during the development of wheat plants four major growth stages representing important developmental phases have been defined as possible critical stages during the FRR progression:1) the ʻseedling stage' (Z13, three unfolded leaves) at ≥10 dai associated with successful root colonization and beginning of disease spread in susceptible interactions; 2) the ʻtillering stage' (Z21-22) as switch from the seedling to the adult plant stage which is assumed to be an important switch in the pathogenesis of FRR; 3) the ʻstem elongation stage' (Z32) in which the plant gains in length, associated with the important question whether the vascular pathogen has the potential to follow plant elongation; and 4) the ʻflowering stage' (Z60-64), usually beginning about three days after head emergence and representing a very critical stage for FHB infection. In fact, the presence of *F. graminearum* at this developmental stage could lead to negative severe impact on the fertilization and subsequent grain development as an important yield parameter.

At each growth stage the wheat plant has been separated in defined zones from which respective tissues samples were collected and screened for fungal presence (Fig. 3). Each growth stage was characterized by specific plant tissues (e.g. leaf number or stem internode number) to test whether the pathogen had reached the newly developed plant parts. In addition, lower tissues (e.g. roots or stem base) were analyzed for the presence/absence of the pathogen as well.

5.3.1 *F. graminearum* colonization progress in wheat distal plant parts

This study showed a general mode of spread in which *F. graminearum* was able to follow the plant development, because at each growth stage fungal biomasses was always detected in newly developed plant parts (stem and leaf blade). Finally, the pathogen could be detected in the flag leaves and spikes of all wheat genotypes in the ʻflowering stage' (Fig. 16a, 17b).

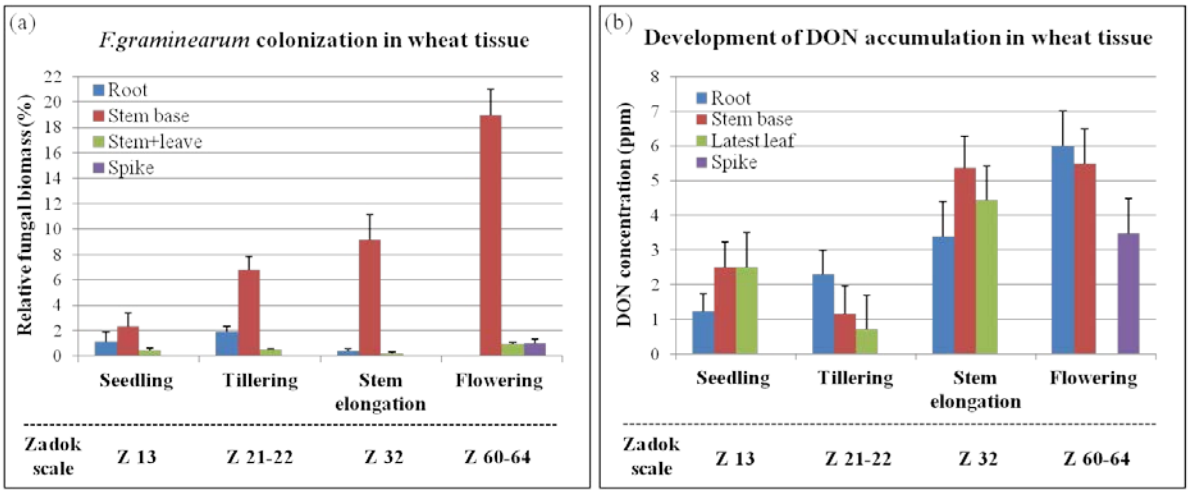

Figure 16: General mode of *F. graminearum* colonization and DON accumulation in different wheattissues at different growth stages. (a) Relative fungal biomass in the roots, stem base, distal plant and head of wheat at four growth stages (Fig. 3). The average relative fungal biomass of cultivars Florence-Aurore, Sumai 3, Frontana and Ning 7840 was used to describe the *F. graminearum* colonization progression in wheat after seedling root inoculation. (b) DON accumulation level in the roots, stem base, youngest leaves and head of wheat measured at four growth stages (Fig. 3). The average DON level of four cultivars (Florence-Aurore, Sumai 3, Frontana and Ning 7840) was used to describe the DON accumulation after seedling root inoculation. Growth stages according to the Zadok's scale.

In addition to the finding that *F. graminearum* can systemically reach the wheat spikes after seedling root inoculation, four other observations were remarkable: 1) the colonization of wheat roots and stem bases was consistent throughout the 'tillering and stem elongation stage'. However, fungal biomass was no more detectable in the roots at the 'flowering stage' of all four genotypes (Fig. 16a). Thus, from the 'stem elongation stage' on, it seemed as if the roots were less attractive for the pathogen. 2) In contrast to the roots, the stem base was found to be a site of constantly increasing fungal accumulation until a peak of the fungal biomass (RFB) while the full flowering stage (Fig. 16a). In contrast to the seedling stage, at 'tillering' RFB showed an increase in the stem bases of partially resistant genotypes (Fig. 17a), even to a higher level than mean calculated for susceptible genotypes. This might be explained by the inversion of plant resposes to FRR between the seedling and adult plant stages which seems to occur around the 'tillering stage'. 3) From the 'tillering stage' on the pathogenic invasion of above-ground plant parts in the tested genotypes was not distinguishable (Fig. 17b). 4) While visible symptoms on the stem bases were detectable insusceptible genotypes, the upper stem internodes were symptomless since neither necrotic nor chlorotic lesions were detectable.

5.3.2 Deoxynivalenol accumulation in wheat plants

In this part of the work it was studied whether the mycotoxin deoxynivalenol (DON) is associated with or necessary for the disease spread and to which plant tissues DON might be transported or released. The DON measurements were performed in a similar manner as the analyses of colonization progress by testing five individual plants per genotype for each wheat growth stage and plant part. At each growth stage roots and stem bases were sampled; from the ‘tillering stage’ on the uppermost leaves were collected; and at the ‘flowering stage’ the spikes were sampled. It was considered that the detection of DON in the youngest plant tissues would indicate that DON might also be present in all tissues below. In this study, 6 ppm was the maximum concentration that could be measured with the applied ELISA-kit (implemented standard curve).The DON toxin was found in all *Fusarium*-inoculated plant tissues during the entire period of plant development (Fig. 16b; Fig. 17c and d). Similar to fungal biomass after succesful stem base colonization none of the tested cultivars was able to suppress DON release by the fungus and/or DON transmission. During the time-course fungal biomass decreased in the roots (Fig. 16a), but DON was increasing at the same time (Fig. 16b). Threfore, the rising DON accumulation in roots might be due to toxin transmission from upper stem base. In all tested apex tissues, DON showed relative high concentration (Fig. 17d) as compared to the relatively low fungal biomass (Fig. 17b), which indicates that DON may even be distributed in advance of fungal spread. Finally, since this is prelimary data from first experiments, repetition is needed to confirm these results.

5.4 Examinations on the Fusarium-wheat root pathosystem during adult plant stages

This study was performed to to investigate (i) whether *F. graminearum* has the capability to infect wheat roots at the post-seedling (adult) stages; and in case of a successful fungal root infection, (ii) whether the FRR disease progresses similar or different in seedlings and adult plants. Results on the fungal accumulation and the FRR disease index ranking in the seedling and adult plant roots are presented as direct comparisons between the two developmental stages. For this study four spring wheat cultivars were selected based on their seedling responses to FRR and their adult plant responses to FHB. The wheat set comprised the partially FRR resistant cv. Florence-Aurore (susceptible to FHB), the highly susceptible genotypes Frontana and Ning 7840 (resistant to FHB) as well as the FRR susceptible cv. Sumai 3 (resistant to FHB) which represents a specific case due to its high sensitivity to relatively intermediate fungal biomass accumulations. All genotypes were subjected to the FRR bioassay and analysed in a time-course

comprising seven timepoints evenly distributed throughout the plant development between early stem elongation (two nodes, Z32) and Flowering (Z60-64).

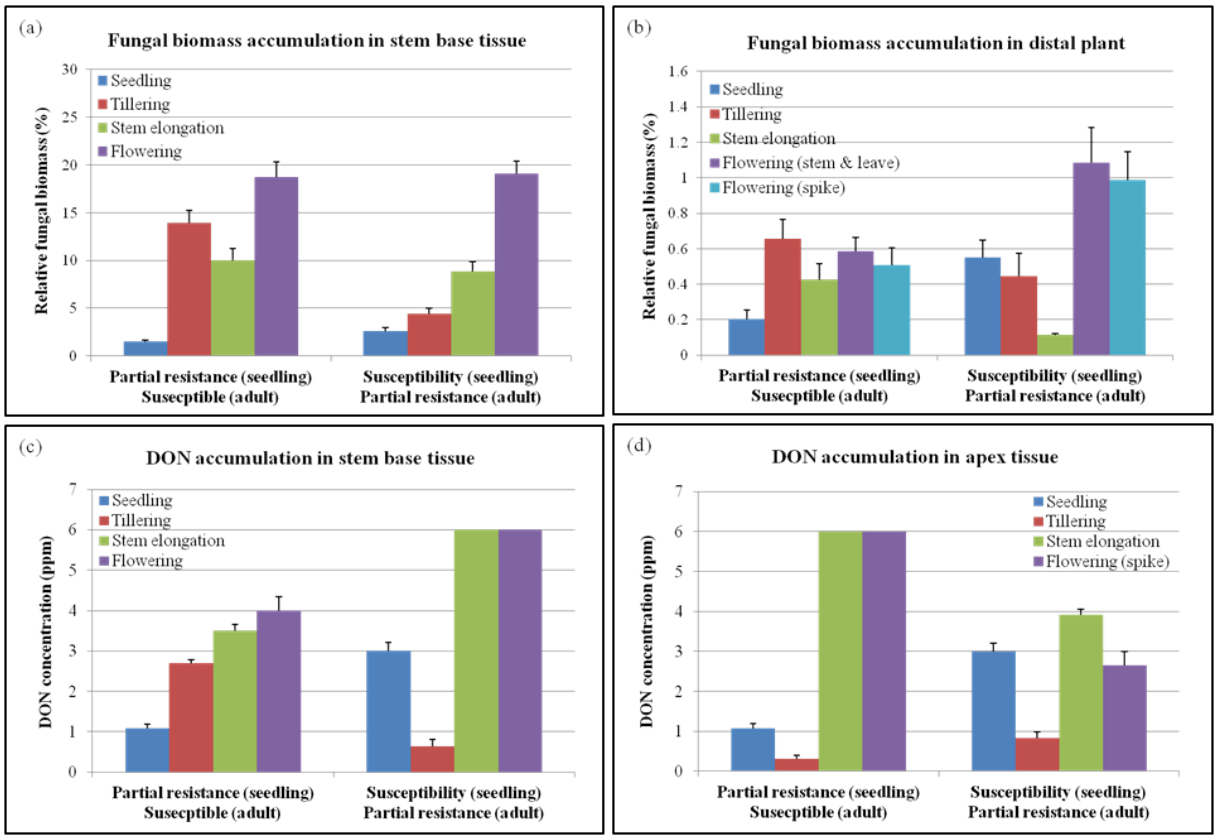

Figure 17: F. graminearum colonization and DON accumulation in partially resistant and susceptible interactions at different plant growth stage. (a) Relative fungal biomass in stem base. (b) Relative fungal biomass in distal plant. (c) DON accumulation level in stem base. (d) DON accumulation level in apex tissue. Relative fungal biomass and DON levels are compared between two groups of wheat genotpyes: cv. Florence-Aurore with seedling partial resistance (left) and cultivars Sumai 3, Frontana and Ning 7840 with seedling susceptibility (right). Growth stages are determined according to the Zadok's scale.

5.4.1 Assessment of relative fungal biomass

The disease progression curves shown in Figure 16 reveal three relevant aspects. First, *F. graminearum* was able to infect wheat roots even at the post-seedling, stem elongation stage. Thus, resistance against initial infection was not observed in adult plant roots, equal to observations made in the seedling stage. Second, the further pathogen progression showed differential *F. graminearum*-wheat interactions in response to a successful root infection. Third, these results demonstrate that *F. graminearum* is able to colonize wheat roots until the heading stage, thus during the pre-flowering stages important for spikelet initiation and development, processes that are also sensitive to abiotic stresses.

In adult roots of cv. Florence-Aurore, known for its partial seedling resistance to FRR, much higher RFB values were found at all timepoints (Fig. 18a). A first peak of biomass accumulation

was found at 3 and 5 dai, which was corresponding to the root colonization phase identified in the previous study seedling stages. Interestingly, the pathogen biomass peaked again at 21 dai, a phenomenon that was found to be characteristic for a high susceptibility at seedling stages. The *F. graminearum* development in adult roots of cv. Sumai 3 was fitting a quadratic trend which peaked at 5 dai (Fig. 18b) which was equal observations in seedling roots. However, the RFB values were considerably higher than those from seedlings. The pathogen accumulation in adult cv. Frontana roots (Fig. 18c) showed a positive linearity similar to observations in seedling roots until the timepoints 14 and 21 dai. In adult roots the sudden increase of fungal biomass was absent which was characteristic for the susceptibility at seedling stages. The phenomenon of an interrupted fungal biomass increase was likewise observed for the cv. Ning 7840 (Fig. 18d) which, however, showed generally much lower fungal accumulations in adult roots compared to seedling roots.

The mixed rANOVA revealed significant 'Time' effect and 'Time x Genotype' interaction for the trait RFB (Table 5) which confirmed the observed developmental changes in fungal growth over time (Fig. 18a-d), and demonstrated that the factor genotype had an influence on the fungal development. For the fungal development in adult roots the post-hoc pairwise comparisons (Bonferroni) showed similar significant changes in the general fungal growth between 1 to 3 dai and 10 to 14 dai. Hence, the model of a three-phase pathogen progression was also supported for adult plant stages since no significant differences were found between the timepoints 0.5 and 1 dai (phase I), between 3 to 10 dai (phase II) and between the final timepoints 14 to 21 dai (phase III), respectively. A difference between both wheat growth periods was the slightly extended disease phase II in adult roots.

In addition, similar to the seedling stages it was reasonable to assume the presence of a genotypic variation in the *F. gramiearum*-wheat root interactions also for the adult plant stages. To illustrate this genotypic variation, the respective mean values of fungal load across all timepoints were ranked in an ascending order (Fig. 19). This kind of benchmarking revealed a spectrum of mean RFB values ranking from 2.45% (cv. Ning 7840) to 4.23% (cv. Florence-Aurore). In contrast to the seedling stage, cv. Ning 7840 exhibited the lowest RFB ranking here, while cv. Florence-Aurore in this study showed the highest RFB ranking. Consequently, at adult plant stage the cv. Ning 7840 expressed a relative partial resistance to FRR, while the cv. Florence-Aurore showed the relative highest level of susceptibility. However, the mean RFB values observed for adult cv. Ning 7840 roots were, nevertheless, higher compared to those observed for cv. Florence-Aurore at the seedling stage (Fig. 19). Also, the cv. Sumai 3 exhibited higher RFB values compared to the seedling stage, and solely the cv. Frontana had a similar FRR

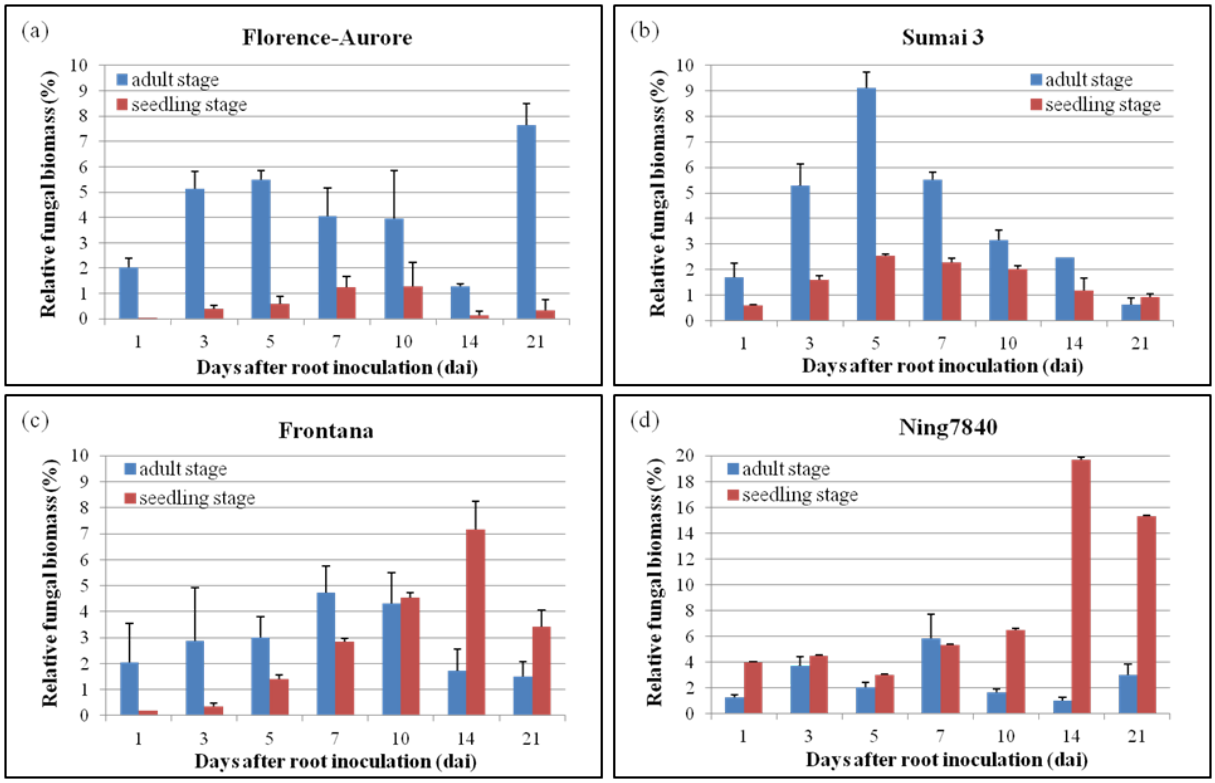

Figure 18: Comparision of RFB development between the seedling and adult stages of four wheat genotypes. qPCR based quantification of fungal biomass: Relative fungalbiomass is expressed as ratio between *F. graminearum* DNA and wheat root DNA by using gene-based qPCR approach. In each diagram the error indicator represents the average standard error of the mean (SEM).

Table 5: Results of the repeated measures ANOVA for relative fungal biomass (RFB) and root biomass reduction (RBR)

	Relative fungal biomass				Root biomass			
	F-value	p-value	Effect	Trend [1)]	F-value	p-value	Effect	Trend [1)]
Adult plant growth								
Treatment [2)]	-	-	-	-	16.22	.001 **	0.52	Linear
Time [2)]					1.25	n.s.	-	
Time × Treat. [2)]	-	-	-	-	1.61	n.s.	-	
Time [3)]	5.26	.004 **	0.31	Cubic	1.74	n.s.	-	-
Time × Genotype [3)]	3.14	.007 **	0.44	Cubic	1.83	.043 *	0.31	Linear

* Significant at level $p \leq 0.05$; ** significant at level $p \leq 0.01$; *** significant at level $p \leq 0.001$; n.s. non-significant. In all rANOVA analyses no sphericity could be assumed ($P < 0.05$, Mauchly's test) and results were therefore corrected based on the Greenhouse-Geisser F-test. The F-value indicates that differences between timepoints are greater than would be expected by chance or by error. The effect size gives the strength of associations between effect (main effect or interaction) and dependent variable (measurement).

[1)] Results of the trend analysis (test of inter-subjects contrast) on significant time effects, reasonable (significant) pattern in means are: linear trend; quadratic; cubic; and SMA (simple moving average) as non-linear trends. [2)] Two-way rANOVA on root and shoot development in infected and uninfected seedlings. [3)] Mixed rANOVA on disease progression in terms of fungal growth, reduction in seedling root and shoot biomass, and visible symptom development, including data of all 12 wheat genotypes.

Table 6: Results of the repeated measures ANOVA for relative fungal biomass (RFB) and root biomass reduction (RBR)

	Root length					Shoot length				
	F-value	*p-value*		Effect	Trend [1)]	*F-value*	*p-value*		Effect	Trend [1)]
Adult plant growth										
Treatment [2)]	26.69	.001	**	0.79	Linear	28.92	.000	***	0.43	Linear
Time [2)]	4.51	.018	*	0.39	Linear	6.69	.000	***	0.15	Cubic
Time × Treat. [2)]	5.75	.048	*	0.45	Linear	5.10	.000	***	0.12	Linear
Time [2)]	4.39	.036	*	0.52	Linear	6.75	.000	***	0.16	Linear
Time × Genotype [3)]	1.44	.288	n.s.	-	-	2.35	.004	**	0.16	SMA

* Significant at level $p \leq 0.05$; ** significant at level $p \leq 0.01$; *** significant at level $p \leq 0.001$; n.s. non-significant. In all rANOVA analyses no sphericity could be assumed ($P < 0.05$, Mauchly's test) and results were therefore corrected based on the Greenhouse-Geisser F-test. The F-value indicates that differences between timepoints are greater than would be expected by chance or by error. The effect size gives the strength of associations between effect (main effect or interaction) and dependent variable (measurement).
[1)] Results of the trend analysis (test of inter-subjects contrast) on significant time effects, reasonable (significant) pattern in means are: linear trend; quadratic; cubic; and SMA (simple moving average) as non-linear trends. [2)] Two-way rANOVA on root and shoot development in infected and uninfected seedlings. [3)] Mixed rANOVA on disease progression in terms of fungal growth, reduction in seedling root and shoot biomass, and visible symptom development, including data of all 12 wheat genotypes.

response at both developmental plant stages. Nevertheless, for the adult plant stages an altered response of wheat to *F. graminearum* root invasion was observed which obviously represents a genotypic inversion in the responses, especially with regard to the opposite extremes of the ranking scale.

5.4.2 Phenotypic evaluation of adult stage wheat root responses to FRR

In order to understand the interaction between wheat and *F. graminearum* during the adult wheat development, developmental traits were monitored in terms of root biomass reduction (RBR), root length reduction (RLR) and shoot length reduction (SLR) (Fig. 20).

Also, for adult wheat plants successful root invasions by *F. graminearum* were accompanied by quantifiable adverse impacts on the root and plant growth (Fig. 20). Moreover, as previously reported for seedlings, high RFB values were associated with higher levels of root biomass reduction, while low RFB values were associated with lower impacts on root biomass. The root biomass reduction observed for cv. Florence-Aurore showed an average of 61% and root length reduction was on average 15%, while in the case of cv. Ning 7840 the corresponding average reductions were 29% and 8%, respectively.

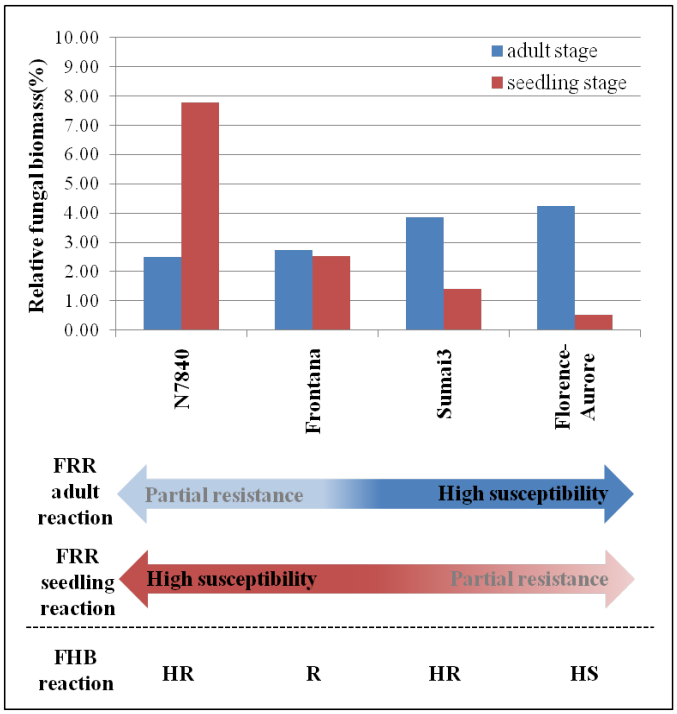

Figure 19: Comparision of relative fungal biomass (RFB) values based Fusarium root rot severity between seedling and adult stage. Wheat genotypes are ranked according to mean values of RFB (ratio between fungal DNA and wheat root DNA) over the time period between 1 to 21 days after root inoculation. The observed FRR measures show a range of severity from partial reisistance to high susceptibility. For all genotypes the known reactions to Fusarium head blight (FHB) are indicated: HR, highly resistant; R, resistant; HS, highly susceptible.

The two-way rANOVA demonstrated significant 'treatment' effects for all three developmental traits (Table 5 and 6) and thus, the root infections by *F. graminearum* were confirmed as causative for the observed developmental differences between inoculated and non-inoculated plants. While the significant 'time' effects demonstrated changes in the general time trend of root and shoot growth during the course of wheat developments, the significant 'treatment × time' interactions showed that FRR is not only characterized by significantly reduced wheat growth rates, but also by a basically non-parallel disease dynamics between treated and control plants (Fig. A2b, c). The biomass development of roots was the only exception from the non-parallel dynamics since 'time' effects and 'treatment × time' interactions were non-significant (Table 5), indicating a parallel trend across time in which root biomass levels of healthy and diseased plants develop at different levels, but with a constant distance between them (Fig. A2a). The mean profile plots demonstrated the begin of an increase in deviations in root and shoot length between diseased and healthy plants at 7 (root length) and 10 dai (shoot length), respectively (Fig. A2b, c). Thus, also during the interactions between F. graminearum and adult wheat roots, the phase II in fungal progression was found to critical by being associated with significantly increasing impacts on the plant development. For root biomass the rANOVA made the assumption of a

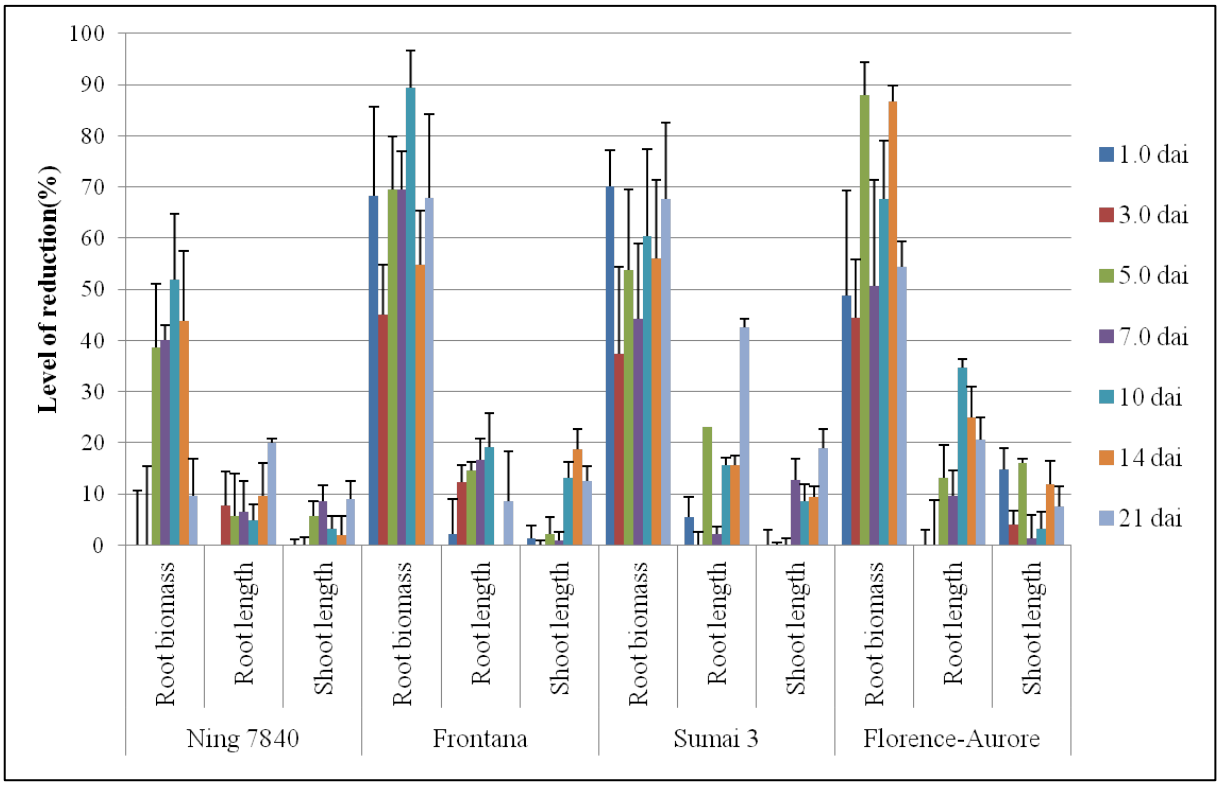

Figure 20: Time-course assessment of *F. graminearum*-wheat root interactions at adult stage of cultivarsFlorence-Aurore, Frontana, Sumai3 and Ning 7840.Time-course reduction of root biomass (qPCR based), reduction of root length and reduction of shoot length. The level of reduction is expressed as the ratio ofthe average uninfected and and infected root biomasses, root length or shoot length, respectively. Vertical bars represent the average standard error of mean (SEM).

significant 'treatment × time' interaction (F = 10.52; p = 0.005) under consideration of a simple moving average (SMA) trend. Although such an assumption has to be considered with caution due to the non-significance of 'time' and 'treatment × time' interaction, it was obvious that the predicted trend of a sequence of peaks and valleys coincides with the root biomass profiles observed for healthy as well as diseased plants (Fig. A2a). Finally, the results obtained by two-way rANOVA statistics indicated for both inoculation experiments a disease dynamics which was characterized by a sudden increase in the impacts on wheat plants, early for roots than for shoots.

This dynamics was further elucidated by using a mixed rANOVA on the general FRR progression (across all four genotypes) in terms of relative fungal growth (RFB) and reductions in root and shoot growth (RBR, RLR, SLR). This analysis confirmed significant effects of time showing that the FRR disease progression basically changed in seedling and adult plants at one or more timepoints (Table 5 and 6). Also, for the trait adult root biomass reduction the tested 'time' effect was not significant, demonstrating constant root reductions over time as could be expected due to the non-significant 'treatment × time' interaction (Table 5). Significant 'time ×

genotype' interactions were obtained for all severity traits, except the root lenght reduction (Table 5 and 6). This demonstrated that also for adult plants basically genotype effects on the developments of fungal biomass and seedling performances can be assumed.

Finally, by the examination of FRR in adult plants it was not possible to obtain reliable results on the visible symptom development on roots and stem bases. This may also be explained by specifities of the adult root development which will be particularly discussed in chapter 6.2.2. Nevertheless, the general progression and impact of FRR on the root and plant biomass were consistent with previous observations on the root rot severity in wheat seedlings. The rANOVA of RFB data even support the three-period pattern of pathogen progression already described for the seedling stage. In addition, an inverse response to FFR between seedling and adult plant/root developmental stages as reported for the RFB was supported by the data obtained for the impact of FRR on adult plants.

5.4.3 Comparison of FRR disease index at seedling and adult stages

To illustrate the genotypic variation in the wheat root - *F. graminearum* interactions at adult plant stages suggested by mixed rANOVA, all genotypes were ranked according to to the FRR disease index (Fig. 21) as a comparative presentation of seedling and adult plant root inoculation experiments. By combining the developmental traits (RBR^{SI}, RLR^{SI}, SLR^{SI}) with the relative fungal biomass (RFB^{SI}), a Fusarium disease index (FDI) was calculated for each cultivar. Finally, the FDI from seedling and adult stage testing were compared (Fig. 21). A lower FDI is considered equivalent with higher resistance against FRR, while a higher FDI is considered synonymous with higher susceptibility. Compared to other cultivars at the adult stage, cv. Florence-Aurore, partially resistant in the seedling stage, showed high FRR susceptibility in the adult stage. On the other hand, cv. Ning7840, highly susceptible in the seedling stage expressed partial resistance at the adult stage. The comparison of FDI ranking consequently indicated inverse FRR reactions in the seedling and adult plant stages. To my knowledge, such an inverse reaction was first time reported in this study. Morever, the adult-plant FRR reaction was similar to the FHB reaction: cv. Ning 7840, partially FRR resistant in the adult stage shows high resistance to FHB, but cv. Florence-Aurore, highly FRR susceptible in the adult stage shows high susceptibility to FHB. The similarity reactions regarding both FRR and FHB reactions in the adult stage gives hint that the FRR resistance mechanism in both cases may share common features, and that the FRR resistance switch between FRR in seedlings and FRR or FHB in adult plants may have similar mechanisms in these three "diseases".

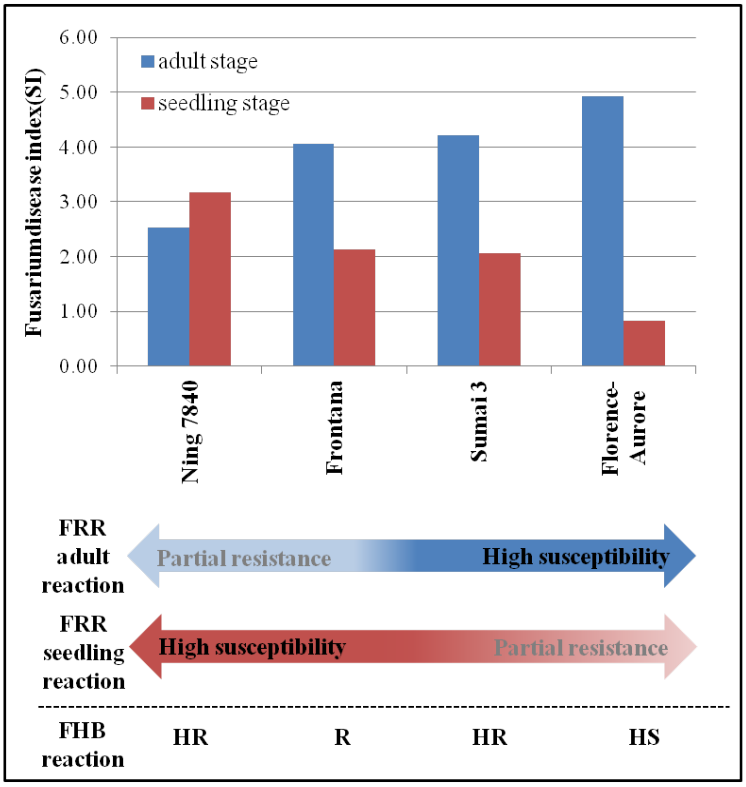

Figure 21: Comparison of FRR disease index (FDI) at seedling and adult plant stage. The FDI is calculated based on susceptibility indices (SI) for (i) relative fungal biomass (RFB), (ii) root biomass (RB); root length (RL) and shoot length (SL) reduction; and (iii) root symptoms (RS) [FDI= RFB^{SI}+RBR^{SI}+RLR^{SI}+SLR^{SI}]. The observed FDI values show a range of severity form partial resistance to high susceptibility. For all genotypes the known reactions to FHB were listed: HR highly resistant; R resistant; HS highly susceptible, and the known reaction to FRR in the seedling stage were illustrated.

5.5 Gene expression analyses of FHB/DON resistance candidate genes in wheat seedlings and adult roots

The differences and possible similarities of wheat defence against the floral disease FHB and the soil-borne diseases FRR and FCR are currently discussed. In this context, the activity of different resistance candidate genes involved in two main defence mechanisms (DON detoxification and JA-triggered basal defence) as well as miscellaneous pathogenesis- or defence-related genes were tested in this work - to my knowledge for the first time in wheat roots (Table 2). At the seedling and adult stages, reverse reactions of wheat to the FRR and FRR diseases were observed, and the fungal biomass level indicated that the resistance mechanism might be similar between these two stages. Meanwhile, many FHB related genes were identified in extensive research work. Such genes can be applied as candidate genes to study FRR adult resistance. Four cultivars, Florence-Aurore, Sumai3, Frontana and Ning 7840 were selected from 0.5 to 21 dai to detect the possible FRR resistance mechanism(s) based on genes involved in detoxification, the JA pathway and other mechanisms: to study (i) whether these FHB related genes can be induced

at seedling stage FRR; (ii) how does these genes react to seedling FRR; (iii) whether they are associated to seedling FRR resistance; (iv) whether these FHB related genes can be induced in adult stage FRR; (v) whether they are associated to adult FRR resistance; (vi) whether these genes can also react inversely between the seedling and adult plant stage corresponding to the inverse reaction in FDI ranking (Fig. 21); (vii) whether these genesare (equally) involved in resistance mechanisms regarding seedling FRR, adult FRR and FHB.

5.5.1 Analyses of resistance candidate genes associated to the DON detoxification mechanism

Detoxification is one of the main resistance mechanisms in wheat spikes against *Fusarium* species. Therefore, the analysis of detoxification-related genes was also targeted at defense mechanisms against the FRR disease, at both the seedling and adult stage. For this purpose, genes associated with DON detoxification, i.e.*TaUGT3* (UDP glucosyltransferase protein), *HvUGT13248,* a homologue of the barley UDP-glucosyltransferase gene, *CYP709C1* (cytochrome P450 gene) and *TaMDR1* (MDR-like ABC transporter) were analyzed.

In seedling roots, *HvUGT13248* and *TaUGT3* were induced early and peaked around 3 dai during the early infection stage (Fig. 22a, c) in cv. Florence-Aurore (partial seedling resistant). On the opposite, these two genes only showed slightly changed expression in three other susceptible cultivars at the same timepoint (Fig. 22a, c), which is the main infection and colonization stage. In adult roots, these two genes peaked around 1 dai during the early infection stage in cv. Ning 7840 (adult partially resistant), but reacted late (around 5 dai) at main infection and colonization stage in cv. Florence-Aurore, adult highly susceptible (Fig. 22b, d). Similarly, in seedling roots, *CYP709C1* showed a high expression change (55-fold at 0.5 dai, 350-fold at 5 dai and 60 fold change in 7 dai) in cv. Florence-Aurore (partially FRR seedling resistant) (Fig. 22e). During the same time points, susceptible cultivars almost showed no expression at the main infection and colonization stages until 7 dai (Fig. 22e). In adult roots, *CYP709C1* was relatively higher and constantly expressed as expected during the early infection stage in cv. Ning 7840 (partially FRR adult resistant), but relative low level and late change during the main infection and colonization stages in the susceptible cv. Florence-Aurore (Fig. 22f). As compared to the three genes above, *TaMDR1* expression pattern is completely different. In seedling roots, *TaMDR1* peaked the main infection and colonization stages after 10 dai in cv. Florence-Aurore (Fig. 22g). But in cv. Ning 7840, it peaked already at 5 to 7 dai (Fig. 22g). Such similar expression pattern for both cultivars was also seen in adult roots (Fig. 22h). Thus, the gene *TaMDR1* may not be involved in seedling FRR resistance.

Summarizing, at the seedling and adult stages the main defense candidate genes *TaUGT3*, *HvUGT13248* and *CYP709C1* possibly involved in the assumed wheat detoxification mechanism showed exclusive expression during early infection stages in roots of partially resistant genotypes. Their expression was associated with significantly impaired fungal accumulation, or partial resistance to FRR, respectively. The expression of detoxification related genes suggests that FHB induced detoxification genes also can be triggered by FRR disease, and were associated to FRR resistance and FRR disease progression at both seedling and adult stages; moreover, the inverse reaction of the three genes corresponded to the inverse resistance in seedling and adult stages.

5.5.2 Analyses of resistance candidate genes associated to the Jasmonate-triggered defence mechanism

The jasmonate (JA)-triggered defence mechanism includes: JA biosynthesis, JA signal transduction and the expression of JA-response genes. In this work, *Lox* (lipoxygenase), which respond to JA biosynthesis; *COI1* (coronatine insensitive1), *JAZ* (jasmonate ZIM domain) and *MYC2*, involved in JA signaling transduction; *PR-4* (vacuolar defense proteins) and *PR-14* (non-specific lipid transfer proteins), regulated by the JA pathway, were tested in the roots of adult and seedling stages to analyze whether the JA pathway is involved in the root-pathogen interaction and associated with FRR resistance at the adult and/or seedling stages.

Lox-2 and *COI1* were no differently expressed in partially resistant and susceptible cultivars at the seedling and adult stages, in all cultivars (Fig. 23a-d). *MYC2* was up-regulated in all other cultivars at both seedling and adult stages, except cv. Frontana at the seedling stage and cv. Sumai3 at the adult stage (Fig. 23e, f).

In seedling roots, *JAZ* was induced with early (0.5 dai) and 20-fold change vs control and peaked in 5 dai (>250-fold), a period which covers the early infection stage in cv. Florence-Aurore (Fig. 24a). On the opposite, the highly susceptible cv. Ning 7840 showed a later expression (at 3 dai) and peaked at 7 dai (Fig. 24a) i.e. at main colonization and the beginning of distal plant colonization stages. In adult roots, the expression of *JAZ* was first induced in cv. Ning 7840 (1 dai) and Sumai3 (3 dai) in the early infection stage; whereas, the cv. Florence-Aurore showed gene expression from 5 dai on (Fig. 24b). The expression pattern of *JAZ* in both seedling and adult roots was consistent with its expression in spike (Fig. A3). In seedling roots, the *PR-4* gene peaked at the early infection stage (3 dai) of the partially resistant cv. Florence-Aurore However, this gene peaked later at 5 dai in roots of the highly susceptible cv. Ning 7840 (Fig. 24c). In adult roots, the cultivars Sumai 3 and Frontna showed an up-regulation of *PR-4* gene at 1 dai and 5 dai, respectively (Fig. 24d). But, the cultivars Ning 7840 and Florence-Aurore showed a late reaction

at 10 dai. *PR-14* showed an expression pattern similar to *PR-4* in seedling roots (Fig. 24e). In adult roots, *PR-14* was expressed in the early period (0.5 to 1 dai) in the cultivars Sumai 3 and Ning 7840, while *PR-14* expression occurred in roots of cv. Frontana at 5 dai. Expression of *PR-4* in cv. Florence-Aurore was similar to *PR-4* much later (at 10 dai) consistent with the cultivar's higher susceptibility at post-seedling developmental stages (Fig. 24f).

The expression patterns of *JAZ, PR-4* and *PR-14* gave some indication that JA-triggered defence mechanism may be associated with FRR partial resistance in both seedling and adult stages, similar to the detoxification related mechanism. In fact, such an involvement of JA-triggered defense was demonstrated for FHB in a current study performed in our lab (Fig. A3, 4). JA-defense was active much earlier during the first tissue infection compared to the DON resistance. Moreover, very recent results from a gene expression study in seedling roots covering an earlier period than presented here (2h after root inoculation and 3 dai), confirmed this assumption at least for the seedling stages (Fig. A3).

5.5.3 Analyses of miscellaneous resistance candidate genes

Besides hormone-related and detoxification defense, there are other mechanisms and genes involved in the wheat resistance to *F. graminearum*. In this study, *WZF1 a* zink finger transcription factor and *WFhb1-C1* a recent published candidate gene for the major resistance QTL *Fhb1* was tested (Table 2).

In seedling roots, *WZF1* was constantly up-regulated from 0.5 dai on and peaked at 5 dai and thus, expression covered the critical disease stages I to III during interactions between the pathogen and cv. Florence-Aurore leding to partial resistance (Fig. 25a). In contrast, in roots of highly susceptible cv. Ning 7840 the gene was up-regulated and peaked not before 7 dai (Fig. 25a) through the whole time course tested. In adult roots, the gene *WZF1* showed an expression pattern similar to seedling roots, but early up-regulated in the genotype cv. Ning 7840 and late up-regulated in the cv. Florence-Aurore (Fig. 25b). Similar to *WZF1*, in seedling roots *WFhb1-C1* was not induced in susceptible genotypes Sumai3, Frontana and Ning 7840, while it showed high and continued fold change (0.5 to 5 dai) during the early infection stage in partially resistant cv. Florence-Aurore (Fig. 25c). In adult roots, *WFhb1-C1* showed strong expressions in the cultivars Ning 7840, Sumai3 and Frontana between 0.5 and 1 dai, while there was no fold-change in the roots of highly susceptible cv. Florence-Aurore until 3 dai (Fig. 25d). Finally, the reaction of these two genes indicated that *WZF1* and *WFhb1-C1* were all associated with FRR partial resistance in both seedling and adult stages and also showed inverse reaction which was consistent with wheat response to *F. graminearum* infection at the seedling and adult stages.

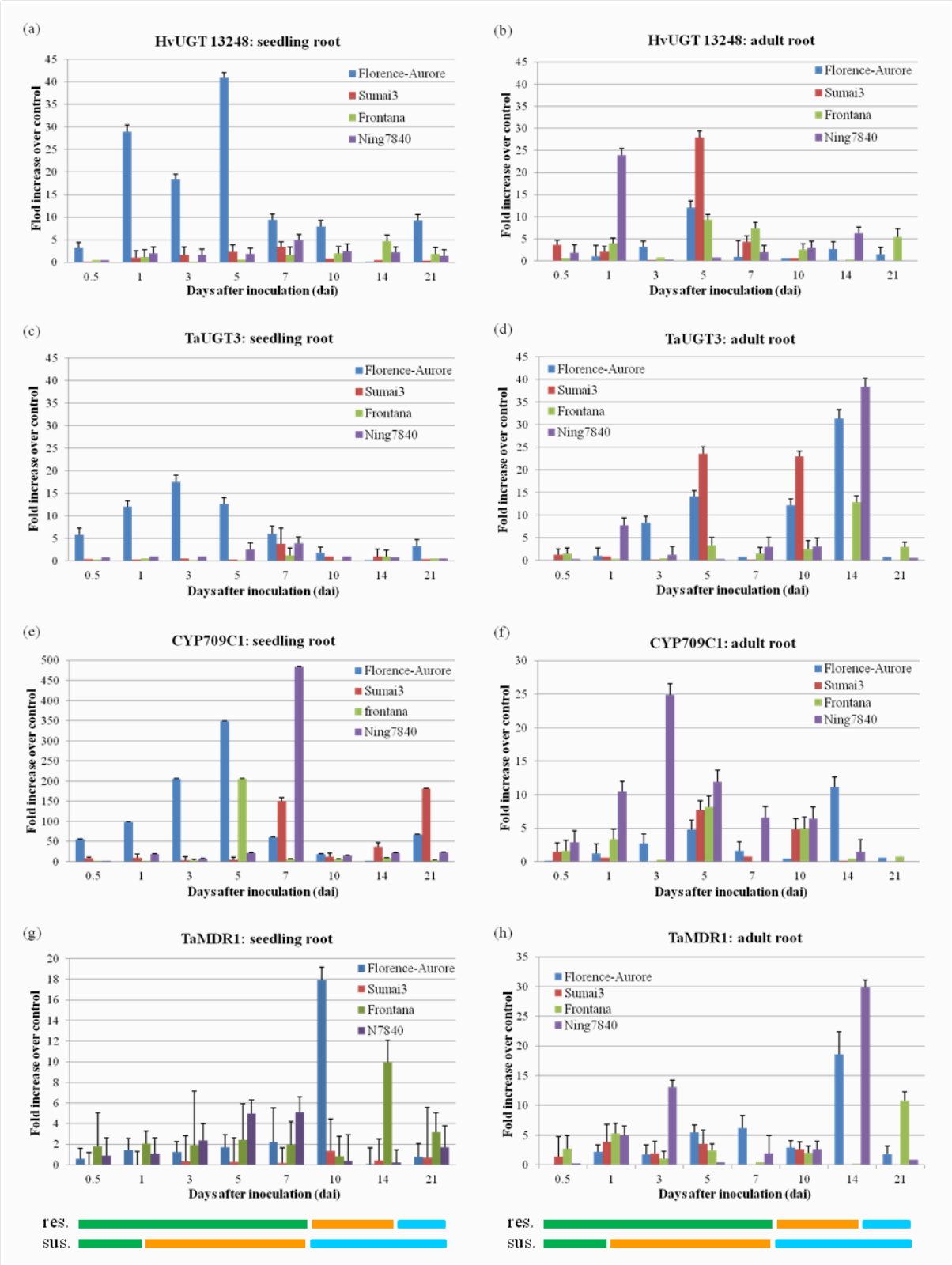

Figure 22: qRT-PCR results of detoxification related genes in Florence-Aurore, Sumai 3, Frontana and Ning 7840 in seedling and adult stage roots after inoculation with *F. graminearum* IFA65. The expression levels on the y-axis were relative to non-inoculated sample from each genotype after normalization with the wheat Ubiquitin gene. The experiment was repeated twice, and data were presented as average+-S.D with n=3. The color bar blow indicated disease progression of partially resistant and highly susceptible genotypes. Green: root early infection; orange: root main infection and colonization; blue: root and distal plant colonization.

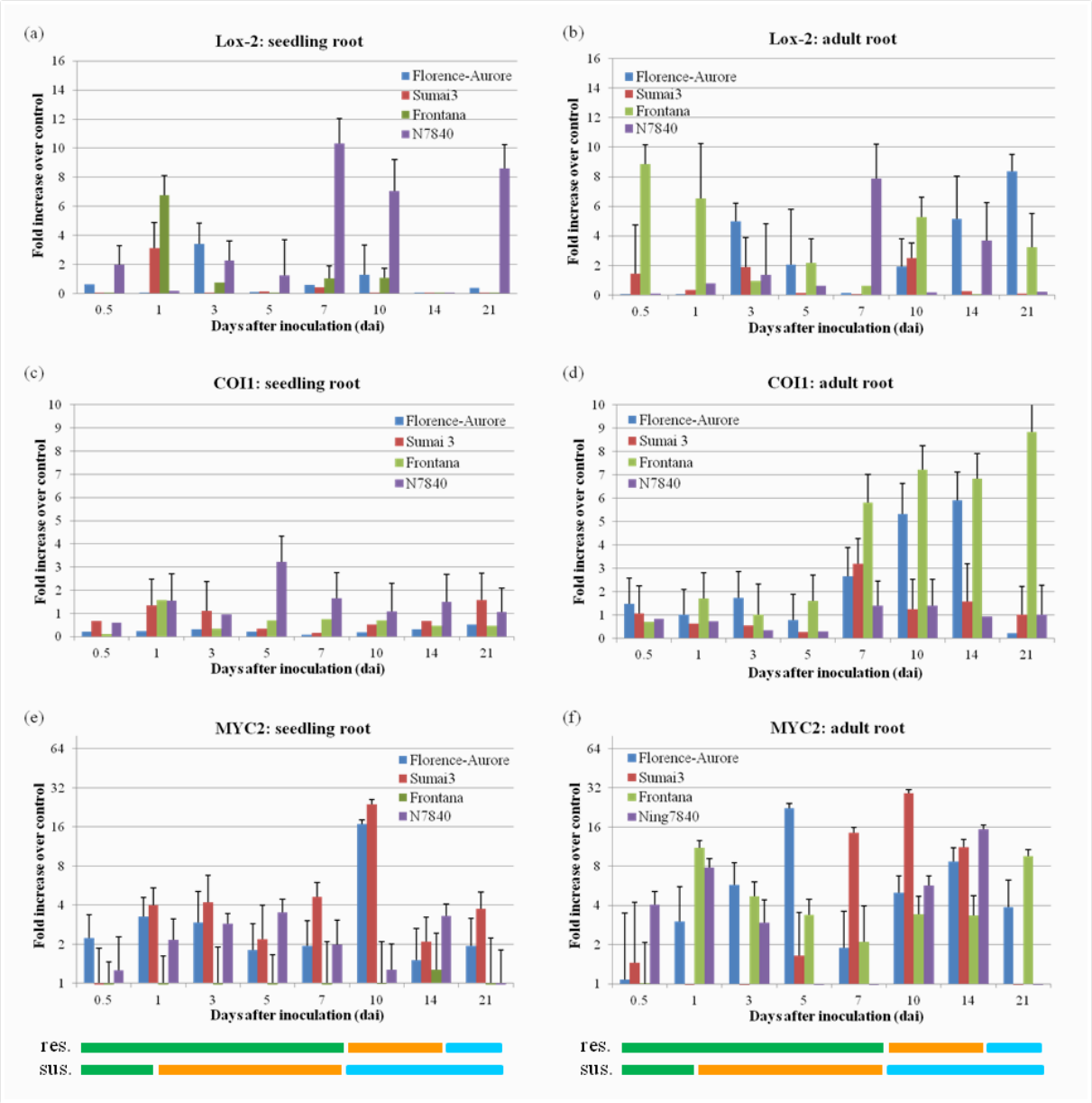

Figure 23: qRT-PCR result of the genes involved in the JA-signaling pathway in Florence-Aurore, Sumai 3, Frontana and Ning 7840 in seedling and adult stage roots after inoculation with *F. graminearum* IFA65. The expression levels on the y-axis were relative to non-inoculated sample from each genotype after normalization with the wheat Ubiquitin gene. The experiment was repeated twice, and data were presented as average+-S.D with n=3. The color bar blow indicated disease progression of partially resistant and highly susceptible genotypes. Green: root early infection; orange: root main infection and colonization; blue: root and distal plant colonization.

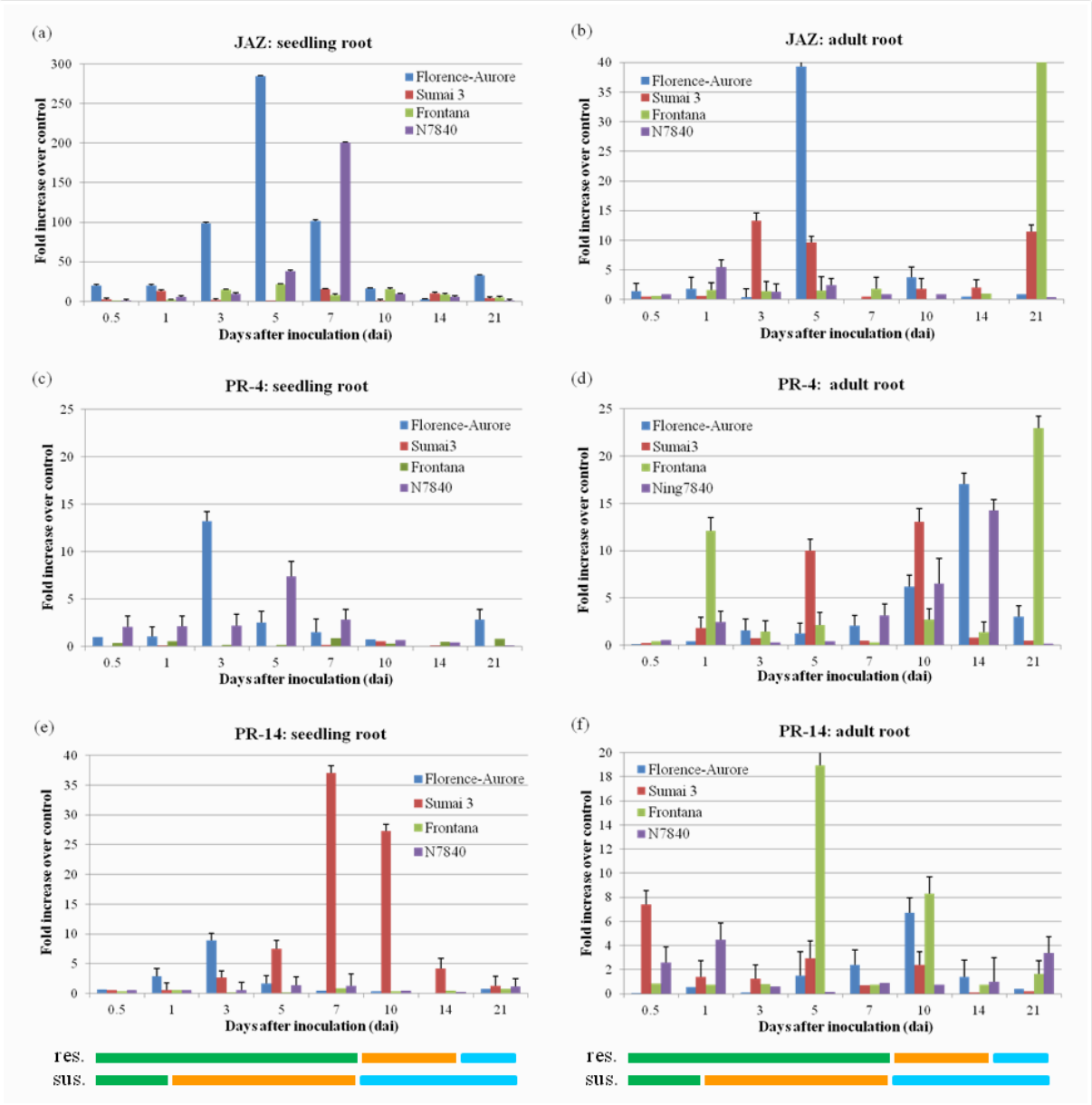

Figure 24: qRT-PCR result of the JA pathway responsive genes in Florence-Aurore, Sumai 3, Frontana and Ning 7840 in seedling and adult stage roots after inoculation with *F. graminearum* IFA65. The expression levels on the y-axis were relative to non-inoculated sample from each genotype after normalization with the wheat Ubiquitin gene. The experiment was repeated twice, and data were presented as average+-S.D with n=3. The color bar blow indicated disease progression of partially resistant and highly susceptible genotypes. Green: root early infection; orange: root main infection and colonization; blue: root and distal plant colonization.

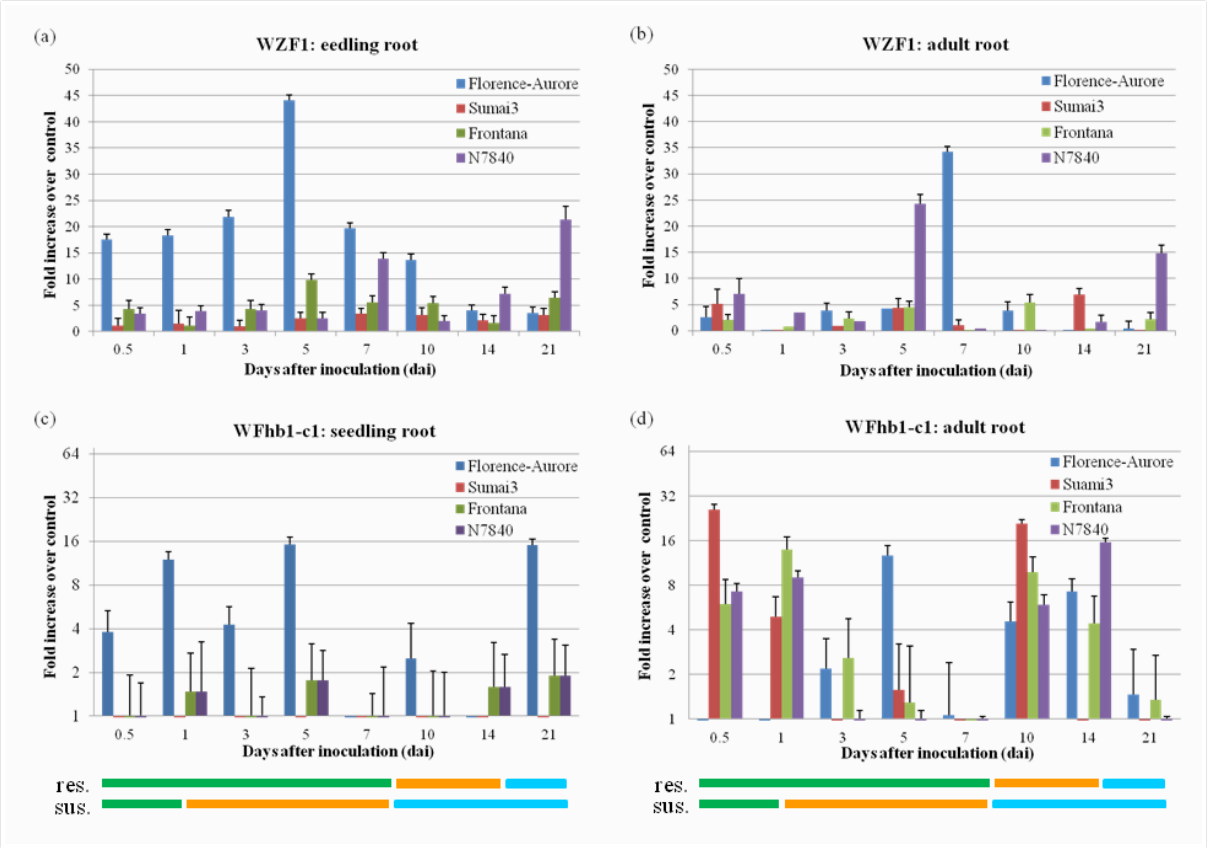

Figure 25: qRT-PCR result of plant defense related genes in Florence-Aurore, Sumai 3, Frontana and Ning 7840 in seedling and adult stage roots after inoculation with *F. graminearum* IFA65. The expression levels on the y-axis were relative to non-inoculated sample from each genotype after normalization with the wheat Ubiquitin gene. The experiment was repeated twice, and data were presented as average+-S.D with n=3. The color bar blow indicated disease progression of partially resistant and highly susceptible genotypes. Green: root early infection; orange: root main infection and colonization; blue: root and distal plant colonization.

6 Discussion

6.1 'Sensitive' and 'Tolerant' responses to FRR

The genotype ranking reflects the relationship between fungal accumulation (Fig. 6) and the negative effects on the seedling (Fig. 7). However, concerning RLR (Fig. 7b) and SLR (Fig. 7c) the partially resistant genotypes were not the best, and the highly susceptible genotypes were not always the worst, even if exceptionless showing relative less impact on seedlings. For instance, the cv. Sumai 3 demonstrated high negative effects on RLR (Fig. 7b), SLR (Fig. 7c) and CSI (Fig. 7e), while cv. Tabasco showing low impacts on RLR (Fig. 7b) and SLR (Fig. 7c), although the observed RFB levels for both genotypes suggested an opposite situation as well as an intermediate ranking (Fig. 6).

To understand these alterations the terms tolerance and sensitivity were consulted. Indeed, these terms have to be used with caution since they bring some subjectivity into the description of disease severity. However, the conducted rankings allowed a precise definition for both terms. In this study, the term relative "tolerance" was used and applied to a wheat genotype in which RFB could be accumulated (Fig. 6) and symptom developed without causing (substantial) growth and biomass reduction. In contrast, the term relative "sensitivity" was used for a genotype which showed disease symptoms accompanied by significant growth reduction compared to relative low RFB. The terms partial resistance and susceptibility refereed to genotypes which demonstrated rates of RFB and FRR severity with consistent low or high levels.

A relative tolerance could be stated for the cv. Tabasco which, despite its location in the susceptible category (Fig. 6), did not display significant reductions in root and seedling length (Fig. 7b, c). Moreover, root biomass reductions were comparable moderate (Fig. 7a) and were not significant before 10 dai (Fig. 4e). In contrast, the cv. Wangshuibai was displaying considerable root and shoot length reductions (Fig. 4e). Interestingly, root biomass reductions were similar for cultivars Tabasco and Wangshuibai, further supporting the observation that the loss of root biomass is the most severe impact coming along with FRR. The relative better performance of cv. Tabasco seedlings after *F. graminearum* root invasion was also displayed by relatively low ratings of root and stem base symptoms which, however, were still higher than those of the partially resistant genotypes (Fig. 7d, e). A relative sensitivity was stated for the susceptible cv. Sumai 3 (Fig. 6) by exhibiting biomass reduction rates (Fig. 7a, b, c) and visible symptoms (Fig. 7d, e) significantly exceeded the rates typically observed for other genotypes in same category. In all rankings except for RFB, cv. Sumai 3 was the most susceptible genotype (Fig. 6). The high sensitivity of Sumai 3 is also supported by a direct comparison with

Wangshuibai which at similar fungal biomass levels (Fig. 6) was ranked better than Sumai3 (Fig. 7).

The cv. Remus was ranked very low for all developmental traits (Fig. 7a, b, c) which were determined by an extraordinary pathogen-host interaction. This genotype-specific reaction was characterized by a temporary suppression of the root rot disease and a sudden increase of disease symptoms at 10 dai. In fact, FRR started gradually with intermediate RFB levels (1.38 -2.10%, Fig. 4c) associated with a tolerant seedling reaction expressed as a low disease severity since no significant RBR, RLR and SLR values were observed in Remus (Fig. 4f). However, from timepoint 10 dai on the root invasion by *F. graminearum* began to increase considerably and cumulated at 14 -21 dai with sharp RFB peaks from initially 3.60% to 8.80 and 9.24%, respectively. In fact, this pattern of RFB progression in Remus fully agreed with the observed response pattern of plant biomass (RBR) which, for example, reached a value of 79.0% at timepoint 21 dai (Fig. 4c, f). Whereas the RBR and RLR values were statistically significant before 14 dai, the values for SLR was not significant before 21 dai (Fig. 4f). While the pathogen spread and the immediate impact on seedling development of cv. Remus were temporarily suppressed, visible symptoms on the roots were already present at 3 dai indicating a severe impact on the root tissue.

Although the cv. Remus demonstrated a ʻtemporary disease suppressionʼ, the early fungal accumulation was still higher than observed in the roots of cv. Florence-Aurore and Line 162.11 (Fig. 4a, c). In addition, visible symptoms on the roots and stem bases of cv. Florence-Aurore and Line 162.11 appeared generally later and weaker (Fig. 4g, i). Besides a remarkable pathogen-host interaction, these observations also demonstrated a high level of accordance between different FRR severity traits representing different assessment approaches such as qPCR and size measurements as well as symptom ratings. Finally, differences between the RFB and phenotypic rankings were clearly due to significant genotype-specific responses of wheat to FRR rather than environmental effects.

6.2 The head blight pathogen *F. graminearum* undergoes developmental processes typical of root-infecting fungi

One of the most important outcomes of this study was the disclosure of a new aspect of the *F. graminearum* life cycle: The fungus can undergo a number of previously uncharacterized programmed developmental events that are typical of root-infecting pathogens (chapter 6.2.1 and 6.2.2). Thereby, *F. graminearum* was found to exhibit a high variability in its mode of infection, differentiation of infection structures and nutritional strategy. The observed developmental events resemble the mechanisms and timing described for spike colonization which is not

unexpected when considering the common aetiology between the different *Fusarium* diseases concerning the spikes and the roots, repectively (chapter 6.2.3).

Plant-pathogen interaction studies were performed by combining qPCR quantification of relative fungal biomass with bright-field and fluorescence as well as confocal laser scanning microscopy. The microscopy confirmed observations and measurements made during the analysis of FRR disease progression and could explain the causative fungal mechanisms of root infection and colonization. To discuss the general mode and mechanism of root infection and colonization emphasis was subsequently put on the susceptible interaction between the pathogen and Line 1105.16, while the specific characteristics which differentiate partial resistance from susceptibility will be discussed in chapter 6.4.

Finally, the different disease stages are presented as successive events since each stage is characterized and distinguishable from the others by specific fungal structures and disease events. However, this does not mean that disease stages are temporally limited to the respective timepoints of initial observation. In fact, developed hyphae structures were typically maintained and appeared simultaneously with newly developed structures, especially during the early disease stages. Nevertheless, the observed consecutive events characterise a programmed sequence of root disease development.

6.2.1 *F. graminearum* shows complex infection morphology in early disease stages

Stage I: The early infection stage was symptomless as observed on WGA Alexa Fluor 488® stained longitudinal root sections prepared at 0.5 and 1 dai. Stage I at 0.5 dai was characterized by first hyphae developing at the root surfaces originating for germinating macroconidia (Fig. 12a). It is likely that macroconidia are also the major source of inoculum during natural root infection. Macroconidia are produced already in the early stage of residue decomposition, while perithecia (fruiting bodies with ascospores) are produced much later, more advanced and growth conditions are less favourable.

At 1 dai roots were found to be completely enclosed by advanced hyphal networks (Fig. 12b) indicating a successful pathogen establishment. The formation of such networks prior to the initial host tissue penetration has been reported for different obligate soil-borne pathogens, for example, *Colletotrichum graminicola* causing anthracnose of maize (*Zea mays*) (Sukno et al., 2008), and *Verticillium longisporum* causing wilt diseases on many economically important crops such as oilseed rape (*Brassica napus*), tomato (*Solanum lycopersicum*) and potato (*Solanum tuberosum*) (Eynck et al., 2007). Interestingly, for both diseases the time lapse of infection was similar to rot root caused by *F. graminearum*. At 1 to 2 dai an intense hyphae colonization at the root surface was observable. These hyphae nets were commonly developed

from hyphae that initially grew parallel to the longitudinal root axis; subsequently hyphae branched and grew perpendicularly to the axis. At 2 to 3 dai, hyphae had already invaded the epidermal cells without causing macroscopically visible disease symptoms (Eynck et al., 2007; Sukno et al., 2008).

F. graminearum performs an equal strategy up to the initially symptomless penetration of root epidermis. At 1 dai initial hyphae were observed in epidermal and cortex cells of Line 1105.16, showing an inter- and intracellular growth (Fig. 12d). This corresponds to observations made for *F. culmorum* infecting roots of the wheat cv. Genio (Beccari et al., 2011) and of *Brachypodium distachyon*, a close wild relative of small grain cereals (Peraldi et al., 2011). Both studies reported a simultaneous colonization of epidermis and first cortex layer by inter- and intracellular growth at 1 dai. In accordance with observations by Beccari et al. (2011) and Peraldi et al. (2011) in the presented study macroscopic symptoms were observable at 1 dai first on the roots of a few susceptible and all highly susceptible genotypes (Fig. 5g-i) which developed rapidly until necrosis of the whole root (Fig. 8).

Simultaneously with first root infections *F. graminearum* frequently developed hyphal structures which are morphologically distinct from the net forming vegetative mycelium. Those were characterized by an obvious hyphal swelling formed on specialized hyphal branches (Fig. 12c). Additionally, from these hyphal swellings typically penetration pegs originated which had entered the root epidermis (Fig 12c). Those penetration pegs were distinguishable due to their much narrower structure compared to the normal hyphae in accordance with descriptions of Eynck et al. (2007). Therefore, these hyphal structures were referred to as infection hyphae. Short infection hyphae which developed during spike infections have been described for different *Fusarium* species (Kang & Buchenauer, 2000; Wanjiru et al., 2002; Kang et al., 2005). According to these reports infection hyphae originated from dense mycelia networks which were formed at the surfaces of the glume, lemma, palea or ovary by 0.5 to 1.5 dai. The described infection hyphae did not produce appressoria, but penetrated the epidermal cell wall directly with penetration pegs.

However, the morphological characteristics of putative infection hyphae observed in the present study were more similar to hyphal swellings which the leaf blast pathogens *Magnaporthe grisea* and *M. oryzae* specifically develop on rice roots (Sesma & Osbourn, 2004; Marcel et al., 2010; Tucker et al., 2010) than to those *Fusarium* infection hyphae observed during floret infection. The infection hyphae developed by *M. grisea* and *M. oryzae* resembled simple penetration structures of root-infecting fungi known as hyphopodia. Similar to the observations for *F. graminearum*, hyphopodia on rice roots were typically associated with infection pegs. Moreover,

also *M. grisea* and *M. oryzae*, originally described as leaf pathogens, were found to display a high ability to infect roots (Sesma & Osbourn, 2004; Marcel et al., 2010; Tucker et al., 2010). In addition, a high similarity was also visible to hyphopodia formed by the pathogen *Gaeumannomyces graminis*, causal agent of the soil-borne cereal disease take-all (Sesma & Osbourn, 2004), and to those formed at 3 dai by *C. graminicola* penetrating maize roots (Sukno et al., 2008). Generally, hyphopodia refer to simple penetration structures developed by root-infecting fungi at infection sites, often associated with infection pegs similar to those originatimg from appressoria. However, in contrast to appressoria that develop from swellings at the tips of conidial germ tubes originating from conidia, hyphopodia are structures that arise from mature vegetative hyphae (Howard, 1997).

Finally, it is likely that *F. graminearum* forms hyphopodia or hyphopodia-like structures on wheat roots for initial epidermis penetration which probably accounts for the observed early root infection at 1 dai. The finding of hyphopodia or hyphopodia-like structures is an interesting outcome of the present study since *Fusarium* has never been reported as a hyphopodiate fungal pathogen such as *G. graminis* causing take-all in wheat seedling roots (Asher & Shipton, 1981). However, systematic examinations of the *Fusarium* root infection process have not previously been performed (Kazan et al., 2012). Further microscopic investigations on the early root infection biology of *F. graminearum* will allow final confirmation of hyphopodia. In that case, another interesting question would be whether *F. graminearum* also forms hyphopodia on senescent tillers which are a severe result of fungal spread into distal plant parts. A similar phenomenon has been observed for the pathogen *C. graminicola* which after successful root colonization formed hyphopodia also on senescent leaves. Sukno et al. (2008) hypothesized that these hyphopodia might also serve as survival structures and a source of inoculum for subsequent fungal spread to adjacent plants during the same or even in the following growing season.

The assumption of an active penetration mode causing root rot disease is also supported by the observation that *F. graminearum* was found to enter root tissue exclusively via the epidermal layer and not via the root hairs which would allow a passive migration of hyphae into the root cortex (Fig. 14e). Generally, root hairs are particularly vulnerable to invasions by microbes (Prieto et al., 2011). Among the fungal pathogens *M. oryzae* (Marcel et al., 2010) and *V. dahliae* causing Verticillium wilt in *Brassicaceae* crops (Eynck et al., 2007) enter the plants via root hairs in addition to epidermal penetration. Also, for some *Fusarium* pathogens root hairs are the main sites of penetration, for example *F. verticillioides* in maize (Oren et al., 2003) or *F.*

oxysporum in tomato (*Solanum lycopersicum*) (Lagopodi et al., 2002), and cotton (*Gossypium barbadense*) (Rodŕiguez-Gálvez &Mendgen, 1995).

Moreover, many pathogens are reported to preferentially infect their hosts at specific root regions, while others demonstrated an unlimited ability to penetrate roots (Gunawardena & Hawes, 2002). The specificity for certain root regions may indicate a tissue-specific variation in factors that determine susceptibility to a pathogen which are of general interest for the development of resistance strategies (Sukno et al., 2008). While *C. graminicola* obviously has no root infection site preference since the hyphae could colonize the surfaces of mature maize roots, root caps, root elongation zones and root hairs, *V. longisporum* was never found to colonize the root caps of oilseed rape by Eynck et al. (2007). In the present study dense hyphae networks of *F. graminearum* were equally present in the maturation and elongation zone of seminal roots. At the root caps hyphal masses were not observed, however a reduced mycelium growth was nevertheless observable.

Stage II: The main infection stage was attested by investigating root sections prepared at 3 dai. Here, trypan blue staining revealed first necrotic cells (Fig. 13a) surrounding infection cushions. Generally, runner hyphae that branched to form foot structures (Fig. 13b), infection cushions (Fig. 13c) and sporodochia (Fig. 13d) at the root surface were typical for this disease stage. Consequently, at 3 dai a new level in the development of *F. graminearum* could be evidenced which demonstrated that root penetration had reached a higher level of intensity.

Previous publications on the FHB disease had already provided first microscopic evidence for complex infection structures formed by *F. graminearum*. Two different structures were described as important for floret infection: coral-like hyphal mats (Pritsch, et al., 2000; Boddu et al., 2006; Rittenour & Harris, 2010) and bulbous infection hyphae (Rittenour & Harris, 2010). Boenisch & Schäfer (2011) suggested that the coral-like hyphal mats actually are infection cushions, whereas the bulbous infection hyphae correlate to foot structures. Concerning the infection cushions this suggestion is supported by the present study since the cushion observed at the root surface appeared as coral-like hyphal mats (Fig. 13c). Besides the infection cushions, also the foot structures observed at the root surface (Fig. 13b) were morphologically similar to those observed by Boenisch & Schäfer (2011). Thus, bulbous infection hyphae might be formed at the root surface as well. In this context, necrotic root cells were apparent around infection cushions consistent with observations from glumes infected by *F. graminearum* (Boenisch & Schäfer, 2011).

Using *in vitro* experiments on the infection-related morphogenesis of *F. graminearum* Rittenour & Harris (2010) found bulbous infection hyphae that developed at 2 dai on wheat glumes. Those hyphae were morphologically similar to previously reported intracellular hyphal structures such as the dikaryotic hyphae in stem tissue (Guenther & Trail, 2005) and the wide hyphae in ovary tissue of spikes (Jansen et al., 2005). Rittenour & Harris (2010) assumed that their bulbous infection hyphae were, however, specific to initial host tissue infection. The development of these hyphae was dependent on the fungal gene *Gpmk1* encoding a mitogen-activated protein kinase (MAPK) which previously had been shown to be involved in *F. graminearum* pathogenicity as regulator for the induction of specific enzymes' secretion (Jenczmionka et al., 2003; Urban et al., 2003). In the rice blast fungus *M. oryzae*, however, *pmk1*is required for the development of appressoria (Xu & Hamer, 1996; Lev et al., 1999). In addition, *pmk1* homologues are needed for the pathogenicity of fungi that do not form appressoria, including *F. graminearum* and *F. oxysporum* (Di Pietro et al., 2001; Mey et al., 2002; Jenczmionka et al., 2003; Urban et al., 2003).

In addition, Boenisch & Schäfer (2011) identified hyphal structures similar to lobate appressoria on caryopses, paleas, lemmas, and glumes of FHB susceptible and resistant wheat cultivars. Lobate appressoria and infection cushions are two types of so called compound appressoria and are described as multicellular types of appressoria, formed by irregularly shaped hyphae (Emmett & Parbery, 1975). Boenisch & Schäfer, (2011) proposed that foot structures, lobate appressoria, and infection cushions developed at stage II of floret infection actually mirror different developmental stages of infection cushion formation, similar to *Rhizoctonia solani*, a soil-borne pathogen which attacks below ground as well as above ground plant parts (Armentrout & Downer, 1987; Keijer& Sinclair, 1996). The development of lobate appressoria into infection cushions was described for *R. solani* (Keijer & Sinclair, 1996), *Sclerotinia sclerotiorum* causing root, crown, and stem rots on various plant hosts (Emmett & Parbery, 1975) and *Botrytiscinerea* (Tenberge, 2004). Lobate appressoria on roots were not observed in the present study. However, a high level of accordance was found between FRR and FHB for the early disease stages with regard to hyphal structures and timing of the infection process. Particularly, the detection of infection cushions on roots suggests that at 3 dai lobate appressoria was no longer present at high frequency and are instead further developed to infection cushions. In contrast, the reports on *C. graminicola* (Sunko et al., 2008), *M. oryzae* (Wilson & Talbot, 2009) and *M. grisea* (Sesma & Osbourn, 2004) suggest that *F. graminearum* does not produce lobate appressoria during root penetration but during floret penetration. Instead, hyphopodia or hyphopodia-like structures are developed on the roots.

For *M. oryzae* and *M. grisea* the authors assumed that the ability to use either hyphopodia or appressoria permits the pathogen to adapt its penetration mechanisms to the properties of the target organ (Sesma & Osbourn, 2004; Wilson & Talbot, 2009). The cAMP (cyclic 39,59-adenosine monophosphate)-mediated signalling process which is essential for the formation of functional appressoria on rice leaves (Mitchell et al., 1995; Xu et al., 1997) is not required for the ability of *M. grisea* to form hyphopodia and to penetrate intact roots (Sesma & Osbourn, 2004). Interestingly, it has recently been found that the same signalling process has an equal function during *F. graminearum* spike infection (Bormann et al., 2014). Finally, Sesma & Osbourn (2004) found indications for critical differences between the signal transduction pathways for penetration of leaves and roots by *M. grisea*, a phenomenon that might apply likewise to floret and root penetrations by *F. graminearum*.

At present it is unknown whether the infection hyphae of *F. graminearum*, observed during stage I are involved in the development of infection cushions at stage II similar to reports on lobate appressoria (Keijer & Sinclair, 1996). It is, however, very likely that the increase in fungal biomass in the period between 3 and 5 dai which was disclosed by the qPCR-based time-course examinations on the FRR progression (Fig. 4 and 5) and by rANOVA statistics (Table 4 and 5) is a result of the complex infection structures that were identified on *F. graminearum* inoculated roots. In chapter 6.2.2 it will be discussed that the following disease stage is actually characterised by heavy root cortex colonisations.

6.2.2 Stage III shows root colonization, disease dispersal and increasing necrosis

Stage III: By fluorescence microscopy of wheat roots harvested at 5 and 7 dai it was shown that stage III was characterized by the abundant presence of macroconidia (Fig. 13e) and chlamydospores (Fig. 13f) on the root surface. Therefore, one important aspect of this stage is the explicit formation of fungal structures that mainly serve for repeating the infection stages I and II with multiple subsurface infection sites and for further infestation of the soil and the dispersal of disease by soil movement or transportation. *F. graminearum* produces ascospores and macroconidia spores for the inoculum dispersal (Markell & Francl, 2003). Macroconidia and chlamydospores (the long-term survival structures in soil) produced at the root surface represent the inoculum for further infections since both can germinate on the roots (Sitton & Cook, 1981).

Against this background it is noteworthy that some susceptible and all highly susceptible genotypes (including Line 1105.16) from 10 dai on showed a second phase of increasing fungal accumulations in root samples in this work (Fig. 4c, 5a-c) which seems to be promoted by a repetition of the infection stages via additional infection sites in the wheat root system. For

example, for root rot on common bean (*Phaseolus vulgaris* L.) caused by *F. solani* it was found that chlamydospores are the main source for infection of deep roots (Nash et al., 1961). This also applies to sporodochia (Fig. 13d), asexual structures which were already found at stage II (Mitter et al., 2006). The presence of conidiophores and conidia by 5 dai has also been found for *F. culmorum* and *F. oxysporum* on the epidermal root surface of wheat (Beccaria et al., 2011). In contrast, *V. longisporum* never formed conidia outside the roots of rapeseed (Eynck et al., 2007).

Besides the formation of fungal structures for a disease dissemination and persistence, the second important aspect associated with stage III is the transition to a systematic colonization of root tissues at the site of infection (Fig. 4, 5, 16, and 18). The following aspects determine the outstanding important of this phase: (i) the significant increases of fungal biomass accumulation and visible root symptoms; (ii) the transition from a root disease to a disease that also affects aerial plant parts around 7 dai; and (iii) the fact that this phase clearly separated the susceptible wheat-Fusarium interaction from the partially resistant interaction.

The hypothesis that stage III represents the actual root colonization stage was visualized by confocal laser scanning microscopy of root cross sections in a time-course between 7.0 to 21 dai. Root sections of Line 1105.16 at 7 dai showed an entire cortex invasion (Fig. 14c). Thereby, hyphae both used the intercellular pathway in extracellular spaces as well as the symplastic cell to cell growth (Fig. 14d). This mode of cortex colonization has previously been documented for *F. culmorum* in roots of *Brachypodium* (Peraldi et al., 2011), wheat (Beccari et al, 2011) and rye (*Secale cereale*) (Jaroszuk-Scisel et al., 2008), as well as for *F. oxysporum* in tomato roots (Lagopodi et al., 2002) and *M. grisea* in wheat roots (Sesma & Osbourn, 2004). Although the entire cortex parenchyma cells were invaded, *F. graminearum* did not penetrate the endodermis, was absent from the stele which contains the root vasculature. This was equally observed in roots of *Brachypodium* (Peraldi et al., 2011) and wheat (Beccari et al., 2011) where *F. culmorum* was never observed to enter the stele. This absence from root stele gives the impression that the hyphae growth could be stopped in front of the Casparian strip, a waxy layer inside the root endodermis which is chemically different from other layers of the cell wall and represents an effective barrier for the passive flow of materials into the stele. Whether the Casparian strip stops fungal migration cannot be answered yet.

However, it is more likely that *F. graminearum* uses tissue-adapted invasion strategies. First, it was observed in rye that *F. culmorum* was able to colonize the entire root tissue from epidermis to central vasculature (Jaroszuk-Scisel et al., 2008). In addition, hyphae of *G. graminis* were found to spread through the wheat roots and to destroy the vascular tissue (McMillan et al., 2011). Second, in all stem tissues, including leaf sheath of stem bases *F. graminearum* was

found in this work to grow more or less as a vascular pathogen (Fig. 14f, n and p) while similar to roots it was absent from the vasculature in leaf blades (Fig. 14j and l). Roots function as supplier of water and nutrients via a route that goes from root hairs to stele for the supply of aerial plant parts via the xylem vessels (Smith & De Smet, 2012). Another route is the transport of photosynthate (sugars) from leaves to the roots via the phloem vessels for the allocation of energy to growing root tissues. Moreover, the colonised parenchyma cells, referred to as the "filler" tissue of cortex, are known to be storage sites for starch, protein, fats, oils and water (Lemoine et al., 2013). Therefore, it is conceivable that the *F. graminearum* invasion is not restricted, but rather that the pathogen limits it presence to the cortex can supply the pathogen everything necessary for its survival and further development.

An important outcome of the present study was the finding that the reduction of root biomass is the most immediate and severe impact on both wheat seedlings (Fig. 4 and 5) and adult plants (Fig. 16 and 18). Such reductions were already significant during the early stage of root infection 1 to 3 dai. Root length reductions were in comparison less drastic suggesting that reduced root branching essentially contributes to this phenomenon. However, both the reduced branching and length growth might result from a substantially impaired carbohydrate energy supply to growing root tissues during source to sink relationships. In fact, roots are highly plastic and respond rapidly with developmental and physiological adaptations to changing environmental conditions as well as to plant-microbe interactions (Shen et al., 2013). In addition, the probably impaired uptake and supply of growing aerial plant parts could account for observations such as shoot length reduction, delayed seedling and plant development as wells as seedling mortality. This situation is likely reinforced by the later hyphae spread into the stem base and other aboveground plant parts. The senescence of plant tillers was a common and drastic phenomenon at later disease stages which besides a possible pathogen migration, as observed for *F. graminearum* and *F. pseudograminearum* by Mudge et al. (2006), could also be a consequence of nutrient and water shortage.

Besides a possible nutritional competition between pathogen and host, another problem associated with several root pathogens is the premature cell death, either due to endogenous programmed cell death (PCD) as a possible defence reaction or due to necrosis caused by the pathogen (Greenberg, 1996; Roger & Lamb, 1997). In a previous study on FRR, root necrosis was described as co-responsible for reductions of seedling vigour, root and crown functions, plant stability, yield and grain quality (Mergoum et al., 1998).

As a consequence for *F. graminearum* root infection, brown discoloration was evident during the advanced stages of root rot, especially on the roots of susceptible wheat genotypes (Fig. 8). Such

root discolouration was likewise found on roots of *Brachypodium* (Peraldi et al., 2011) and bread wheat (Beccari et al. 2011) colonized by *F. culmorum*. In both studies, similar to observations made in the present research, from 2 dai on lesions became dark brown and symptoms spread in both directions along the root until the whole root was necrotic between 4 and 5 dai (Peraldi et al., 2011). Also for the take-all disease caused by *G. graminis* necrotic lesions on the roots are typical symptoms which can spread to the stem base (McMillan et al., 2011) as well as for the advanced stages of maize root colonization by *C. graminicola* (Sukno et al., 2008). Desmond et al. (2008) and Boenisch & Schäfer, (2011) found strong indications that DON is involved in the development of necrotic lesions on the stem base and spikelet tissue and that the toxin is released from infection cushions. In contrast, even an extensive intra- and intercellular growth of *V. longisporum* hyphae in the root cortex of oilseed rape was not associated with any responses such as discolouration or necrotic lesions, and invaded host cells still showed an intact structure of the cytoplasm (Eynck et al., 2007; Floerl et al., 2008). A more detailed discussion on the possible role of DON during *F. graminearum*-wheat root interactions is provided in chapter 6.3.2.

Besides the secretion of mycotoxins, the release of cell wall-degrading enzymes such as proteinases by infection hyphae can also result in host cell death (Wanjiru et al., 2002; Martinez et al., 2008; Kikot et al. 2009). *F. graminearum* is known to secrete a broad spectrum of enzymes that can degrade the middle lamella and cell wall during infection of cereal crops (Annis & Goodwin, 1997; Kang & Buchenauer, 2000). The genome of *F. graminearum* harbours 103 genes encoding cell wall-degrading enzymes (Horbach et al., 2011). For instance, *Fusarium* lipases might play a central role in degrading long-chain fatty acids present in the plant epidermis, because the knock-out of the *F. graminearum* lipase gene *Fgl-1* was shown to reduce the fungal virulence on both wheat and maize (Voigt et al., 2005). The hemibiotrophic pathogens *M. grisea* and *M. oryzae* practice a biotrophic phase (up to 8 dai) during rice leaf and root infection which allows them to grow intra- and intercelluarly without damaging the plant cells. The switch of infectious hyphae to a necrotrophic phase, however, results in cell death whereby the release of hydrolytic, cell wall-degrading enzymes plays an important role (Wilson & Talbot, 2009; Marcel et al., 2010; Horbach et al., 2011).

Whether invaded cortex cells show senescence has not been specifically investigated during this study. However, root and stem sections obtained from necrotic regions with heavy hyphae enrichments showed a characteristic highly fragile structure which challenged the preparation of tissue sections. This indicates a general loss of root cell integrity in consequence of fungal accumulation. For example, in a study on FHB, intracellular hyphae were never seen within

living host cells, but after host cell death numerous intracellular hyphae grew within the cell lumen (Brown et al., 2010). Necrosis caused by *C. graminicola* was a consequence of maize root cells that were densely packed with hyphae and acervuli; the asexual fruiting bodies (Sukno et al., 2008).

The non-pathogenic, programmed root cortex cell death (RCD), a known feature of root aging in wheat and barley is usually accompanied by progressive root browning similar to root diseases caused by fungi and bacteria (Henry & Deacon, 1981). RCD is an interesting aspect in (wheat) root development that likely affects the root rot disease. In fact, during the study on adult plant FRR, the RCD phenomenon affected the disease assessment by complicating the rating of macroscopic root symptoms. The early RCD probably have important implications for the root microflora. For example, the avirulent fungal root parasite *Phialophora radicieola* colonises cereal root cells only just before or just after their death (Henry & Deacon, 1981). The discovery that *F. graminearum* colonizes adult plant roots similar to the seedling root rot raises the question which strategy enables the pathogen to survive and progress in tissue that is also characterized by a RCD in the maturation zone of seminal roots. Henry & Deacon (1981) suggested that RCD to a certain extent provides an advantageous environment, especially for microorganisms with a saprophytic mode of life. During the earliest stages of cortical senescence, around early tillering (Z20-22), the resistance of the host cells is declining shortly before their nutrients become available. In fact, *F. graminearum* is also a known saprophyte with a good adaptability to changing environments (Hatsch et al., 2006). Therefore, after seedling and adult root inoculations wheat roots could provide also an environment which enables the pathogen to express both its parasitic and saprophytic way of life.

6.2.3 *F. graminearum* root colonisation is reminiscent of spike colonization

The common aetiology between Fusarium head blight and root rot raises the question whether important commonalities between both diseases can be found which would have important implications for the development of resistance strategies for a broad spectrum of *Fusarium* disease. Moreover possible commonalities would uncover developmental processes that would be critical for the pathogenicity of *F. graminearum* in both diseases. Stephens et al. (2008) already have reported significant similarities in the fungal gene expression patterns at early disease stages of FHB and FCR.

In FHB *F. graminearum* undergoes a series of well-defined developmental steps before and during wheat spike infection. The floret infection is sub-divided into the processes surface colonization, penetration and sporulation (Boenisch & Schäfer, 2011). On wheat and barley

spike tissues the initial *Fusarium* infection process (stage I) was observed during the first two days after spike inoculation (Pritsch et al., 2000; Jansen et al., 2005). Generally, *Fusarium* spores germinate on the abaxial surface of the glume and in the floral cavity within 0.5 dai (Pritsch et al., 2000; Wanjiru et al., 2002). At 1 to 2 dai, immediately after conidia germination and prior to epidermis penetration hyphae networks are formed on caryopses without causing symptoms (Kang & Buchenauer, 2000; Bushnell et al., 2003; Goswami & Kistler, 2004; Boenisch & Schäfer, 2011). During stage II of *F. graminearum* spike infection runner hyphae begin to branch at high frequency and form foot structures, lobate appressoria and infection cushions surrounded by necrotic lesions. This was initially observed at 3 dai. In the further course the appearance of necrosis follows the spread of homogenous hyphal networks over the entire floret and both appear at 4-5 dai on paleas and at 6-7 dai on glumes and lemmas (Boenisch & Schäfer, 2011). The first minor tissue colonization was microscopically observed in the palea by 2 dai and was limited to subepidermal and intercellular hyphal growth. At stage III the entire tissue of husks was found to be necrotic, aerial hyphae and sporodochia were produced (Boenisch & Schäfer, 2011). Brown et al. (2010) reported that by 4-5 dai all cell-types of the palea were rapidly colonized by *F. graminearum* resulting in a lost cell integrity of the non-lignified lower parenchyma. The main colonization of spike tissues was characterized by inter- and intracellular growth of *F. culmorum* (Kang & Buchenauer, 2000) and *F. graminearum* (Guenther & Trail, 2005). In addition, stage III was the junction towards the disease spread into non-colonized plant parts. By 5 dai *F. graminearum* started to spread from initially infected and colonized spikelets and the advancing fronts of hyphal infection were already located in the third rachis node (Brown et al., 2010).

The direct comparison between different studies on the FHB disease establishment and progression with corresponding observations made in the present study on FRR uncovered common features which concern the infection structures developed and a remarkably high level of analogy in the time courses of all phases of the infection process. This was hitherto unknown since information about the fungal development on wheat root tissues and its penetration strategy were very limited (Kazan et al., 2012), only recently examined extensively in spike tissues (Boenisch & Schäfer, 2011). All three disease stages comprising the events surface colonization, penetration, sporulation, host tissue colonization, symptom development and spread into non-infected plant parts show an almost equal chronology between both diseases, in spite of different tissues and environments. This conformity essentially explains the high capability of *F. graminearum* as a root pathogen since obviously no root and/or soil specific environmental conditions seem to prevent the fungus from acting as a pathogen.

However, there are also important aspects differentiating between FRR and FHB. Firstly, lobate appressoria (Boenisch & Schäfer, 2011) were not observed (at least not yet), although foot structures and infection cushions similarly developed on roots. Instead, strong indications for the development of hyphopodia or hyphopodia-like infection structures were found in accordance with previous reports on root pathogens including *M. grisea* and *M. oryzae* (Sesma & Osbourn, 2004; Marcel et al., 2010; Tucker et al., 2010), *G. graminis* (Asher & Shipton, 1981; Sesma & Osbourn, 2004), and *C. graminicola* (Sukno et al., 2008).

Secondly, during floret infection *F. graminearum* and *F. culmorum* frequently use different passive penetration strategies in which hyphae extend either into the apical floret mouth (Bushnell, 2001; Lewandowski et al., 2006), into the stomata of a glume (Rittenour & Harris, 2010), or into crevices between lemma and palea (Lewandowski et al., 2006). Such a passive route, for example via root hairs, could not be observed for root rot. *F. graminearum* root infection was characterised by the absence of specific infection sites, such as the origin of secondary roots, root tips, or wounded tissues.

Thirdly, during FHB the stages I to III likewise occurred in the resistant wheat cv. Sumai 3, the semi-resistant cv. Amaretto and the susceptible cv. Nandu (Boenisch & Schäfer, 2011). In fact, the major resistance of wheat against FHB represents Type II which acts against the spread of the infection within a spike, but does not prevent floret colonization at the infection sites. Type I resistance against initial flower infection, however, occurs much more rarely and therefore, has been less explored (Schweiger et al., 2013). During the FRR disease stages I to III important differences were already found between the partial resistant cv. Florence-Aurore and the highly susceptible Line 1105.156. The constantly reduced fungal biomass accumulation observed in roots of Florence-Aurore (Fig. 4a) could finally be explained by an absent root cortex invasion during stage III. This situation continued until the beginning of plant tillering (Z 21). Therefore, partial FRR resistance shows characteristics of a defence that lowers the rate of root colonization at initial infection sites (in fact, epidermal root layers of cv. Florence-Aurore showed penetration, Fig. 14c) similar to the FHB Type I resistance. In fact, in case of cv. Florence-Aurore the infection process during the stages I to II was associated with an early induction of known FHB resistance gene candidates from Jasmonate-mediate defence and DON detoxification processes (Li et al., 2010a; Gottwald et al., 2012; Zhuang et al., 2013).

6.3 *F. graminearum* can spread from the roots to aerial plant tissues

Another major outcome of this study is the discovery that upon successful colonization of the root system, *F. graminearum* can enter the vascular system of the stem and spread systemically

to aerial plant parts without causing visible disease symptoms in the upper main stem and leaves. This was a noticeable difference to the heavy symptom development on the root and lower stem (stem base) tissues associated with FRR susceptibility and to the early senescence of tillers at later disease stages. Taken together, the observations made in the present study in agreement with previous work indicate two different colonization strategies used by the pathogen. Moreover they show, in accordance with previous findings, that the ability to colonize host tissue and the ability to cause disease seem to be separate traits with independent genetic control (Jansen et al., 2005; Kogel et al., 2006; Sukno et al., 2008).

The combination of confocal laser scanning microscopy, qPCR-based fungal biomass detection and ELISA-based DON quantification revealed (i) specific patterns of fungal colonization in the stem and leaf blade that both differentiate from root colonization; (ii) the fungal ability to reach wheat spikes at the onset of flowering after seedling and adult plant root inoculations; (iv) the presence of DON in all plant parts from the roots to the spikes; (v) the importance of the stem base as the main site of pathogen persistence during later disease stages, probably responsible for steady hyphae and DON infestations; and (vi) a disease spread that is almost undifferentiated between the investigated wheat genotypes, after the fungus has managed to migrate into upper internode(s) of the main stem.

6.3.1 *F. graminearum* shows specific patterns of colonization in the stem and the leaf blade

Confocal microscopic analyses of stem base and stem sections have been conducted to investigate the magnitude and mode of *F. graminearum* migration into distal plant parts in consequence of a successful root colonization. At 7 dai the wheat seedling stem base was found to be composed of three leaf sheaths. In cross sections of Line 1105.16 sampled at 7 dai, *F. graminearum* was found to be mainly present in the outer leaf sheath (L1) and to a lower extent in the second sheath (L2), but was still absent from the central sheath (L3). Interestingly, in both leaf sheaths fungal hyphae were observed to colonize in the vascular bundles. Especially, in L2 the migration into the vasculature was nearly exclusive since hyphae in the parenchyma were rare. At 14 dai, except L1 and L2 *F. graminearum* was also present in the vascular tissues of stem (Fig. 14f and g). From that timepoint on microscopic examinations showed that colonized vascular bundles appear dark which indicates cell death or loss-of-function (not shown). A collapse of vascular bundles after intracellular colonisation has also been reported for FHB (Brown et al., 2010, 2011; Boenish & Schäfer, 2011).

Previous studies on FCR caused by *F. culmorum* (Beccari et al., 2011; Covarell et al., 2012) and *F. graminearum* (Stephens et al., 2008) have reported a colonization route via L1 to L3 after stem base inoculation. Beccari et al. (2011) and Stephens et al. (2008) reported for both pathogens a colonization of L1 by 2 to 3 dai at the point of inoculation. In both cases L1 infections were associated with small necrotic lesions, while the centre of stem base was not colonized before 21 to 28 dai. Thus, for both *Fusarium* species a delayed progression of FCR disease was reported between 2 to 21/28 dai. Such a delay in stem base colonization was not observed in susceptible *F. graminearum*-wheat root interactions. Stephens et al. (2008) explained the delayed FCR disease progression with air cavities between each layer of leaf sheath which seem to represent a stratum of physical barriers restricting lateral shoot penetration by *F. graminearum*. This effect will only be repealed by growing internode tissue during the later stem elongation which permits more rapid colonization of stem parenchyma. The reasonable possibility of such physical barriers for a lateral pathogen migration together with the relatively fast stem base invasion support the assumption of an internal, systemic migration route for FRR. Such an internal route into the stem base could take place via the root-stem junction at the retained seed coat. For example, it is possible that hyphae migrate into the stem via the joint epidermis cells and/or parenchyma cells of root and stem, respectively leaf sheath. Beccari et al. (2011) have observed colonization of parenchyma by *F. culmorum* 5 dai at the contact point between root and retained seed. In addition, for FHB Brown et al. (2010) reported that after floral invasion, the advancing hyphae infected the spike rachis solely via the junctions of neighbouring parenchyma cells and not through the vasculature. Behind the advancing front of infection, however, hyphae started to colonise also the vascular bundles. Therefore, a possible scenario for the fungal migration into the stem base tissue might be that after initial stem base infection the pathogen turns to an advanced colonisation of vascular tissues, more or less simultaneously in L1 and L2. In contrast, the rice leaf blast pathogen *M. grisea* has shown systemic spread through the vascular tissue from roots into to aerial plant parts (Sesma & Osbourn, 2004). However, *F. graminearum* has not been found in the vasculature of roots in the period between 7 and 28 dai.

Finally, an important finding of the present study was that, in contrast to the roots (Fig. 13c), *F. graminearum* predominantly acts as a vascular pathogen in stem and leaf sheath tissues (Fig. 13f and g), from the first discovery to later disease stages, and from the respective lower stem base to the stem apex (Fig. 13n, o, p and q).

The infection of seedling leaf blades probably route via junctions of colonised parenchyma cells between leaf sheath and leaf blade. This would explain while leaf blade migrations occurred in

accordance with first colonisations of the stem base. First leaf blade colonisations were observed in Line 1105.16 at 7 dai. In addition, in all cross sections *F. graminearum* revealed a highly specific colonization pattern by being exclusively present directly beneath or even inside the leaf hairs (trichomes) and to a lower extent close to substomatal cavities. This pattern was maintained during the entire examinations period until 28 dai (Fig. 13j, k, l and m). A fungal migration into the leaf veins and vasculature has never been observed, neither for Line 1105.16 nor for cv. Florence-Aurore. This indicates a colonization strategy in which trichome (at adaxial and abaxial surface) and stomata are the preferential targets.

The specificity of *F. graminearum* for leaf hairs is interesting, because hyphae in root hairs have never been observed. Moreover, studies on *F. graminearum-Brachypodium* interactions demonstrated that the fungus has the ability for an endogenous growth in plant hairs since both the lemma of florets and the leaf blades were infected via the respective macro-hairs (Peraldi et al. 2011). In contrast, the latter authors have not found evidence for direct penetration via stomata which corresponds to observations in the present study that hyphae at stomata were much less frequent. After the penetration of leaves via their hairs, hyphae were observed within the cells directly beneath the base of a macro-hair (Peraldi et al., 2011), the same position at which hyphae were observed in the present study. The following process of leaf colonization was not examined by Peraldi et al. (2011), but the authors assumed that from there on infection will proceed, possibly via the globose structures that formed at the base of hairs. At least for FRR no migration into other tissue such as mesophyll cells was observed in the investigated period. In contrast to external leaf colonisation (Peraldi et al. 2011), the colonization from inside as a consequence of FRR was symptomless. This was not unexpected since the pathogen did not invade the ground tissue involved in regular physiological processes (for example, photosynthesis or nitrate metabolism and storage).

It is reasonable to ask whether the observed pattern of leaf colonization, indeed, represents a passage towards the leaf surface to enable the dispersal to neighbouring plants and/or to higher plant parts such as spikes. After successful spike colonisation by *F. graminearum* Guenther & Trail (2005) could demonstrate that by 10-12 dai the pathogen continued host colonization via the rachis into the stem. Thereby, the fungus developed perithecia on wheat stems as well as on leaf sheaths, exclusively associated with stomatal openings and silica cells. Moreover, while perithecia were developed on leaf sheaths, they were not developed at leaf blade surfaces, instead germinating conidia were observed here. Finally, in accordance with Guenther & Trail (2005) in the investigated period between 7 to 28 dai no perithecia were observed on leaf blades. Interestingly, at 28 dai stained hyphae at trichome tips outside the leaf were found indicating a

possible excite from the leaf. Finally, whether the pattern of leaf colonization observed during FRR aims at the production of macroconidia (and/or perithecia) at the leaf surface or rather at the further migration into leaf tissues as suggested by Peraldi et al. (2011) still remains to be answered.

6.3.2 *F. graminearum* uses a different strategy for aerial plant colonization than for root and stem base colonization

Besides the histopathological examinations of stem colonisation during wheat seedling stages, the potential of *F. graminearum* to colonize aboveground plant parts up to the developing inflorescence has been investigated. This examination was accompanied by DON toxin measurements in all relevant plant tissues and *F. graminearum* colonization of the stem, leaf and spike by qPCR. The qPCR detection was preferred since this method is based on natural amplification or growth, respectively, to detect the fungal presence and was successfully used by Covarelli et al. (2012) and Mudge et al. (2006) for the same reason. So far, the number of studies which address this issue is quite limited and contradictory results were reported even if the same *Fusarium* species was examined. Moreover, most of the studies cover plant colonization and DON accumulations that initiate from stem base infection by *F. culmorum* and *F. pseudograminearum* but not from root infection with *F. graminearum*.

In the presented study only preliminar examinations could be carried out which initially had the main objective to indentify tissues and timepoints with relevance for further detailed studies, in case *F. graminearum* can colonize upper plant parts. However, results from the investigation of after seedling root and adult plant root inoculations shown *F. graminearum* can spread from the roots of wheat into the aboveground parts. Although the preformed fungal biomass and DON measurements currently represent preliminary data they could already provide aspects of agricultural relevance which justify a discussion.

The stem colonization as a consequence of root and stem base infection was symptomless and undistinguishable between the four tested wheat genotypes, Florence-Aurore, Sumai 3, Frontana and Ning 7840, irrespective of their response during root colonisations (partial resistance or susceptibility). The reports on plant colonisations by *Fusarium* pathogens as a consequence of FCR are similar. One of the most complete studies was conducted by Mudge et al. (2006) who isolated *F. graminearum* and *F. pseudograminearum* from flag leaf nodes and spike tissues after stem base inoculation of wheat plants at the seedling stage. This is in accordance with observations made for FRR. Interestingly, as observed in the present study, the systemic colonisation of aerial plant parts was not associated with visible symptoms apart from necrotic

lesions at the stem base and lower nodes that are typical for crown rot (Mudge et al., 2006). In this context, Mudge et al. (2006) suggested that the pathogen had colonised the upper areas of the host plant as an endophyte or biotroph rather than as a necrotroph as observed at the infection sites on stem base where necrosis was evident. However, in contrast to Mudge et al. (2006) who did not observe spike symptoms such as “whitehead” the whitehead symptom was observed in the present study. After seedling infection of 45 plants tested for each genotype, 21% of cv. Florence-Aurore, 19% of cv. Sumai 3, 59% of cv. Frontana and 33% of cv. Ning 7840 displayed this symptom. This was the case although the plants were well watered, a measure that Mudge et al. (2006) applied to avoid premature plant death and whiteheads. Finally, the possibility that aerial ascospores or macroconidia originating from the stem base were responsible for upper plant infestations could be excluded by Mudge et al. (2006). In addition, Poels et al. (2006) reported the migration of *F. graminearum* from the infected seeds up to the heads.

Other studies on plant colonization, however, reported that *F. culmorum* can extensively colonize stem tissues, but not reach the head by the time of plant maturity (Covarelli et al., 2012), or it was even concluded that none of the *Fusarium* species can colonize spikes via stem colonization (Purss, 1971; Burgess et al., 1975; Snijders, 1990; Clement & Parry, 1998; Moretti et al., 2014). Different environmental factors and the relative aggressiveness of the different *Fusarium* species or strains are probably the reasons for these contrasting results (Diaz & Mercedes, 2012).

In this context, there is also an ongoing discussion regarding the mode of stem colonization. Previous papers on crown rot have reported non or only a sporadic colonization of vascular bundles in the non-inoculated upper internodes by *F. graminearum* (Mudge et al., 2006) and *F. culmorum* (Covarell et al., 2012). Instead, the fungus was microscopically observed in the pith parenchyma and lumen of stems. Other studies, however, report *Fusarium* migration into the vascular system of stem and spike tissues demonstrating that there is no principle limitation for the pathogen to invade the vasculature. For the stem colonization from an inoculated spike downwards both modes were observed, a spread via the pith parenchyma and lumen, as well as via the vascular system (Guenther et al., 2005). In addition, Clement & Parry (1998) observed *F. culmorum* hyphae in the vascular system at nodes distant from the point of inoculation. The mode of fungal spread in wheat from floret to floret within spikelet and from spikelet to spikelet is through the vascular bundles in the rachis and rachilla. In the vasculature of spike rachis, the phloem was predominantly the first cell-type to be colonised, followed by the vascular parenchyma and finally the xylem (Ribichich et al., 2000; Jansen et al., 2005; Brown *et al.*, 2010; 2011).

In the present study a nearly exclusive colonization of vascular tissues was observed in leaf sheath of young stem base through the stem apex at 28 dai. Hence, until the beginning stem elongation stage (Z32) *F. graminearum* behaved demonstrably as a vascular pathogen and it is unlikely that the fungus is changing its mode of spread at later plant developmental stages. Concerning the absence of the pathogens from the vascular tissues Mudge et al. (2006) stated that these tissues of wheat are surrounded by a layer of lignified parenchyma cells which could be difficult to penetrate coming from the adjacent pith parenchyma. In contrast, the lumen would provide a pathway for vertical growth that is free of host structural barriers and the surrounding parenchyma cells provide a potential nutrient source, for example stored soluble carbohydrates (Rae et al., 2005a; Mudge et al., 2006).

In fact, the vascular bundle provides the pathogen both with nutrients and serves as a pathway for hyphae extension. Some pathogens have been shown to manipulate the sucrose transporter SWEETs localized in the plasma membrane of phloem and parenchyma cells for their own purpose to release more sucrose for pathogen growth (Chen LQ et al., 2010, 2014). Generally, *F. graminearum* present in the vasculature of the wheat stem is a competitor for nutrients, especially during the critical flower development and grain filling phases. In fact, the stems are the most important sources of carbon for grain filling in cereal crops. This is because water soluble carbohydrates are mobilized from the stem during the grain filling (Ruuska et al., 2006; Dreccer *et al*., 2009; Xue *et al*., 2013). Moreover, such reserves contribute as much as 70% to the yield under severe stress (Goggin & Setter, 2004, Ehdaie et al., 2006, Rebetzke et al., 2008). Therefore, the ability of *F. graminearum* to occupy and to destroy vascular bundles may be a main reason for the “whitehead” symptom observed in the present study as a consequence of FRR. In case of the take-all disease caused by *G. graminis* whiteheads are accompanied by premature ripening of the crop. White heads are sterile or produce shrivelled kernels and can significantly reduce grain yield and quality. Consequently, losses of up to 60% have been reported in the UK (Sunko et al., 2008).

The role of the DON trichothecene toxin during Fusarium root and crown rot is also still unclear. On the one hand, it was stated that DON production is not essential for the infection process of *F. graminearum* or *F. pseudograminearum* causing FCR, while the toxin was found to play a role during the colonization to suppress the produce of cell walls (Okubara et al., 2002; Mudget et al., 2006; Diamond et al., 2013). For instance, the expression of the *Tri5* gene which encodes the first enzyme of trichothecene biosynthesis was only expressed in the stem and remained stable between 3 and 28 dai (Mudge et al., 2006). Similar observations have been made for FHB. Here, DON was found to be unnecessary for the initial infection, but was required for the disease

spread in the spike rachis (Jansen et al., 2005; Boenisch & Schäfer, 2011; Pasquet et al., 2014). In the spike rachis DON is supposed to play a role in inhibiting plant defence to promote disease spreading (Bai G et al., 2001; Cuzick et al., 2008; Brown et al., 2011).

On the other hand, in a study on FRR caused by *F. culmorum* the *Tri5* gene was shown to be consistently expressed in wheat roots at 1, 2 and 3 dai, demonstrating that trichothecenes were already synthesized during the early stages of infection (Beccari et al., 2011). In co-operation with the Institute of Inorganic and Analytical Chemistry (JLU Giessen) to establish liquid chromatography mass spectrometry (LC-MS) as a tool for the rapid detection of the DON toxin in low quantity plant tissue samples such as FRR infested seedling roots, the toxin presence could be evidenced at 3 to 7 dai in infected roots of the highly FRR susceptible cultivars Ning 7840 and Tabasco (data not shown). Although this study was not applied to the genotypes used for light and fluorescence microscopy and did not aim at DON quantification, this finding is consistent with the observations of Beccari et al. (2011). Moreover, it is consistent with the observed expression of genes form a recently described putative DON detoxification mechanism (Gottwald et al., 2012) that were induced in association with partial FRR resistance (Fig. 21) during the three stages of root infection and colonization. These genes peaked at the colonization stage III. Therefore, the present study indicates that DON released by the fungus probably plays a similar role for the virulence of *F. graminearum* to facilitate tissue colonization and necrotrophic growth as reported for FHB (Boddu et al., 2006; Brown et al., 2010; Boenisch & Schaefer, 2011). Similarly, the accumulation of DON in the necrotrophic stage III of crown rot was found to coincide with necrosis on wheat tissue and a significant increase in fungal biomass (Desmond et al., 2008; Stephens et al., 2008).

The first ELISA measurements carried out in the present study during a period comprising the seedling stage around 10 dai (Z 13, three unfolded leaves); early tillering (Z21-22); stem elongation (Z32) and flowering (Z60-69) demonstrated the continuous presence of DON (Fig. 15b). The DON contamination followed the plant development and fungal spread, and finally was measurable in roots, stem bases, uppers stems, leave and spike tissues (Fig. 15b). This observation is consistent with reports from Mudge et al. (2006) and Beccari et al. (2011). Moreover, similar to the present study, Beccari et al. (2011) detected DON even in those plant tissues that did not exhibit any symptoms.

In the present study DON concentrations up to 6.0 ppm (the maximum content measurable with current ELISA assay) were observed in the stem base and spike tissues, whereas they were always <6.0 ppm in stem and leave samples (Fig. 17). Although the ELISA values in the present study are are based on one repetition only and are limited by the detectable maximum of 6.0

ppm, our observations are reminiscent to observations made by Covarelli et al. (2012) who detected high levels of DON in treated stem bases in the range of 111.0 - 438.0 ppm, while the levels of DON in the wheat spikes ranged from 1.0 to 11.0 ppm.

The observation of DON in stem, leave and spike tissues very distant from the initial infection sites (stem bases or roots) raises questions related to the possible origin and role of DON in higher plant parts, especially since the colonization of upper plant regions is symptomless. Current observations suggest a double source for DON: first, due to a release from hyphae (Beccari et al., 2011) and second, due to a transmission into non-infected tissues (Covarelli et al., 2012).

In case DON is released by the pathogen the absence of visible symptoms associated with DON could be explained by the relatively low level of DON production in stems as observed by Stephens et al. (2008), Covarelli et al. (2012) and Moretti et al. (2014) as well as in the present study (preliminary data). For example, during the movement in the spike rachis and for the growth in un-infected florets via the rachis nodes trichothecene toxins are released at low levels to inhibit wheat defence response (Jansen et al., 2005). For FCR, Covarelli et al. (2012) suggested that DON may also have a role in fungal progression through the plant stem. DON may be suppresses the production of host defense responses (Okubara et al., 2002; Mudget et al., 2006; Diamond et al., 2013).

In case of a DON transmission in long distance from heavily colonized stem bases (Covarelli et al., 2012), observations in the present study suggest transport together with water and nutrients via the xylem in the vascular bundles. For example, DON was reported to appear in maize and wheat heads prior to *Fusarium* hyphae (Young & Miller, 1985; Kang & Buchenauer, 2002; Covarelli et al., 2012). Particularly, Kang & Buchenauer (1999) proved for FHB that toxins can be transported in xylem and phloem of the rachis to distal uninfected florets.

6.4 Characteristics of partial wheat resistance against root rot

6.4.1 Systematic examination of pathogen growth patterns and observational studies of the host-pathogen interaction

For the FCR disease only very few major wheat resistance sources are reported, and compared to FHB only a limited number of genotypes have been screened since the FCR screening methods are technically demanding (Wildermuth et al., 2001; Mitter et al., 2006; Li et al., 2008). One important example is the wheat accession CSCR6 identified in a screening of 2,400 wheat genotypes (Ma et al., 2010) which carries one of the most stable resistance QTL *Qcrs.cpi-3B* on chromosome 3BL. *Qcrs.cpi-3B* accounts for up to 49% of the phenotypic variance for FCR

reaction in different genetic backgrounds (Ma et al., 2012) which is similar to the *Fhb1* QTL of the genotypes Sumai 3 and Ning 7840 providing FHB resistance (Buerstmayer et al., 2009). Also similar to FHB, wheat resistance against FCR is partial and a typical quantitative trait (Wallwork et al., 2004; Collard et al., 2005; Bovill et al., 2006).

Wheat genotypes with partial resistance to FRR have so far not been described and therefore, the identification of two wheat genotypes (cv. Florence-Aurore and Line 162.11) which show characteristics of partial resistance to root colonization was one of the major outcomes of this study. This allowed comparative studies on the growth pattern of *F. graminearum* in roots of genotypes with different responses to FRR. To the author's knowledge, this is the first comparative study of this kind.

Genotype rankings based on relative fungal biomass (Fig. 6), developmental traits evaluation (Fig. 7) and the FRR disease index developed in this work (Fig. 8) have uncovered significant differences between the 12 tested wheat genotypes concerning their respective performance under FRR. These results were used to define three categories of FRR severity which were characterized as relative partial resistance, susceptibility and high susceptibility. The respective disease progression values obtained from a time course study (Fig. 4 and 5; Fig. 16 and 18) were subjected to rANOVA' statistics to test for significant differences in the dynamics of the FRR disease process, but also between the three FRR severity categories (Table 3 and 4; Fig. 11). Finally, based on severity analyses partial resistance to FRR could be explained by relatively low fungal accumulations in roots and low impacts on the seedling as well as by a specific dynamics of interactions (Fig. 11a).

By using confocal laser scanning microscopy it was possible to confirm and characterize the partial resistance in the cultivar Florence-Aurore. For these investigations the Line 1105.16 was used as a respective highly susceptible genotype (Fig. 9). Combining observations from the study on FRR severity and the histopathological study, the initial root colonization (phase II in disease progression and stage III of fungal development) was found to be particularly critical with regard to the differentiation between partial resistance and susceptibility. While root cross sections of the susceptible Line 1105.16 at 7 dai were completely colonized including epidermis and cortex, cross sections of the partially resistant cv. Florence-Aurore showed a remarkably reduced root invasion since hyphae invasion was restricted to the epidermal layer (Fig. 14e). Only from timepoint 21 dai on first cortex colonisations by *F. graminearum* were observable in roots of cv. Florence-Aurore. Thus, in first instance partial resistance to FRR was found to be characterized by the un-ability of the pathogen to enter the root cortex layer.

A similar delayed colonization has been observed for stem base tissues of Florence-Aurore in accordance with observations made for macroscopic symptoms (Fig. 4g). For the susceptible Line 1105.16 a successful pathogen migration into the stem base was observed at 7 dai, whereas at the timepoint 14 dai the investigated stem bases and lower stem parts of Florence-Aurore still remained almost un-colonized. Instead, at 14 dai green fluorescence signals of non-fungal origin were detected in all investigated stem sections of partially resistant Florence-Aurore. These signals were limited to the parenchyma cells in direct contact with the vascular bundles (Fig. 14h and i). The WGA Alexa Fluor 488® conjugate can selectively bind to N-acetylglucosamine (GlcNAc) and N-acetylneuraminic acid (sialic acid) residues and therefore, enables the specific detection of chitin in fungal cell walls (Sahai & Manocha, 1993). However, previous studies have demonstrated that WGA Alexa Fluor 488® can also label enriched hydroxyproline-rich glycoproteins, single plant components located in secondary cell walls (Lannoo et al., 2006). Such glycoproteins can indeed constitute a protective function by cell-wall strengthening (Chazotte, 2011), and cell wall thickening or deposition of amorphous material within the vascular bundles of wheat can slow the growth of *F. graminearum* (Ribichich et al., 2000). Therefore, it is possible that the observed fluorescence signals represent a plant response to an initial stem migration by *F. graminearum* as a plant reaction to specifically protect the vascular system.

Beccari et al. (2011) observed a similar autofluorescence of cortical cells in seedling roots three days after *F. culmorum* inoculation. This autofluorescence just in advance of the fungal hyphal colonization front was interpreted as evidence for host response. However, hyphae were also observed in these cells indicating that the autofluorescence did not inhibit penetration of cells. Indeed, in contrast to cv. Florence-Aurore, the wheat genotype Genio used by Beccari et al. (2011) was susceptible to FRR and FCR. Thus, in second instance partial resistance to FRR was found to be characterized by the non-ability of the pathogen to enter the stem tissue and particularly the stem vasculature.

Finally, three aspects were found to characterise partial FRR resistance: (1) no resistance to initial epidermis penetration and invasion, but (2) resistance to the infection of cortical root cells which is assumed to result in a delayed and reduced migration into the stem base, and (3) a resistance to vascular bundle infection in stem tissues. These findings are in accordance with the definition that partial resistance is first characterized by quantitative limitation of pathogen growth (Vergne et al., 2010).

However, confocal laser scanning microscopy in this work has uncovered another aspect, that partial FRR resistance in the seedling stage is limited. From the timepoint 21 dai typically

corresponding to the subsequent beginning of tillering (Z21-22), roots and stem tissues of cv. Florence-Aurore were colonized by *F. graminearum* (14p). Two explanations for this time-limited presence of partial FRR resistance during the seedling stages are considered. First, the fungus overcomes the molecular mechanisms behind partial resistance. Previous reports showed that *Fusarium* spp. can release several virulence factors like toxins and extracellular enzymes that can directly suppress defence mechanisms (Proctor et al., 1995, Kang & Budenauer, 1999, 2000, Phalip et al., 2005, Voigt et al., 2005). Second, the observed partial resistance is plant age dependent, a scenario that has been suggested by Li X et al. (2010) for the Fusarium seedling blight disease. The authors observed for the plant cytochrome P450 gene *CYP709C1* (Table 2) clearly association with the resistance reactions in both seedling and spike. The FHB-resistant genotype Sumai 3 accumulated 7-fold more P450 transcripts than did the FHB-susceptible cv. Annong 8455, while 84-fold more P450 transcripts were accumulated in the FSB-resistant cv. Annong 8455 than the FSB-susceptible cv. Sumai 3. In addition, Wu et al. (2005) already observed a consistent susceptible reaction at the seedling stage for the FHB resistant wheat cultivars Sumai 3, Wangshuibai, and Fanshanxiaomai and proposed an adult plant resistance (APR) for these cultivars, reminiscent of APR reported for resistance of wheat to leaf rust (Seyfarth et al., 1999; Barcellos et al., 2000), stripe rust (Yang et al., 2001), or powdery mildew (Liu et al., 2001). The hypothesis was supported by the finding that major FHB resistance genes did not protect against FRR at the seedling stage in the present study (Fig. 9). In fact, for the development of new resistance strategies it would be of high relevance to obtain more information on this particular aspect.

6.4.2 Root invasion by *F. graminearum* is accompanied by plant age dependent activation of defence responses known from FHB

The molecular responses to root infection by pathogens are largely unknown, as well as root defence markers were not described (Marcel et al., 2010). To characterize wheat root invasion by *F. graminearum* at the molecular level, well-established spike defence genes were analysed (Table 2). A comprehensive analysis of *Fusarium* resistance candidate genes in root tissues has not been performed so far. Generally, for the development of new resistance strategies it would be necessary to analyze whether the common aetiology found for different *Fusarium* diseases may involve the same defence mechanisms and key genes.

6.4.2.1 Does DON detoxification play a role in partial FRR resistance?

Gene expression in correlation to partial FRR resistance and to the critical main infection and first root colonization stages I-III were observed for resistance candidate genes representing a possible DON detoxification mechanism known from FHB resistance (Gottwald et al., 2012). *TaUGT3* and *HvUGT13248* are two DON detoxification genes which encode glucosyltransferases that can convert DON into the less virulent DON-3-glucosid (D3G) (Ma LL et al., 2010; Schweiger et al., 2010). Particularly, *HvUGT13248* has been identified as remarkable DON resistance related gene in wheat and barley (Boddu et al., 2007; Walter et al., 2008; Gardiner et al., 2010; Gottwald et al., 2012) with a proven DON detoxification ability (Schweiger et al., 2010). Both glucosyltransferase genes were significantly induced in FRR seedling and adult resistant cultivars around 1 to 5 dai (Fig. 22).

P450 cytochromes form a large protein family which catalyze most of the oxidation steps in the plant secondary metabolism (Howe et al., 2002; Noordermeer et al., 2001; Weber et al., 2002); they are also involved in signal transmission of plant defences against insects and pathogens (Weber et al., 1999). Plant P450 cytochrome genes are known to be induced by the stress hormone signal methyl jasmonate as well as by fungal pathogens (Kandel et al., 2005; Kong et al., 2005; Walter et al., 2008). The P450 gene *CYP709C1* was initially cloned from wheat and described as being implicated in plant defense events, particularly with a possible function in DON detoxification (Kandel et al., 2005). High level expression of *CYP709C1* in the FSB resistant cv. Annong 8455 already indicated a role in the defence against *Fusarium* pathogens (Li X et al., 2010). Therefore, *CYP709C1* was an interesting candidate to be tested in FRR treated roots, also because the gene represents a link between the investigated detoxification and JA-mediate defence mechanisms. In fact, in seedling roots of partially resistant cv. Florence-Aurore *CYP709C1* revealed high expressions with an increasing trend during the period 0.5 to 5 dai and peaked by 5 dai, a critical timepoint for a successful root colonization (Fig. 22e). A similar pattern has been observed in adult roots of cv. Ning 7840 which was the best performing genotype during these plant development stages (Fig. 22f). The observed expression pattern of *CYP709C1* was also in accordance to observations from Li X et al. (2010) and thus, supports their assumption of APR against *Fusarium* spp.

The MDR-like ABC transporter gene *TaMDR1* was originally isolated from wheat roots as a candidate gene for aluminum toxicity (Sasaki et al., 2002). *TaMDR1* encodes a multidrug resistance (MDR) protein which is known as a member of the ATP-binding cassette (ABC) protein superfamily. *TaMDR1* was found to be up-regulated in cv. Wangshuibai as induced by DON and *F. graminearum* (Shang et al., 2009) and was likewise induced in the FHB resistant

cultivars Dream and Sumai 3 (Gottwald et al., 2012). Therefore, *TaMDR1* was an interesting candidate to be tested in FRR treated roots. In seedling roots of cv. Florence-Aurore and in the adult plant roots of Ning 7840 the expression of *TaMDR1* peaked much later and only temporarily compared to the other three genes (Fig. 22 g and h). However, such a later induction was equally found during gene expression studies in FHB treated spikes of (partially) resistant cultivars Dream and Sumai 3. ABC transporter genes where generally expressed later than glucosyltransferase genes (Gottwald et al., 2012).

Three of the four tested genes were similarly expressed the critical stages of infection (stage I and III, 1 to 5 dai), when in seedling roots of cv. Florence-Aurore the colonization of cortex tissue was impaired as shown by microscopic examinations. Finally, these observations strongly indicate that an early induction of a detoxification process essentially contribute to impaired low fungal biomass accumulations at early disease stages. Second, for all four genes the observed expression patterns strongly indicate a form of age-related resistance. Moreover, the gene expressions in adult plant roots compared to seedling roots were more similar to those observed for FHB (Gottwald et al., 2012). Third, the age-related change of gene expression also supports the assumption that these detoxification genes play a role for the observed partial FRR resistance and that the DON toxin is already present at the disease stages I to III. There are strong indications that the FRR disease process is accompanied by the accumulation of trichothecene mycotoxins such as deoxynivalenol (DON). As mentioned above, Beccari et al. (2011) demonstrated continuous expression of the DON biosynthesis gene *Tri5* in *F. culmorum* treated wheat roots at 1, 2 and 3 dai. In addition, in the present study DON was detected from 5 dai on in infected seedling roots (chapter 6.3.2). The presence of DON is also supported by the appearance of necrotic lesions on the roots of infected plants. Finally, the activity of DON detoxification was likewise demonstrated for *CYP709C1* in root and spike tissues by Li X et al. (2010).

It is interesting that in the case of FHB both the toxin release by *F. graminearum* and the DON resistance by wheat are typically present during the pathogen spread within the rachis, but not during the initial penetration of spike tissue (Jansen et al., 2005; Boenisch & Schäfer, 2011; Pasquet et al., 2014). Moreover, since the genes were induced depending on age- but independent from genotype and thus, even in the highly FHB susceptible cv. Florence-Aurore, it is possible that the detoxification mechanism is mainly regulated indirectly via cellular signals such as MeJA and/or directly via decreased levels of [Ca^{2+}] (Desmond et al., 2008; Meriño-Gergichevich et al., 2010) and not by the major *Fhb1* QTL as stated by Lemmens et al. (2005).

6.4.2.2 Jasmonate-mediate defence might play a role in partial FRR resistance

Jasmonic acid is a volatile fatty acid-derived compound that participates in response to pathogen attack (Farmer et al., 1992), especially in the response against necrotrophic pathogens (Li et al., 2008; Laluk et al., 2010; Ding et al., 2011). Recent reports confirm that the JA pathway is important for FHB resistance (Li et al., 2008; Jia et al., 2009; Ding et al., 2011; Gottwald et al., 2012; Xiao et al., 2013; Pasquet et al., 2014). This pathway includes three steps: 1) JA biosynthesis; 2) JA signal transduction and finally 3) the expression of JA-responsive genes (Fonseca et al., 2009). Representative genes for thsee steps were tested for their expression in roots: The *Lox*-2 gene is known as a key enzyme in JA biosynthesis (Creelman et al., 1997; Feussner & Wasternack, 2002; Schaller et al., 2004). The analysed *Lox-2* gene was up-regulated in association with FHB resistance in the cultivars Dream (Gottwald et al., 2012) and Sumai 3 (Zhuang et al., 2013). The genes *JAZ, COI1* and *MYC2* were identified as resistance associated and up-regulated in *Fusarium* spp. treated spikes (Xiao et al., 2013; Zhuang et al., 2013) as well as the pathogenesis-related proteins *PR-4* (Bertini et al., 2003) and *PR-14* (Gottwald et al., 2012).

It has been demonstrated that JA-signalling and responses depend on the key compounds *COI1*, *JAZ* and *MYC* (Chini et al., 2007; Thines et al., 2007). The activation of JA-mediated responses relies on JA-Ile (JA conjugated with isoleucine) promoted protein-protein interaction between *COI1* and *JAZ* leading to the degradation of *JAZ* proteins (Devoto et al., 2002). In this way, the *COI1*-dependent removal of pre-existing *JAZ* proteins provides the liberation of *MYC2* proteins which finally allows transcriptional activation of jasmonate responses. The product of *MYC2* is a key transcriptional activator of JA-regulated gene expression (Lorenzo et al., 2004; Chico et al., 2008; Katsir et al., 2008; Fernandez-Calvo et al., 2011; Kazan & Manners, 2013). In contrast, a rapid synthesis of new *JAZ* proteins ensures the decrease of JA response (Thines et al., 2007), because it is suggested that *JAZ* act as repressors of *MYC2* (Chini et al., 2007). Moreover, *MYC2* and *JAZ* proteins are associated in a negative feed-back regulatory loop in which *MYC2* regulates *JAZ* gene expression levels leading to slow down of JA-mediated gene expressions (Chini et al., 2007; Fernandez-Calvo et al., 2011). Genes encoding PR proteins such as the *PR-4* and *PR-14* are known targets for JA signalling after fungal attack (Kunkel & Brooks, 2002; Caporale et al., 2004). For instance, *PR*-4 can bind to the fungal chitin to “neutralize” the pathogen by inhibiting *Fusarium* germination (Hejgaard et al., 1992; Ponstein et al., 1994). Zhuang et al. (2013) observed that *PR-4* is much higher expressed in the case of FHB resistance than susceptibility.
For the genes *JAZ, PR-4* and *PR-14* expression patterns could be associated to partial FRR resistance at the seedling stage (Fig. 24a, c, e). However, the patterns were less clear compared

to the patterns obtained from detoxification genes (Fig. 23). For all three genes infection-related expressions in adult roots of cv. Florence-Aurore disappeared as observed for the DON detoxification genes, whereas their expression in post-seedling roots of the genotypes Ning 7840, Sumai 3 and Frontana was predominant corresponding to their resistance at adult plant stages. In seedling roots, however, all three genes were induced at 3 dai and *JAZ* even peaked at 5 dai. The observed JAZ expression indicates a down-regulation of JA-dependent defence responses, due to the negative regulatory effect on the transcriptional activator MYC2 (Chini et al., 2007).

In seedling and post-seedling roots *Lox-2*, *MYC2* and *COI*1 did not show expression patterns that could be associated to partial resistance or susceptibility, respectively (Fig. 23). The similarly expression of *MYC2* (Fig. 23e and f) in all genotypes can be explained by its wide spectrum of functional roles, including the natural root development (Grunewald et al., 2009; Sun J et al., 2009; Chen Q et al., 2011;Yamada et al., 2011; De Geyter et al., 2012). For instance, *MYC2* has a greater effect on root growth in Arabidopsis compared to *MYC*3 or *MYC*4 (Fernandez-Calvo et al., 2011). Therefore, the increased *MYC2* activity in infected compared to control roots indicates a stimulation of root growth and correspondingly enhanced defense response to *F. graminearum* invasion in wheat roots.

Currently, the expressions of all six genes in spikes of the FHB resistant cv. Sumai 3 and the highly susceptible Florence-Aurore is analysed in our lab to examine the possible role of JA-mediated defence during early disease stages (Fig. A3). The results preliminary hypothesized a model for resistant pathogen-floret interactions: It is here that the JA-mediated defense response is activated already 4 h after single spikelet inoculation and remains active until the timepoint 2 dai from which on *JAZ* gene expression starts to rise until 4 dai. During this time between 4 hai and 2 dai, expressions of the genes *Lox-2*, *PR-4* and *PR-14* were higher in *F. graminearum* infected spikelets of Sumai 3 (Fig. A3, A4). In the susceptible genotype Florence-Aurore the whole process was delayed by about 1 to 2 days and *Lox-2* activity occurred at 16 hai that is about 12 h later (Fig. A3b). The fact that susceptibility is characterized rather by a delayed response to infection than by a complete absence of a response has previously been observed for genes associated to DON detoxification, too (Gottwald. et al., 2012; Xiao et al., 2013). This model tentatively supports the assumption that the JA-mediated defence might be active already during the first stages of spikelet infection (Gottwald et al., 2012), while detoxification becomes active during later disease stages (Jansen et al., 2005; Boenisch & Schäfer, 2011; Pasquet et al., 2014).

Based on the observations made in the FHB study it was suggested that a FRR assay for gene expression analyses covering a period between 2 hai to 3 dai might lead to clearer insights into

early gene activities. Very recently this analysis has been completed for seedling roots of the genotypes Florence-Aurore, Ning 7840, Sumai 3 and Frontana (Fig. A3). First, relative fungal biomass values measured at eight timepoints between 0.5 to 3 dai are in accordance with results from the previous study on FRR severity (Fig. 4 and 5) and thus, the previous assignment of genotypes to respective severity categories was confirmed. Second, the observed gene expressions were in accordance with the model hypothesized for FHB. The gene expressions of *Lox-2*, *PR-4* and *PR-14* peaked at 1 dai in roots of Florence-Aurore and remained until 3 dai (Fig. A3a, A4). For *PR-4* and *PR-14* (Fig. A4a, c), this is consistent with observations made in the previous FRR study (Fig. 24c and e). Interestingly, only for the timepoint 1 dai a sudden and temporary peak was observed for *Lox-2* and *PR-4* in infected roots of cv. Sumai 3. However, these inductions amounted at best half to 50% of Florence-Aurore. The strong induction in cv. Sumai 3 is not unexpected since this variety was characterized as having relatively low RFB values as shown by genotype ranking (Fig. 6), but with a comparatively high sensitivity to FRR (see chapter 5.1.4). In Florence-Aurore roots of all three genes were suddenly expressed at 1 dai. In contrast, the expression of the negative regulator gene *JAZ* peaked at 3 dai, indicating a two-day-window until increased *JAZ* expressions seems to slow-down the JA activation of defence.

Similarly, an induction of several JA-triggered PR-genes was observed at 1 to 2 dai after *F. pseudograminearum* inoculation related to partial FCR resistance (Desmond et al., 2006). In addition, a methyl jasmonate treatment prior to fungal inoculation not only induces related defence genes, but also significantly delays FCR-lesion development for two weeks in a genotype-independent manner (Desmond et al., 2006). Moreover, the observed two-day-window between *Lox-2* and *JAZ* expression is in accordance with observations on FHB. This supports the assumption of a time-limited activation of wheat defences against initial penetration by *F. graminearum* via jasmonate signals. Generally, derivatives of the 13-LOX pathway to which the *Lox-2* gene belongs are precursors of plant defence compounds such as jasmonates (signalling), thaumatin and phytoalexins (antimicrobial activity), commonly referred to as phyto-oxylipins (Blée, 2002; Feussner & Wasternack, 2002; Prost et al., 2005). Plant oxylipins are produced from cuticle-or cell membrane-associated fatty acids often derived via fungal degradation of plant cuticles or cell membranes (Wasternack, 2007). In fact, changes in membrane lipids such as phosphatidylcholines (PC) and LysoPCs occur at the site of fungal infection (Tayeh et al., 2013) and both lipid classes are e.g. involved in the synthesis of jasmonates(van Loon et al., 2006). The sudden induction of *Lox-2* and both PR-genes coincides with first epidermal and cortical penetrations by *F. graminearum* at 1 dai during stage I (Fig. 12c and d) and may represent first, immediate reactions in the partial resistant wheat genotype. In the same way, the

early induction of JA-mediated defence mechanisms supports the finding of an active root penetration by infection hyphae. It is interesting to study the expression patterns of these genes in roots that have been inoculated at an adult plant stage, an investigation that is currently in progress.

6.4.2.3 Wheat zinc finger protein might be a candidate for a central regulator of Fusarium resistance

The gene *Wzf1* is a member of the plant specific Q-type C2H2 zinc finger subfamily, and contains an ERF-associated amphiphilic repressor (EAR) motif with a general repressor function (Kam et al., 2008). Several previous studies have characterized zinc finger proteins (ZFPs) as transcriptional repressors in association with tolerance against biotic or abiotic stresses (Ohta et al., 2001; Sakamoto et al., 2004; OH et al., 2005; Uehara et al., 2005; Ciftci-Yilmaz et al., 2007). The possible mechanism of EAR containing repressors is protecting cellular components from self-inflicted permanent damage by modulating the action of defense and stress responses (Kazan et al., 2006).

Wzf1 was up-regulated after *F. graminearum* infection in the highly FHB-resistant cultivar Sumai 3 (Li & Yen, 2008; Gottwald et al., 2012; Zhuang YB et al., 2013). At the seedling stage, relatively high expression of *Wzf1* in partially FRR resistant cv. Florence-Aurore appeared during the infection and colonization phase (0.5 to 5 dai) and peaked at 5 dai. In addition, in a time-course study covering the period between 2 hai and 3 dai, similar expressions were found for the timepoints 1 to 3 dai (data not shown). In adult plant roots the early *Wzf1* expression was no longer observed in roots of Florence-Aurore, but in roots of Ning 7840 with an induction peak at 5 dai. Generally, *Wzf1* showed an expression pattern highly similar to genes from the DON detoxification (Fig. 22), particularly with *CYP709C* (Fig. 23c). The activity of *Wzf1* on FRR observed in the present study together with its frequent occurrence in studies on FHB provide strong indication for this gene being an interesting candidate as a transcriptional regulator involved in *Fusarium* resistance.

6.4.2.4 Activitiy of the *Fhb1* candidate resistance gene in wheat roots

The major FHB resistance QTL *Fhb1* was initially identified in the Chinese cv. Sumai 3 (Waldron et al., 1999; Bai G et al., 1999). Wheat genotypes carrying *Fhb1* typically have a high ability to convert DON into DON-3-O-glycoside. Therefore, *Fhb1* was assumed to encode or regulate a DON-specific glucosyltransferase (Lemmens et al., 2005). More recent efforts of fine mapping were able to locate *Fhb1* to a 261kb genomic region in wheat which contains seven

putative genes which, however, were found to be unfunctional (Liu S et al., 2008). In a combined approach including transcriptome analysis, genetic studies, expression QTL (eQTL) mapping and physical mapping, the functional gene *WFhb1_c1* has been identified as co-segregating with *Fhb1* and therefore, was assumed to be a strong candidate for the *Fhb1* locus (Li & Yen, 2008; Basnet et al., 2012; Zhuang YB et al., 2013).

Further, Zhuang YB et al. (2013) assumed that the *WFhb1_c1* gene encodes a pectin methyl esterase inhibitor (PMEI). Pectin methyl esterases (PME) can enhance the susceptibility to fungal cell wall infections since they can hydrolyze pectin compounds in the middle lamella. In their study *WFhb1_c1* showed a non-significant up-regulation in cv. Sumai 3, but a down-regulation in infected spikes of the FHB susceptible genotype Y1193.6. Therefore, the authors assumed that down-regulate of *WFhb1_c1* leading to an increased FHB susceptibility. If *WFhb1_c1* encodes a PME-inhibitor its down-regulation by the fungus would promote fungal cell wall infection. On the other hand, in the resistant genotype the gene is constitutively expressed, but not induced in response to the disease (Zhuang YB et al., 2013). However, in current work on FHB in our lab a sharp induction of *WFhb1_c1* has exclusively been observed in cv. Sumai 3 at 16 hai (Fig. A5), a timepoint was not included in the time-course expression study by Zhuang et al. (2013). This observation demonstrates an involvement *of WFhb1_c1* in FHB resistance, not in the sense of a functional role as stated by Zhuang et al. (2013) In fact, the sequence similarity between *WFhb1_c1* and the PME-inhibitor gene from *Arabidopsis* was low (Zhuang et al., 2013) and thus, *WFhb1_c1* is thought to be a gene that directly causes *Fusarium* resistance, instead of indirectly reducing susceptibility by lack of expression.

This assumption is consistent with the FRR resistance-associated expression patterns in seedling and post-seedling roots which show a gene activity from 0.5 dai on until 21 dai (Fig. 25c and d). If the gene expression in consequence of FRR disease can be confirmed than it is questionable whether *WFhb1_c1* really represents the major gene behind the *Fhb1* resistance-QTL, because the cultivars Florence-Aurore and Frontana both do not carry *Fhb1*.

6.4.2.5 Are resistances of wheat against FRR, FCR and FHB different?

Stephens et al. (2008) reported significant similarities in the *F. graminearum* gene expression between early stages of FHB and FCR. Moreover, corresponding to the present study they found that the early pathogen-wheat stem interactions are characterized by three distinct stages. Beyond that they could demonstrate that each stage is associated with a specific fungal gene expression program. During the stages I and II *F. graminearum* was found to express a large number of genes to facilitate host penetration and first establishment inside plant tissues (317 genes up-

regulated), while already at stage III during the further tissue colonisation considerably fewer genes were expressed (25 genes up-regulated). Generally, Stephens et al. (2008) concluded that especially the stages I to III in the pathogen-host interaction are most critical for *F. graminearum* since they determine whether the pathogen can successfully colonize the plant or not. Besides the expression of pathogenesis-related plant genes, several fungal genes observed *in planta* seem to have protective functions. Stephens et al. (2008) compared their expression data from stem base tissues with published data on fungal gene expressions during the FHB disease in wheat and barley. Particularly during the early disease stages high similarities between the respective infection-related gene expression patterns were uncovered.

This observation initially leads to a hypothesis assumed in the present study. The pathogen possibly expresses a similar set of genes for the invasion of different plant tissues, as stated by Stephens et al. (2008). This is supported by observations in the present study (chapter 6.2.3) demonstrating that a similar set of fungal developmental events is present during wheat root and floret penetration. Therefore, it is reasonable to assume that comparable similarities should be present regarding the molecular and cellular responses of different tissues.

In this context it was remarkable that all putative wheat resistance genes analysed in the present study showed high activities between 1 to 5 dai, a period in which, on the other side, the pathogen was found to express the majority of pathogenesis-related genes and which has been described to be most critical for disease establishment (Stephens et al., 2008). An intense molecular crosstalk seems to occur during this early disease stages in which the analysed wheat genes was probably part of an immediate plant response to the arsenal of virulence factors released by *F. graminearum*. However, this hypothesis needs further confirmation. In contrast, in susceptible wheat responses gene activities occurred much later, typically around 10 to 21 dai. This phase during the FRR disease development is accompanied by the systemic spread into aerial plant parts in consequence of successful root colonisation. Nevertheless, strong indications were found for a high similarity among *Fusarium* disease particularly during the early stages which is an important finding also with respect to understanding wheat defences against early FHB development. Such knowledge will help to finally propose effective strategies to breed resistant varieties for a better control of devastating *Fusarium* diseases.

There is still an ongoing discussion whether resistances to FHB and FCR in wheat are genetically related. The current status based on QTL studies is that despite a common aetiology, different host genes are involved in the resistance against head blight and crown rot of wheat (Xie et al., 2006; Li HB et al., 2010). In their study using the winter wheat cv. Ernie resistant against FHB and FCR Li HB et al. (2010) found that QTL conferring resistance to the two

diseases were located on different chromosomes (Li HB et al., 2010). In fact, published major QTL against FCR (Zheng et al., 2014) and FHB (Buerstmayr et al., 2009) do not share the same chromosomal locations. Miedaner et al. (1997) also reported a lack of association between Fusarium root rot and head blight resistance in winter rye (*Secale cereale*). Corresponding *Fusarium*-wheat root interactions have not been considered so far. Nevertheless, Li HB et al. (2010) did not exclude that genes affecting both diseases may exist. In fact, similar resistance-associated gene expressions in spike and stem base tissues (Li HB et al., 2010) demonstrated that genes with putative defence functions can be found in different plant tissues infested by *Fusarium*

In the present study the FRR and FHB reactions of wheat genotypes did not show a strong correlation: major FHB resistances as present in the cultivars Sumai 3 and Ning 7840 did not protect against FRR in seedling stages (Fig. 9). This observation initially supported the assumption of a lack of genetic association between genes conferring resistance to these two diseases and was in contrast to the hypothesis that both diseases may have similar resistant mechanism. One explanation for the discrepancy between wheat responses to FRR and FHB would be an age-dependent response of wheat against *Fusarium* spp. similar to an APR as mentioned before. QTL studies on FCR were typically carried out with plants in the seedling stage (Collard et al., 2005, 2006; Bovill et al., 2006, 2010; Ma et al., 2009; Li HB et al., 2010), whereas FHB studies necessarily have to be performed at adult plant stages. Only a single FCR study has been done on adult plants (Wallwork et al., 2004). Moreover, only a single QTL study reports on FCR resistance in both seedlings and adult plants and, in fact, has demonstrated that QTL for seedling and adult plant resistance were located in different genomic regions of bread wheat (Poole et al., 2012). However, the respective genetic studies on seedlings and adult plants were performed using different mapping populations and environmental conditions (greenhouse vs. field). Already Mesterhazy (1987) suggested that discrepancies in resistances against different *Fusarium* diseases could be explained by the fact that some genotypes may express seedling and adult plant resistances simultaneously, while others may not.

To test whether the responses to FRR are vary between different developmental plant stages wheat roots which were inoculated with *F. graminearum*. In fact, within the selected set of four genotypes wheat responses were different at post seedling stage from FRR at seedlings. Especially, the contrasting wheat responses - partial resistance versus high susceptibility - were found to be reverse. Morever, between FHB and FRR a similar wheat responses could be observed. This inversion of wheat responses to FRR was accompanied by different expression of the putative resistance genes. Both findings support the assumption of an age-dependent wheat

response against *Fusarium* spp. reminiscent of APR as described for several biotrophic fungal diseases (Seyfarth et al., 1999; Barcellos et al., 2000; Liu et al., 2001; Yang et al., 2001). The observed inversion can also explain the time limitation in the partial FRR resistance of Florence-Aurore which seems to change around the beginning of plant tillering (Z21-22).

In fact, APR is typically initiated at the tillering stage, the transition from the seedling to adult growth stage, and effective throughout the whole adult stages (Mallard et al., 2008; Ingala et al., 2012). Another, specific type of resistance is the high-temperature, adult-plant resistance, initiated at the tillering stage which is usually quantitatively inherited, as shown in stripe rust of cereals (Line, 2002). Changes in disease resistance phenotypes associated with the plant physiological age have also been reported for other fungal diseases. For instance, Mallard et al. (2008) have reported for the resistance of wheat against the yellow rust pathogen *Puccinia striiformis* that the resistant/susceptible cultivar seems to modify the expression of some defence-related genes during its transition from the seedling to adult growth stages. Ingala et al. (2012) reported that the wheat leaf rust resistance genes Lr27 and LrSV2 were detected each at the seedling and at adult plant stage. The rice variety Wase Aikoku 3 is not resistant to the blight pathogen *Xanthomonas oryzae* in the seedling stage, but shows resistance in the adult plant. Here, Peng & Zhang (2009) found that most polymorphic loci have a higher level of methylation in adult plants than in seedlings, which may contribute to adult plant resistance (APR) in rice plants. Besides the methylation as a possible mechanism behind age-dependent transcriptional changes, genetic factors could also account for such changes. For instance, the *Arabidopsis* gene *NPR1* was found to cause inverse responses to FSB (susceptibility) and FHB (resistance) in the same transgenic wheat line via the regulation of the respective resistance QTL (Gao CS et al., 2013). In addition, common signal transduction pathways were found to activate defence genes against seedling FCR and adult plant FHB such as the pathogeneses-related gene *PR-1* (Gao CS et al., 2013) and different P450 cytochrome genes (Li HB et al., 2010; Li X et al., 2010).

The hexaploidy of bread wheat allows asking whether and to which extent polyploidy contributes to age-dependent gene expression. Polyploidy has extensive effects on gene expression since duplicated genes/genomes typically diversify in function or undergo subfunctionalization (Adams & Wendel, 2005). In fact, the expression of most genes depends on regulatory networks, such as transcription factors that are organized in hierarchies. Polyploid networks are much more complex than diploid networks due to possible (much) higher numbers of alleles and regulators. Hence, the overall effects on the expression of genes at the ends of regulatory cascades are difficult to predict, but in some cases, altered interactions could change the developmental timing or tissue specificity of gene expression (Osborn et al., 2003; Adams &

Wendel, 2005). Whether the polyploidy of bread wheat has an effect on the observed changes in FRR phenotypes is a question that is currently addressed in our lab (data not shown).

Finally, the assumption of the present study that the changes in the wheat response to FRR probably associated with the physiological plant age, respectively with transcriptional changes of defence-related gene expressions is also supported by the observation that the expression patterns of candidate resistance genes were similar to those previously observed for FHB. These FHB related patterns were characterised by early-stage and steady-state inductions associated with resistance, while transcript induction generally occurred later and temporarily in the susceptible cultivars (Gottwald et al., 2012). To conclude, already Mesterhazy (1983) suggested that breeding for *Fusarium* resistance in the seedling stage together with breeding for adult resistance (FHB), may help to significantly enhance overall (wheat) crop resistance to Fusarium damage on crowns, roots, or spikes.

7 Summary

In the present study the *F. graminearum*-wheat root pathosystem has been systematically examined. This pathosystem represents a complex of *Fusarium* diseases including root rot (FRR), crown rot (FCR) and seedling blight (FSB). Several molecular tools are nowadays available for investigating plant-host pathosystems including virulence determinants and resistance research. The knowledge on the mechanisms of *Fusarium* pathogenesis is still relatively sparse, particularly in case of soil-borne diseases. However, such knowledge is required to exploit molecular tools and currently available 'omics' technologies to support research towards the implementation of efficient and sustainable defense strategies.

A comprehensive bioassay has been established to study and elucidate the causes and features of FRR, a hidden disease which affects below-ground plant parts. The bioassay combines different phenotypic evaluations, such as qPCR-based quantification, size measurement and symptom rating as well as statistics. The combined bioassay yielded consistent and significant results which prove its usefulness for resistance research and wheat breeding.

The FRR bioassay combined with different microscopy techniques was applied for studies of plant-pathogen interaction in a set of 12 diverse wheat genotypes. An important result of the studies was the identification of different wheat responses ranging from partial resistance to high susceptibility. Partial resistance was characterised by an impaired fungal accumulation in roots accompanied by a delayed disease spread better plant performance (biomass production, yield, etc.). This was confirmed by comparative confocal laser scanning microscopy of the partially resistant cv. Florence-Aurore and the highly susceptible Line 1105.16. A reduction of root biomass was the most severe effect on wheat caused by root rot, most probably responsible for the negative effects on seedlings and plant fitness. Finally, the phytopathological and histopathological examinations carried out in this study allowed the definition of three distinct phases of FRR disease comprising i) root infection; ii) root colonization at infection sites; and iii) progressive root colonization accompanied with a successful disease spread. The first two phases were found to be critical for the disease establishment and therefore, provide targets for further research and selective phenotyping in the course of genetic studies and/or wheat breeding.

Soil-borne inoculum and root infection were found to be significant components of the *F. graminearum* life cycle, although the pathogen is usually regarded as affecting above-ground plant parts. In addition, it was demonstrated that the life cycle of the pathogen shares common features with other root-infecting fungi. This explains the observed high capability of *F. graminearum* to infect wheat roots. In fact, microscopic examinations demonstrated the early

formation of fungal structures on root surfaces which either serve for an active root penetration, or for repeating infection stages and further soil contamination.

An important outcome of this study was the discovery that upon successful root colonization, *F. graminearum* can enter the vascular system of the wheat stem and spread systemically to leaves and spikes without causing visible disease symptoms. Tissue-adapted invasion strategies were uncovered in which the root cortex cells, the vascular stem tissues and the leaf hairs are preferential targets for colonization. At later disease stages the stem base was increasingly used as storage for the pathogen and source for the dispersal of mycotoxins and hyphae into the developing plant, probably contributing to the frequently observed senescence of tillers and whitehead symptoms. Consequently, at later disease stages the DON mycotoxin was detected in all plant parts. Thus, FRR has the potential to affect critical growth stages, especially since both the pathogen and the toxin were detected in spikes at anthesis (flowering).

Major FHB resistance genes were shown not to protect against root rot at seedling stages since even highly FHB resistant genotypes have shown a high susceptibility to FRR. Hence, there is a high risk that new elite cultivars with enhanced FHB resistance are susceptible to FRR at seedling stages. On the other side, besides features that are unique for root rot, other features of the FRR pathogenesis were reminiscent of spike colonization. The hypothesis that such similarities of the pathogens activities might be causal for similarities of wheat responses was strongly supported by the finding that partial FRR resistance is accompanied by the activation of different defence mechanisms (DON detoxification and jasmonate-triggered basal defence) known from FHB, too. In roots the tested 12 FHB/DON resistance genes were up-regulated in the FRR resistant genotype Florence-Aurore which is, however, highly susceptible to FHB. Nevertheless, the respective expression patterns were basically similar to those in spikes by covering all phases of main infection and early colonization, indicating perception of the pathogen by the wheat root. In addition, a zinc finger transcription factor has been reported as an interesting candidate gene possibly involved in the regulation of *Fusarium* resistance.

The hypothesis that resistance against *Fusarium* diseases including FRR and FHB is plant age dependent has been tested in this study. This hypothesis is supported by the finding that the transition from seedling to post-seedling stages is associated with changes in wheat responses to FRR leading similar responses to FRR and FHB. In fact, upon adult root infection the early resistance of cv. Florence-Aurore turned to FRR susceptibility correlated with absent defence gene inductions. On the contrary, wheat genotypes susceptible during seedling stages showed better performances and absence of defence gene inductions. This finding is especially remarkable since it could also be demonstrate in this study that no fundamental differences exist

in the course and severity of root rot after seedling and adult root infection, indicating that such infections can be a major threat even after the seedling stage. These results strongly indicate that resistance of wheat to different *Fusarium* diseases may not rely on the presence of different genes, but rather on transcriptional modifications related to the physiological plant age, reminiscent of adult plant resistance.

Although many open questions still exist, the results of this study allow the hypothesis that root infection confers a selective advantage to *F. graminearum* and therefore, is likely more common in the field than previously assumed. In fact, due to their saprotrophic life cycle *Fusarium* fungi are an integral part of the rhizosphere community to which crop plants are exposed. It has previously been stated that it would be unlikely that a fungus maintains such an ability if it were not advantageous since successful root infection is associated with complex, specialized structures and processes. This insight has major implications for the development of new strategies for plant breeding and disease control. In fact, growing resistant varieties is the most promising strategy to protect against FRR since chemical plant protection is ineffective here due to the specific characteristics of this disease. Consequently, the present study provides new insights into a long time underestimated threat to wheat production and can provide new resistance strategies against a complex, multifaceted plant pathogen causing significant damage to wheat and other cereals.

8 Zusammenfassung

Gegenstand und Ziel dieser Arbeit war eine systematische Untersuchung des Pathosystems *F. graminearum*-Weizen (*Triticum aestivum*). Dieses Pathosystem beinhaltet einen Komplex von *Fusarium*-Krankheiten, die den Weizenbau erheblich beeinträchtigen können; dazu gehören die Wurzelfäule (FRR), die Kronenfäule (FCR) und die Ähren-Fusariose (FHB). Unsere Kenntnis der Mechanismen der *Fusarium*-Pathogenese ist nach wie vor relativ gering. Dies gilt insbesondere für die bodenbürtigen Krankheiten, insbesondere die Wechselwirkungen zwischen *F. graminearum* und Weizenwurzeln waren zu Beginn dieser Studie nahezu unbekannt. Eine umfangreichere Kenntnis ist jedoch Grundlage und Voraussetzung für eine gezielte Nutzung molekularer Werkzeuge inkl. „Omics"-Technologen zur Unterstützung der Forschung hinsichtlich einer Implementierung effizienterer und nachhaltiger Abwehrstrategien.

Ein notwendiger, erster Schritt war die Weiterentwicklung und Anwendung eines zuverlässigen und praktikablen Bioassay für die Fusarium-Wurzelfäule, die primär unterirdische Pflanzenorgane befällt und sich einer herkömmlichen, frühen Phänotypisierung entzieht. Auf der Basis der relativen Pilz-Biomasse (RFB) und verschiedener phänotypischer Parameter (RBR, RLR, SLR, FSI) wurde ein Fusarium-Krankheitsindex (FDI) entwickelt und für die Differenzierung von 12 Weizen-Genotypen bezüglich Resistenz oder Anfälligkeit eingesetzt. Dieser Index kann für weiterführende QTL-Analysen und Resistenzzüchtung eingesetzt werden.

Diese Untersuchungen zeigten das FRR mit einem breiten Schadspektrum einhergeht, das signifikante Beeinträchtigungen der Weizenentwicklung sowohl im Sämlings- als auch im Erwachsenen-Stadium zur Folge hat. Insbesondere die Reduktion der Wurzelmasse erwies sich als der gravierendste Negativ-Effekt den FRR bei Weizen verursacht. Ein wichtiges Ergebnis war die Identifikation von zwei Genotypen mit partieller Resistenz gegen FRR. Ferner zeigen die Untersuchungen zur Wurzelinfektion im Sämlings- und Erwachsenen-Stadium eine inverse Reaktion des Weizens bezüglich der Wurzelfäule und Ähren-Fusariose. Zudem wurden Hinweise auf altersbedingte Änderungen in Weizenreaktion auf *Fusarium*-Krankheiten gefunden, die bisher in diesem Umfang noch nicht diskutiert wurden.

In einem vergleichenden Ansatz wurden die pilzlichen Strategien der Wurzel- und Pflanzenbesiedlung in der partiell resistent Sorte Florence-Aurore und der anfälligen Line 1105.16 mittels konfokaler Laser-Scanning Mikroskopie untersucht. Diese Studie ermöglichte bisher unbekannte Einblicke in die unterschiedlichen, pflanzen-gewebespezifischen Pilzstrategien, aber auch in den Charakter der Resistenz gegen FRR. Während die anfängliche Penetration der Wurzelepidermis noch bei beiden Genotypen beobachtet werden konnte, wurde

die anschließende Migration des Pathogens in den Cortex (Rindengewebe) vom resistenten Genotyp deutlich vermindert.

Eine Resistenz des Weizens gegen die Wurzelinfektion wurde nicht beobachtet, weder im Sämlings- noch im Erwachsenen-Stadium. Tatsächlich zeigten die mikroskopischen Untersuchungen zur Wurzelinfektion bei Sämlingen, das *F. graminearum*, bisher als Ährenpathogen angesehen, über komplexe hyphale Strukturen zur Wurzelinfektion verfügt. Es wurde eine zwei-phasige Strategie beobachtet bestehend aus (1) Strukturen wie sie von anderen Wurzelpathogenen bekannt sind, und (2) solchen wie sie von der Ähren-Fusariose bekannt sind. Dies ist, meines Wissens, im Bereich der Pflanzenpathogene eine Besonderheit. Auch zeigten die Untersuchungen bereits früh nach Inokulation Pilzstrukturen, die zur Vermehrung und nachfolgende Kontamination des Bodens dienen.

Ein wichtiges Resultat der Arbeit ist die Erkenntnis, dass *F. graminearum* nach erfolgreicher Wurzelkolonisierung das Gefäßsystem des Weizenhalm besiedeln und sich ohne erkennbare Symptome in periphäre Organe ausbreiten kann. Wie bereits für die Wurzeln berichtet, ist auch die Ausbreitung in Halm und Blätter im resistenten Genotyp deutlich verzögert und reduziert. Während das Mycotoxin DON zunächst nur in der Wurzel nachzuweisen ist, kann es später in allen Geweben bzw. Entwicklungsstadien von Weizenpflanzen gefunden werden. Sowohl das Pathogen selbst als auch das Mykotoxin wurden schließlich zu Beginn der Blüte auch in Ähren detektiert. Für das Pathogen wurde dieses Ausbreitungspotential auch nach Wurzelinokulationen im Erwachsenen-Stadium beobachtet.

Die phytopathologischen und histopathologischen Untersuchungen im Zeitverlauf ermöglichten die Definierung distinkter FRR-Stadien: i) frühe Infektion, ii) Hauptinfektion, iii) Kolonisierung der Wurzel und danach auch distaler Gewebe/Organe. Dieser skizzierte Krankheitsverlauf zeigt Ähnlichkeit mit der FHB-Pathogenese.

Offenbar geht partielle FRR-Resistenz mit der Aktivierung von Abwehrmechanismen (DON-Detoxifikation und Jasmonsäure (JA)-gesteuerte generelle Abwehr) einher, die schon von FHB bekannt sind. In den Wurzeln waren FHB- bzw. DON-Resistenzgene in der FRR-resistenten Sorte Florence-Aurore hochreguliert, obwohl diese gegen FHB hochanfällig ist und alle getesteten Gene in den Ähren keine Induktion zeigten. In den Wurzeln der FHB resistenten Kultivare Sumai 3 und Ning 7840 hingegen waren die getesteten Gene nicht induziert, bzw. wesentlich später induziert. Unter den getesteten Genen erwies sich ein Zinkfinger-Transkriptionsfaktor als interessantes Kandidatengen für die Resistenzregulation. In einer vergleichenden Zeitreihenstudie zwischen Wurzel und Ähren konnte gezeigt werden, dass unterschiedliche Schlüsselgene der JA-gesteuerte generellen Abwehr sowohl im Sämlings- (FRR)

als auch im Erwachsenen-Stadium (FHB) im Zusammenhang mit Resistenz induziert sind. Auch für diese Gene zeigten sich inverse Expressionsmuster hinsichtlich der Genotypen. Dies war umso interessanter als die Expressionsmuster in Wurzeln grundsätzlich denen in Ähren entsprachen: Resistenz assoziiert mit frühen und oft anhaltenden Expressionen, die typischerweise während kritischer Phasen im Krankheitsverlauf gipfeln; Anfälligkeit assoziiert mit (wesentlich) späteren und oft kurzzeitigen Expressionen. Auch die Studie zu Genexpressionen erbrachte Hinweise auf altersbedingte Änderungen in Weizenresistenz gegen *Fusarium*-Krankheiten. Dazu konnte gezeigt werden, (1) dass die Resistenz gegen *Fusarium*-Erkrankungen der unter- und oberirische Pflanzenorgane möglicherweise hinsichtlich der beteiligten Gene nicht so verschieden ist, wie bisher in der einschlägigen Forschung angenommen wird; und (2) dass sich eine quantitative Resistenz sich nicht notwendigerweise durch das Spektrum induzierter Gene von einer Anfälligkeit unterscheidet, sondern vielmehr durch den Zeitpunkt der Geninduktionen.

Sicherlich müssen viele Fragen zur den Wechselwirkungen zwischen Weizenwurzeln und *F .graminearum* (z.B. hinsichtlich der Resistenzmechanismen und der Epidemiologie im Feld) in dieser Arbeit unbeantwortet bleiben. Dennoch gestatten die Ergebnisse die Hypothese, dass die Wurzelinfektion für *F. graminearum* einen selektiven Vorteil darstellt und daher im Feld möglicherweise weiter verbreitet ist, als bisher angenommen. Tatsächlich sind *Fusarium*-Pathogene wegen ihrer primär saprophytischen Lebensweise in der Rhizosphäre weit verbreitet und stellen damit eine unmittelbare Gefahr für kompatible Nutzpflanzen (Getreide) dar. Die Befähigung zum Wurzelbefall, ein komplexer und aufwändiger Vorgang, ist ein starker Hinweis auf den Nutzen dieser Strategie für das Pathogen. Mithin muss hierauf bei der Entwicklung neuer Züchtungs- bzw. Pflanzenschutz-Strategien Rücksicht genommen werden. Tatsächlich ist die Sortenresistenz die beste Strategie zur Bekämpfung von Fusariosen, da chemischer Pflanzenschutz hier nicht effektiv ist. Diese Tatsache unterstreicht die Bedeutung der vorliegenden Arbeit: Das Verständnis eine bisher wenig beachteten Krankheit als ernsthafte Bedrohung für die Weizenproduktion ermöglicht nunmehr die Implementierung neuer Strategien für eine Resistenzzüchtung, die sich gegen ein Pflanzenpathogen richten muss, das in seinen Möglichkeiten vielseitiger ist als bisher angenommen.

9 References

Adams LK, Wendel FJ. 2005. Polyploidy and genome evolution in plants. *Curr. Opin. Plant Biol.* 8: 135-141.

Agrios GN. 2004. *Plant Pathology-5th ed***.** Elsevier Press, 984.

Alam A, Xue F, Wang C, Ji C. 2011. Powdery mildew resistance genes in wheat: identification and genetic analysis. *J Mol Biol Res.* 1: 20-39.

Anderson JA, Stack RW, Liu S, Waldron BL, Fjeld AD, Coyne C, Moreno-Sevilla B, Fetch JM, Song QJ, Cregan PB and Frohberg RC. 2001. DNA markers for Fusarium head blight resistance QTLs its two wheat populations. *Theor. Appl. Genet.* 102: 1164-1168.

Anderson JP, E Badruzsaufari, PM Schenk, JM Manners, OJ Desmond, C Ehlert, DJ Maclean, PR Ebert, K Kazan. 2004. Antagonistic interaction between Abscisic Acid and Jasmonate-Ethylene singnaling pathways modulates defense gene expression and disease resistance in Arabidopsis. *Plant Cell* 16: 3460-3479.

Annis SL, Goodwin PH. 1997. Production and regulation of polygalacturonase isozymes in Canadian isolates of Leptosphaeria maculans differing in virulence. *Can. J. Plant Pathol.* 19: 358-65.

Armentrout VM, Downer AJ, Grasmick DL, Weinhold AR. 1987. Factors affecting infection cushion development by *Rhizoctonia solani* on cotton. *Phytopathology* 77: 623-630.

Audenaert K, De Meyer GB, Hofte MM. 2002. Abscisic acid determines basal susceptibility of tomato to *Botrytis cinerea* and suppresses salicylic acid-dependent signaling mechanisms. *Plant Physiol.* 128: 491-501.

Bachmann A, Hause B, Maucher H, Garbe E, Vörös K, Weichert H, Wasternack C, Feussner I. 2002. Jasmonate-induced lipid peroxidation in barley leaves initiated by distinct 13-LOX forms of chloroplasts. *Biol Chem.* 383: 1645-1657.

Backhouse D, Abubakar AA, Burgess LW, Dennis JI, Hollaway GJ, Wildermuth GB, Wallwork H, Henry FJ. 2004. Survey of *Fusarium* species associated with crown rot of wheat and barley in eastern Australia. *Aus. Plant Path.* 33: 255-261.

Badea A, Eudes F, Graf RJ, Laroche A, Gaudet DA, Sadasivaiah RS. 2008. Phenotypic and marker-assisted evaluation of spring and winter wheat germplasm for resistance to fusarium head blight. *Euphytica* 164: 803-819.

Bai G, Kolb FL, Shaner G, Domier LL. 1999. Amplified fragment length polymorphism markers linked to a major quantitative trait locus controlling scab resistance in wheat. *Phytopathology* 89: 343-348.

Bai G, Desjardins AE, Plattner RD. 2001. Deoxynivalenol-nonproducing *Fusarium graminearum* causes initial infection, but does not cause disease spread in Wheat spikes. *Mycopathologia* 153: 91-98.

Balmer D, Flors V, Glauser G, Mauch-Mani B. 2013. Metabolomics of cereals under biotic stress: current knowledge and techniques. *Front.PlantSci*. 4:82.

Barcellos AL, Roelfs AP, Moraes-Fernandes MIBde. 2000. Inheritance of adult plant leaf rust resistance in the Brazilian wheat variety Toropi. *Plant Dis.* 84: 90-93.

Bärlocher F. 1999. Biostatistik. Praktische Einführung in Konzepte und Methoden. *Georg Thieme Verlag Stuttgart.*

Basnet B, Glover K, Ibrahim A, Yen Y, Chao S. 2012. A QTL on chromosome 2DS of 'Sumai 3' increases susceptibility to Fusarium head blight in wheat. *Euphytica* 186: 91-101.

Beccari G, Covarelli L and Nicholson P. 2011. Infection processes and soft wheat response to root rot and crown rot caused by *Fusarium culmorum*. *Plant Pathol.* 60: 671-684.

Becker H. 2011. Pflanzenzüchtung.2nd edition. *Verlag Eugen Ulmer Stuttgart.*

Belien T, Van Campenhout S, Robben J, Volckaert G. 2006. Microbial endoxylanases: effective weapons to breach the plant cell-wall barrier or, rather, triggers of plant defense systems? *Mol Plant-Microbe Interact.* 19: 1072-1081.

Belova T, Zhan Bj, Wright J, Caccamo M, Asp T, Šimková H, Kent M, Bendixen C, Panitz F, Lien S, Doležel J, Olsen O, Sandve RS. 2013. Integration of mate pair sequences to improve shotgun assemblies of flow-sorted chromosome arms of hexaploid wheat. *BMC Genomics* 14: 222.

Bennett JW and Klich M. 2003. Mycotoxins. *Clin. Microbiol. Rev.* 16: 497-516.

Ben-David R, Xie Wl, Peleg Z, Saranga Y, Dinoor A, Fahima T. 2010. Identification and mapping of PmG16, a powdery mildew resistance gene derived from wild emmer wheat. *Theor. Appl. Genet.* 121: 499-510.

Berkman PJ, Skarshewski A, Manoli S, Lorenc MT, Stiller J, Smits L, Lai K, Campbell E, Kubaláková M, Simková H, Batley J, Doležel J, Hernandez P, Edwards D. 2012. Sequencing wheat chromosome arm 7BS delimits the 7BS/4AL translocation and reveals homoeologous gene conservation. *Theor. Appl. Genet.* 124:423-432.

Berthiller F, Dallasta C, Corradini R, Marchelli R, Sulyok M, Krska R, Adam G, Schuhmacher R. 2009. Occurrence of deoxynivalenol and its 3-beta-D-glucoside in wheat and maize. *Food Addit Contam A.* 26: 507-511.

Bertini L, Caporale C, Testa M, Proietti S, Caruso C. 2009. Structural basis of the antifungal activity of wheat PR4 proteins. *FEBS (Fed. Eur. Biochem. Soc.) Lett* 583: 2865-2871.

Berzonsky WA, Gebhard BL, Gamontine E, Leach GD. 2007. A reciprocal backcross monosomic analysis of the scab resistant spring wheat (Triticum aestivum L.) cultivar, 'Frontana'. *Plant Breeding* 126: 234-239.

Blée E. 2002. Impact of phyto-oxylipins in plant defense. *Trends Plant Sci.* 7: 315-22.

Boddu J, Cho S, Kruger WM, Muehlbauer GJ. 2006, Transcriptome analysis of the barley-*Fusarium graminearum* interaction. *MPMI* 19(4): 407-417.

Boddu J, Cho S, Muehlbauer GJ. 2007. Transcriptome analysis of trichothecene induced gene expression in barley. *Mol Plant Microbe Interact.* 20: 1364-1375.

Boenisch JM, Schäfer W. 2011. *Fusarium graminearum* forms mycotoxin producing infection structures on wheat. *BMC Plant Biol.* 11:110.

Bollina V, Kumaraswamy GK, Kushalappa AC, Choo TM, Dion Y, Rioux S. 2010. Mass spectrometry based metabolomics application to identify quantitative resistance related metabolites in barley against Fusarium head blight. *Mol.Plant.Pathol.*11:769-782.

Bormann J, Boenisch MJ, Brückner E, Firat D, Schäfer W. 2014. The Adenylyl Cyclase Plays a Regulatory Role in the Morphogenetic Switch from Vegetative to Pathogenic Lifestyle of *Fusarium graminearum* on Wheat. *PLoS ONE* 9(3): e91135.

Bovill WD, Horne M, Herde D, Davis M, Wildermuth GB, Sutherland MW. 2010. Pyramiding QTL increases seedling resistance to crown rot (*Fusarium pseudograminearum*) of wheat (*Triticum aestivum*). *Theor. Appl.Genet.*121:127-136.

Bovill WD, Ma W, Ritter K, Collard BCY, Davis M, Wildermuth GB, Sutherland MW. 2006. Identification of novel QTL for resistance to crown rot in the doubled haploid wheat population 'W21MMT70' X 'Mendos'. *Plant Breeding* 125: 538-543.

Brenchley R, Spannagl M, Pfeifer M, Barker GLA, D'Amore R, Allen AM, McKenzie N, Kramer M, Kerhornou A, Bolser D. 2012. Analysis of the bread wheat genome using whole-genome shotgun sequencing. *Nature* 491: 705-710.

Brown NA, Urban M, van de Meene AM, Hammond-Kosack KE. 2010. The infection biology of *Fusarium graminearum*: defining the pathways of spikelet to spikelet colonisation in wheat ears. *Fungal Biol.* 114: 555-571.

Brown AN, Bass C, Baldwin KT, Chen HG, MassotF, Carion WCP, Urban M, van deMeene MLA, Hammond-Kosack EK. 2011. Characterisation of the *Fusarium graminearum*-Wheat Floral Interaction. *J. Pathog.* 2011: 626345.

Brummell DA, Harpster MH. 2001. Cell wall metabolism in fruit softening and quality and its manipulation in transgenic plants. *Plant Mol. Biol.* 47: 311-339.

Brunner K, Paris PKM, Paolino G, Bürstmayr H, Lemmens M, Berthiller F, Schuhmacher R, Krska R, Mach LR. 2009. A reference-gene-based quantitative PCR method as a tool to determine *Fusarium* resistance in wheat. *Anal Bioanal Chem.* 395: 1385-1394.

Buerstmayr H, Ban T, Anderson JA. 2008. QTL mapping and marker assisted selection for *Fusarium* head blight resistance in wheat. In: Mesterhazy. A. and Toth, B. (eds.): Proceedings of the 3rd International Symposium on *Fusarium* Head Blight, Szeged, Hungary, September 1-5, 2008, Cereal Research Communications, 36, Suppl. B: 1-3.

Buerstmayr H, Ban T and Anderson JA. 2009. QTL mapping and marker assisted selection for Fusarium head blight resistance in wheat: a review. *Plant Breeding* 128: 1-26.

Buerstmayr H, Lemmens M, Hartl L, Doldi L, Steiner B, Stierschneider M and Ruckenbauer P. 2002. Molecular mapping of QTLs for Fusarium head blight resistance in spring wheat. I. Resistance to fungal spread (type II resistance). *Theor. Appl. Genet.* 104: 84-91.

Buerstmayr H, Steiner B, Hartl L, Griesser M, Angerer N, Lengauer D. 2003. Molecular mapping of QTLs for Fusarium head blight resistance in spring wheat. II. Resistance to fungal penetration and spread. *Theor. Appl. Genet.* 107: 503-508.

Burgess LW, Wearing AH, Toussoun TA. 1975. Survey of Fusaria associated with crown rot of wheat in Eastern Australia. *Aust. J. Agric. Res.* 26: 791-9.

Burgess L. 2005. Intermediate hosts and the management of crown rot and head blight. In: Annual Report of GRDC strategic initiative on crown rot, common root rot and Fusarium head blight. *Grains Research and Development Corporation, Kingston, Australia*: 34-36.

Bushnell WR, Hazen BE and Pritsch C. 2003. Histology and physiology of Fusarium head blight. In Fusarium Head Blight of Wheat and Barley (Leonard, K.J. and Bushnell, W.R., eds). *St. Paul, MN: APS Press*.

Bustin SA, Nolan T. 2009. Analysis of mRNA expression by Real-time PCR. In: Real-time PCR-Current Technology and Applications (Logan J, Edwards K, Saunders N., eds). *Caister Academic Press, Norfolk, UK.*

Caporale C, Di Bernardino I, Leonardi L, Bertini L, Cascone A, Buonocore V, Caruso C. 2004. Wheat pathogenesis–related proteins of class 4 have ribonuclease activity. *FEBS Letters* 575: 71-76.

Chakraborty S, Luck J, Hollaway G, Freeman A, Norton R, Garrett KA et al., 2008. Impacts of global change on diseases of agricultural crops and forest trees. *CAB Reviews* 3: 054.

Chakraborty S, Newton AC. 2011. Climate change, plant diseases and food security: an overview. *Plant Pathol.*. 60: 2-14.

Charmet G. 2011. Wheat domestication: Lessons for the future. *C. R. Biologies* 334: 212–220.

Chazotte B. 2011. Labeling membrane glycoproteins or glycolipids with fluorescent wheat germ agglutinin. *Cold Spring Harb Protoc* doi: 10.1101.

Chen F, Zhang J, Song X, Yang J, Li H, Tang H and Liao YC. 2011. Combined metabolomic and quantitative real-time PCR analyses reveal systems metabolic changes of *Fusarium graminearum* induced by *Tri5* gene deletion. *J. Proteome Res.* 10: 2273-2285.

Chen LQ, Hou BH, Lalonde S, Takanaga H, Hartung ML, QuXQ, Guo WJ, Kim JG, Underwood W, Chaudhuri B et al. 2010. Sugar transporters for intercellular exchange and nutrition of pathogens. *Nature* 468: 527-532.

Chen LQ. 2014. SWEET sugar transporters for phloem transport and pathogen nutrition. *New Phytol.* 201: 1150-1155.

Chen Q, Sun J, Zhai Q, Zhou W, Qi L, Xu L, Wang B, Chen R, Jiang H, Qi J, et al. 2011. The basic helix-loop-helix transcription factor MYC2 directly represses *PLETHORA* expression during jasmonate-mediated modulation of the root stem cell niche in *Arabidopsis* . *Plant Cell* 23:3335-3352.

Chen XM. 2005. Epidemiology and control of stripe rust [*Puccinia striiformis f. sp. tritici*] on wheat. *Can J Plant Pathol.* 27: 314-337.

Chen XM. 2013. High-Temperature Adult-Plant Resistance, Key for Sustainable Control of Stripe Rust. *Am.J.Plant Sci.* 4 (3): 608-627.

Chico JM, Chini A, Fonseca S, Solano R. 2008. JAZ repressors set the rhythm in jasmonate signaling. *Curr Opin Plant Biol.* 11: 486-494.

Chini A, Fonseca S, Fernandez G, Adie B, Chico JM, Lorenzo O, Garcıa-Casado G, Lopez-Vidriero I, Lozano F.M, Ponce MR, Micol JL, and Solano R. 2007. The JAZ family of repressors is the missing link in jasmonate signalling. *Nature* 448: 666-671.

Chomczynski P, Sacchi N. 1987. Single-step method of RNA isolation by acid guanidinium thiocyanate-pheno-chloroform extraction. *Anal Biochem.* 162: 156-159.

Chongo G, Gossen BD, Kutcher HR, Gilbert J, Turkington TK, Fernandez MR. 2000. Reaction of seedling roots of 14 crop speciese of *Fusarium graminearum* from wheat heads. *Can. J. Plant Pathol.* 23:132-137.

Chongo G, Gossen BD, Kutcher HR, Gilbert J, Turkington TK, Fernandez MR and Mclaren D. 2001. Reaction of seedling roots of 14 crop species to *Fusarium graminearum* from wheat heads. *Can. J. Plant Pathol.* 23: 132-137.

Chu C, Niu Z, Zhong S, Chao S, Friesen T, Halley S et al., 2011. Identification and molecular mapping of two QTLs with major effects for resistance to Fusarium head blight in wheat. *Theor. Appl. Genet* . 123: 1107-1119.

Ciftci-Yilmaz S, MittlerR. 2008. The zinc finger network of plants. *Cell. Mol. Life Sci.* 65: 1150 -1160.

Clement JA, Parry DW. 1998. Stem-base disease and fungal colonisation of winter wheat grown in compost inoculate with *Fusarium culmorum, F. graminearum* and *Microdochium nivale*. *Eur. J. Plant Pathol.* 104: 323-330.

Collard BCY, Grams RA, Bovill WD, Percy CD, Jolley R, Lehmensiek A, Wildermuth G, Sutherland MW. 2005. Development of molecular markers for crown rot resistance in wheat: mapping of QTL for seedling resistance in a '2-49' x 'Janz' population. *Plant Breeding* 124: 532-537.

Collard BCY, Jolley R, Bovill WD, Grams RA, Wildermuth GB, Sutherland MW. 2006. Confirmation of QTL mapping and marker validation for partial seedling resistance to crown rot in wheat line '2-49'. *Aust J Agric Res.* 57: 967-973.

Collins TJ. 2007. ImageJ for microscopy. *Bio. Techniques* 43: S25–30.

Cook RJ. 1992. Wheat root health management and environmental concerns. *Can. J. Plant Pathol.* 14: 76-85.

Covarelli L, Beccari G, Steed A, Nicholson P. 2012. Colonization of soft wheat following infection of the stem base by *Fusarium culmorum* and translocation of deoxynivalenol to the head. *Plant Pathol.* 61: 1121-1129.

Creelman RA, Mullet JE. 1997. Biosynthesis and action of jasmonates in plants. Ann. Rev. Plant Physiol. *Plant Mol. Biol.* 48: 355-381.

Cumagun CJR, Miedaner T. 2004. Segregation for aggressiveness and deoxynivalenol production of a population of *Gibberella zeae* causing head blight of wheat. *Eur. J. Plant Pathol.* 110: 789-799.

Cuomo, CA, Guldener U, Xu JR, Trail F, Turgeon BG, Di Pietro A, Walton JD, Ma LJ, Baker SE, Rep M, et al. 2007. The *Fusarium graminearum* genome reveals a link between localized polymorphism and pathogen specialization. *Science* 317: 1400-1402.

Cuthbert PA, Somers DJ, Thomas J, Cloutier S, Brule-Babel A. 2006. Fine mapping Fhb1, a major gene controlling fusarium head blight resistance in bread wheat (*Triticum aestivum L.*). *Theor. Appl. Genet.* 112: 1465-1472.

Cuzick A, Urban M, Hammond-Kosack K. 2008. *Fusarium graminearum* gene deletion mutants map1 and tri5 reveal similarities and differences in the pathogenicity requirements to cause disease on *Arabidopsis* and wheat floral tissue. *New Phytol.* 177 (4): 990-1000.

Dalcero A, Torres A, Etcheverry M, Chulze S, Varsavsky E. 1997. Occurrence of deoxynivalenol and *Fusarium graminearumin* Argentinian wheat. *Food Addit Contam* 14 (1): 11-14.

Daniel R, Simpfendorfer S. 2008. The impact of crown rot on winter cereal yields. http://www.grdc.com.au/uploads/documents/GRDC%20update%202008%20crown%20rot%20impact%20on%20yield.doc

De Geyter N, Gholami A, Goormachtig S, Goossens A. 2012. Transcriptional machineries in jasmonate-elicited plant secondary metabolism. *Trends Plant Sci*. 17: 349-359.

Del Ponte EM, Fernandes JMC, Bergstrom GC. 2007. Influence of growth stage on fusarium head blight and deoxynivalenol production in wheat. *J. Phytopathology* 155: 577-581.

Demeke T, Clear RM, Patrick SK, Gaba D. 2005. Species-specific PCR-based assays for the detection of *Fusarium* species and a comparison with the whole seed agar plate method and trichothecene analysis. *Int. J. Food Microbio*l. 103(3): 271-284.

Demeke T, Gräfenhan T, Clear MR, Phan A, Ratnayaka I, Chapados J, Patrick KS, Gaba D, Lévesque b CA, Seifert AK. 2010. Development of a specific TaqMan® real-time PCR assay for quantification of *Fusarium graminearum* clade 7 and comparison of fungal biomass determined by PCR with deoxynivalenol content in wheat and barley. *Int. J. Food Microbiol.* 141: 45-50.

Desjardins AE. 2008. Natural product chemistry meets genetics: when is a genotype a chemotype? *J Agr Food Chem*. 56:7587-7592.

Desmond OJ, Manners JM, Stephens AE, Maclean DJ, Schenk PM, Gardiner DM, Munn AL and Kazan K. 2008. The *Fusarium* mycotoxin deoxynivalenol elicits hydrogen peroxide production, programmed cell death and defence responses in wheat. *Mol. Plant Pathol.* 9: 435-445.

Devoto A, Ellis C, Magusin A, Chang HS, Chilcott C, Zhu T, Turner JG. 2005. Expression profiling reveals COI1 to be a key regulator of genes involved in wound- and methyl jasmonate-induced secondary metabolism, defence, and hormone interactions. *Plant Mol. Biol.* 58: 497-513.

Di Pietro A, García-Maceira FI, Méglecz E, Roncero MIG. 2001. A MAP kinase of the vascular wilt fungus *Fusarium oxysporum* is essential for root penetration and pathogenesis. *Mol Microbiol.* 39(5): 1140-1152.

Di R, Blechl A, Dill-Macky R, Tortora A, Tumer NE. 2010. Expression of a truncated form of yeast ribosomal protein L3 in transgenic wheat improves resistance to Fusarium head blight. *Plant Sci.* 178: 374-380.

Diamond M, Reape TJ, Rocha O, Doyle SM, Kacprzyk J. 2013. The *Fusarium* Mycotoxin Deoxynivalenol Can Inhibit Plant Apoptosis-Like Programmed Cell Death. *PLoS ONE* 8(7): e69542.

Diaz A, Maria M. 2012. *Fusarium* species infectiong soybean roots: Frequency, aggressiveness, yield impact and interaction with the soybean cyst nematode. *Graduate theses and Dissertations*. 12314.

Ding L, Xu H, Yi H, Yang L, Kong Z, Zhand L, Xue S, Jia H. 2011. Resistance to hemi-biotrophic *F. graminearum* infection is associated with coordinated and ordered expression of diverse defense signaling pathways. *PLoS One* 6(4):e19008.

Divon HH, Fluhr R. 2007. Nutrition acquisition strategies during fungal infection of plants. *FEMS Microbiology Letters* 266: 65–74.

Dombrecht B, Xue GP, Sprague SJ. 2007. MYC2 differentially modulates diverse jasmonate-dependent functions in *Arabidopsis*. *The Plant Cell* 19: 2225-2245.

Doyle JJ, Doyle JL. 1990. A rapid total DNA preparation procedure for fresh plant tissue. *Focus* 12: 13-15.

Dreccer MF, van Herwaarden AF, Chapman SC. 2009. Grain number and grain weight in wheat lines contrasting for stem water soluble carbohydrate concentration. *Field Crops Res.* 112*:* 43-54.

Dvorak J, Akhunov E. 2005. Tempos of gene locus deletions and duplications and their relationship to recombination rate during diploid and polyploid evolution in the *Aegilops-Triticum* alliance. *Genetics* 17: 323-332.

Ehdaie B, Alloush GA, Madore MA, Waines JG. 2006. Genotypic variation for stem reserves and mobilization in wheat. *Crop Science* 46: 2093-2103.

Emmett RW, Parbery DG. 1975. Appressoria. Annu Rev Phytopathol. 13(1): 147-165.

Eynck C, Koopmann B, Grunewaldt-Stoecker G, Karlovsky P, von Tiedemann A. 2007. Differential interactions of *Verticillium longisporum* and *V. dahliae* with Brassica napus detected with molecular and histological techniques. *Eur. J. Plant Pathol.* 118: 259-274.

Faize M, Faize L, Ishizaka M, Ishii H. 2004. Expression of potential responses of Asian and European pears to infection with *Venturia nashicola*. *Physiol. Mol. Plant Pathol.* 64: 319-330.

FAO. 2013. *Food Outlook Report. November 2013. p. 13. FAO Trade and Markets Division.* http://www.fao.org/giews/, Rome, Italy.

Fahima T, Röder M, Grama A, Nevo E. 1998. Microsatellite DNA polymorphism divergence in Triticum dicoccoides accessions highly resistant to yellow rust. *Theor. Appl. Genet.* 96: 187-195.

Farmer EE, Ryan CA. 1992. Octadecanoid precursors of jasmonic acid activate the synthesis of wound-inducible proteinase inhibitors. *Plant Cell* 4:129-134.

Farr DF, Bills GF, Chamuris GP, Rossman AY. 1989. Fungi on Plants and Plant Products in the United States. St. Paul, MN: APS Press, p.1252.

Fernández-Calvo P et al., 2011. The Arabidopsis bHLH transcription factors MYC3 and MYC4 are targets of JAZ repressors and act additively with MYC2 in the activation of jasmonate responses. *Plant Cell* 23: 701-715.

Feuillet C, Eversole K. 2007. Physical mapping of the wheat genome: a coordinated effort to lay the foundation for genome sequencing and develop tools for breeders. *Isr J Plant Sci.* 5: 307-313.

Feussner I, Wasternack C. 2002. The lipoxygenase pathway. Ann. Rev. *Plant Biol.* 53:275-297.

Floerl S, Druebert C, Majcherczyk A, Karlovsky P, Kues U, Polle A. 2008. Defence reactions in the apoplastic proteome of oilseed rape (Brassica napus var. napus) attenuate Verticillium longisporum growth but not disease symptoms. *BMC Plant Biol.* 8: 129.

Fonseca S, Chico JM, Solano R. 2009. The jasmonate pathway: the ligand, the receptor and the core signalling module. *Curr Opin Plant Biol.* 12(5): 539-547.

Foroud NA, Eudes F. 2009. Trichothecenes in cereal grains. *Int J Mol Sci.* 10:147-173.

Gao CS, Kou XJ, Li HP, Zhang JB, Saad ASI and Liao YC. 2012. Inverse effects of Arabidopsis NPR1 gene on fusarium seedling blight and fusarium head blight in transgenic wheat. *Plant Pathol.* 62: 383-392.

Gale LR, Harrison SA, Ward TJ, O"Donnell K, Milus EA, Gale SW, Kistler HC. 2011. Nivalenol-type populations of *Fusarium graminearum* and *F. asiaticum* are prevalent on wheat in southern Louisiana. *Phytopathology* 101(1): 124-134.

Gardiner SA, Boddu J, Berthiller F, Hametner C, Stupar R, Adam G, Muehlbauer GJ. 2010. Transcriptome analysis of the barley-deoxynivalenol interaction: Evidence for a role of glutathione in deoxynivalenol detoxification. *Mol Plant Microbe Interact.* 23: 962-976.

Goggin DE, Setter TL. 2004. Fructosyltransferase activity and fructan accumulation during development in wheat exposed to terminal drought. *Plant Biol.* 31: 11-21.

Golkari S, Gilbert J, Ban T, Procunier JD. 2009. QTL-specific microarray gene expression analysis of wheat resistance to Fusarium head blight in Sumai-3 and two susceptible NILs. *Genome* 52(5): 409-418.

Goswami RS, Kistler HC. 2004. Heading for disaster: *Fusarium graminearum* on cereal crops. *Mol Plant Pathol.* 5: 515-525.

Gottwald S, Samans B, Luck S, and Friedt W. 2012. Jasmonate and ethylene dependent defence gene expression and suppression of fungal virulence factors: Two essential mechanisms of Fusarium head blight resistance in wheat? *BMC Genomics* 13:369.

GRDC (Grains Research & Development Corporation). 2012. *Adult plant resistance fact sheet.*http://www.google.de/url?sa=t&rct=j&q=&esrc=s&frm=1&source=web&cd=6&ved=0CGQQFjAF&url=http%3A%2F%2Fwww.grdc.com.au%2FDownloads.ashx%3Fq%3D%2F~%2Fmedia%2F50129E82BA0B408592D954376A44C746.pdf&ei=StyOU8udB5HA7AbquoGgCQ&usg=AFQjCNFrTNdgJmIhyxG03ZbeqiQPJtCY3Q&sig2=JVNuFebJQ8RWMvCCsEN4pQ, Sydney, Australia.

Greenberg TJ. 1996. Programmed cell death: A way of life for plants proc. *Natl. Acad. Sci. USA.* 93: 12094-12097.

Grunewald W, Vanholme B, Pauwels L, Plovie E, Inzé D, Gheysen G, Goossens A. 2009. Expression of the *Arabidopsis* jasmonate signalling repressor JAZ1/TIFY10A is stimulated by auxin. *EMBO Rep.* 10: 923–938.

Guenther JC, Trail F. 2005. The development and differentiation of Gibberella zeae (anamorph: *Fusarium graminearum*) during colonization of wheat. *Mycologia* 97(1): 229-237.

Gunawardena U, Hawes MC. 2002. Tissue specific localization of root infection by fungal pathogens: role of root border cells. *Mol. Plant-Microbe Interact.* 15: 1128-1136.

Gunnaiah R, Kushalappa AC, Duggavathi R, Fox S Somers DJ. 2012. Integrated metabolo-proteomic approach to decipher the mechanisms by which wheat QTL (Fhb1) contributes to resistance against *Fusarium graminearum* .*PLoS ONE* 7: e40695.

Häberle J, Schmolke M, Schweizer G, Korzun V, Ebmeyer E, Zimmermann G, Hartl L. 2007. Effects of two major fusarium head blight resistance QTL verified in a winter wheat backcross population. *Crop Sci.* 47: 1823-1831.

Hallen-Adams HE, Wenner N, Kuldau GA, Trail F. 2011. Deoxynivalenol biosynthesis-related gene expression during wheat kernel colonization by *Fusarium graminearum*. *Phytopathology* 101: 1091-1096.

Hammond-Kosack K, Urban M, Baldwin T, Daudi A et al. 2004. Plant pathogens: how can molecular genetic information on plant pathogens assist in breeding disease resistant crops."New directions for a diverse planet". Edited by RA Fischer. Proceedings of the 4th International Crop Science Congress. Brisbane, Australia, 26 September - 1 October 2004.

Hamzehzarghani H, Kushalappa AC, Dion Y, Rioux S, Comeau A, Yaylayan V. 2005. Metabolic profiling and factor analysis to discriminate quantitative resistance in wheat cultivars against fusarium head blight. *Physiol.Mol. Plant Pathol.* 66: 119-133.

Hamzehzarghani H, Paranidharan V, Abu-Nada Y, Kushalappa AC, Mamer O, Somers D. 2008. Metabolic profiling to discriminate wheat ner isogenic lines, with quantitative trait loci at chromosome 2DL, varying in resistance to Fusarium head blight. *Can J Plant Sci.* 88: 789-797.

Hatsch D, Phalip V, Petkovski E, Jeltsch JM. 2006. *Fusarium graminearum* on plant cell wall: No fewer than 30 xylanase genes transcribed. *Biochem. Biophys. Res. Commun.* 345: 959-966.

He J, Boland GJ, Zhou T. 2009. Concurrent selection for microbial suppression of *Fusarium graminearum*, Fusarium head blight and deoxynivalenol in wheat. *J. Appl. Microbiol.* 106: 1805-1817.

Hejgaard J, Jacobsen S, Bjorn S, Kragh KM. 1992. Antifungal activity of chitin-binding PR-4 type proteins from barley grain and stressed leaf. *FEBS (Fed. Eur. Biochem. Soc.) Lett.* 307: 389-392.

Henczmionka NJ, Maier FJ, Losch AP, Schäfer W. 2003. Mating conidiation and pathogenicity of *Fusarium graminearum*, the main causal agent of the head bloight disease of wheat, are regulated by the MAP kinase gpmk1.*Curr.Genet.* 43: 87-95.

Henkes GJ, Jousset A, Bonkowski M, Thorpe MR, Scheu S, Lanoue A, Schurr U and Röse US. 2011. *Pseudomonas fluorescens* CH0 maintains carbon delivery to *Fusarium graminearum*-infected roots and prevents reduction in biomass of barley shoots through systemic interactions. *J. Exp.Bot.* 62: 4337-4344.

Henry CM, Deacon JW. 1981. Natural (non-pathogenic) death of the cortex of wheat and barley seminal roots,as evidenced by nuclear staining with acridine orange. *Plant and Soil* 60: 255-274.

Hohn TM, Beremand MN. 1989. Isolation and nucleotide sequence of a sesquiterpene cyclase gene from the trichothecene-producing fungus *Fusarium* sporotrichioides. *Gene*. 79: 131-138.

Horbach R, Navarro-Quesada AR, Knogge W, Deising HB. 2011. When and how to kill a plant cell: Infection strategies of plant pathogenic fungi. *J. Plant Physiol.* 168: 51-62.

Howard RJ. 1997. Breaching the outer barriers—cuticle and cell wall penetration, p. 43–60. In G. Carroll and P. Tudzynski (ed.), Plant relationships, vol. 5A. Springer-Verlag, New York, NY.

Howe GA, Schilmiller A L. 2002. Oxylipin metabolism in response to stress. *Curr. Opin. Plant Biol.* 5: 230-236.

Hsam SLK, Zeller FJ. 2002. Breeding for powdery mildew resistance in common wheat (*Triticum aestivum L.*). In: Belanger RR, Bushnell WR, Dik AJ, Carver TLW (eds) The powdery mildews, a comprehensive treatise. *St. Paul, MN, USA*: 219-238.

Huang S, Sirikhachornkit A, Su X, Faris J, Gill B, Haselkorn R, Gornicki P. 2002. Genes encoding plastid acetyl-CoA carboxylase and 3-phosphoglycerate kinase of the *Triticum/ Aegilops* complex and the evolutionary history of polypoid wheat. *Proc. Nat. Acad. Sci. USA* 99:8133-8138.

Hwang SF, Howard RG, Chang KF, Park B and Burnett PA. 1994. Etiology and severity of fusarium root rot of lentil in Alberta. *Can. J. Plant Pathol.* 16: 295-303.

Inch S, Gilbert J. 2003. The incidence of *Fusarium* species recovered from inflorescences of wild grasses in southern Manitoba. *Can. J. Plant Pathol.* **25**: 379-383.

Inda LA, Segarra-Moragues JG, Müller J, Peterson PM, Catalan P. 2008. Dated historical biogeography of the temperate LoHinae (Poaceae, Pooideae) grasses in the northern and southern hemispheres. *Mol Phylogenet Evol.* 46:932-957.

Ingala L, López M, Darino M, Pergolesi MF, Diéguez MJ, Sacco F. 2012. Genetic analysis of leaf rust resistance genes and associated markers in the durable resistant wheat cultivar Sinvalocho MA. *Theor. Appl. Genet.* 124: 1305–1314.

Jackowiak H, Packa D, Wiwart M, Perkowski J, Buśko M, Borusiewicz A. 2002. Scanning electron microscopy of mature wheat kernels infected with *Fusarium culmorum*. *J Appl Genet*. 43A: 167-176.

Jaroszuk-Scisel J, Kurek E, Winiarczyk K, Baturo A,Lukanowski A. 2008. Colonization of root tissues and protection against Fusarium wilt of rye (Secale cereale) by nonpathogenic rhizosphere strains of *Fusarium culmorum*. *Biol. Control* 45: 297-307.

Jayatilake DV, Bai GH, Dong YH. 2011. A novel quantitative trait locus for Fusarium head blight resistance in chromosome 7A of wheat. *Theor. Appl. Genet.* 122:1189-1198.

Jansen C, von Wettstein D, Schäfer W, Kogel KH, Felk A, Maier FJ. 2005. Infection patterns in barley and wheat spikes inoculated with wild-type and trichodiene synthase gene disrupted *Fusarium graminearum*. *PNAS* 102(46): 892-897.

Jenczmionka NJ, Maier FJ, Losch AP, Schafer W. 2003. Mating, conidiation and pathogenicity of *Fusarium graminearum*, the main causal agent of the head-blight disease of wheat, are regulated by the MAP kinase *GPMK1*. *Curr. Genet.* 43: 87-95.

Jia HY, Cho SH, Muehlbauer GJ. 2009. Transcriptome analysis of a wheat nearisogenic line pair carrying Fusarium head blight-resistant and -susceptible alleles. *Mol Plant Microbe In.* 22(11):1366-1378.

Kam J, Gresshoff MP, Shorter R, Xue GP. 2008. The Q-type C2H2 zinc finger subfamily of transcription factors in Triticum aestivum is predominantly expressed in roots and enriched with members containing an EAR repressor motif and responsive to drought stress. *Plant Mol Biol.* 67: 305-322.

Karlovsky P. 2011. Biological detoxification of the mycotoxin deoxynivalenol and its use in genetically engineered crops and feed additives. *Appl Microbiol Biotechnol* 91: 491-504.

Katan T, Shlevin E, Katan J. 1997. Sporulation of *Fusarium oxysporum* f. sp. *lycopersici* on stem surfaces of tomato plants and aerial dissemination of inoculum. *Phytopathology* 87: 712-719.

Kandel S, Morant M, Benveniste I, Blee E, Werck-Reichhart D, Pinot F. 2005. Cloning, functional expression, and characterization of CYP709C1, the first sub-terminal hydroxylase of long chain fatty acid in plants: Induction by chemicals and methyl jasmonate. *J. Biol. Chem.* 280: 35881-35889.

Kang Z, Buchenauer H. 1999. Immunocytochemical localization of *fusarium* toxins in infected wheat spikes by *Fusarium culmorum*. *Physiol. Mol. Plant Pathol.* 55: 275-288.

Kang Z, Buchenauer H. 2000. Ultrastructural and immunocytochemical investigation of pathogen development and host responses in resistant and susceptible wheat spikes infected by *Fusarium culmorum*. *Physiol. Mol. Plant Pathol.* 57(6): 255-268.

Kang ZS, Zingen-Sell I, Buchenauer H. 2005. Infection of wheat spikes by *Fusarium avenaceum* and alterations of cell wall components in the infected tissue. *Eur. J. Plant Pathol.* 111(1): 19-28.

Katsir L, Chung HS, Koo AJK, Howe GA. 2008. Jasmonate signaling: a conserved mechanism of hormone sensing. *Curr. Opin. Plant Biol.* 11: 428-435.

Kazan K, Gardiner DM, Manners JM. 2012. Onthe trail of a cereal killer: recent advances in *Fusarium graminearum* pathogenomics and host resistance. *Mol.PlantPathol.* 13: 399-413.

Kazan K, Manners JM. 2013. MYC2: the Master in Action. *Molecular Plant, in press*.

Kazan K. 2006. Negative regulation of defence and stress genes by EAR-motif-containing repressors. *Trends Plant Sci.* 11: 109-112.

Kellogg EA. 2001. Evolutionary history of the grasses. *Plant Physiol.* 125:1198-1205.

Keijer JWA, Sinclair JB. 1996. Plant-Pathogen Interactions of *Rhizoctonia spp.* In *Rhizoctonia* species: Taxonomy, molecular biology, ecology, pathology and disease control. Edited by: Sneh B, Jabaji-Hare S, Neate SM, Dijst G. Dordrecht. The Netherlands: Kluwer Academic Publishers: 147-174.

Khonga EB, Sutton JC. 1988. Inoculum production and survival of *Gibberella zeae* in maize and wheat residues. *Plant Pathol.* 10: 232-239.

Kikot GE, Hours RA, Alconada TM. 2009. Contribution of cell wall degrading enzymes to pathogenesis of *Fusarium graminearum*: a review. *J. Basic Microb.* 49: 231-241.

Knight NL and Sutherland MH. 2013. Histopathological assessment of wheat seedling tissues infected by *Fusarium pseudograminearum*. *Plant Pathol.* 62: 679-687.

Kogel KH, Franken P, Huckelhoven R. 2006. Endophyte or parasite-what decides? *Curr. Opin. Plant Biol.* 9: 358-363.

Kong L, Anderson JM, Ohm H W. 2005. Induction of wheat defense and stress-related genes in response to *Fusarium graminearum*. *Genome* 48:29-40.

Kubo Ki, Kawada N, Fujita M, Hatta K, Oda S, Nakajima T. 2010. Effect of cleistogamy on Fusarium head blight resistance in wheat. *Breeding Sci.* 60(4): 405.

Kunkel, BN and Brooks DM. 2002. Cross talk between signaling pathways in pathogen defense, *Curr.Opin. Plant Biol.* 5: 325-331.

Lannoo N, Peumans WJ, Van Damme EJM. 2006. The presence of jasmonate-inducible lectin genes in some but not all Nicotiana species explains a marked intragenus difference in plant responses to hormone treatment. *J Exp Bot.* 57: 3145-3155.

Lagopodi AL, Ram AF, Lamers GE, Punt PJ, Van den Hondel CA, Lugtenberg BJ, Bloemberg GV. 2002. Novel aspects of tomato root colonization and infection by *Fusarium oxysporum* radicis-lycopersici revealed by confocal laser scanning microscopic analysis using the green fluorescent protein as a marker. *Mol. Plant Microbe Interact.*15: 172-179.

Laluk K, Mengiste T. 2010. Necrotroph attacks on plants: wanton destruction or covert extortion? *Arabidopsis Book* 8: e0136.

Ledingham RJ, Atkinson TG, Horricks JS, Mills JT, Piening LJ, Tinline RD. 1973. Wheat losses due to common root rot in the prairie provinces of Canada, 1976-71. *Can. Plant Dis. Surv.* 53: 113-122.

Lemmens M, Scholz U, Berthiller F, Dall_Asta C, Koutnik A, Schuhmacher R, Adam G, Buerstmayr H, Mesterhazy A, Krska R and Ruckenbauer P. 2005. The ability to detoxify the mycotoxin deoxynivalenol colocalizes with a major quantitative trait locus for fusarium head blight resistance in wheat. *Mol. Plant Microbe Interact.* 18:1318-1324.

Lemoine R, Camera LS, Atanassova R, Dédaldéchamp F, Allario T, Pourtau N, Bonnemain JL, Laloi M, Coutos-Thévenot P, Maurousset L, Faucher M, Girousse C, Lemonnier P, Parrilla J, Durand M. 2013. Source-to-sink transport of sugar and regulation by environmental factors. *Front Plant Sci.* 4: 272.

Leplat J, Friberg H, Abid M, Steinberg C. 2012. Survival of *Fusarium graminearum*, the causal agent of Fusarium head blight. A review. Agron. Sustain. Dev. DOI 10.1007/s13593-012-0098-5.

Leslie JF, Summerell AB. 2006. Media–Recipes and Preparation. *The Fusarium Laboratory Manual* 2: S6-7.

Lev S, Sharon A, Hadar R, Ma H, Horwitz BA. 1999. A mitogen-activated protein kinase of the corn leaf pathogen *Cochliobolus heterostrophus* is involved in conidiation, appressorium formation, and pathogenicity: Diverse roles for mitogen-activated protein kinase homologs in foliar pathogens. *Proc Natl Acad Sci. USA* 96(23): 13542-13547.

Lewandowski KE, Barrantes–Vidal N, Nelson–Gray RO, Clancy C, Kepley HO, Kwapil TR. 2006. Anxiety and depression symptoms in psychometrically identified schizotypy. *Schizophr Res.* 83: 225-235.

Li G, Yin Y. 2008. Jasmonate and ethylene signaling pathway may mediate Fusarium Head Blight resistance in wheat. *Crop Sci.* 48: 1888-1896.

Li HB, Xie GQ, Ma J, Liu GR, Wen SM, Ban T, Chakraborty S, Liu CJ. 2010. Genetic relationships between resistances to Fusarium head blight and crown rot in bread wheat (*Triticum aestivum L.*). *Theor. Appl. Genet.* 121: 941-950.

Li X, Zhang JB, Song B et al. 2010. Resistance to fusarium head blight and seedling blight in wheat is associated with activation of a cytochrome P450 gene. *Phytopathology* 100:183-91.

Li X, Zhang JB, Song B, Li HP, Xu HQ, Qu B, Dang FJ, and Liao YC. 2010. Resistance to Fusarium Head Blight and seedling blight in wheat as associated with activation of a Cytochrome P450 gene. *APS* 100 (2): 183-191.

Lin F, Kong Z X, Zhu HL, Xue SL, Wu JZ, Tian DG, Wei JB, Zhang CQ and Ma ZQ. 2004. Mapping QTL associated with resistance to Fusarium head blight in the Nanda2419 * Wangshuibai population. I. Type II resistance. *Theor. Appl. Genet.* 109: 1504-1511.

Line RF. 2002. Stripe rust of wheat and barley in North America: a retrospective historical review. *Annu. Rev. Phytopathol.* 40: 75-118.

Liu S, Pumphrey MO, Gill BS, Trick HN, Zhang JX, Dolezel J, Chalhoub B and Anderson JA. 2008. Toward positional cloning of Fhb1, a major QTL for Fusarium head blight resistance in wheat. *Cereal Res. Comm.* 36:195-201.

Liu S, Zhang X, Pumphrey MO, Stack RW, Gill BS, Anderson JA. 2006. Complex microcolinearity among wheat, rice, and barley revealed by fine mapping of the genomic region harboring a major QTL for resistance to Fusarium head blight in wheat. *Funct.Integr. Genomics* 6: 83-89.

Livak KJ, Schmittgen TD. 2001. Analysis of relative gene expression data using real-time quantitative PCR and the $2^{-\Delta\Delta C}{}_{T}$ method. *Method 25*:402-408.

Loake G, Grant M. 2007. Salicylic acid in plant defence–the players and protagonists. *Curr Opin. Plant Biol.* 10(5): 466-472.

Lorenzo O, Chico JM, Sanchez-Serrano JJ, Solano R. 2004. JASMONATEINSENSITIVE1 encodes a MYC transcription factor essential to discriminate between different jasmonate-regulated defense responses in *Arabidopsis*. *Plant Cell* 16:1938-50.

Luck J, Spackman M, Freeman A, Trebicki P, Griffiths W, Finlay K et al., 2011. Climate change and diseases of food crops. *Plant Pathol.* 60: 113-121.

Lysøe E, Seong KY, Kistler C. 2011. The transcriptome of *Fusarium graminearum* during the infection of wheat. *Mol. Plant–Microbe Interact.* 24: 995-1000.

Ma HX, Zhang KM, Gao L, Bai GH, Chen HG, Cai ZX, Lu WZ. 2006. Quantitative trait loci for resistance to fusarium head blight and deoxynivalenol accumulation in Wangshuibai wheat under field conditions. *Plant Pathol.* 55: 739-745.

Ma J, Li H, Zhang C, Yang X, Liu Y, Yan G, Liu C. 2009. Identification and validation of a major QTL conferring crown rot resistance in hexaploid wheat. *Theor. Appl. Genet.* 6:1119-1128.

Ma LJ, van der Does HC, Borkovich KA, Coleman JJ, Daboussi MJ, Di Pietro A, Dufresne M, Freitag M, Grabherr M, Henrissat B, Houterman PM. 2010. Comparative genomics reveals mobile pathogenicity chromosomes in *Fusarium*. *Nature* 464: 367-373.

Ma LL, Shang Y, Cao AZ , Qi ZJ, Xing LP, Chen PD, Liu DJ, Wang XE. 2010. Molecular cloning and characterization of an up-regulated UDP-glucosyltransferase gene induced by DON from *Triticum aestivum L.* cv. Wangshuibai. *Mol. Biol. Rep.* 37: 785-795.

Mach RL, Kullnig-Gradinger CM, Farnleitner AH, Reischer G, Adler A, Kubicek CP. 2004. Specific detection of *Fusarium langsethiae* and related species by DGGE and ARMS-PCR of a beta-tubulin (tub1) gene fragment. *Int. J. Food Microbiol.* 95(3): 333-339.

Madgwick JM, West JS, White RP, Semenov M, Townsend JA, Turner JA, Fitt B. 2011. Impacts of climate change on wheat anthesis and fusarium ear blight in the UK, *Eur. J. Plant Pathol.* 130: 117-131.

Maldonado AM, Doerner P, Dixon RA, Lamb CJ, Cameron RK. 2002. A putative lipid transfer protein involved in systemic resistance signalling in *Arabidopsis*. *Nature* 419(6905):399-403.

Mallard S, Nègre S, Pouya S, Gaudet D, Lu Z-X, Dedryver F. 2008. Adult plant resistance-related gene expression in 'Camp Remy' wheat inoculated with *Puccinia striiformis*. *Mol Plant Pathol.* 9: 213-25.

Maier FJ, Miedaner T, Hadeler B, Felk A, Salomon S, Lemmens M, Kassner H and Schäfer W. 2006. Involvement of trichothecenes in fusarioses of wheat, barley and maize evaluated by gene disruption of the trichodiene synthase (Tri5) gene in three field isolates of different chemotype and virulence. *Mol. Plant Pathol.* **7**: 449-461.

Marcel S, Sawersa R, Oakeleyb E, Anglikerb H, Paszkowskia U. 2010. Tissue-Adapted Invasion Strategies of the Rice Blast Fungus Magnaporthe oryzae. *Plant Cell* 22: 3177-3187.

Mardi M, Pazouki L, Delavar H, Kazemi MB, Ghareyazie B, Steiner B, Nolz R, Lemmens M, and Buerstmayr H. 2006. QTL analysis of resistance to Fusarium head blight in wheat using a Frontana-derived population. *Plant Breeding* 125: 313-317.

Markell SG, Francl LJ. 2003. Fusarium head blight inoculum: species prevalence and *Gibberella zeae* spore type. *Plant Dis.* 87: 814-820.

Martinez D, Berka RM, Henrissat B, Saloheimo M, Arvas M, Baker SE, Chapman J, Chertkov O, Coutinho PM, Cullen D, et al., 2008. Genome sequencing and analysis of the biomass-degrading fungus *Trichoderma reesei* (syn. Hypocrea jecorina). *Nat Biotech*. 26:553-560.

Massman J, Cooper B, Horsley R et al. 2011. Genome-wide as-sociation mapping of Fusarium head blight resistance in contemporary barley breeding germplasm. *Mol. Breeding* 27: 439-54.

Matsuoka Y, Nasuda S. 2004. Durum wheat as a candidate for the unknown female progenitor of bread wheat: an empirical study with a highly fertile F1 hybrid with Aegilops tauschii Coss. *Theor*. *Appl* .*Genet.* 109:1710-1717.

McCartney CA, Somers DJ, Fedak G, Cao W. 2004. Haplotype diversity at fusarium head blight resistance QTLs in wheat. *Theor. Appl. Genet.* 109: 261-271.

McMillan VE, Hammond-Kosack KE, Gutteridge RJ. 2011. Evidence that wheat cultivars differ in their ability to build up inoculum of the take-all fungus, *Gaeumannomyces graminis var. tritici*, under a first wheat crop. *Plant Pathol.* 60: 200-206.

McMullen M. 2003. Impacts of FHB on the North American agriculture community-The power of one disease to catapult change. Pages 484-503 in: Fusarium Head Blight of Wheat and Barley. K. J. Leonard and W. R. Bushnell, eds. American Phytopathological Society, St. Paul, MN.

McMullen MP, Jones R, Gallenberg D. 1997. Scab of wheat and barley-A re-emerging disease of devastating impact. *Plant Dis.* 81:1340-1348.

Mergoum M, Pfeiffer WH, Crossa JL. 1998. Triticale mixtures: A way to improve and/or stabilize yield under adverse environments. p. 245-251. In: Proc. of the 4th International Triticale Symposium. (Ed.): P.E. Juskiw. Vol. 1. Oral Presentations. Red Deer, AB, Canada. 26-31 July 1998. International Triticale Assoc., Sidney, Australia.

Meriño-Gergichevich C, Alberdi M, Ivanov AG, Reyes-Díaz M. 2010. Al^{3+}-Ca^{2+} Interaction in plants growing in acid soils: Al-phytotoxicity response to calcareous amendments. *J. Soil. Sci. Plant Nutr.* 10: 217-243.

Mesterhazy A. 1987. Selection of head blight resistant wheat through improved seedling resistance. *Plant Breeding* 98: 25-36.

Mesterhazy A. 1996. Types and components of resistance against Fusarium head blight of wheat. *Plant Breeding* 114: 377-386.

Mew TW, Veera Cruz CM, Reyes RC. 1981. Characterization of resistance in rice to bacterial blight. *Ann Phytopathol Soc Jpn.* 47: 58-67.

Mey G, Oeser B, Lebrun MH, Tudzynski P. 2002. The biotrophic, non-appressorium-forming grass pathogen *Claviceps purpurea* needs a Fus3/Pmk1 homologous mitogen-activated protein kinase for colonization of rye ovarian tissue. *Mol Plant-Microbe Interact.* 15(4): 303-312.

Miedaner T, Risser P, Paillard S, Schnurbusch T, Keller B, Hartl L, Holzapfel J, Korzun V, Ebmeyer E, Utz HF. 2012. Broad-spectrum resistance loci for three quantitatively inherited diseases in two winter wheat populations. *Mol. Breed.* 29:731-742.

Miller JD, Young JC, Sampson RD. 1985. Deoxynivalenol and Fusarium head blight resistance in spring cereals. *Phytopath Z* 113: 359-367.

Mitchell TK, Dean RA. 1995. The cAMP-dependent protein kinase catalytic subunit is required for appressorium formation and pathogenesis by the rice blast pathogen *Magnaporthe grisea*. *Plant Cell* 7: 1869-1878.

Mitter V, ZhangMC, Liu CJ, Ghosh R, GhoshM, Chakraborty S, 2006. A high-throughput glasshouse bioassay to detect crown rot resistance in wheat germplasm. *Plant Pathol.* 55: 433-41.

Montiel G, Zarei A, Korbes AP, Memelink J. 2011. The jasmonate-responsive element from the ORCA3 promoter from Catharanthus roseus is active in *Arabidopsis* and is controlled by the transcription factor AtMYC2. *Plant Cell Physiol.* 52:578-587.

Morant M, Bak S, Moller BL, Werck-Reichhart D. 2003. Plant cytochromes P450: Tools for pharmacology, plant protection and phytoremediation. *Curr. Opin. Biotechnol.* 14: 151-162.

Moretti A, Panzarini G, Somma S, Campagna C, Ravaglia S, Logrieco FA, Solfrizzo M. 2014. Systemic growth of *F. graminearum* in wheat plants and related accumulation of deoxynivalenol. *Toxins (Basel)* 6(4): 1308-1324.

Mudge AM, Macky DR, Dong Y, Gardiner DM, White RG, Manners JM. 2006. A role for the mycotoxin deoxynivalenol in stem colonisation during crown rot disease of wheat caused by *Fusarium graminearum* and *Fusarium pseudograminearum*. *Physiol. Mol. Plant Pathol.* 69: 73-85.

Nash SM, Christou T, Snyder WC. 1961. Existence of *Fusarium solani* f. sp. *phaseoli* as chlamydospores in soil. *Phytopathology* 51: 308-312.

Nasri T, Bosch RR, Voorde ST, Fink-Gremmels J. 2006. Differential induction of apoptosis by type A and B trichothecene in Jurkat T-lymphocytes. *Toxicology in Vitro* 20 (6): 832-840.

Nicholson P, Simpson D R, Weston G, Rezanoor H N, Lees A K, Parry D W, Joyce D. 1998. Detection and quantification of *Fusarium culmorum* and *Fusarium graminearum* in cereals using PCR assays. Physiol. *Mol. Plant Pathol.* 53: 17-37.

Nicolardot B, Bouziri L, Bastian F, Ranjard L. 2007. A microcosm experiment to evaluate the influence of location and quality of plant residues on residue decomposition and genetic structure of soil microbial communities. *Soil Biol. Biochem.* 39: 1631-1644.

Noordermeer MA, Veldink GA, Vliegenthart JF. 2001. Fatty acid hydroperoxide lyase: a plant cytochrome p450 enzyme involved in wound healing and pest resistance. *Chembiochem.* 2:494-504.

Oh SK, Park JM, Joung YH, Lee S, Chung E, Kim SY, YuSH, Choi D. 2005. A plant EPF-type zinc-finger protein, CaPIF1, involved in defence against pathogens. *Mol. Plant Pathol.* 6 (3): 269-285.

Ohta M, Matsui K, Hiratsu K, Shinshi H, Ohme-Takagi M. 2001. Repression domains of class II ERF transcriptional repressors share an essential motif for active repression. *Plant Cell* 13: 1959-1968.

Okubara P, Blechl AE, McCormick SP, Alexander NJ, Dill-Macky R, Hohn TM. 2002. Engineering deoxynivalenol metabolism in wheat through the expression of a fungal trichothecene acetyltransferase gene. *Theor. Appl. Genet.* 106: 74-83.

Olivieri F, Zanetti ME, Oliva CR, Covarrubias AA, Casalongué CA. 2002. Characterization of an extracellular serine protease of *Fusarium eumartii* and its action on pathogenesis related proteins. *Eur. J. Plant Pathol.* 108: 63-72.

Oren L, Ezrati S, Cohen D, Sharon A. 2003. Early events in the *Fusarium verticillioides*-maize interaction characterized by using a green fluorescent protein-expressing transgenic isolate. *Appl. Environ. Microbiol.* 69: 1695-1701.

Osborn TC, Pires JC, Birchler JA, Auger DL, Chen ZJ, Lee H-S, Comai L, Madlung A, Doerge RW, Colot V et al. 2003. Understanding mechanisms of novel gene expression in polyploids. *Trends Genet*. 19: 141-147.

Paper JM, Scott-Craig JS, Adhikari ND, Cuomo CA and Walton JD. 2007. Comparative proteomics of extracellular proteins *in vitro* and *in planta* from the pathogenic fungus *Fusarium graminearum*. *Proteomics* 7: 3171-3183.

Parry DW, Jenkinson P, McLeod L. 1995. Fusarium ear blight (scab) in small grains-a review. *Plant Pathol.* 44: 207-238.

Pasquet JC, Chaouch S, Macadre C et al. 2014. Differential gene expression and metabolomic analyses of *Brachypodium distachyon* infected by deoxynivalenol producing and non-producing strains of *Fusarium graminearum*. *BMC Genomics* 15: 629.

Paulitz TC, Smiley RW, Cook RJ. 2002. Insights into the prevalence and management of soilborne cereal pathogens under direct seeding in the Pacific Northwest, USA. *Can. J. Plant Pathol.* 24: 416-28.

Paulitz TC. 2006. Low input no-till cereal production in the Pacific Northwest of the U.S.: the challenges of root disease. *Eur. J. Plant Pathol.* 115: 271-81.

Pauwels L, Goossens A. 2011. The JAZ Proteins: A Crucial Interface in the Jasmonate Signaling Cascade. *Plant Cell* 23: 3089-3100.

Paux E, Roger D, Badaeva E, Gay G, Bernard M, Sourdille P, Feuillet C. 2006. Characterizing the composition and evolution of homoeologous genomes in hexaploid wheat through BAC-end sequencing on chromosome 3B. *Plant J.* 48: 463-474.

Pekkarinen AI, Jones LB. 2002. Trypsin-Like Proteinase Produced by *Fusarium culmorum* Grown on Grain Proteins *J. Agric. Food Chem.* 50: 3849-3855.

Pekkarinen Longstaff C, Jones BL. 2007. Kinetics of the inhibition of *Fusarium* serine proteinases by barley (*Hordeum vulgare L.*) inhibitors. *J. Agric. Food Chem*. 55: 2736-2742.

Peng JH, Sun DF, Nevo E. 2011. Domestication evolution, genetics and genomics in wheat. *Mol. Breeding* 28: 281-301.

Peng J, Zhang J. 2009. Plant genomic DNA methylation in response to stresses: Potential applications and challenges in plant breeding. *Progress in Natural Science* 19: 1037-1045.

Pereyra SA, Dill-Macky R. 2008. Colonization of the residues of diverse plant species by *Gibberella zeae* and their contribution to Fusarium head blight inoculum. *Plant Dis.* 92(5):800-807.

Peraldi A, Beccari G, Steed A, Nicholoson P. 2011. *Brachypodium distachyon*: a new pathosystem to study Fusarium head blight and other *Fusarium* diseases of wheat. *BMC Plant Biology* 11: 100.

Pestka JJ, Smolinski AT. 2005. Deoxynivalenol: toxicology and potential effects on humans. *J Toxicol Environ Health* 8: 39.

Petti C, Khan M, Doohan F. 2010. Lipid transfer proteins and protease inhibitors as key factors in the priming of barley responses to Fusarium head blight disease by a biocontrol strain of *Pseudomonas fluorescens*. *Funct. Integr. Genomics* 10: 619-627.

Phalip V, Delalande F, Carapito C, Goubet F, Hatsch D, Leize-Wagner E, Dupree P, Dorsselaer AV and Jeltsch JM. 2005. Diversity of the exoproteome of *Fusarium graminearum* grown on plant cell wall. *Current Genetics* 48: 366-379.

Philippe R, Paux E, Bertin I, Sourdille P, Choulet F, Laugier C. 2013. A high density physical map of chromosome 1BL supports evolutionary studies, map-based cloning and sequencing in wheat. *Genome Biol.* 14: R64.

Poels P, Sztor E, Cannaert F. 2006. Fusariose elle peut migrer de la semence à l'épi. *Phytoma.* 593: 9-12.

Ponstein AS, Bres-Vloemans AA, Sela-Buurlage MB, Cornelissen BJC, Melchers LS. 1994. The ''missing'' class I PR-4 protein from bobacco exhibits antifungal activity. *J. Cell. Biochem. Suppl.* 18A: 90.

Ponstein AS, Bres-Vloemans AA, Sela-Buurlage MB, van den Elzen PJM, Melchers LS, Cornelissen BJC. 1994. A novel pathogen- and wound-inducible tobacco (Nicotiana tabacum) protein with antifungal activity. *Plant Physiol.* 104: 109-118.

Poole GJ, Smiley RW, Paulitz TC, Walker CA, Carter AH, See DR, Garland-Campbell K. 2012. Identification of quantitative trait loci (QTL) for resistance to Fusarium crown rot (*Fusarium pseudograminearum*) in multiple assay environments in the Pacific Northwestern US. *Theor. Appl. Genet.* 125: 91-107.

Poppenberger B, Berthiller F, Lucyshyn D, Sieberer T, Schuhmacher R, Krska R, Kuchler K, Glössl J, Luschnig C and Adam G. 2003. Detoxification of the *Fusarium* mycotoxin deoxynivalenol by an UDP-glucosyltransferase from *Arabidopsis* thaliana. *J. Biol. Chem.* 278: 47905-47914.

Postnikova OA, Minakova NY, Boutanaev AM, Nemchinov LG. 2011. Clustering of Pathogen-Response Genes in the Genome of Arabidopsis thaliana. *J. Integrative Plant Biol.* 53: 824-834.

Prieto P, Schiliro E, Maldonado-Gonzalez MM, Valderrama R, Barroso-Albarracin JB, Mercado-Blanco J. 2011. Root hairs play a key role in the endophytic colonization of olive roots by *Pseudomonas spp.* with biocontrol activity. *Microb Ecol.* 62: 435-445.

Pritsch C, Muehlbauer GJ, Bushnell WR, Somers DA, Vance CP. 2000. Fungal development and induction of defense response genes during early infection of wheat spikes by *Fusarium graminearum*. *MPMI* 13(2): 159-169.

Proctor RH, Hohn TM, Mccormick SP. 1995. Reduced virulence of *Gibberella zeae* caused by disruption of a trichothecene toxin biosynthetic gene. *MPMI* 8: 593.

Prost I et al. 2005. Evaluation of the antimicrobial activities of plant oxylipins supports their involvement in defense against pathogens. *Plant Physiol.* 139: 1902-1913.

Puri KD, Zhong S. 2010. The 3-ADON population of *Fusarium graminearum* found in North Dakota is more aggressive and produces a higher level of DON than 212 the prevalent 15-ADON population in spring wheat. *Phytopathology* 100(10): 1007-1014.

Purss GS. 1971. Pathogenic specialization in *Fusarium graminearum*. *Aus. J. Agr. Res.* 22: 553-61.

Raats D, Frenkel Z, Krugman T, Dodek I, Sela H, Šimková H, Magni F et al., 2013. The physical map of wheat chromosome 1BS provides insights into its gene space organization and evolution. *Genome Biol.* 14: R138.

Raaijmakers JM, Paulitz TC, Steinberg C, Alabouvette C, Moënne-Loccoz Y. 2009. The rhizosphere: a playground and battlefield for soilborne pathogens and beneficial microorganisms. *Plant Soil* 321: 341-361.

Rae A, Grof C, Casu R, Bonnett G. 2005. Sucrose accumulation in the sugarcane stem: pathways and control points for transport and compartmentation. *Field Crops Res.* 92: 159-168.

Rebetzke GJ, van Herwaarden AF, Jenkins C, Weiss M, Lewis D, Ruuska S, Tabe L, Fettell NA, Richards RA. 2008. Quantitative trait loci for water-soluble carbohydrates and associations with agronomic traits in wheat. *Aus. J. Agri. Res.* 59: 891-905.

Reischer GH, Lemmens M, Farnleitner A, Adler A, Mach RL. 2004. Quantification of *Fusarium graminearum* in infected wheat by species specific real-time PCR applying a TaqMan Probe. *J Microbiol Methods* 59(1): 141-146.

Ribichich KF, Lopez SE, Vegetti AC. 2000. Histopathological spikelet changes produced by *Fusarium graminearum* in susceptible and resistant wheat cultivars. *Plant Dis.* 84: 794-802.

Rittenour WR, Harris SD. 2010. An in vitro method for the analysis of infectionrelated morphogenesis in Fusarium graminearum. *Mol. Plant Path.* 11(3):361-369.

Rocha O, Ansari K, Doohan FM. 2005. Effects of trichothecene mycotoxins on eukaryotic cells: A review. *Food Addit Contam.* 22(4): 369-378.

Rodŕiguez-Gálvez E, Mendgen K. 1995. The infection process of *Fusarium oxysporum* in cotton root tips. *Protoplasma* 189: 61-72.

Roger P, Lamb C. 1997. Programmed Cell Death in Plants. *The Plant Cell* 9: 1157-1168.

Rojas M L, Montes De Gomez V, Ocampo CA. 1993. Stimulation of lipoxygenase activity in cotyledonary leaves of coffee reacting hypersensitively to the coffee leaf rust. *Physiol. Mol. Plant Pathol.* 43: 209-219.

Ruuska S, Rebetzke GJ, van Herwaarden A, Richards RA, Fettell NA, Tabe L, Jenkins C. 2006. Genotypic variation for water soluble carbohydrate accumulation in wheat. *Plant Biol.* 33: 799-809.

Sahai AS, Manocha MS. 1993. Chitinases of fungi and plants: their involvement in morphogenesis and host-parasite interaction. *FEMS Microbiol Rev.* 11: 317-338.

Sakamoto A, Minami M, Huh GH, Iwabuchi M. 1993. The putative zinc-finger protein WZF1 interacts with a cis-acting element of wheat histone genes. *Eur. J. Biochem.* 217: 1049-1056.

Sakamoto A, Omirulleh S, Nakayama T, Iwabuchi M. 1996. A Zinc-Finger-Type Transcription Factor WZF-1 That Binds to a Novel cis-Acting Element of Histone Gene Promoters Represses Its Own Promoter. *Plant Cell Physiot.* 37(4): 557-562.

Sakamoto H, Maruyama K, Sakuma Y, Meshi T, Iwabuchi M, Shinozaki K, Yamaguchi-Shinozaki K. 2004. Arabidopsis Cys2/His2-type zinc-finger proteins function as transcription repressors under drought, cold and high-salinity stress conditions. *Plant Physiol.* 136: 2734-2746.

Sambrook J, Fritsch EF, Maniatis T. 1989. Molecular cloning-A laboratory manual. 2nd edition. *Cold Spring Harbor Laboratory Press, New York.*

Sasaki T, Ezaki B, Matsumoto H. 2002. A gene encoding multidrug resistance (MDR)-like protein is induced by aluminum and inhibitors of calcium flux in wheat. *Plant Cell Physiol.* 43: 177-185.

Schaller F, Schaller A, Stintzi A. 2004. Biosynthesis and metabolism of jasmonates. *J. Plant Growth Regul.* 23: 179-199.

Schaller, F. 2001. Enzymes of the biosynthesis of octadecanoid-derived signalling molecules. *J. Exp. Bot.* 52: 11-23.

Schnerr H, Niessen L, Vogel RF. 2001. Real time detection of the tri5 gene in *Fusarium* species by lightcycler-PCR using SYBR Green I for continuous fluorescence monitoring. *Int J Food Microbiol.* 71(1): 53-61.

Schnerr H, Vogel RF, Niessen L. 2002. Correlation between DNA of trichothecene-producing *Fusarium* species and deoxynivalenol concentrations in wheat-samples. *Lett Appl Microbiol.* 35(2): 121-125.

Schreiber KJ, Nasmith CG, Allard G, Singh J, Subramaniam R, Desveaux D. 2011. Found in translation: high-throughput chemical screening in *Arabidopsis thaliana* identifies small molecules that reduce Fusarium head blight disease in wheat. *Mol. Plant–Microbe Interact* 24: 640-648.

Schroeder HW, Christensen JJ. 1963. Factors affecting resistance of wheat to scab caused by *Gibberella zeae*. *Phytopathology* 53: 831-838.

Schweiger W, Boddu J, Shin S, Poppenberger B, Berthiller F, Lemmens M, Muehlbauer GJ, Adam G. 2010. Validation of a candidate deoxynivalenolinactivating UDP-glucosyltransferase from barley by heterologous expression in yeast. *Mol. Plant. Microbe Interact* 23: 977-986.

Schweiger W Stein B, Ametz C, Siegwart G,Wiesenberger G, Berthiller F, Lemmens M, Jia H, Adam G, Muehlaruer JG, Kreil PD, Buerstmary H. 2013. Transcriptomic characterization of two major *Fusarium* resistance quantitative trait loci (QTLs), Fhb1 and Qfhs.ifa-5A, identifies novel candidate genes. *Mol. Plant Pathol.* 14(8): 772-785.

Sesma A, Osbourn A E. 2004. The rice leaf blast pathogen undergoes developmental processes typical of root-infecting fungi. *Nature* 431: 582-586.

Seyfarth R, Feuillet C, Schachermayr G, Winzeler M, Keller B. 1999. Development of a molecular marker for the adult plant leaf rust resistance gene Lr35 in wheat. *Theor. Appl. Genet.* 99: 554-560.

Shang Y, Xiao J, Ma L, Wang H, QI Z, Chen P, Liu D, Wang X. 2009. Characterization of a PDR type ABC transporter gene from wheat (*Triticum aestivum L.*). *Chinese Sci. Bull* 54: 3249-3257.

Shen X, Zhou M, Lu W, Ohm H. 2003. Detection of Fusarium head blight resistance QTL in a wheat population using bulked segregate analysis. *Theor. Appl. Genet.* 106: 1041-1047.

Shen J, Li C, Mi G, Li L, Yuan L, Jiang R, Zhang F. 2013. Maximizing root/rhizosphere efficiency to improve crop productivity and nutrient use efficiency in intensive agriculture of China. *J Exp Bot.* 64(5): 1181-1192.

Sitton JW, Cook RJ. 1981. Comparative morphology and survival of chlamydospores of Fusarium roseum 'Culmorum' and 'Graminearum'. *Phytopathology* 71: 85-90.

Smiley WR, Gourlie JA, Easley SA, Patterson LM, Whittaker RG. 2005. Crop damage estimates for crown rot of wheat and barley in the Pacific Northwest. *Plant Dis.* 89: 595-604.

Smiley WR, Yan H. 2009. Variability of fusarium crown rot tolerances among cultivars of spring and winter wheat. *Plant Dis.* 93 (9): 954-961.

Smith S, De Smet I. 2012. Root system architecture: insights from Arabidopsis and cereal crops. *Phil. Trans. R. Soc. B.* 367: 1441-1452.

Snijders CHA. 1990. Systemic fungal growth of *Fusarium culmorum*. *Journal of Phytopathology* 129: 133-40.

Son H et al. 2011. A phenome-based functional analysis of transcription factors in the cereal head blight fungus, *Fusarium graminearum*. *PLoS Pathog.* 7: e1002310.

Steiner B, Lemmens M, Griesser M, Scholz U, Schondelmaier J, Buerstmayr H. 2004. Molecular mapping of resistance to Fusarium head blight in the spring wheat cultivar Frontana. *Theor. Appl. Genet.* 109: 215-224.

Spannagl M, Martis M M, Pfeifer M, Nussbaumer T, Mayer FX K. 2013. Analysing complex Triticeae genomes –concepts and strategies. *Plant Methods* 9:35.

Stephens AE, Gardiner DM, White RG, Munn AL, Manners JM. 2008. Phases of infection and gene expression of *Fusarium graminearum* during crown rot disease of wheat. *Mol. Plant–Microbe Interact* 21: 1571-1581.

Steiner B, Lemmens M, Griesser M, Scholz U, Schondelmaier J, Buerstmayr H. 2004. Molecular mapping of resistance to Fusarium head blight in the spring wheat cultivar Frontana. *Theor. Appl. Genet.* 109: 215-224.

Strausbaugh AC, Overturf K, Koehn CA. 2005. Pathogenicity and real-time PCR detection of *Fusarium spp.* in wheat and barley roots. *Can. J. Plant Pathol.* 27: 430-438.

Sukno SA, Garcia VM, Shaw BD, Thon MR. 2008. Root infection and systemic colonization of maize by *Colletotrichum graminicola*. *Appl. Environ. Microbiol.* 74: 823-832.

Sutton JC. 1982. Epidemiology of wheat head blight and maize ear rot caused by *Fusarium graminearum*. *Can. J. Plant Pathol.* **4**: 195-209.

Sun J, Xu Y, Ye S, Jiang H, Chen Q, Liu F, Zhou W, Chen R, Li X, Tietz O, et al. 2009. *Arabidopsis* ASA1 is important for jasmonate-mediated regulation of auxin biosynthesis and transport during lateral root formation. *Plant Cell* 21*:* 1495–1511.

Tamburic-Ilincic L, Somers D, Fedak G, Schaafsma A. 2009. Different quantitative trait loci for *Fusarium* resistance in wheat seedlings and adult stage in the Wuhan/Nyubai wheat population. *Euphytica* 165: 453-458.

Tayeh N, Bahrman N, Sellier H, Bluteau A. 2013. A tandem array of CBF/DREB1genes islocated in a major freezing tolerance QTL region on *Medicago truncatula* chromosome 6. *BMC Genomics.* 14:814.

Taylor RD, Saparno A, Blackwell B, Anoop V, Gleddie S, Tinker NA, Harris LJ. 2008. Proteomic analyses of *Fusarium graminearum* grown under mycotoxin-inducing conditions. *Proteomics* 8: 2256-2265.

Tenberge KB. 2004. Infection sites and infection structures. In Botrytis: Biology, Pathology and Control. Edited by: Elad Y, Williamson B, Tudzynski P, Delen N. Dordrecht, The Netherlands: Kluwer Academic Publishers: 74-84.

Terzi V, Morcia C, Faccioli P, Faccini N, Rossi V, Cigolini M, Corbellini M, Scudellari D, Delogu G. 2007. *Fusarium* DNA traceability along the bread production chain. *Int. J. Food Sci. Technol.* 42: 1390-139.

Thines B, Katsir L, Melotto M, Niu Y, Mandaokar A, Liu G, Nomura K, He SY, Howe GA, Browse J. 2007. JAZ repressor proteins are targets of the SCF (COI1) complex during jasmonate signalling. *Nature* 448: 661-665.

Tian Q, Wang W, Miao C, Peng H, Liu B, Leng F, Dai L, Chen F, Bao J. 2008. Purification, characterization and molecular cloning of a novel mannosebinding lectin from rhizomes of Ophiopogon japonicus with antiviral and antifungal activities. *Plant Sci.* 175: 877-884.

Trail F, Xu H, Loranger R, Gadoury D. 2002. Physiological and environmental aspects of ascospore discharge in *Gibberella zeae*. *Mycologia* 94: 181-189.

Trail F, Xu JR, San Miguel P, Halgren RG, Kistler HC. 2003. Analysis of expressed sequence tags from *Gibberella zeae* (anamorph *Fusarium graminearum*). *Fungal Genet Biol.* 38(2): 187-197.

Trail F. 2009. For blighted waves of grain: *Fusarium graminearum* in the postgenomics era. *Plant Physiol.* 149(1): 103-110.

Trusov Y, Sewelam N, Rookes JE, Kunkel M, Nowak E. 2009. Heterotrimeric G proteins-mediated resistance to necrotrophic pathogens includes mechanisms independent of salicylic acid-, jasmonic acid/ethyleneand abscisic acid-mediated defense signaling. *Plant J.* 58: 69-81.

Tucker SL, Besi MI, Galhano R, Franceschetti M, Goetz S, Lenhert S, Osbourn A, Sesma A. 2010. Common genetic pathways regulate organ-specific infection-related development in the rice blast fungus. *Plant Cell* 22: 953-972.

Uehara Y, Takahashi Y, Berberich T, Miyazaki A, Takahashi H, Matsui K, Ohme-Takagi M, Saitoh H, Terauchi R, Kusano T. 2005. Tobacco ZFT1, a transcriptional repressor with a Cys2/His2 type zinc finger motif that functions in spermine-signaling pathway. *Plant Mol Biol.* 59: 435-448.

Urban M, Mott E, Farley T, Hammond-Kosack K. 2003. The *Fusarium graminearum* MAP1 gene is essential for pathogenicity and development of perithecia. *Mol. Plant Pathol.* 4: 347-359.

Van den Brink J, de Vries Ronald P. 2011. Fungal enzyme sets for plant polysaccharide degradation. *Appl Microbiol Biotechnol.* 91:1477-1492.

Van Eeuwijk FA, Mesterhazy A, Kling CI, Ruckenbauer P, Saur L, Bürstmayr H, Lemmens M, Keizer LCP, Maurin N, Snijders CHA. 1995. Assessing non-specificity of resistance of wheat to head blight caused by inoculation with European strains of *Fusarium culmorum, F. graminearum* and *F. nivale*, using a multipöicative model for interaction. *Theor. Appl. Genet.* 90: 221-228.

Van Loon LC, Geraats BPJ, Linthorst HJM. 2006. Ethylene as a modulator of disease resistance in plants. *Trends Plant Sci.* 11: 184–191.

Van Sanford DV, Anderson J, Campbell K, Costa J, Cregan P, Griffey C, Hayes P, Ward R. 2001. Discovery and deployment of molecular markers linked to fusarium head blight resistance: An integrated system for wheat and barley. *Crop Sci.* 41: 638-644.

Vergne P, Maene M, Gabant G, Chauvet A, Debener T, Bendahmane M. 2010. Somatic embryogenesis and transformation of the diploid *Rosa chinensis* cv Old Blush. *Plant Cell, Tissue and Organ Culture* 100: 73-81.

Voigt CA, Schäfer W and Salomon S. 2005. A secreted lipase of *Fusarium graminearum* is a virulence factor required for infection of cereals. *Plant J.* 42: 364-375.

Volpi C, Janni M, Lionetti V, Bellincampi D, Favaron F, D'Ovidio R. 2011. The ectopic expression of a pectin methyl esterase inhibitor increases pectin methyl esterification and limits fungal diseases in wheat. *Mol. Plant-Microbe Interact* 24: 1012-1019.

Waalwijk C, Koch SH, Ncube E, Allwood J, Flett B, de Vries I, Kema GHJ. 2008. Quantitative detection of *Fusarium spp.* and its correlation with fumonisin content in maize from South African subsistence farmers. *World Mycotox* 1(1): 39-47.

Waalwijk C, van der Heide R, de Vries I, van der Lee T, Schoen C, Corainville GC, Häusler-Hahn I, Kastelein P, Köhl J, Lonnet P, Demarquet T, Kema GHJ. 2004. Quantitative detection of *Fusarium* in wheat using TaqMan. *Eur J Plant Pathol.* 110: 481-494.

Waldron BL, Moreno-Sevilla B, Anderson JA, Stack RW, Frohberg RC. 1999. RFLP mapping of QTL for fusarium head blight resistance in wheat. *Crop Sci.* 39: 805-811.

Wallwork H, Butt M, Cheong JPE, Williams KJ. 2004. Resistance to crown rot in wheat identified through an improved method for screening adult plants. *Aus. Plant Pathol.* 33: 1-7.

Walter S, Brennan JM, Trognitz F, Trognitz B, Leonard G, Egan D, Doohan FM. 2008. Components of the gene network associated with genotype dependent response of wheat to the *Fusarium* mycotoxin deoxynivalenol. *Funct Integr Genomics* 8:421-427.

Walter S, Nicholson P, Doohan FM. 2010. Action and reaction of host and pathogen during Fusarium head blight disease. *New Phytol.* 185: 54-66.

Wang H, Hwang SF, Eudes F, Chang KF, Howard RJ, Turnbull GD. 2006. Trichothecenes and aggressiveness of *Fusarium graminearum* causing seedling blight and root rot in cereals. *Plant Pathol.* 55: 224-230.

Wang C et al., 2011. Functional analysis of the kinome of the wheat scab fungus *Fusarium graminearum*. *PLoS Pathog.* 7: e1002460.

Wang Y, Yang LM, Xu HB, Li QF, Ma ZQ, Chu CG. 2005. Differential proteomic analysis of proteins in wheat spikes induced by *Fusarium graminearum*. *Proteomics* 5: 4496-4503.

Wanjiru WM, Kang ZS, Buchenauer H. 2002. Importance of cell wall degrading enzymes produced by *Fusarium graminearum* during infection of wheat heads. *Eur. J. Plant Pathol.* 108(8): 803-810.

Wasternack C. 2007. Jasmonates: an update on biosynthesis, signal transduction and action in plant stress response, growth and development. *Annals of Botany* 100: 681-697.

Weber H, Chetelat A, Caldelari D, Farmer EE. 1999. Divinyl ether fatty acid synthesis in late blight-diseased potato leaves. *Plant Cell* 11: 485-493.

Weber H. 2002. Fatty acid-derived signals in plants. *Trends. Plant Sci.* 7: 217-224.

Wildermuth GB, McNamara RB, Quick JS. 2001. Crown depth and susceptibility to crown rot in wheat. *Euphytica* 122: 397-405.

Wilson R, Talbot NJ. 2009. Under pressure: investigation the biology of plant infection by magnaparthe oryzae. *Nature Rev. Microbiol.*7: 185-195.

Woriedh M, Hauber I, Martinez-Rocha AL, Voigt C, Maier FJ, Schröder M, Meier C, Hauber J, Schäfer W. 2011. Preventing fusarium head blight of wheat and cob rot of maize by inhibition of fungal deoxyhypusine synthase. *Mol. Plant–Microbe Interact* 24: 619-627.

Wu AB, Li HP, Zhao CS, Liao YC. 2005. Comparative pathogenicity of *Fusarium graminearum* isolates from China revealed by wheat coleoptile and floret inoculations. *Mycopathologia* 160: 75-83.

Xia Y. 2004. Proteases in pathogenesis and plant defence. *Cell Microbiol.* 6:905-913.

Xiao J et al. 2013. Transcriptome-based discovery of pathways and genes related to resistance against Fusarium head blight in wheat landrace Wangshuibai. *BMC Genomics* 14:197.

Xu JR, Hamer JE. 1996. MAP kinase and cAMP signaling regulate infection structure formation and pathogenic growth in the rice blast fungus *Magnaporthe grisea*. *Genes Dev.* 10(21): 2696-2706.

Xu JR, Urban M, Sweigard JA, Hamer JE. 1997. The CPKA gene of Magnaporthe grisea is essential for appressorial penetration. *Mol. Plant Microbe Interact.* 10: 187-194.

Yamada Y, Koyama T, Sato F. 2011. Basic helix-loop-helix transcription factors and regulation of alkaloid biosynthesis. *Plant Signal Behav.* 6: 1627-1630.

Yabwalo DN, Mergoum M, Berzonsky WA. 2011. Further characterization of the scab resistance of Frontana spring wheat and the relationships between resistance mechanisms. *Plant Breeding* 130: 521-525.

Yang J, Bai GH, Shaner GE. 2005. Novel quantitative trait loci (QTL) for Fusarium head blight resistance in wheat cultivar Chokwang. *Theor. Appl. Genet.* 111: 1571-1579.

Yang F, Jacobsen S, Jørgensen HJL, Collinge DB, Svensson B, Finnie C. 2013. *Fusarium graminearum* and its interactions with cereal heads: studies in the proteomics era. Front. *PlantSci*. 4: 37.

Yli-Mattila T, Paavanen-Huhtala S, Jestoi M, Parikka P, Hietaniemi V, Gagkaeva T, Sarlin T, Haikara A, Laaksonen S, Rizzo A. 2008. Real-time PCR detection and quantification of *Fusarium poae, F. graminearum, F. sporotrichioides* and *F. langsethiae* in cereal grains in Finland and Russia. *Arch Phoytopathol Plant Protection* 41(4): 243-260.

Young JC, Miller JD, 1985. Appearance of fungus, ergosterol and *Fusarium* mycotoxins in the husk, axial stem and stalk after ear inoculation of field corn. *Can. J.Plant Sci.* 65: 47-53.

Yu JB, Bai GH, Zhou WC, Dong YH, Kolb FL. 2008. Quantitative trait loci for Fusarium head blight resistance in a recombinant inbred population of Wangshuibai/Wheaton. *Phytopathology* 98: 87-94.

Zhan X, Zhou MP, Ren LJ, Bai GH, Ma HX, Scholten OE, Guo PG, Lu WZ. 2004. Molecular characterizationof Fusarium head blight resistance from wheat variety Wangshuibai. *Euphytica* 139: 59-64.

Zhou WC, Kolb FL, Yu JB, Bai GH, Boze LK, Domier LL. 2004. Molecular characterization of Fusarium head blight resistance in Wangshuibai with simple sequence repeat and amplified fragment length polymorphism markers. *Genome* 47: 1137-1143.

Zhuang Yb, Gala A, Yen Y. 2013. Identification of Functional Genic Components of Major Fusarium Head Blight Resistance Quantitative Trait Loci in Wheat Cultivar Sumai 3. *MPMI* 26(4): 442-450.

10 Appendix

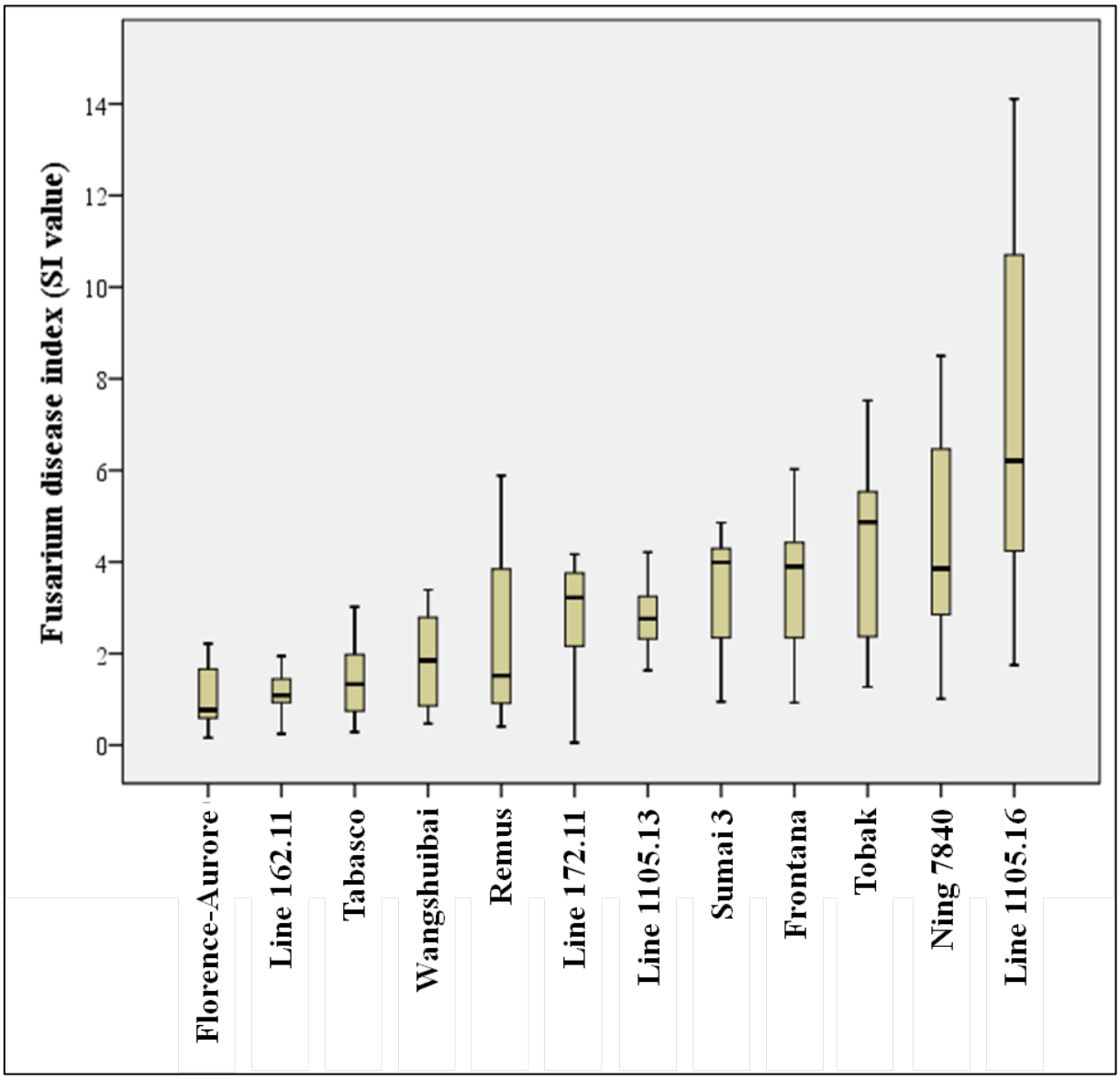

Figure A1: Box plot showing the FDI values for 12 wheat genotypes. The box indicates 75% of the distribution while the top and bottom box edges denote the first and third quartile. Medians are denoted by solid black lines. It should be noted, that the grouping of FDI genotype rankings into FRR severity categories by Mann Whitney U-Test is based on calculated medians (Fig. 9). Whiskers denote the maximum and minimum values. The box plot helps to understand the grouping of FDI genotype rankings. It also illustrates the variability inside the category susceptibility leading to two subgroups as well as the subgrouping in the category high susceptibility. The separation of category partial resistance is explained by minimum median as well as by relatively low maximum values.

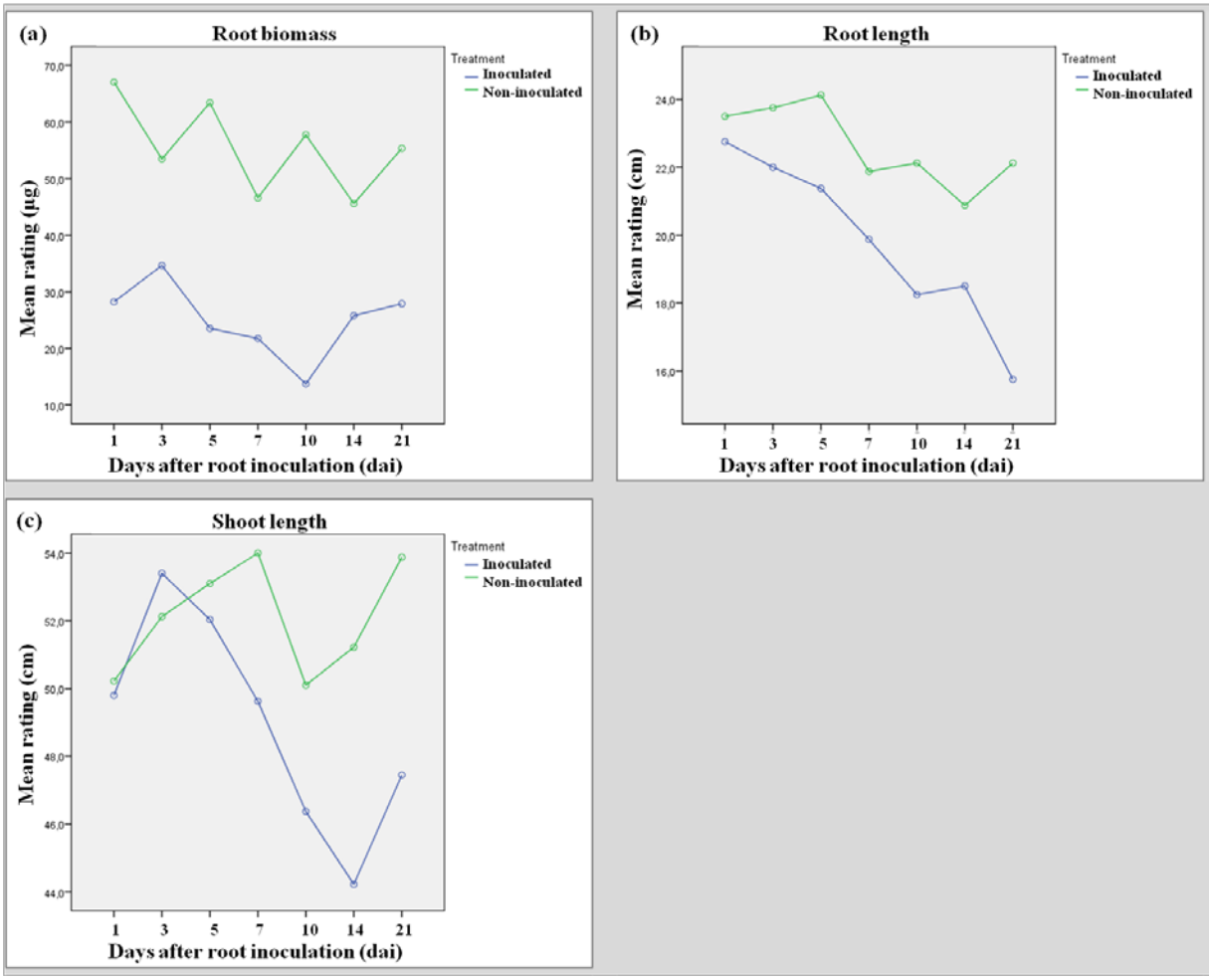

Figure A2: The mean profile plots displaying 'Treatment × Time' interactions during adult plant stages. The mean profile plots (4 wheat genotypes) show the general trends of change present in the developments of (a) root biomass; (b) root length; and (c) shoot length for inoculated and non-inoculated seedlings (two-way rANOVA).

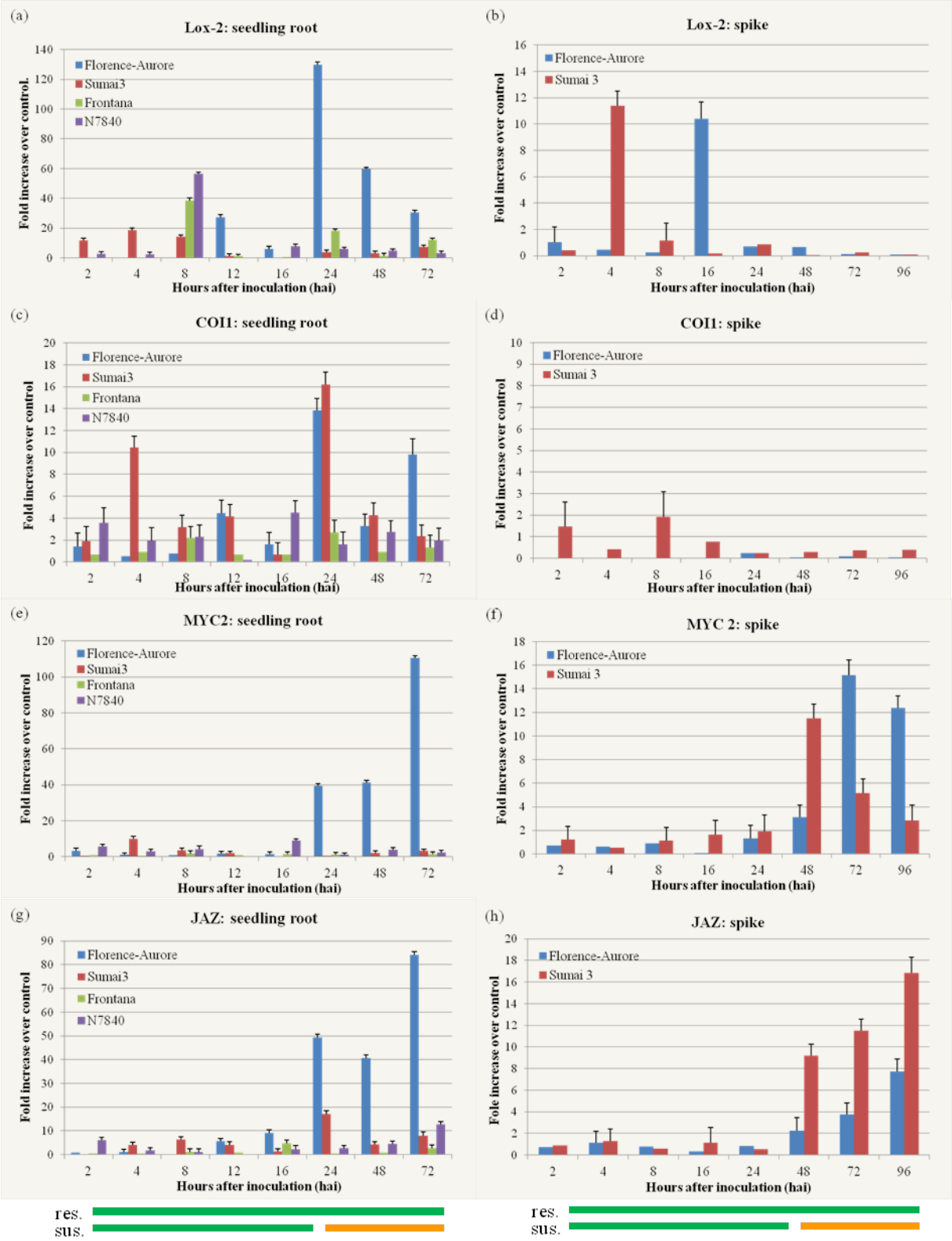

Figure A3: qRT-PCR results of the genes involved in the JA-signaling pathway in spike and seedling roots of Florence-Aurore, Sumai 3, Frontana and Ning 7840 after inoculation with *F. graminearum* IFA65. The expression levels on the y-axis were relative to non-inoculated sample from each genotype after normalization with the wheat Ubiquitin gene. The experiment was repeated (2 replicates), and data were presented as average+-S.D with n=3. The color bar indicated disease progression of resistant and susceptible genotypes. Green: early infection; orange: root main infection and colonization.

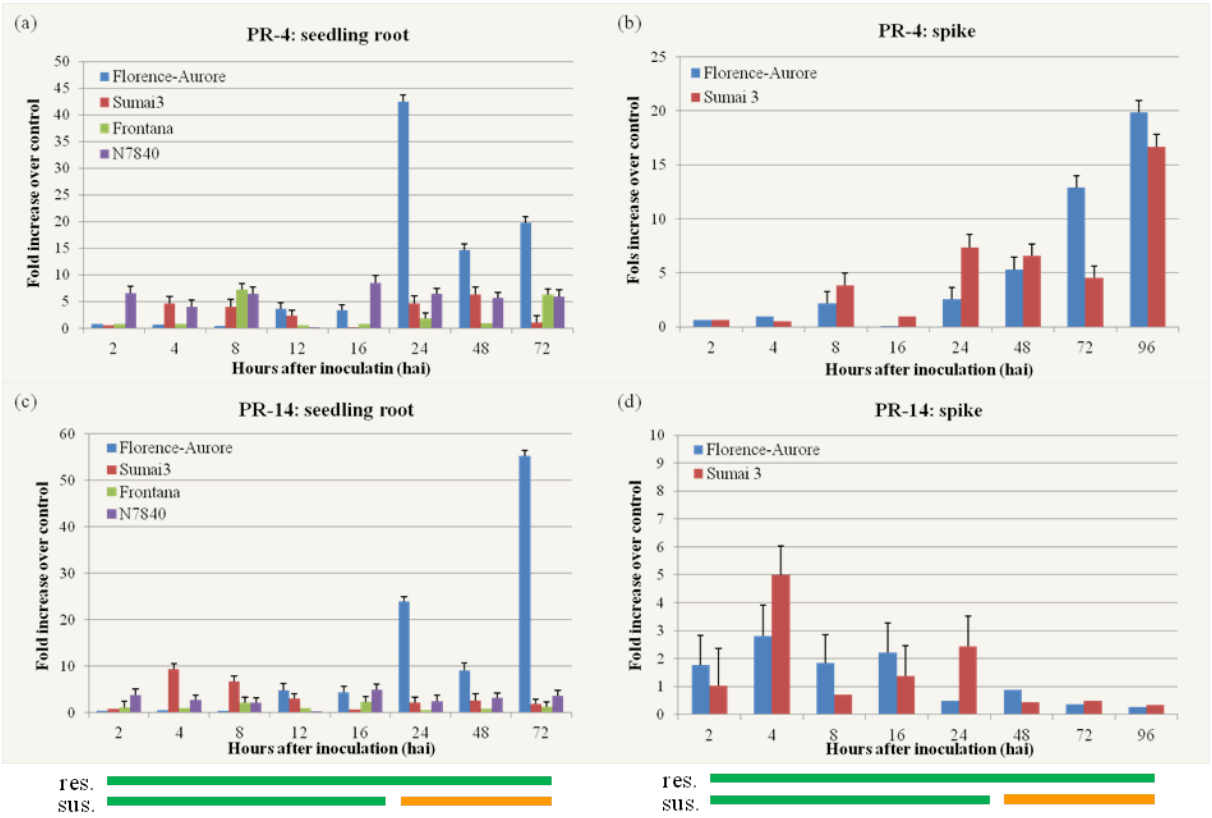

Figure A4: qRT-PCR results of JA responsive genes in spike and seedling roots of Florence-Aurore, Sumai 3, Frontana and Ning 7840 after inoculation with *F. graminearum* IFA65. The expression levels on the y-axis were relative to non-inoculated sample from each genotype after normalization with the wheat Ubiquitin gene. The experiment was repeated (2 replicates), and data were presented as average+-S.D with n=3. The color bar indicated disease progression of resistant and susceptible genotypes. Green: early infection; orange: root main infection and colonization.

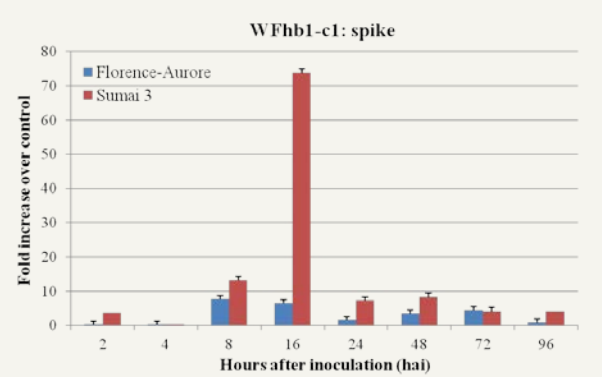

Figure A5: qRT-PCR results of FHB candidate gene in spike of Florence-Aurore, Sumai 3 after inoculation with *F. graminearum* IFA65. The expression levels on the y-axis were relative to non-inoculated sample from each genotype after normalization with the wheat Ubiquitin gene. The experiment was repeated (2 replicates), and data were presented as average+-S.D with n=3.

Erklärung

Ich erkläre: die vorgelegte Dissertation habe ich selbständig und ohne unerlaubte fremde Hilfe und nur mit den Hilfen angefertigt, die ich in der Dissertation angegeben habe. Alle Textstellen, die wörtlich oder sinngemäß aus veröffentlichten Schriften entnommen sind, und alle Angaben, die auf mündlichen Auskünften beruhen, sind als solche kenntlich gemacht. Bei den von mir durchgeführten und in der Dissertation erwähnten Untersuchungen habe ich die Grundsätze guter wissenschaftlicher Praxis, wie sie in der „Satzung der Justus-Liebig-Universität Gießen zur Sicherung guter wissenschaftlicher Praxis“ niedergelegt sind, eingehalten.

Giessen, Febuary, 2015 Qing Wang

Acknowledgement

First of all, I would like to express my sincere gratitude to Prof. Dr. Dr. h.c. Wolfgang Friedt who gave me the opportunity to work in the Institute of Plant Breeding and for the continuous support and encouragement to my Ph.D research. Thanks for his patience, motivation, enthusiasm, and immense knowledge of plant breeding. His guidance helped me in all the time of research and writing of thesis.

I also thankful to Prof. Dr. Karl-Heinz Kogel, Institute of Phytopathology and Applied Zoology, Justus Liebig University, Giessen, Germany for acceptiong to be the co-supervisor for my work and his valuable suggestions to improve the manuscript.

My sincere thanks go to Dr. Sven Gottwald under whose guidance I chose this topic. I thank him so much for his great help, guidance, constructive thought during the project and valuable advice and comments on my thesis. I am very grateful to work with him and learn a lot from him.

I am also thankful to Dr. Alexandra Furch and Dr. Steffanie Buxa from phytopathology and applied zoology institute of Justus Liebig University, Giessen for Confocal laser scanning microscopy analysis.

This work would not have been done without the help of many people in the laboratory, especially the valuable technical support from Stavros Tzigos. I also thank to the help, advice and encouragement from all of the colleague and friends.

I express my gratitude goes to my parents, without their support I would never able to finish my study. I would like to thank them for their encouragement and supporting in my life.

Last but not the least; I am very grateful to the China Scholarship Council (CSC) for financing my studies.